

**Dynamic Remodeling Events Drive the Removal of the ITS2  
Spacer Sequence During Assembly of 60S Ribosomal Subunits  
in *S. cerevisiae***

Salini Konikkat

M.Sc. Biochemistry

2009

University of Madras, TN, India

Submitted in partial fulfillment of the requirement for the degree of

Doctor of Philosophy

Department of Biological Sciences

Carnegie Mellon University

4400 Fifth Avenue

Pittsburgh, PA-15213

February 08, 2016

Thesis Advisor: Dr. John L. Woolford Jr.

## ACKNOWLEDGEMENTS

I owe my gratitude to a number of people for their support and presence in my life during the past four and a half years

My advisor, Dr. John L. Woolford Jr., for giving me the opportunity to be a part of his excellent research group and for the ample freedom to work on my projects. I immensely enjoyed working on this thesis under his guidance. His sincerity and dedication to science is a legacy I will strive to carry forth.

Members of my thesis committee, Dr. Gordon Rule, Dr. Joel McManus, and Dr. Jeffrey Brodsky for their valuable advice and challenging me to think deeply. I sincerely thank Dr. Rule for giving me plenty of opportunities to enhance my teaching skills while I worked as a teaching assistant for his Biochemistry course.

Anne Stanley and Dr. Bruce Stanley at the Core Proteomics Facility, Penn State University, Hershey, PA for the mass spectrometry experiments and Dr. Jill Dembowski for help with mass spectrometry data analysis.

Present and past members of the Woolford lab for constructive scientific discussions and company: Dr. Madhumitha Ramesh, Karen Kormuth, Beril Tutuncuoglu, Dr. Jill Dembowski, Jelena Jakovljevic, Dr. Jason Talkish, Dr. Michael Gamalinda, Stephanie Biedka, Luke Diorio-Toth, Anna Park, Joe Park, Hailey Brown, and Ben Kuo. I especially thank my friends Madhu, Karen, and Jill for their support, guidance and help when life and experiments looked particularly challenging.

The undergraduate and rotation students I had an opportunity to train or work with: Elena Shuvaeva, Laura Anderson-Lehman, Olumide Martins. I learned a lot about mentoring working with them.

My colleagues and classmates, Suchitra Ramachandran, Jigar Desai, Sahil Sangani, Olivia Molinar, Shana Bowersox, John Petersson, Zhonling, Ting Liu, Gino Gallo, and Swati Venkat, for fun times and being a part of my grad-school journey.

My family and friends, for their love and support. This work would not have been possible without their help. If there is any merit in my actions, I wish they would inspire my little nephew, Shambhu, to courageously pursue what his heart desires.

This work is dedicated to my teachers, for instilling the love for logic, beauty, and truth in me.

# Dynamic Remodeling Events Drive the Removal of the ITS2 Spacer Sequence During Assembly of 60S Ribosomal Subunits in *S. cerevisiae*

Salini Konikkat  
Carnegie Mellon University  
Department of Biological Sciences  
Pittsburgh, PA -15213

## Abstract

Ribosome assembly in eukaryotes require ~200 trans-acting proteins that drive the concerted processes of pre-rRNA processing and modification, RNA folding and r-protein binding. Previous work has identified the steps of ribosome assembly in which most trans-acting ‘assembly factors’ and r-proteins function. Yet, we are only beginning to understand the mechanistic details of remodeling events facilitated by assembly factors and r-proteins during ribosome assembly.

The objective of my work is to understand mechanistic details underlying the removal of spacer sequences ITS1 and ITS2 in pre-ribosomal RNA (pre-rRNA) during assembly of 60S ribosomal subunits in *S. cerevisiae*. The steps I focused on are (1) the exonucleolytic processing of the ITS1 spacer in 27SA<sub>3</sub> pre-rRNA, and (2) the removal of the ITS2 spacer sequence in 27SB pre-rRNA and 7S pre-rRNAs.

In the first part of my work, I explored the functions of the evolutionarily conserved assembly factor Erb1 in 60S subunit assembly. Previous research from our lab demonstrated that depletion of Erb1 blocks the removal of ITS1 spacer sequence and affects the association of the interdependent A3 factors with pre-ribosomes. This results in destabilization of the pre-ribosomes resulting in their turnover. Since depletion of Erb1 disrupts its multiple contacts in pre-ribosomes, we hypothesized that more careful mutagenesis perturbing specific intermolecular interactions of Erb1 could reveal additional functions, if any, for Erb1 in 60S ribosomal subunit assembly. I constructed internal deletion mutations targeting the evolutionarily conserved N-terminal half of Erb1 and explored the effects of these mutations on ribosome assembly using molecular and proteomic approaches. My studies revealed a new role for Erb1 in the removal of the ITS2 spacer sequence, in addition to its initial role in processing the ITS1 spacer sequence. I demonstrated that the folding of 5.8S rRNA and stable association of rRNA domain V binding assembly factors are affected in *erb1* mutants, thus blocking ITS2 removal. I also demonstrate a role for ES26/ES20 helical structures in domain III of 25S rRNA for 60S ribosomal subunit assembly. Based on these observations, I predict a model in which remodeling events triggered by the removal of Erb1 together with its interacting partner Ytm1 facilitate rearrangements in domain III of 25S rRNA in pre-ribosomes necessary to initiate the removal of the ITS2 spacer sequence.

In the second part of my thesis research, I investigated the roles of r-proteins L21 and L28 in processing of the ITS2 spacer sequence. Based on comparative analysis of structures of pre-ribosomes and ribosomes, I hypothesized that these r-proteins facilitate

RNA folding in between domains II /V of 25S rRNA. Biochemical analysis of the composition of pre-ribosomes revealed specific changes in the association of assembly factors binding to the domain II/V interface of 25S rRNA, adjacent to the peptidyl transferase center, revealing that the organization of this interface is crucial to processing of the ITS2 spacer in 7S pre-rRNA.

In addition to understanding specific mechanisms driving 60S ribosomal subunit assembly, my studies demonstrate coordination between the organization of the active centers in the 60S subunit (peptidyl transferase activity and tRNA binding sites in domain V and the polypeptide exit tunnel in domain III of 25S rRNA) and removal of the ITS2 spacer sequence. Thus, the ITS2 spacer might have evolved in eukaryotes as a mechanism to ensure accurate assembly of the translational apparatus.

## Table of Contents

<b>Chapter 1</b>	<b>Introduction: Ribosome structure and assembly</b>	
<b>1.1</b>	<b>Fundamental molecular processes driving ribosome biogenesis</b>	9
1.1.1	Pre-rRNA processing and modification	9
1.1.2	RNA folding	17
1.1.3	The roles of r-proteins in rRNA folding and assembly of the 60S subunit in <i>S. cerevisiae</i>	24
1.1.4	Formation of pre-ribosomal intermediates	31
<b>1.2</b>	<b>Our current understanding of 60S ribosomal subunit assembly</b>	37
1.2.1	Very early steps during and transcription of rRNA: Initial folding and compaction of 60S subunit precursors	37
1.2.2	Early steps: processing of ITS1 in 27SA <sub>3</sub> pre-rRNA to generate 27SB <sub>5</sub> pre-rRNA	44
1.2.3	Middle and late steps involving cleavage and processing of the ITS2 spacer	56
1.2.4	Preparing for nuclear export	76
1.2.5	Cytoplasmic maturation events release assembly factors that enter the cytoplasm with 66S preribosomes	82
<b>1.3</b>	<b>Concluding remarks</b>	83
<b>Chapter 2</b>	<b>The assembly factor Erb1 functions in a molecular interaction network to facilitate the cleavage of the ITS2 spacer during 60S subunit assembly</b>	85
<b>2.1</b>	<b>Introduction</b>	85
<b>2.2</b>	<b>Results</b>	98
2.2.1	Conserved regions in the N-terminal half of Erb1 are essential for growth	98
2.2.2	Most of the N-terminal half of Erb1 is not required for its interaction with Ytm1	111

2.2.3	Erb1 is required for the processing of both 27SA <sub>3</sub> and 27SB pre-rRNAs during 60S ribosomal subunit assembly	114
2.2.4	The pre-ribosomal composition of the three classes of erb1 mutants concurs with their pre-rRNA processing defects	122
2.2.5	Stable association of specific assembly factors required for 27SB pre-rRNA processing are affected in <i>erb1<sub>class 2</sub></i> mutants	129
2.2.6	Structure of the bowtie region in 5.8S rRNA is affected in <i>erb1<sub>class 2</sub></i> mutants	141
<b>2.3</b>	<b>Discussion</b>	154
<b>2.4</b>	<b>Future directions</b>	163
<b>2.5</b>	<b>Materials and methods</b>	164
<b>Chapter 3</b>	<b>Proper structuring of helices ES20 and ES26 in Domain III of 25S rRNA is required for 60S Ribosomal Subunit Assembly</b>	166
<b>3.1</b>	<b>Introduction</b>	166
<b>3.2</b>	<b>Results</b>	171
3.2.1	The RNA polymerase I Ts <sup>-</sup> system to study rDNA mutants	171
3.2.2	Mutations affecting the structure of ES20/ES26 in domain III of 25S rRNA are lethal	174
3.2.3	rRNA mutations perturbing the structure of the Nop7 cross-link site/ES26 affect ribosome biogenesis	177
<b>3.3</b>	<b>Discussion and Future directions</b>	180
<b>3.4</b>	<b>Materials and methods</b>	186
<b>Chapter 4</b>	<b>4. The role of ribosomal proteins L21 and L28 in late nuclear steps of 60S ribosomal subunit assembly</b>	189
<b>4.1</b>	<b>Introduction</b>	189
<b>4.2</b>	<b>Results</b>	198

4.2.1	Depletion of L21 and L28 does not significantly alter the protein composition of early pre-ribosomal intermediates	199
4.2.2	Association of late-acting assembly factors is affected upon depletion of L21 and L28	202
4.2.3	Depletion of L21 and L28 affects the stable association of proteins during middle and late events of 60S maturation	207
<b>4.3</b>	<b>Discussion</b>	211
<b>4.4</b>	<b>Future directions</b>	220
<b>4.5</b>	<b>Materials and methods</b>	222
	<b>References</b>	223

## List of Figures

Figure 1	Atomic resolution structure of <i>S. cerevisiae</i> ribosomes	3
Figure 2	rRNA expansion segments in the 60S subunit of <i>Saccharomyces cerevisiae</i>	5
Figure 3	Eukaryotic specific 60S ribosomal proteins and extensions cluster adjacent to rRNA expansion segments	7
Figure 4	Organization of rRNA genes in <i>S. cerevisiae</i>	13
Figure 5	Pre-rRNA processing in <i>S. cerevisiae</i>	15
Figure 6	Hierarchy of rRNA folding	20
Figure 7	Protein-assisted folding of RNA	22
Figure 8	Dynamic changes in the RNP architecture initiate and strengthen the association of r-proteins with pre-ribosomes	27
Figure 9	Hierarchical association of 60S subunit r-proteins is required for specific steps of pre-rRNA processing.	29
Figure 10	Pre-rRNA processing and other 60S subunit assembly events occur inside RNA-protein complexes called pre-ribosomes.	35
Figure 11	Ribosomal proteins (green) required for processing of the 27SA <sub>3</sub> pre-rRNA cluster in the domain I and domain II/VI neighborhoods	45
Figure 12	Direct interactions between the interdependent A <sub>3</sub> assembly factors	50
Figure 13	A <sub>3</sub> factors – hierarchy of assembly and interactions	52
Figure 14	Multistep process for removal of the ITS2 spacer during 60S ribosomal subunit assembly.	58
Figure 15	Location of r-proteins required for ITS2 cleavage and processing in 60S subunits.	61
Figure 16	Hierarchy of association of B assembly factors with preribosomes	64
Figure 17	Remodeling events driving ribosome assembly	70
Figure 18	Two Roles of the AAA-ATPase Rea1 in late steps of 60S subunit assembly.	74

Figure 19	Binding of export factors to the subunit interface on preribosomes aids their transit into the cytoplasm	78
Figure 20	Molecular architecture of the Nop7-subcomplex	89
Figure 21	Molecular interaction network of assembly factors involved in 27SA <sub>3</sub> , 27SB, and 7S pre-rRNA processing	94
Figure 22	Molecular assembly events in early and middle preribosomal intermediates	96
Figure 23	The N-terminal half of Erb1 contains stretches of highly conserved residues	100
Figure 24	Bioinformatic prediction of secondary structural elements in Erb1	102
Figure 25	Effects of deletions of discrete regions of Erb1 on growth of yeast	105
Figure 26	Effect of temperature on growth of <i>erb1</i> internal deletions mutants that have no growth defects at 30°C	107
Figure 27	Effects of overexpression of the lethal <i>erb1</i> internal deletion mutants on growth	109
Figure 28	A major portion of the N-terminal half of Erb1 is not required for its interaction with Ytm1	112
Figure 29	<i>erb1</i> - internal deletion mutants are categorized into three classes based on pre-rRNA processing phenotypes (by primer extension)	116
Figure 30	<i>erb1</i> - internal deletion mutants can be categorized into three classes based on pre-rRNA processing phenotypes (by northern blotting)	118 120
Figure 31	Preribosomes purified from <i>erb1<sub>class 2</sub></i> mutants are more stable compared to depletion of Erb1	124- 127
Figure 32	Schematic flow chart for the analysis of iTRAQ data	130
Figure 33	Erb1 is required for stable association of assembly factors involved in 27SB pre-rRNA processing	136
Figure 34	<i>erb1<sub>class 2</sub></i> mutants perturb the association of specific assembly factors involved in ITS2 cleavage and 27SB pre-rRNA processing	138
Figure 35	The structure of ITS2 is largely intact in <i>erb1<sub>class 2</sub></i> mutants	141
Figure 36	The structure 5.8S rRNA is perturbed in <i>erb1<sub>class 2</sub></i> mutants	144

Figure 37	Contacts of r-proteins L26, L35, L17, and L39 on 5.8S rRNA	146
	show increased modification in <i>erb1<sub>class 2</sub></i> mutants	147
Figure 38	Removal of Nop7 or rearrangement of its contacts is needed to	150-
	establish ES3/ES19 contacts in 60S ribosomal subunits	152
Figure 39	(A) Erb1 is required for two consecutive pre-rRNA processing	161
	events during 60S ribosomal subunit assembly	
	(B) A proposed molecular interaction network for ITS2 cleavage	
	in 60S ribosomal subunit precursors	
Figure 40	Nop7 binds to ES26 and helix 54 in domain III of 25S rRNA	169
Figure 41	The pol I <i>Ts</i> - system to study rDNA mutants	172
Figure 42	Effects of ES20/ES26 mutations on cell viability	175
Figure 43	Lethal mutations in ES26 and helix 54 of domain III of 25S rRNA	178
	perturb 60S subunit assembly	
Figure 44	Primer extension analysis of pre-rRNA processing in rDNA	182
	mutants	
Figure 45	The ES20/E26 neighborhood is a hub of interaction with assembly	184
	factors and r-proteins	
Figure 46	A comparative analysis of interactions of L21 and L28 with rRNA	192
	in 60S ribosomal subunits	
Figure 47	Direct contacts of L21 and L28 on 25S rRNA	194
Figure 48	L21 and L28 homologues in prokaryotic ribosomes	196
Figure 49	The protein composition of pre-ribosomes is not altered at early	200
	stages of assembly upon depletion of L21 and L28	
Figure 50	The protein composition of pre-60S particles exhibits specific	204-
	changes upon depletion of L21 and L28	205
Figure 51	The association of assembly factors located in domain V of 25S	208-
	pre-rRNA is affected upon depletion of L21 or L28	209
Figure 52	Helices contacted by L21 and L28 in domains II and V are not in	214
	their mature conformations in pre-ribosomes	
Figure 53	Helices contacted by L21 and L28 in domains II and V are not in	216
	their mature conformations in pre-ribosomes	

Figure 54	Helices in domain V contacted by L21 and L28 undergo extensive changes during late steps of 60S ribosomal subunit maturation	218
-----------	--	-----

**Tables**

Table 1	Assembly factors required for early steps of 60S subunit assembly	40
Table 2	Assembly factors involved in processing of the ITS1 spacer in 27SA <sub>3</sub> pre-rRNA	54

## **CHAPTER 1. Introduction**

Ribosomes are the ribonucleoprotein nanomachines responsible for protein synthesis in all cells. Mature eukaryotic ribosomes contain two asymmetric subunits: the large, 60S subunit, which contains 25S rRNA, 5.8S rRNA, 5S rRNA and 46 r-proteins, and the small, 40S subunit, which contains 18S rRNA and 33 r-proteins (Figure 1). During protein synthesis, the small 40S subunit binds and decodes the information in mRNA and recruits appropriate aminoacyl-tRNAs as substrates. The large 60S subunit hosts the peptidyl transferase center responsible for peptide bond formation and protein synthesis (Figure 1).

Extensive RNA-protein interactions underlie the construction of these macromolecular complexes. Although the core structure of ribosomes is conserved across the three domains of life, eukaryotic ribosomes are larger and more complex than their bacterial counterparts, due to the addition of rRNA segments called expansion segments and r-protein extensions, insertions or eukaryote specific r-proteins (Ben-Shem et al. 2010, 2011; Melnikov et al. 2012; Jenner et al. 2012; Gerbi 1996; Armache et al. 2010; Anger et al. 2013). These additional elements are mostly localized on the solvent-exposed side of ribosomal subunits, away from the functional centers (Figure 2). Even though the eukaryote-specific features are thought to reflect the functional divergence of ribosomes, their potential roles in the assembly and functional specialization of eukaryotic ribosomal subunits are just beginning to be explored.

Ribosome assembly is central to cellular metabolism. In rapidly growing yeast cells, a major fraction of the transcriptional, splicing, translational and intracellular trafficking machinery is dedicated to the production of ribosomes, at a rate of ~4000 subunits/minute (Warner 1999). Since protein synthesis and translational fidelity are crucial to cellular homeostasis, major defects in ribosome assembly or function are lethal to all organisms, often observed as embryonic lethality in higher organisms. Mutations in assembly factors or r-proteins that result in a partial loss of their function, or heterozygous null alleles, result in a variety of diseases collectively referred to as ribosomopathies. These diseases are characterized by hematopoietic, craniofacial or skeletal abnormalities, and a predisposition to cancer (Freed et al. 2010; Kathleen L McCann 2013; Sulima et al. 2014; Kondrashov et al. 2011). Thus, research on ribosome assembly is crucial to dissect the molecular bases of these pathological conditions.

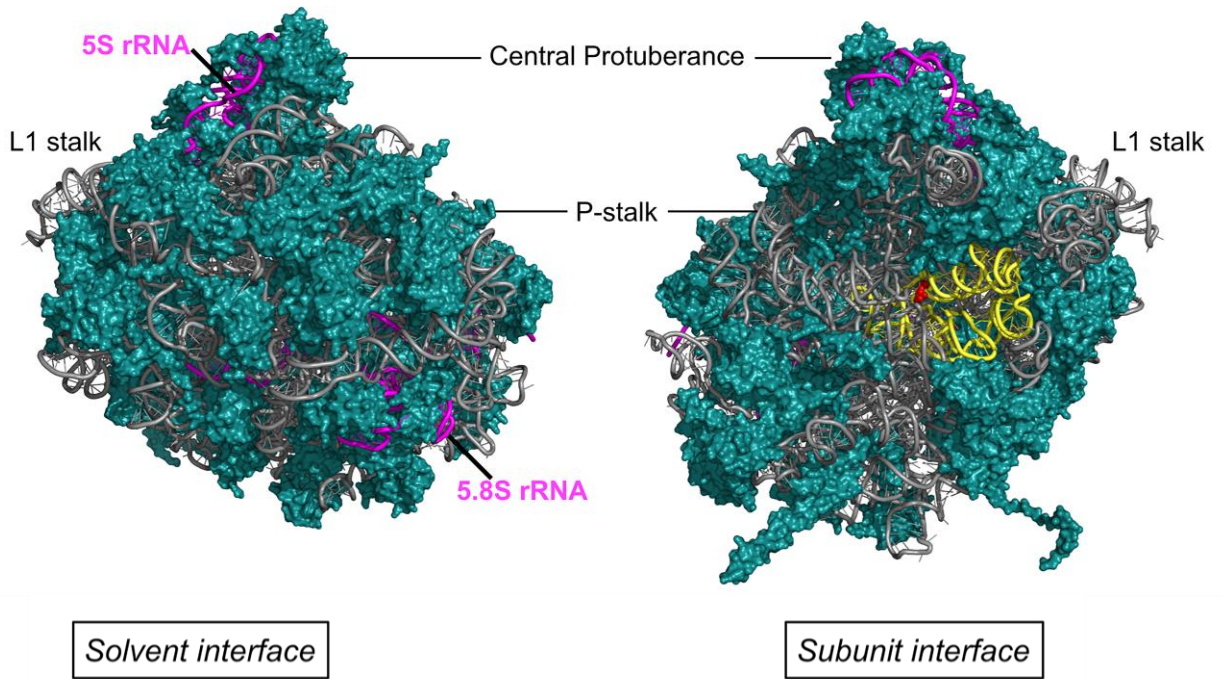
There is an increasing body of evidence indicating that organisms might produce subpopulations of ribosomes with distinct composition for functional specialization or regulatory purposes. This is an exciting arena, since it shifts our view of ribosomes as dynamic regulators of the cellular proteome (Gilbert 2011; Xue and Barna 2013; Bygrazov et al. 2013). Whether or not ribosome assembly is programmed to generate heterogeneous ribosomes with functional diversity is a largely unexplored area.

My thesis work focused on understanding mechanistic processes driving 60S ribosomal subunit assembly in *S. cerevisiae*. In this Introduction, I will briefly discuss molecular processes driving ribosome biogenesis, with a focus on construction of the 60S subunit.

**Figure 1**

**A**

**The Large 60S Subunit**



**B**

**The Small 40S Subunit**

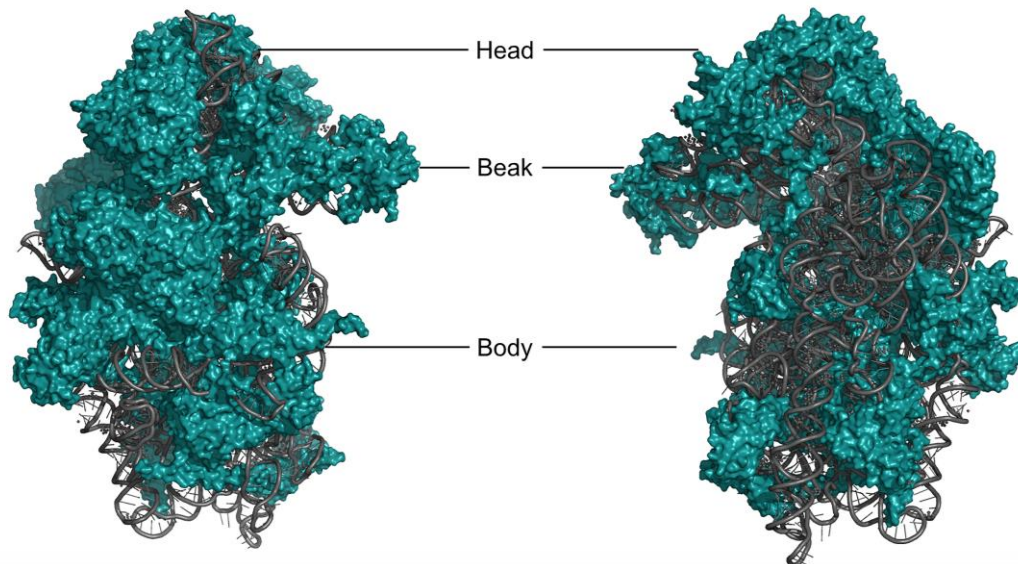


**Figure 1. Atomic-resolution structure of *S. cerevisiae* ribosomes**

Shown are crystal structures of the 60S and 40S ribosomal subunits in *S. cerevisiae*, viewed from either the solvent (left) or subunit (right) interface. (A) The large ribosomal 60S subunit is composed of 25S, 5.8S and 5S rRNAs, and 47 r-proteins. (B) The small ribosomal 40S subunit contains the 18S rRNA and 32 r-proteins. Other structural landmarks on the 60S and 40S subunits are also indicated.

(PDB IDs: 3U5D, 3U5E, 3U5B, 3U5C)

Figure 2

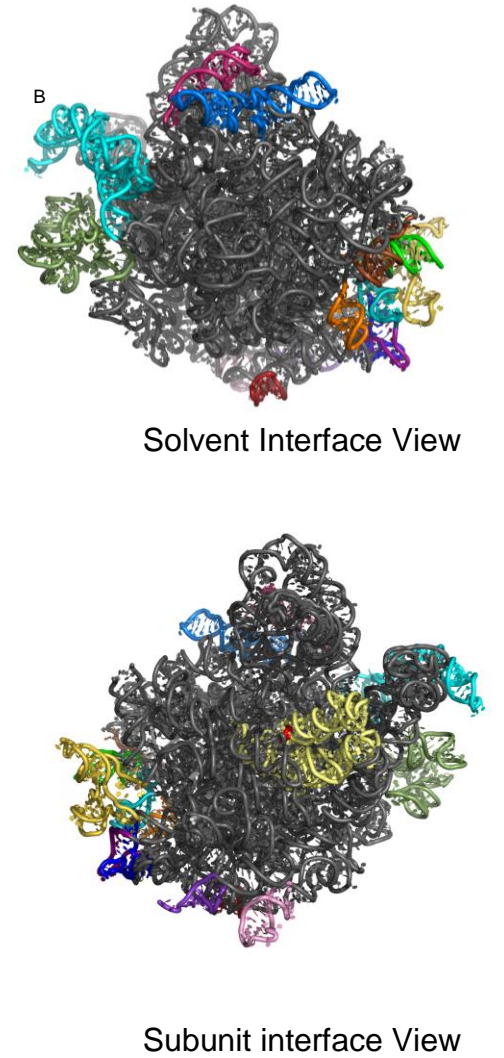
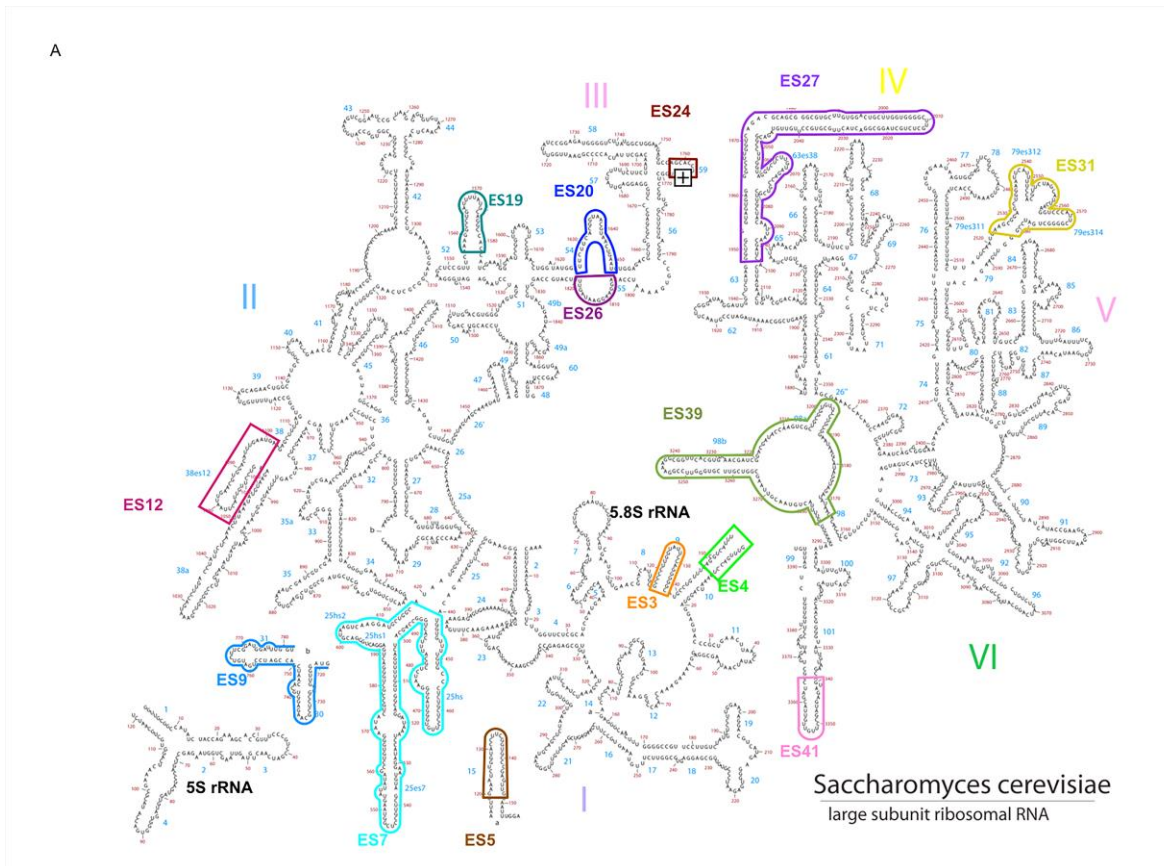


**Figure 2. rRNA expansion segments in the 60S subunit of *Saccharomyces cerevisiae***

(A) Expansion segments (ES) also known as eukaryote-specific rRNA elements in the large subunit are mapped onto the phylogeny-based secondary structure obtained from the ribovision website (<http://apollo.chemistry.gatech.edu/RiboVision/#>). (B) ESs form two clusters on the periphery of the 60S subunit (PDB ID: 3U5D), away from the peptidyl transferase center and tRNA binding sites (red and pale yellow). ES5 in green contains the 5'-end of 5.8S rRNA and the 3'-end of 25S rRNA.

Figure 3

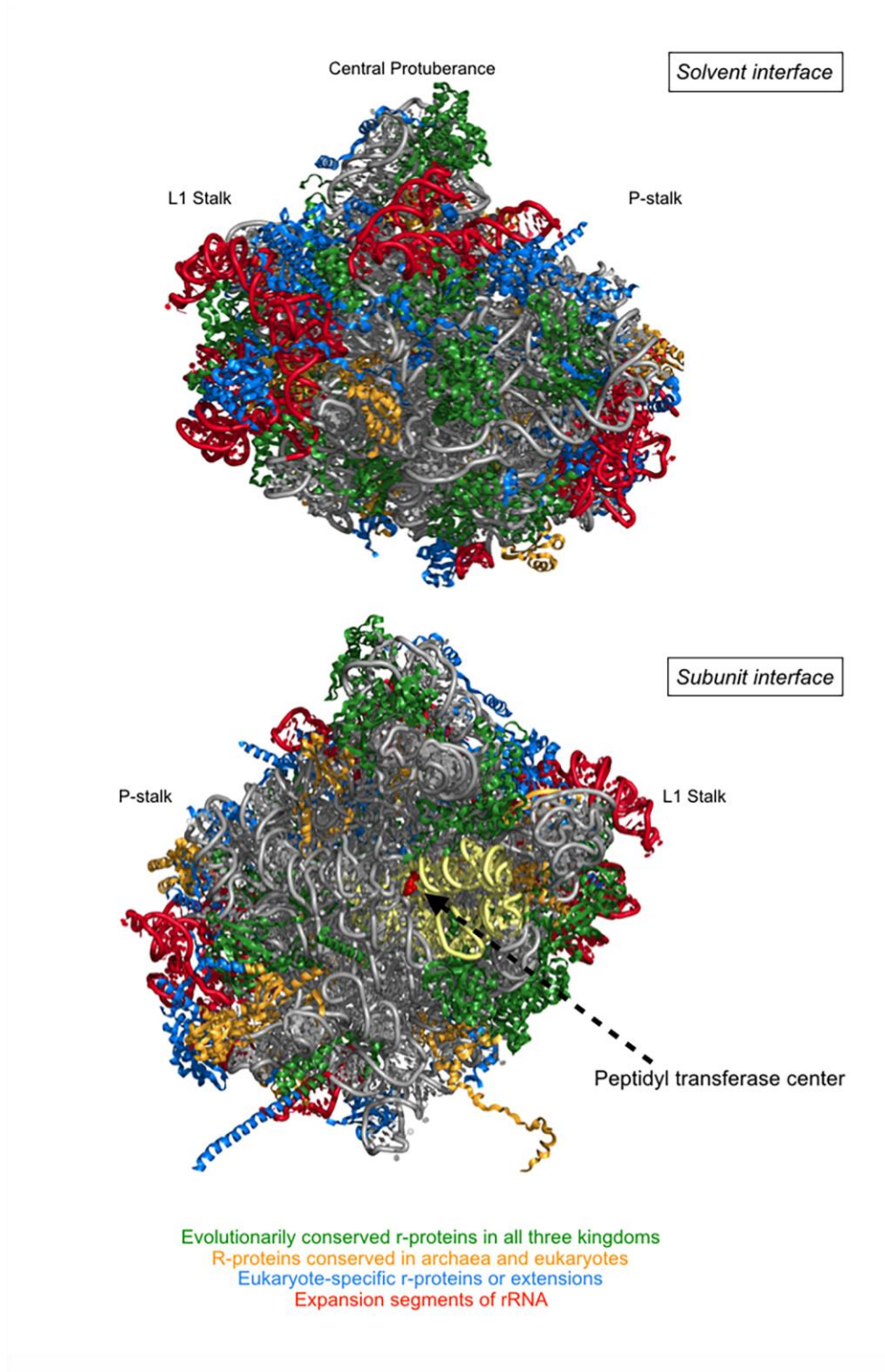


**Figure 3. Eukaryotic specific 60S ribosomal proteins and extensions (blue) cluster adjacent to rRNA expansion segments (red).** Eukaryote specific rRNA (red) and r-protein elements (blue) concentrate around the central protuberance and the 5' and 3'-ends of 25S and 5.8S rRNAs.

(PDB IDs: 3U5D, 3U5E)

## **1.1 Fundamental molecular processes driving ribosome biogenesis**

Ribosome assembly begins with transcription of pre-rRNAs, which undergo co-transcriptional folding, modification, processing, and assembly with r-proteins to form functional ribosomal subunits. These events occur in a series of highly orchestrated events spanning three cellular compartments: the nucleolus, nucleoplasm, and cytoplasm. The wide spectrum of genetic, molecular, and proteomic techniques available to study ribosome assembly in yeast, has enabled it to be the model system of choice to investigate ribosome assembly in eukaryotes. Studies spanning several decades have demonstrated that the concerted action of ~76 snoRNPs and 200 *trans*-acting proteins referred to as ‘assembly factors’ facilitates the production of translation-competent ribosomal subunits in *S. cerevisiae*. The exact functions of most of these assembly factors remain to be understood. A recent study of the human nucleolar proteome revealed that 210 of 286 human ribosome assembly factors have yeast homologs, highlighting the evolutionary conservation of these assembly mechanisms. In this section, I will outline four intertwined molecular processes driving ribosome assembly in eukaryotes: pre-rRNA processing and modification, RNA folding, binding of r-proteins, and formation of pre-ribosomal intermediates.

### **1.1.1 Pre-rRNA processing and modification**

Ribosomal RNAs are encoded by tandem repeats of rDNA genes around which nucleolus, the membrane-less nuclear subcompartment, is organized (Cmarko et al.

2008). Three of the four rRNAs (18S, 5.8S, and 25S rRNAs) are synthesized by RNA polymerase I as a polycistronic precursor called 35S pre-rRNA. The fourth rRNA, 5S rRNA is transcribed in its precursor form by RNA polymerase III. The organization of rDNA repeats in *S. cerevisiae* and the primary transcripts formed by their transcription are schematically depicted in Figure 4. Evolutionarily aspects of rDNA organization and pre-rRNA processing are discussed in more detail in (Lafontaine and Tollervey 2001; 2004; Lafontaine 2015).

The 35S pre-rRNA contains mature rRNA sequences separated by two internal transcribed spacers (ITS1 and ITS2) and flanked by two external transcribed spacers (5'-ETS and 3'-ETS). R-proteins and assembly factors co-transcriptionally bind pre-rRNA to generate RNA-protein complexes called 'pre-ribosomes'. The spacer sequences are removed in a multistep pathway by endonucleases, exonucleases and the nuclear exosome that associate with pre-ribosomes (reviewed in (Fernández-Pevida et al. 2015)) (Figure 5). Because pre-rRNA processing events are irreversible, they contribute to the directionality of the ribosome assembly process.

The pre-rRNA processing pathway is one of the best-understood aspects of ribosome assembly. Hence processing events are used as landmarks to understand the hierarchy of remodeling events driving ribosome assembly. 60S subunit assembly events can be grouped into six categories based on the pre-rRNA content in the pre-ribosomal intermediates (Figure 5) (1) "very early steps" as rRNA is transcribed and initially compacted, (2) "early steps", including removal of the ITS1 spacer sequence in

27SA2 and 27SA3 pre-rRNAs to produce 27SB pre-rRNA (35S pre-rRNA is found in 90S pre-ribosome, 27SA2 or 27SA3 pre-rRNA are in 66S pre-ribosomes) (3) “middle steps”, involving cleavage at the C2 site in ITS2, and exit from the nucleolus (27SB pre-rRNA is in 66S pre-ribosomes), (4) “late nuclear steps” including the removal of the ITS2 spacer and remodeling of the central protuberance in the 60S subunit (25.5S + 7S or 25S + 6S pre-rRNAs are in 66S pre-ribosomes), (5) binding of nuclear export factors to enable transit of pre-ribosomes through the nuclear-pore complex into the cytoplasm, and (6) final maturation events in the cytoplasm. Molecular details of these steps are discussed in section 1.3.

Approximately 2% of rRNA nucleotides undergo chemical modifications such as pseudouridylation and 2'-O-ribose methylation, mediated by snoRNA-guided enzymes or a conventional substrate-specific enzyme. Most modifications occur co-transcriptionally, however, some of them take place during late stages of assembly (Lapeyre and Purushothaman 2004; Osheim et al. 2004; Koš and Tollervey 2010; Lafontaine 2015; Sharma and Lafontaine 2015). Interestingly, rRNA modifications cluster near highly conserved functional sites on the subunit-interface. snoRNA-mediated rRNA modifications are carried out by ~76 box C/D or box H/ACA snoRNPs. These snoRNPs interact with their target RNA by Watson-Crick base pairing, and often have multiple targets on pre-rRNA located far apart in the primary sequence. While the absence of individual modifications or some groups of them has no effect on ribosome assembly, they are known to be essential for optimal ribosome function. Misdirection of rRNA methylation can have lethal consequences (Ben Liu et al. 2008; Baxter-Roshek et al.

2007; Liang et al. 2007; Jack et al. 2011). Depletion of essential proteins associated with the snoRNP machinery or of the substrate-specific 60S subunit methylases Spb1 and Nop2 disrupts ribosome assembly (Kiss et al. 2010; Lafontaine and Tollervey 1999; Lapeyre and Purushothaman 2004; Kressler 1999; Hong et al. 1997; 2001; Sharma et al. 2013; Bourgeois et al. 2015; Lafontaine 2015; Ban et al. 2014). How these snoRNPs and methylases facilitate ribosome assembly is a field of active research. Whether functionally specialized ribosomes are created by varying the combination of modifications on rRNA is not yet known.

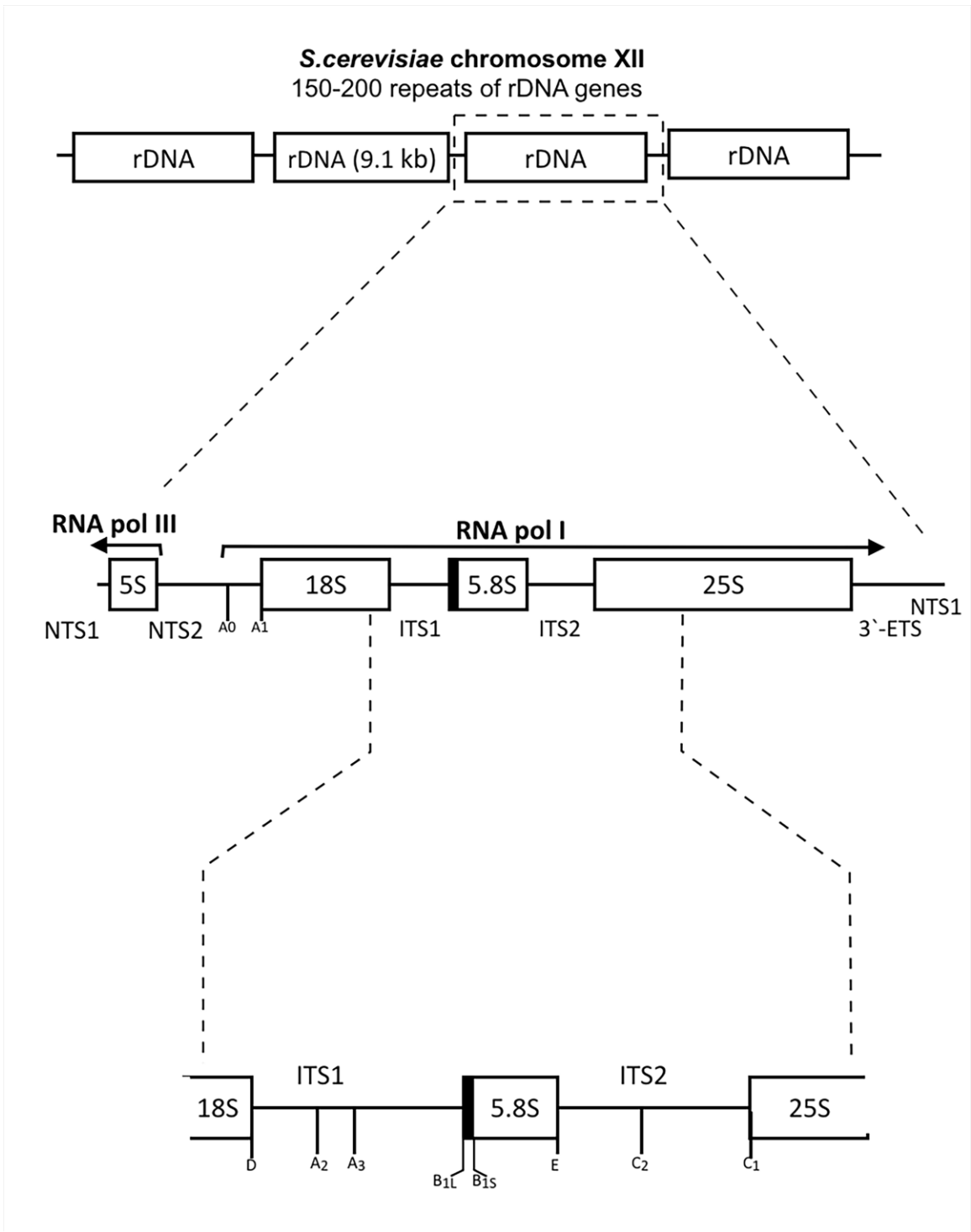


**Figure 4. Organization of rRNA genes in *S. cerevisiae*.** A single yeast cell contains ~150-200 tandem repeats of ~9.1 kb long rDNA genes on chromosome XII. The rDNA repeats are transcribed by RNA polymerase III to produce pre-5S rRNA and by RNA polymerase I to produce 35S pre-rRNA. The 35S pre-rRNA contains 18S, 5.8S, and 25S rRNAs separated and flanked by two internal transcribed spacers (ITS2) and external transcribed spacers (ETSs) respectively. Individual rDNA repeats are separated from each other by the non-transcribed spacers (NTSs). The cleavage sites on rRNA during pre-rRNA processing events are indicated.



**Figure 5. Pre-rRNA processing in *S. cerevisiae*.** The location of the external (5'- and 3'-ETS) and internal transcribed spacers (ITS1 and ITS2), and the processing sites on the primary transcript, 35S pre-rRNA are shown. Processing intermediates (italicized) and nucleases are indicated next to the step in which they function. The primary transcript synthesized by RNA polymerase I, 35S pre-rRNA, undergoes either post- or co-transcriptional cleavage at the A<sub>2</sub> site (not shown here). Despite post- or co-transcriptional cleavage, 60S subunit assembly begins with formation of the 3'-end of 27SA<sub>2</sub> pre-rRNA. In yeast, 27SA<sub>2</sub> pre-rRNA can proceed via two parallel processing pathways, the major pathway (~85%) and the minor pathway (~15%) producing 5.8S rRNA with heterogeneous ends (5.8S<sub>S</sub> and 5.8S<sub>L</sub>, respectively).

### 1.1.2 RNA folding

The tertiary structure RNA is crucial to its function. Higher order structures of RNA molecules consist of secondary structure elements such as helices and loops arranged in three dimensional space to generate a functionally competent tertiary structure (Holbrook 2005) (Leontis et al. 2006; Pyle and Green 1995) (Figure 6).

RNA folding begins co-transcriptionally in the 5`-3` direction with rapid and spontaneous formation of secondary interactions driven by base-pairing. RNA helices are often formed between bases far apart in the primary sequences, resulting in an initial compaction of the linear primary transcript. RNA secondary structural elements are inherently stable due to the large negative net free energy of double helix formation. Consequently, folding into unproductive conformers can result in the formation of kinetically trapped intermediates (Woodson 2008; 2011). Long RNAs such as pre-rRNAs collapse into compact intermediates in which the helices interact and undergo remodeling events before attaining their final conformations(Woodson 2010). The tertiary folding of RNA depends on long-range intra- and inter- molecular interactions resulting from base pairing (Watson-Crick and non-canonical), base stacking, coaxial helical stacking, 2`-OH group interactions, or formation of intercalated strands between the helices and loops in the secondary structure. The strength of tertiary interactions is weaker in comparison to that of secondary interactions in RNA (Butcher and Pyle 2011). The formation of secondary and tertiary structural elements in RNA is not always hierarchical. For example, tertiary structural elements aid the formation of inherently unstable secondary structures such as pseudoknots (Gluick and Draper 1994)

Since rRNA is a ribozyme, its folding determines the functionality and translational fidelity of ribosomes. In order to assemble these long rRNAs at a rate of ~4000 subunits/minute in rapidly growing yeast cells, productive conformers of rRNA need to be selected and favored. Cellular osmolytes and the crowded intracellular environment stimulate the collapse of RNAs into globular shapes (Woodson 2010). Cations such as Mg<sup>2+</sup> ions help to overcome electrostatic barriers to RNA folding (Butcher and Pyle 2011). Additionally, r-proteins and the assembly machinery greatly facilitate rRNA folding by the mechanisms listed below (Figure 7).

- (1) Specific RNA-binding proteins (r-proteins and many assembly factors) promote RNA folding by stabilizing native structure or by guiding folding (Figure 7A) (Pyle and Green 1995; Woodson 2008; Granneman et al. 2011; Dembowski et al. 2013b; Talkish et al. 2014).
- (2) R-proteins and some assembly factors can function as RNA chaperones to resolve mis-folded RNA structures in an energy-independent manner (Figure 7B) (Herschlag 1995; Lorsch 2002; Fedorova et al. 2010; Del Campo et al. 2009).
- (3) Nineteen RNA helicases (15 of which are DEAD-box RNA helicases) function in ribosome assembly in yeast. They can utilize the energy derived from ATP hydrolysis to anneal or fold RNA helices, resolve mis-folded RNA structures or displace RNA-bound assembly factors. Due to this energy-investment, these proteins can drive ribosome assembly in a forward direction (Figure 7C).

(Lamanna and Karbstein 2011; Guenther and Jankowsky 2009; Bohnsack et al. 2009; Dembowski et al. 2013a) reviewed in (Rodríguez-Galán et al. 2013).

- (4) snoRNAs could mediate RNA folding processes by base pairing with mature or spacer sequences on rRNA (Steitz and Tycowski 1995; Dutca et al. 2011). They could also prevent mis-folding of RNA strands before their base-pairing partner sequences are transcribed (Figure 7D).

**Figure 6**

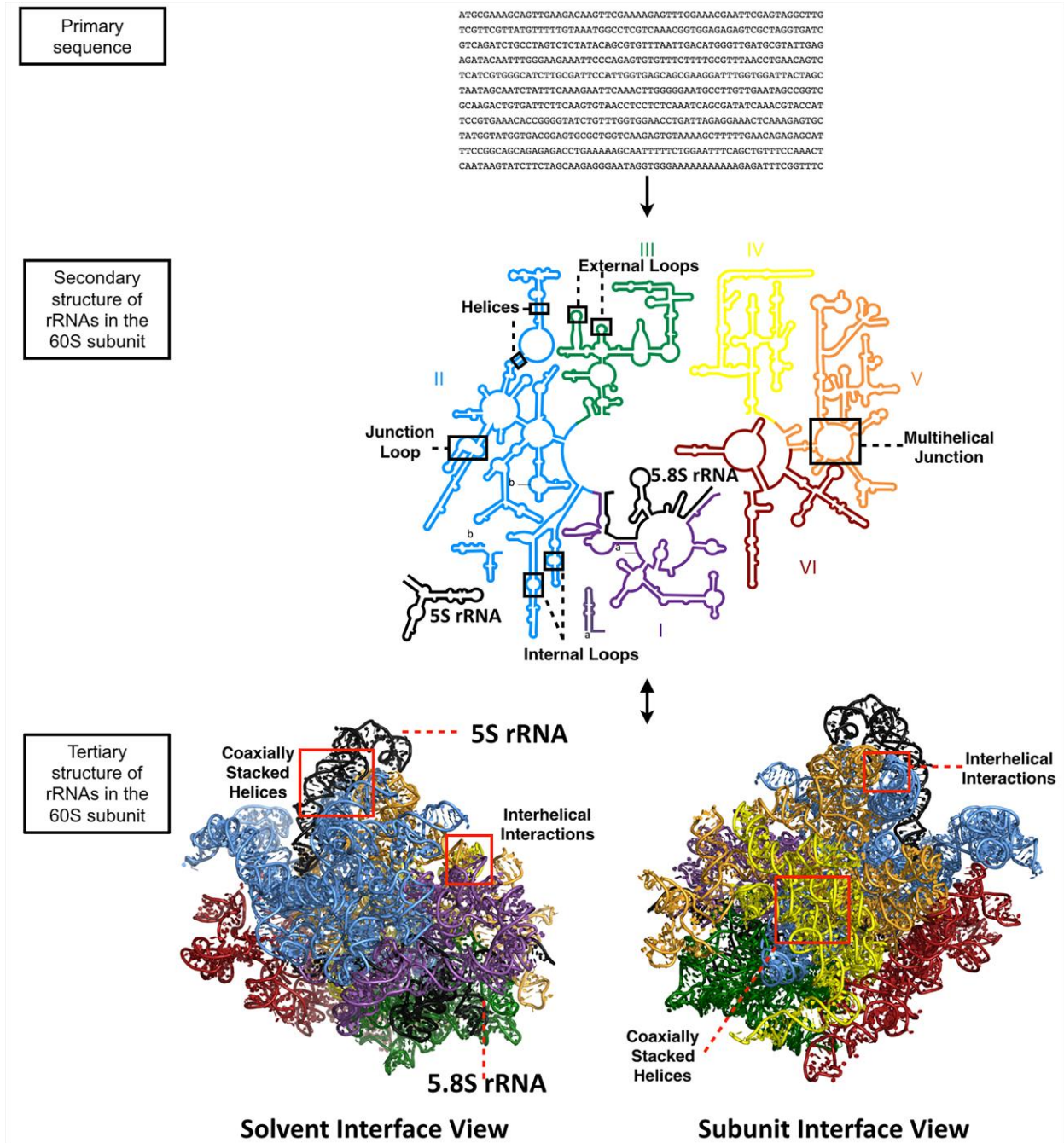
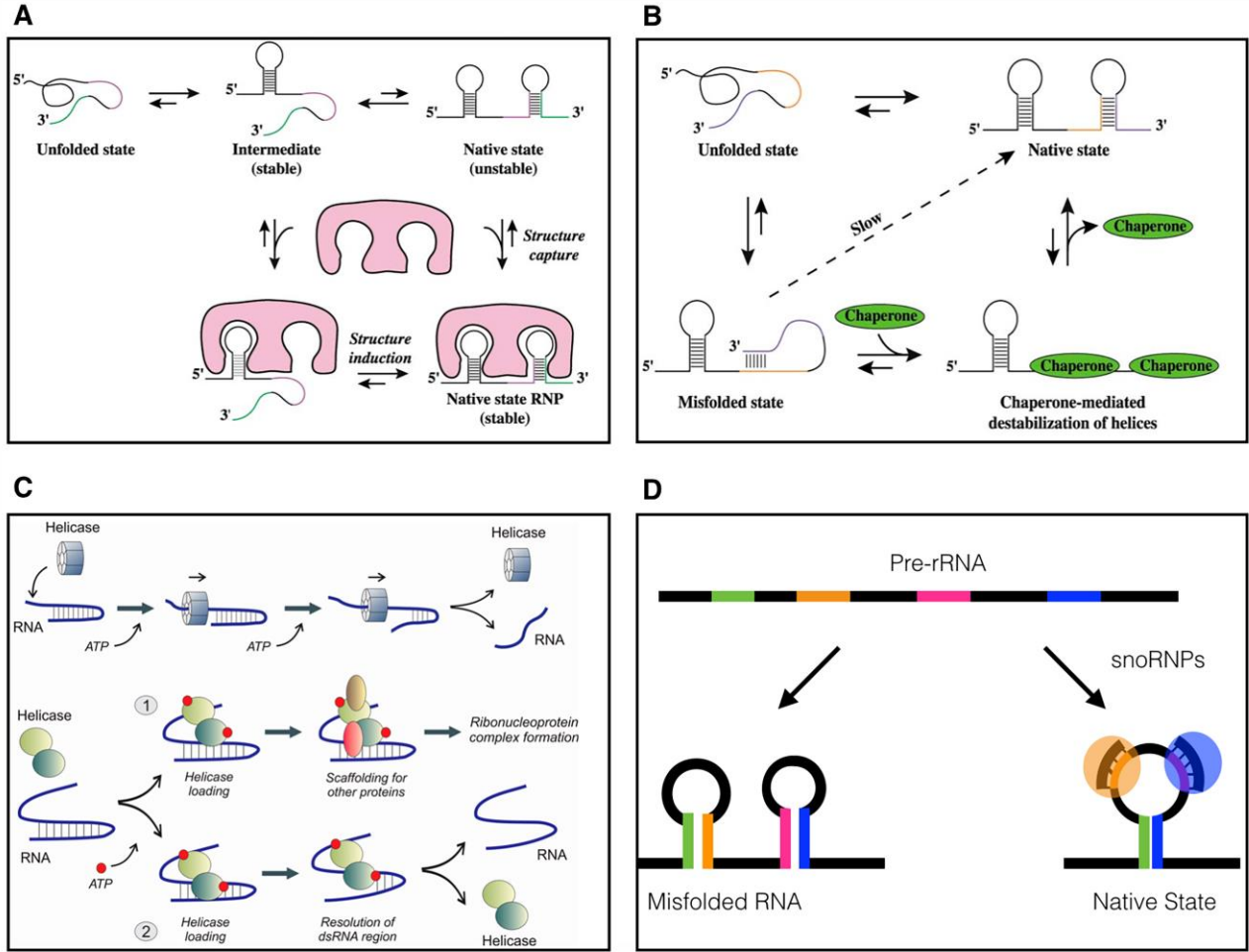


**Figure 6. Hierarchy of rRNA folding.** rRNA sequences in the primary transcript form helices that are ~2-11 base pair long, separated by helical junctions and internal loops, via base-pairing interactions. The 25S rRNA of 60S subunits folds into six domains (I-VI), indicated in different colors. The 5.8S rRNA binds to domain I (purple) of 25S rRNA via base-pairing interactions. The secondary structural elements are compacted and arranged in three-dimensional space via tertiary interactions such as coaxial base stacking and inter-helical base pairing/backbone interactions, to form the tertiary RNA structure of mature 60S ribosomal subunits.

Figure 7



Lorsch J. (2002), Leitao A.L et al (2015)

**Figure 7. Protein-assisted folding of RNA.** (A) RNA binding proteins recognize and bind specific structures on RNA. Their binding can stabilize otherwise unstable active conformations or induce the formation of structures for binding of other proteins. (B) Interaction of RNA chaperones with RNA disrupts mis-folded structures, providing more opportunities for the RNA to fold into its native state. (C) Multitasking RNA helicases. RNA helicase can unwind and resolve mis-folded RNA structures in an energy dependent manner, serve as scaffolds to build RNA-protein complexes, or use the energy of ATP-hydrolysis to initiate local structural changes in an RNA-protein complex. (D) Binding and release of snoRNPs to pre-rRNAs can block specific pre-rRNA mis-folding events.

### **1.1.3 The roles of r-proteins in rRNA folding and assembly of the 60S subunit in *S. cerevisiae***

Most r-proteins (64/79) are essential for growth under standard laboratory conditions, because they are important for the assembly and/or function of ribosomes (Steffen et al. 2012; Pöll et al. 2009; Gamalinda et al. 2014). Non-essential r-proteins also may have important roles in ribosome biogenesis or function (Babiano et al. 2012).

R-proteins are enriched in basic residues, which enables them to bind negatively charged RNA (Figure 8). Interestingly, a significant fraction of r-proteins also contains intrinsically disordered regions (Peng et al. 2014). Thus chaperone proteins are often necessary for their stable expression, to protect them from aggregating, and to escort them through pores in the nuclear envelope for late steps of ribosome assembly in the cytoplasm. Ribosome-associated chaperones and importins, and ubiquitination of the N-termini of r-proteins are known to perform some of these roles. In addition, recent studies demonstrated that dedicated chaperones co-translationally bind r-proteins and escort them across nuclear pores for assembly into ribosomes, for example, AcL4, Rrb1, Syo1, and Sqt1 serve as chaperones for L4, L3, L5, and L10, respectively (Calviño et al. 2015; Pausch et al. 2015; Stelter et al. 2015).

Crystal structures of eukaryotic ribosomes suggested the role for r-proteins in stabilizing inter-domain interactions. Eukaryotic r-proteins typically contain a globular domain and one or more long extensions forming extensive contacts with rRNA, often

spanning long distances across the ribosomal subunit surface or forming deep insertions into the subunit. Typically, the globular domains of r-proteins contact one domain of rRNA, which is thought to act as the primary binding site (Klein et al. 2004). rRNAs and r-proteins undergo co-folding, which increases the specificity of RNA-protein binding. The intrinsically disordered extensions of r-proteins could co-ordinate the folding of rRNA in different regions of ribosomal subunits, and form communication channels to relay changes in the architecture of pre-ribosomes at different stages of assembly (Beril Tutuncuoglu, Personal Communication). Thus, as assembly progresses, r-proteins are more stably integrated with rRNA. Consequently, components of pre-ribosomes proceed through alternating steps of r-protein binding and rRNA conformational changes. The binding of r-proteins to RNA during early steps of assembly can be equated to the formation of an encounter complex. This initial binding event is then followed by rearrangements in RNA structure that allow more stable intermolecular interactions (Figure 8). Such stabilization can result from an independent event promoting RNA-folding, or an induced-fit by the associating protein.

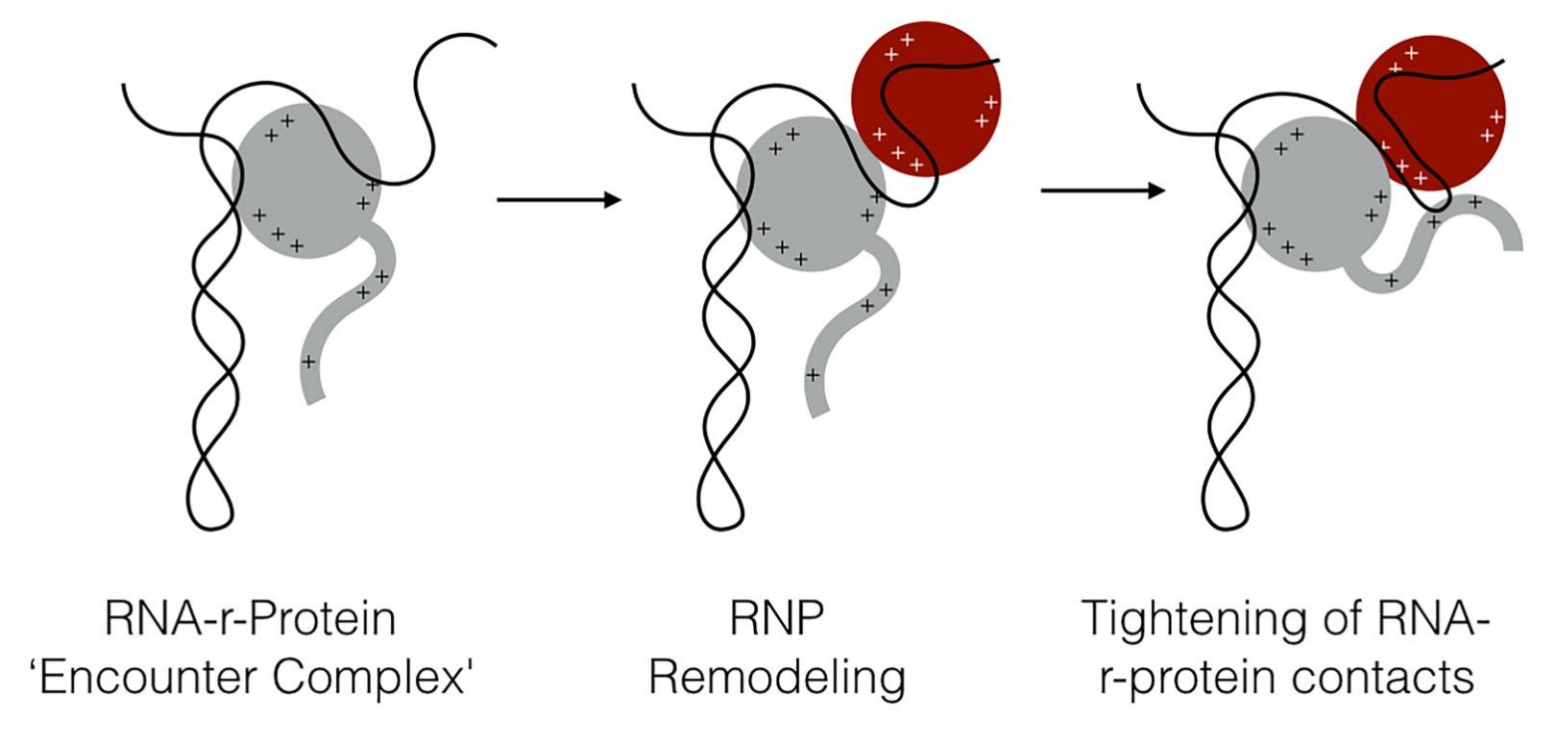
The *in vitro* reconstitution of bacterial 30S and 50S subunits from mature rRNA and r-proteins demonstrated the importance of r-proteins to enhance rRNA folding to its native structure. These studies defined the hierarchy of stable association of each bacterial r-protein with rRNA; primary (direct binding to rRNA), secondary (binding depends on association of primary binding r-proteins with rRNA), and tertiary (binding depends on association of secondary binding r-proteins). R-protein assisted rRNA folding is speculated to be the underlying principle facilitating the binding of secondary and

tertiary binding r-proteins, following the association of primary and secondary binding r-proteins, respectively.

Recent studies using depletion of large subunit r-proteins revealed a correlation between the location of the r-proteins and pre-rRNA processing steps (Figure 9). R-proteins binding to domains I or II, or to the II/IV interface at the equatorial belt of 60S subunits, are required for processing of the ITS1 spacer. R-proteins binding domain III and 5.8S rRNA in the bottom third of 60S subunits are required for cleavage of the ITS2 spacer. ITS2 pre-rRNA processing requires domains IV/V/VI and 5S rRNA, and binding of r-proteins on the solvent interface and central protuberance of 60S subunits (Pöll et al. 2009; Gamalinda et al. 2014; 2013; Ohmayer et al. 2013; Milkereit et al. 2015). Collectively, these studies provided strong evidence for a hierarchical pattern of RNA folding and r-protein binding proceeding from the solvent interface of 60S subunit to its subunit interface. However, it is important to note that the folding hierarchy is not uniquely linear, as late nuclear steps of 60S subunit maturation involve major reorientation of RNA helices such as h38 in domain III and h89 I domain V of 25S rRNA) and 5S rRNA) (Leidig et al. 2014).

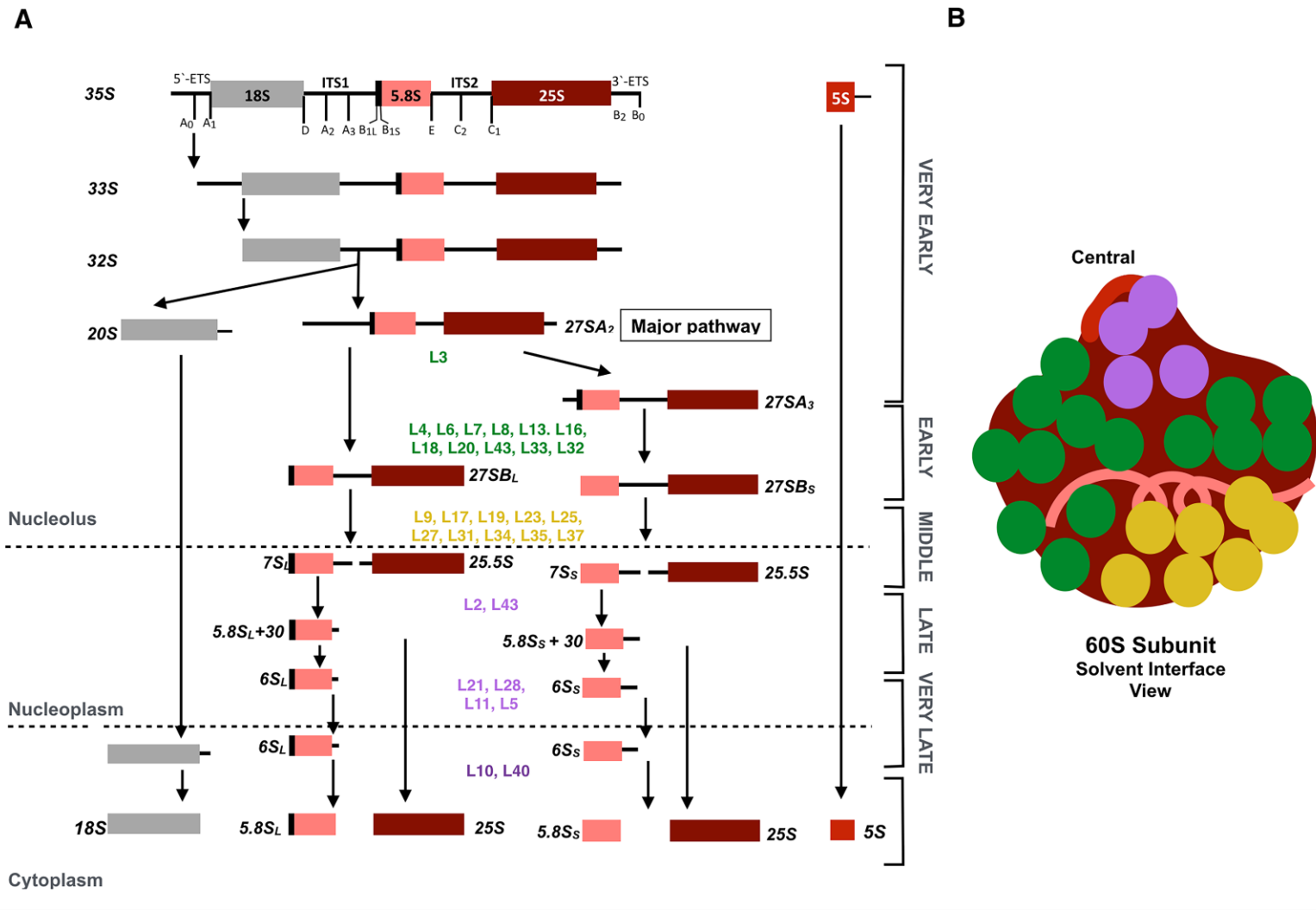
The roles of r-proteins in 60S ribosomal subunits are further discussed in Chapter 4.

Figure 8



**Figure 8. Dynamic changes in the RNP architecture initiate and strengthen the association of r-proteins with pre-ribosomes.** Shown is a schematic for the hierarchical recruitment and sequential tightening of r-protein-rRNA interaction. R-proteins that are initial binders (grey) promote conformational changes in the architecture of RNA required for recruitment of later binding r-proteins (reddish brown). Binding of the second r-protein creates an RNA structure for the interaction of the disordered domain of the first r-protein, tightening its association with pre-ribosomes.

Figure 9



**Figure 9: Hierarchical association of 60S subunit r-proteins is required for specific steps of pre-rRNA processing.** (A) Specific pre-rRNA processing steps affected by depletion of r-proteins in yeast. All r-proteins functioning in a particular step of pre-rRNA processing are indicated in the same color. (B) The r-proteins affecting specific stages of pre-ribosome assembly cluster to specific neighborhoods on the 60S subunit, providing valuable clues for the hierarchy of rRNA folding.

#### 1.1.4 Formation of pre-ribosomal intermediates

As discussed briefly in the beginning of this section, many assembly factors and r-proteins bind to nascent RNA resulting in the formation of pre-ribosomal intermediates or pre-ribosomes. Genetic and proteomic approaches identified ~200 assembly factors that bind pre-ribosomes at specific stages of maturation, perform their function, and then dissociate. Association of assembly factors with pre-ribosomes can also happen in a hierarchical manner determined by structural and compositional remodeling events occurring within the pre-ribosomes.

The simplest classification of pre-ribosomal intermediates is based on their pre-rRNA content (Figure 10). Ribosome biogenesis begins with the formation of 90S pre-ribosomes containing 35S pre-rRNA (post-transcriptional cleavage at site  $A_2$ ), or else 66S and 43S pre-ribosomes, containing 27SA<sub>2</sub> and 20S pre-rRNAs respectively (co-transcriptional cleavage at site  $A_2$ ). In either case, assembly of the large 60S subunit bifurcates from assembly of the small subunit after cleavage at site  $A_2$ . 43S pre-ribosomes containing 20S pre-rRNAs are exported into the cytoplasm, where they undergo final steps of maturation including a translation-like test-drive cycle to check their functional competence (Strunk et al. 2012; Lebaron S et al. 2012; Garcia-Gomez et al. 2014). The maturation of 60S subunits is much more complicated; it involves formation of at least five distinct 66S pre-ribosomal intermediates distinguished by their pre-rRNA content. 66S pre-ribosomes containing 27SA<sub>2</sub>, 27SA<sub>3</sub>, and 27SB pre-rRNAs are found in the nucleolus. Pre-ribosomes containing 27SB pre-rRNA move into the nucleoplasm following cleavage in the ITS2 spacer, to generate 25.5S and 7S pre-rRNAs.

The 25.5S and 7S pre-rRNAs are trimmed into 25S and 6S pre-rRNAs, after which pre-ribosomes are exported into the cytoplasm. The final steps of 60S subunit maturation, including formation of the 5' - end of 5.8S rRNA, occur in the cytoplasm.

The pre-ribosomal intermediates are very dynamic due to the association and dissociation of assembly factors at distinct stages of assembly. Assembly factors include proteins with a wide variety of biochemical activities, such as RNA binding proteins, NTPases (GTPases and DEAD-box helicases), kinases/phosphatases, endo/exonucleases, putative scaffolding proteins, and some proteins that are homologous to r-proteins. Most of the assembly factors have been assigned to a particular step in pre-rRNA processing or subunit maturation based on the phenotypic effects of their depletion. They often exhibit a hierarchical pattern for their stable association with pre-ribosomes (Figure 16)

The lifetime of assembly factors in pre-ribosomes is typically identified by the pre-rRNAs and assembly factors with which they co-purify. Recruitment of assembly factors to pre-ribosomes can be driven by protein-protein interactions with other assembly factors or r-proteins, or protein-RNA interactions with pre-rRNAs. Therefore, the proper structuring of the binding sites on pre-rRNAs could also determine entry of assembly factors into pre-ribosomes. It is important to consider that exit/release of assembly factors from pre-ribosomes may be as impactful on the progress of assembly, as AF entry or the presence of assembly factors in pre-ribosomes. The exit of these assembly factors may be driven by gradual weakening of the intermolecular interactions stabilizing their association, and/or via energy-dependent enzymatic events. For example,

release might be a critical checkpoint that signals proper progress through the assembly pathway. A productive remodeling event might create an RNP structure that activates release of some assembly factors, which in turn might expose or create rRNA binding sites for other assembly factors which associate at the same site during late events of assembly.

While the entry and exit of assembly factors occur throughout maturation steps, three major remodeling events driven by AAA-ATPases – Rix7 (ribosome export), Rea1 (ribosome export associated, or Midasin/Mdn1), and Drg1 (Afg2, dizaborine resistance gene) occur during the maturation of 60S subunits. Rea1 is a mechanoenzyme that uses physical force to release assembly factors in two different steps, before transit of pre-ribosomes from the nucleolus to the nucleoplasm, and then from the nucleoplasm to the cytoplasm (Erzberger and Berger 2006; Thoms et al. 2015a; Galani et al. 2004; Barrio-Garcia et al. 2015; Baßler et al. 2010). It appears that Rix7 functions along with Rea1 in the first remodeling event (Gadal et al. 2001; Kressler et al. 2008). Drg1-mediated remodeling events occur in the cytoplasm (Loibl et al. 2014). These remodeling events result in remarkable changes in the composition of pre-ribosomes.

In addition to the three AAA-ATPases, 19 RNA helicases function in ribosome assembly in *S. cerevisiae* (Woolford and Baserga 2013). They use ATP binding and/or hydrolysis to bind or remodel RNA or RNA-protein complexes (Jankowsky 2011). They can sense RNA-RNA, RNA-protein or protein-protein interactions and convert these into downstream events such as rearrangements of RNA structure, recruitment/release of

assembly factors, stabilization of r-protein contacts, or activation of other NTPases  
(reviewed in ( Rodríguez-Galán et al. 2013; Martin et al. 2013)).

Figure 10

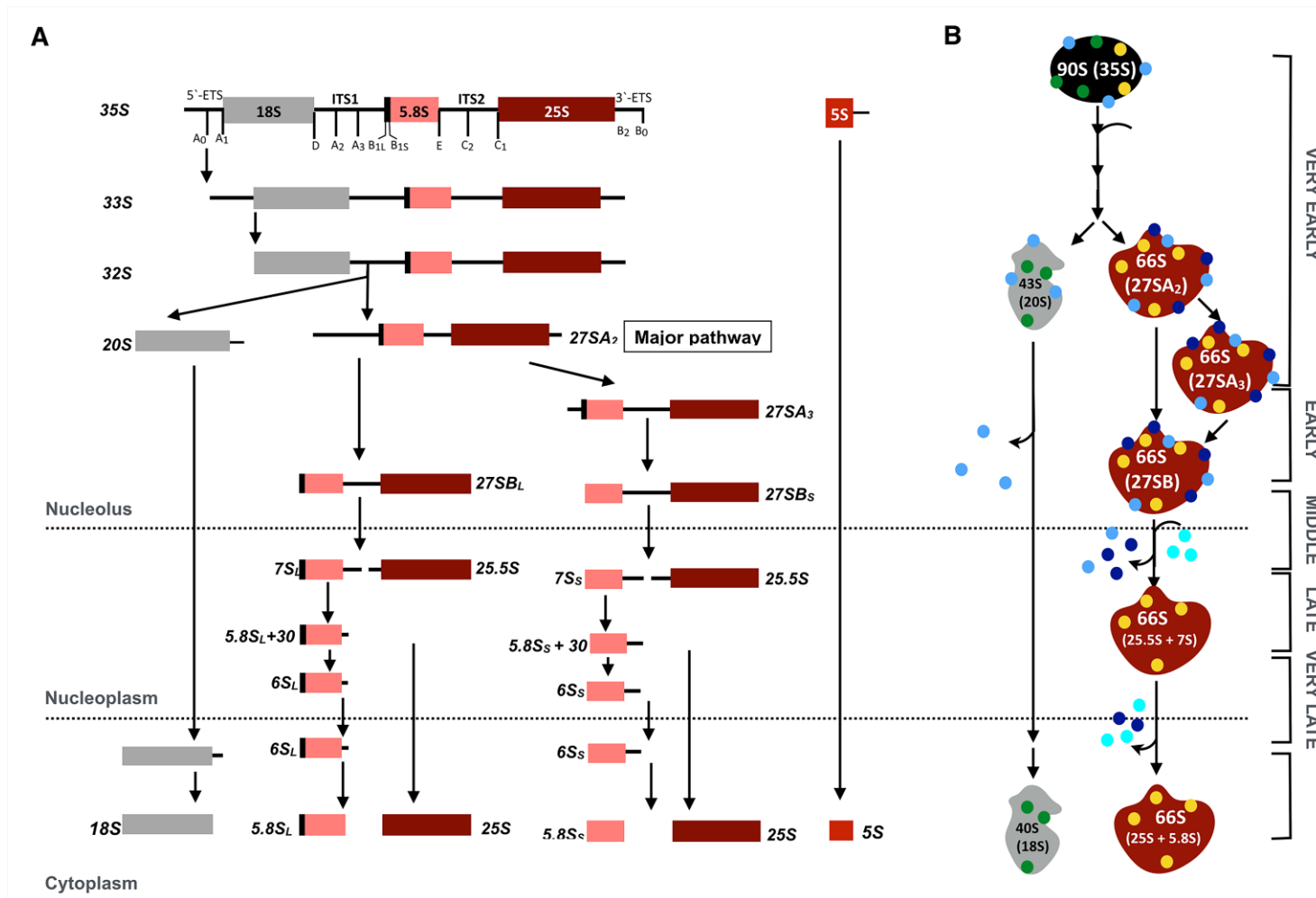


**Figure 10. Pre-rRNA processing and other 60S subunit assembly events occur inside RNA-protein complexes called pre-ribosomes.** Most r-proteins (yellow and green), except the cytoplasmically associating r-proteins, associate with pre-rRNAs co-transcriptionally. The pre-ribosomes are highly dynamic in protein and pre-rRNA composition due to the entry and release of *trans*-acting assembly factors (blue) from pre-ribosomes at specific stages of assembly and processing of pre-rRNAs.

## **1.2 Our current understanding of 60S ribosomal subunit assembly**

In this Section, I outline key steps in maturation of 66S preribosomes and attempt to provide a model for the nuclear steps of 60S subunit assembly in *S. cerevisiae*. I will discuss these events under the six groups described above in Section 1.2.1.

### **1.2.1 Very early steps during and after transcription of rRNA: Initial folding and compaction of 60S subunit precursors**

Upon completion of transcription, one can detect the first precursor to mature 60S large subunits, the 66S particle, containing 27SA<sub>2</sub> pre-rRNA and 5S rRNA. The 27SA<sub>2</sub> pre-rRNA is generated by co- or post-transcriptional cleavage of the primary transcript at site A<sub>2</sub> by the enzyme Rcl1 (Horn et al. 2011). In the co-transcriptional assembly pathway (75-90% in rapidly growing cells), cleavage at site A<sub>2</sub> occurs as transcription proceeds, while in the post-transcriptional assembly pathway, cleavage at the A<sub>2</sub> site occurs after the complete transcription of 35S pre-rRNA. Subsequent processing at the other sites in 27SB pre-rRNA (A<sub>3</sub>, B<sub>S</sub>, B<sub>L</sub>, and C<sub>2</sub>) does not happen until after transcription is completed. Thus, for the 60S subunit, early steps of assembly are in the strictest sense co-transcriptional, but in fact most of the processing and remodeling steps occur post-transcriptionally.

Co-IP of 27SA<sub>2</sub> pre-rRNA with r-proteins and assembly factors indicates that 50 out of 70 of the 60S subunit assembly factors and ~40/47 r-proteins (all but those 8-9 r-proteins that are only assembled in the cytoplasm: L10, L24, L29, L40, L41, L42, P0, P1, and P2), are present in these earliest 66S preribosomes. The association of r-proteins

becomes tightened only as assembly proceeds, as indicated by resistance of r-protein pre-rRNA interactions to high salt washes. This tightening presumably results from multiple remodeling events with 66S preribosomes, similar to those thought to drive the maturation of initial less stable r-protein-rRNA ‘encounter complexes’ to establish more and tighter contacts between r-proteins and rRNA.

A large number of AFs (~25) appear to function very early, defined primarily by the effect of their depletion: only small amounts of 27SA<sub>2</sub> pre-rRNA accumulate, and no later pre-rRNAs are evident (Table 1). This “rapid pre-rRNA turnover” phenotype may reflect that early assembly intermediates require complex folding to compact to a stable state; interruption of such pathways could create especially unstable assembly intermediates. Some of these ‘very early’ assembly factors may assemble together with r-proteins, and others independently of r-proteins.

Two very early assembly factors Nop4 and Rrp5 are particularly large proteins that cross-link to multiple sequences of pre-rRNA and thus may serve as scaffolds to enable compaction of the nascent pre-rRNA (Granneman et al. 2011; Lebaron et al. 2013; Hierlmeier et al. 2013). R-protein L3 contacting the ‘domain linker’ interface on which the six domains of 25S rRNA fold may also serve as a key scaffolding protein, since its depletion has the greatest effect of any r-protein on the stability of 27SA<sub>2</sub> and 27SA<sub>3</sub> pre-rRNAs (Gamalinda et al. 2014; Ohmayer et al. 2015).

Among the very early assembly factors are seven potential RNA-dependent ATPases/RNA helicases/DEAD-box proteins: Dbp2, Dbp3, Dbp6, Dbp7 and Dbp9, Prp43, Mak5 (Bond et al. 2001; Weaver et al. 1997; Daugeron and Linder 1998; Daugeron et al. 2001; Bohnsack et al. 2009; Leeds et al. 2006; Zagulski et al. 2003). Dbp6 forms an RNase-resistant subcomplex with Npa1, Npa2, Rsa3, and rpL3 (Rosado et al. 2007). Assembly of these five r-proteins may form a lid over what becomes the 3'-end of 25S rRNA and/or 5'-end of 5.8S rRNA to protect them from exonucleases (Ohmayer et al. 2015). Many of these proteins also exhibit genetic or direct interactions and hence presumably assemble and/or function together (see Table 1). Very little is known about the role of these DEAD-box enzymes as remodelers of RNP architecture, as timers, or as checkpoints.

Our current understanding of these essential very early-acting r-proteins and assembly factors is mostly based on their depletion phenotype. However, depletion of some early assembly factors results in a specific block in cleavage at the ITS2 site. Many of these assembly factors exit preribosomes prior to or immediately after the cleavage in ITS2. Hence more careful mutational analysis of these assembly factors will be needed to understand their mechanism of action in very early or early 66S preribosomal intermediates and their potential contributions to processing of the ITS2 spacer sequence.

**Table 1. Assembly factors required for very early steps of 60S subunit assembly**

Name	Pre-rRNAs	Comments	Interactions with other 66S pre-ribosomal components	Reference
<a href="#">Rrp5</a>	35S to 27SB pre-rRNAs	N-terminal and C-terminal domains required for 27SA2 and 27SA3 pre-rRNA processing, respectively. Forms a sub-complex with Noc2 and Noc1	ITS1, 25S rRNA (CRAC) Mak21, Dbp9, Urb1, Noc2, Rix1, L1, L8, L3, L22, L23 (CoIP with Rrp5 post RNase treatment) Brx1 (PCA), Noc1 ( <i>in vitro</i> pull down), Noc2 ( <i>sl</i> , PCA), Rlp7 (PCA), Pwp1 (PCA)	(Eppens et al. 1999; Lamanna and Karbstein 2011; Lebaron et al. 2013; Hierlmeier et al. 2013; Tarassov et al. 2008; Merl et al. 2010)
Nop4	27SA <sub>2</sub> to 7S pre-rRNAs	4 RRM Nop4 cross-links to multiple sites on 25S rRNA and interacts with many 60S assembly factors in Y2H assay (see McCann and Baserga, 2015)	Domain II of 25S rRNA, domain linker adjacent to 3'-end of 5.8S rRNA (CRAC)  <i>nsa1</i> (dosage rescue), <i>nop1</i> ( <i>sl</i> )	(Granneman et al. 2011; Sun and John L Woolford 1997; Tarassov et al. 2008; Pratte et al. 2013; McCann et al. 2015)
Npa1 (Urb1)	27SA2 to 27SB pre-rRNAs		<i>dbp3</i> , <i>dbp7</i> , <i>dbp9</i> , <i>nop8</i> , <i>rsa3</i> , and <i>RPL3</i> ( <i>sl</i> ) Rsa3, Dbp6, Nop8 (Y2H)	(Rosado et al. 2007) (Dez et al. 2004a) McCann:2015bm}
Npa2 (Urb2)	35S to 27SB pre-rRNAs		Npa1, Dbp6, Nop8, and Rsa3 (CoIP with Npa2-TAP after RNase treatment) <i>dbp3</i> , <i>dbp7</i> , <i>dbp9</i> , <i>nop8</i> , <i>rsa3</i> , and <i>RPL3</i> ( <i>sl</i> ) Urb1, Dbp6, Rsa3 (Y2H)	(Rosado et al. 2007)
Nop8	CoIPs ITS2 containing pre-rRNAs.	Contains coiled coils and an RRM motif N-terminal half of Nop8 is important for its association with pre-ribosomal intermediates prior to processing of ITS2	<i>rsa3</i> , <i>dbp7</i> , <i>dbp9</i> , and <i>npa1</i> ( <i>sl</i> ) Nip7, Urb1 (Y2H and <i>in vitro</i> pull downs) Rrp6 (GST pull down) Dbp6 ( <i>sl</i> )	(Rosado et al. 2007)(Zanchin and Goldfarb 1999; Santos et al. 2011; la Cruz et al. 2004; McCann et al. 2015)

Rsa3			<i>dbp6, nop8, and rsa3</i> (sl) CoIPs with Npa2-TAP after RNase treatment Urb1, Urb2 (Y2H)	(la Cruz et al. 2004) (Rosado et al. 2007) (McCann et al. 2015)
<a href="#">Noc1 (Mak21)</a>	35S to 27SB pre-rRNAs	Forms a sub-complex with Noc2 and Rrp5	N-terminus of Rrp5 ( <i>in vitro</i> pull down) <i>noc2, noc3</i> (sl)	(Milkereit et al. 2001; Hierlmeier et al. 2013; Merl et al. 2010)
<a href="#">Noc2 (Rix3)</a>	35S to 7S pre-rRNAs	Forms a sub-complex with Noc2 and Rrp5	Noc1 ( <i>in vitro</i> pull down), <i>noc3</i> (sl), <i>noc1</i> (sl) Noc3 (co-purification after high salt washes, Y2H) Rrp1, Mak21, Noc3 (Y2H)	(Hierlmeier et al. 2013; Milkereit et al. 2001; Merl et al. 2010; Ohmayer et al. 2015; McCann et al. 2015)
Noc3	27S and 7S pre-rRNAs	Associated with later preribosomes than Noc1 (see Ref #2) RNA-binding protein	Noc2 (co-purification after high salt washes, Y2H)	(Milkereit et al. 2001)
Loc1	Present in Nop7-TAP and Rlp24-TAP particles	*decreased levels of 27SA2 pre-rRNA and 27SB pre-rRNAs	Interacts with many 60S assembly factors in Y2H assay (see McCann and Baserga, 2015)	(Castle et al. 2010; McCann et al. 2015; Saveanu et al. 2003)
Cbf5	Present in Nop4, Nop15, Cic1 and Mak11-TAP particles	Pseudouridine synthase catalytic subunit of box H/ACA snoRNPs Depletion also causes accumulation of 27SB and 7S re-rRNAs		(Lafontaine et al. 1998) (Saveanu et al. 2007; Nissan et al. 2002; Oeffinger and Tollervy 2003) Ed Horsey (Personal Communication)
Ssf1	27SA2 to 27SB and some 7S pre-RNAs	Brix domain. Paralog of Ssf2. Proposed to prevent premature cleavage at C2 site.	Rrp15 (Y2H)	(Fatica et al. 2002) {McCann:2015bm}
Ssf2		Brix domain, Paralog of Ssf1	Rrp15 (Y2H)	(Fatica et al. 2002) {McCann:2015bm}
Rrp14	Pre-66S rRNAs. Some amount of 35S pre-rRNA	Depletion blocks formation of 27SA <sub>2</sub> pre-rRNA and maturation of 27SB pre-rRNA	Loc1, Ebp2 (Y2H)	(Oeffinger et al. 2007) {McCann:2015bm}

Rrp15	27SA and B pre-rRNAs, some amount of 7S pre-rRNA	HEAT repeats	Ssf1, Ssf2, Mak11 (Y2H)	(MARCHIS et al. 2005){McCann:2015bm}
Mak16		Modest decrease in 27SA <sub>2</sub> pre-rRNA formation, and in stability of 27SB pre-rRNA	Rpf1, Dbp9, Noc2 (Y2H)	(Pellett and Tracy 2006; McCann et al. 2015)
Dbp2		DEAD-box RNA helicase. Helicase activity is important for assembly.		(Bernstein et al. 2006; Bond et al. 2001)
Dbp3		DEAD-box RNA helicase. Helicase activity is important for assembly.	<i>npa1, npa2 (sl), spb4 (sl)</i>	(Weaver et al. 1997; Bernstein et al. 2006)
Dbp6		DEAD-box RNA helicase. Helicase activity is important for assembly.	<i>dbp7 (se)</i> , Dbp9 (Y2H)	(Daugeron and Linder 1998) (Daugeron et al. 2001)
Dbp7		DEAD-box RNA helicase. Helicase activity is important for assembly.	<i>dbp6 (se)</i>	(Daugeron et al. 2001) (Bernstein et al. 2006)
Dbp9		DEAD-box RNA helicase. Helicase activity is important for assembly.	Dbp6 (Y2H), Mak16 (CoIP)	(Daugeron et al. 2001) (Bernstein et al. 2006; McCann et al. 2015)
Prp43	35S, 27SA and 7S pre-rRNAs	DEAD-box RNA helicase Additional role in 40S subunit assembly	Helices 39, 40, 23, 24, 34, and 83 in 25S rRNA Nop15 (pull down from yeast lysate)	(Combs et al. 2006; Leeds et al. 2006; Bohnsack et al. 2009; McCann et al. 2015)
Mak5	Copurifies with Nop7-TAP, Ssf1-TAP and Nsa1-TAP	DEAD-box RNA helicase. Helicase activity is important for assembly.  A functional interaction cluster is formed by Mak5, Ebp2, Nop16, and Rpf1	<i>ebp2 (sl), nop16(sl), rpf1(sl), rpL14(sl)</i> Rpf1 (pull down from yeast lysate) <i>nsa1 (sl)</i>	(Zagulski et al. 2003; Bernstein et al. 2006; Pratte et al. 2013; McCann et al. 2015)

Yeast two-hybrid interactions are denoted by Y2H.

Synthetic lethal or synthetic enhancement effects are indicated by *sl* and *se*, respectively.

### 1.2.2 Early steps: processing of ITS1 in 27SA<sub>3</sub> pre-rRNA to generate 27SB<sub>S</sub> pre-rRNA

Preribosomes containing 27SA<sub>2</sub> pre-rRNA can undergo maturation via two exclusive paths to remove the remaining portion of the ITS1 spacer (Figure 5): (1) The 27SA<sub>2</sub> pre-rRNA can undergo direct endonucleolytic cleavage by an unknown endonuclease to form 27SB<sub>L</sub> pre-rRNA (minor pathway, ~15%), or (2) RNase MRP can cleave the 27SA<sub>2</sub> pre-rRNA at the A<sub>3</sub> site, generating the 27SA<sub>3</sub> pre-rRNA. The 5' most sequences of 27SA<sub>3</sub> pre-rRNA are processed by the 5'-3' exonucleases Rat1, Rrp17 or Xrn1 to form 27SB<sub>S</sub> pre-rRNA. The 27SB<sub>S</sub> and 27SB<sub>L</sub> pre-rRNAs differ in length at their 5'-end by a few nucleotides. Interestingly, this 5'-end is conserved across all eukaryotes, but the functional significance of these multiple forms remains unknown.

R-proteins required for formation of 27SB pre-rRNA from 27SA<sub>3</sub> pre-rRNA localize to domain I of 25S rRNA (L4, L6, L8, L13, and L8), close to the proximal stem from which ITS2 emerges, or to the domain II/VI interface close to the ITS1 sequence removed in this step (L7, L14, L16, L20, L32, L33) (Figure 11A). We believe that the processing of the ITS1 spacer sequence requires stabilization of domains I and II/VI of 25S rRNA, since the association of r-proteins that bind to these domains is strengthened first. Depletion of r-proteins affecting downstream events does not affect association of early associating r-proteins (Pöll et al. 2009; Jakovljevic et al. 2012; Ohmayer et al. 2013; Gamalinda et al. 2014).

Figure 11

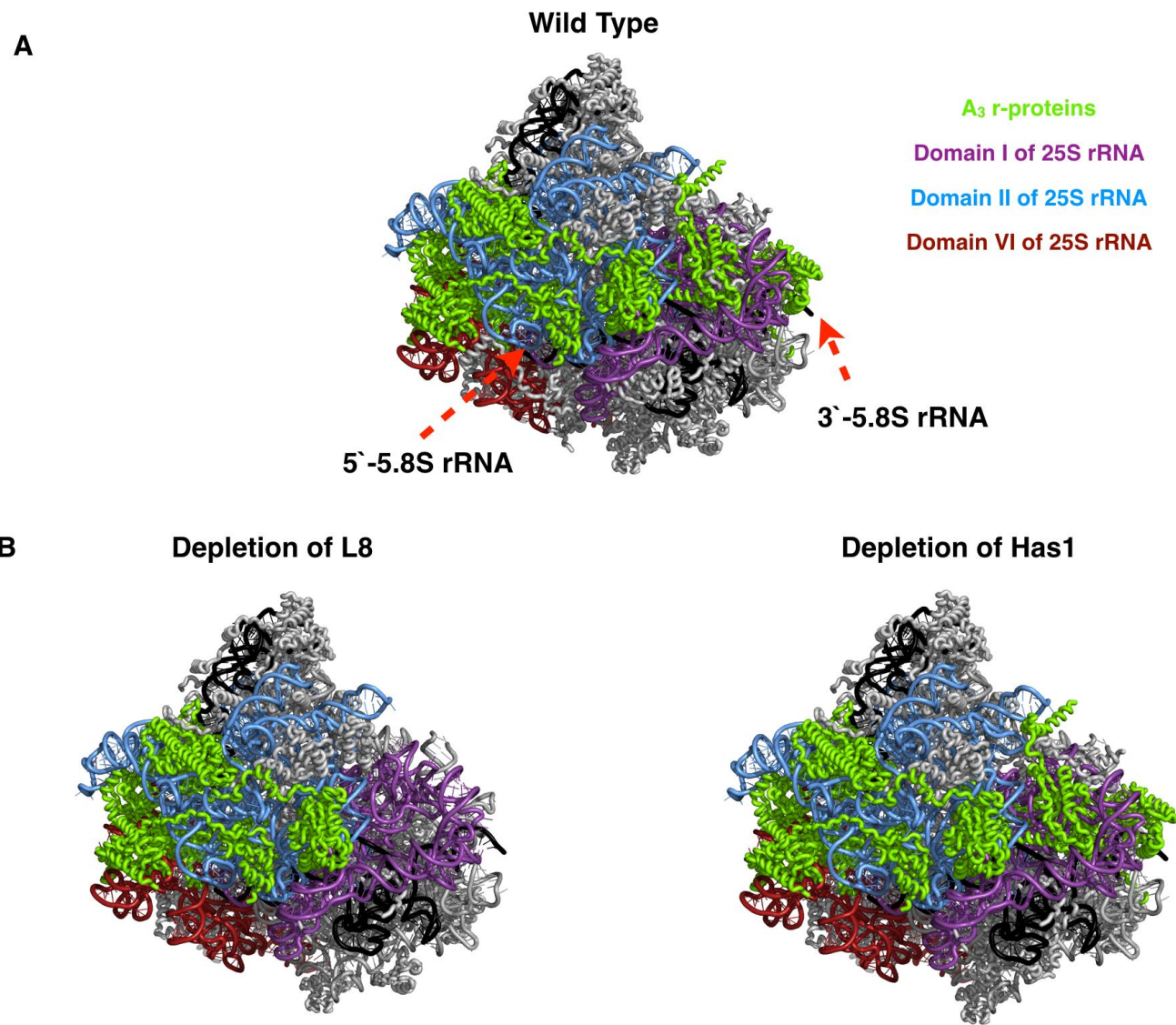


**Figure 11: Ribosomal proteins (green) required for processing of the 27SA<sub>3</sub> pre-rRNA cluster in the domain I (purple), and domain II/VI (blue/maroon) neighborhoods.** Depletion A<sub>3</sub> factors L8 or Has1 affects the association of r-proteins binding to these domains of rRNA. Not all domain I-binding r-proteins are absent in the Has1 depletion mutant (Jakovljevic et al. 2012)(Dembowski et al. 2013a). This places Has1 downstream of L8 in the functional hierarchy of A<sub>3</sub> mutants.

In addition to the r-proteins mentioned above, removal of ITS1 from 27SA<sub>3</sub> pre-rRNA to form 27SB<sub>L</sub> pre-rRNA also requires 13 ‘A<sub>3</sub>’ assembly factors: Rpf1, Ebp2, Brx1, Nop12, Pwp1, Nop7, Ytm1, Rlp7, Nop15, Cic1/Nsa3, Rrp1, Drs1, and Has1. Ebp2, Brx1, Nop12, and Pwp1 form a subcomplex with L8 and L15, which can be isolated from cells. L8 and L15 are located on the solvent-interface of the 60S subunit near the proximal stem. Overexpression of domain I/5.8S rRNA binding proteins L34 and L36 can suppress the growth defects of *ebp2* mutants (Shimoji et al. 2012; Wan et al. 2015; 2014). Several observations indicated that the A<sub>3</sub> factors, Ytm1, Erb1, Nop7, Nop15, Rlp7, and Cic1, together with the DEAD-box proteins Has1 and Drs1, assemble near L8, L13, L15, L36, and the proximal stem and ITS2 of pre-rRNA: (1) Nop15, Rlp7, and Cic1 bind to adjacent sites in ITS2 and are required for structuring of ITS2 spacer sequences (Granneman et al. 2011; Wu et al. 2016, submitted). (2) Nop7, Erb1, and Ytm1 form a stable subcomplex that potentially functions as a hub of protein-protein and protein-RNA interactions. Erb1 and Nop7 cross-link to domains I and I/III of 25S rRNA, respectively (Miles et al. 2005; Granneman et al. 2011). (3) Drs1 can be isolated as a subcomplex with the Nop7-subcomplex (Biedka et al. 2016, submitted; Kellner et al. 2015). (4) There is also evidence suggesting that Has1 interacts directly with the Nop7-subcomplex (Thoms et al. 2015b). Together, these observations suggested that the A<sub>3</sub> r-proteins and assembly factors form a tight molecular interaction network. This model was proven to be true by the recently acquired near-atomic resolution cryo-EM structures of pre-ribosomes containing Nop7, Nop15, Cic1, and Rlp7 (Figure 12).

The assembly of the A<sub>3</sub> factors into preribosomes is hierarchical (Figure 13). Pwp1, Ebp2 and L8 are required for the assembly of Nop7, Erb1, Ytm1, Nop15, Rlp7, Cic1, and Has1 (Jakovljevic et al. 2012; Shimoji et al. 2012; Talkish et al. 2014). Nop7, Erb1, Ytm1, Rlp7, Nop15, and Cic1 are mutually interdependent for their assembly and are necessary for the association of Drs1 and Has1, but not the L8-subcomplex (Miles et al. 2005; Sahasranaman et al. 2011; Tang et al. 2008; Dembowski et al. 2013a; Talkish et al. 2014; Jakovljevic et al. 2012; Thoms et al. 2015a; Wegrecki et al. 2015). Upon depletion of Has1 or Drs1, all other A<sub>3</sub> factors associate stably with preribosomes, placing them as the last assembly factors required for 27SA<sub>2</sub> pre-rRNA processing. The protein composition of pre-ribosomes in the Rrp1 depletion mutant closely resembles that when Has1 is depleted, based on visual inspection (Dembowski et al. 2013a; Sahasranaman et al. 2011; Horsey et al. 2004). Hence, Rpf1 is placed alongside Has1 and Drs1 in the hierarchy pathway (Figure 12A). The effects of these mutations on 27SA<sub>3</sub> pre-rRNA processing are not due to failure to recruit the exonucleases Rrp17, Rat1, or Xrn1 to preribosomes, since these enzymes are present in preribosomes in A<sub>3</sub> mutants (Sahasranaman et al. 2011).

Depletion of L8, Rlp7, or Has1 affects the stable association of r-proteins L17, L35, and L37 that bind to the helices formed between 5.8S rRNA and 25S rRNA. ITS1 and ITS2 emerge from the two ends of these helices (Figure 11B) (Jakovljevic et al. 2012; Dembowski et al. 2013a). Thus, processing of 27SA<sub>3</sub> pre-rRNA might require structuring of 5.8S rRNA and association of r-proteins with 5.8S rRNA/domain I of 25S

rRNA. The absence of these proteins could greatly destabilize the RNP, resulting in the rapid turnover of pre-rRNAs observed in A<sub>3</sub> mutants.

Thus, our favorite explanation for the ribosome assembly defects upon depletion of A<sub>3</sub> assembly factors or r-proteins is that the presence of these proteins is required to make a preribosomal particle stable enough to undergo A<sub>3</sub> processing. Because these proteins form a tight protein-protein and protein-RNA network (Figure 13B), removing one of the components in the network causes all others to fail to stably assemble, consequently causing these particles to turn over. In addition to Has1 and Drs1, most DEAD-box helicases functioning in the previous step are also present in preribosomes blocked in ITS1 processing. Hence more careful analysis will be needed to further dissect the molecular network underlying processing of ITS1. Also, many of the A<sub>3</sub> factors remain associated with preribosomes until a subsequent major remodeling step releases them. Therefore, these proteins could have additional functions in 60S ribosomal subunit assembly. A major part of my work was aimed at transitioning from assaying depletion phenotypes, which suffer from the shortcoming of strongly affecting multiple network interactions, to investigating effects of more subtle mutations, which might help us to better understand the importance of specific intermolecular interactions in 60S subunit assembly.

Figure 12

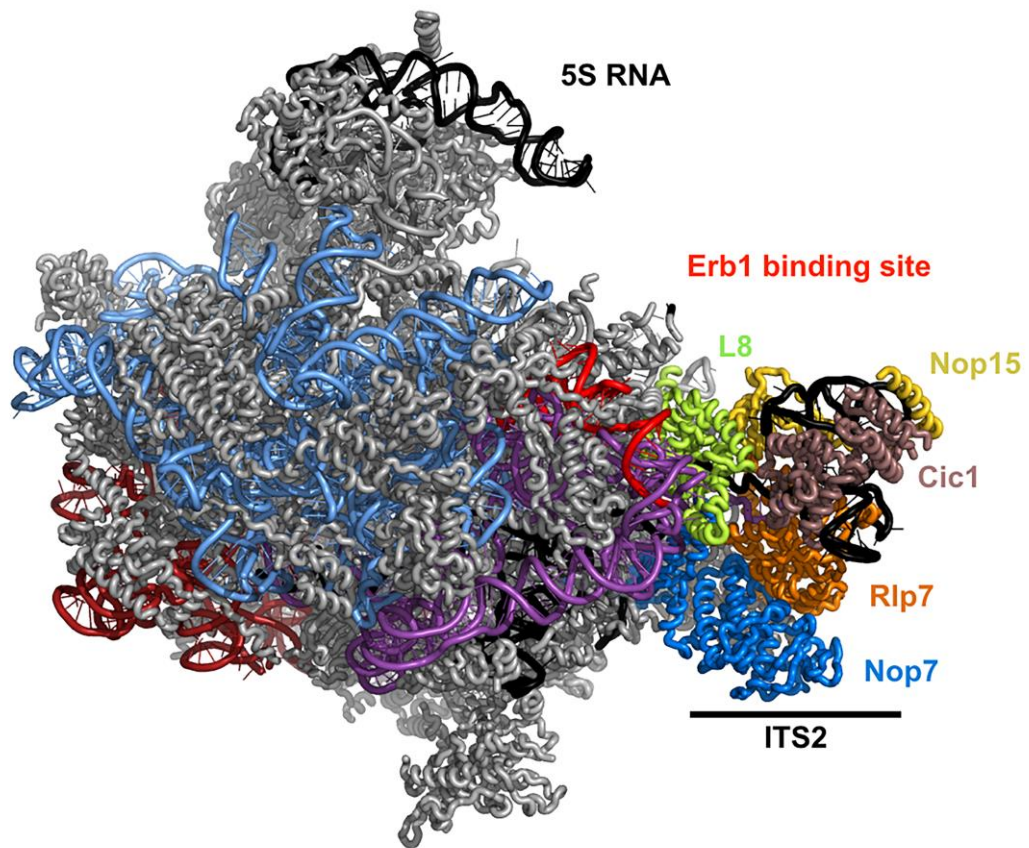


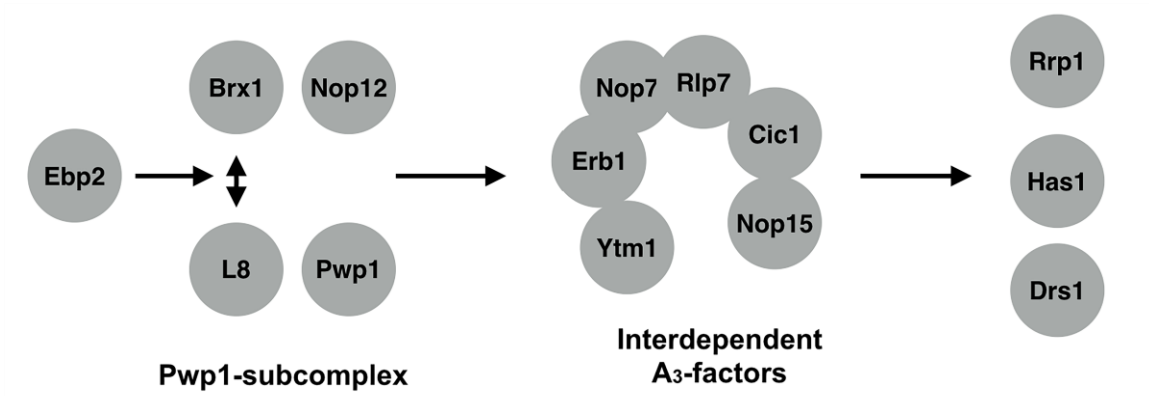
**Figure 12. Direct interactions between the interdependent A<sub>3</sub> assembly factors.**

Shown is the 3A° cryo-EM structure of 66S preribosomes. The interdependent A<sub>3</sub> factors Nop7, Rlp7, Cic1, Nop15, and L8 form a functional cluster around ITS2, adjacent to domain I (violet) of 25S rRNA. Nop7 forms a heterotrimeric subcomplex with Erb1 and Ytm1 (Miller et al. 2003). The UV cross-link site of Erb1 on rRNA is shown in red (Granneman et al. 2011). Domains II/VI of 25S rRNA are also shown in light blue and maroon colors, respectively.

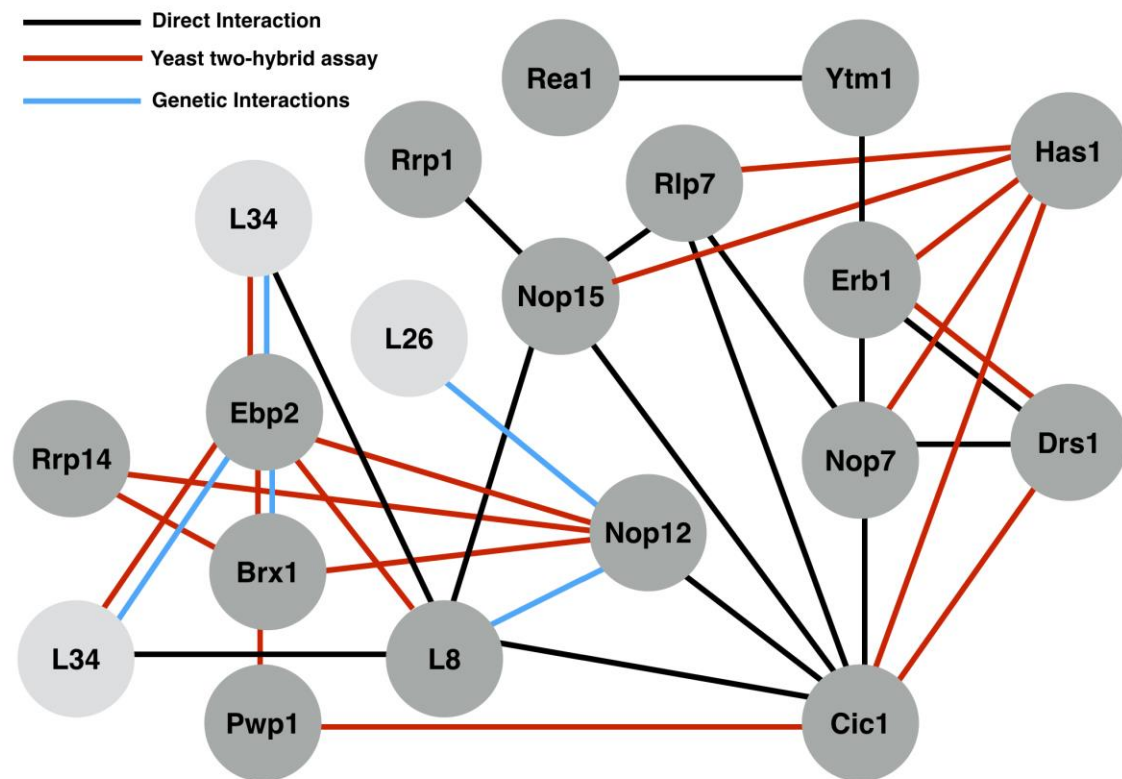
(Pre-ribosome structure: Wu et al. 2016, submitted)

Figure 13.

A



B



**Figure 13. A<sub>3</sub> factors – hierarchy of assembly and interactions.** (A) The hierarchy for association of assembly factors involved in 27SA<sub>3</sub> pre-rRNA processing. (B) The molecular interaction network formed by A<sub>3</sub> assembly factors. If there are direction interactions between two proteins, yeast two-hybrid or genetic interactions are not indicated.

**Table 2. Assembly factors involved in processing of the ITS1 spacer in 27SA<sub>3</sub> pre-rRNA**

Name	Comments	Pre-rRNA CoIP	Interactions with other 66S pre-ribosomal components	Reference
Rrp1		27SA <sub>2</sub> , 27SA <sub>3</sub> , 27SB, 25.5S and 7S pre-rRNAs	Nop15 (Y2H)	(Fabian and Hopper 1987; Horsey et al. 2004; Sahasranaman et al. 2011; McCann et al. 2015)
Pwp1	Non-essential under standard growth conditions. Component of the Pwp1- subcomplex	35S, 27SA <sub>2</sub> , 27SA <sub>3</sub> , and 7S pre-rRNAs	Nop12, Cic1, Brx1 (Y2H), Pwp1- subcomplex (Ebp2, Brx1, Nop12, L8 and Pwp1)	(Talkish et al. 2014; Shimoji et al. 2012)
Ebp2		35S, 27SA <sub>2</sub> , 27SA <sub>3</sub> , and 7S pre-rRNAs	Brx1, Pwp1, Mak5, L8, Rrp14, Nop12 (Y2H) <i>brx1</i> , <i>rpL34</i> , and <i>rpL36</i> ( <i>sl</i> )	(Shimoji et al. 2012)
Brx1	Sigma(70)-like RNA binding motifs	35S, 27SA <sub>2</sub> , 27SA <sub>3</sub> , and 7S pre-rRNAs	<i>ebp2</i> ( <i>se</i> ), Nop12, Ebp2, and Rrp14 (Y2H)	(Shimoji et al. 2012)
Nop12	Non-essential under standard growth conditions	35S, 27SA <sub>2</sub> , 27SA <sub>3</sub> , and 7S pre-rRNAs	Cic1, Brx1, Ebp2 (Y2H)	(Talkish et al. 2014; Shimoji et al. 2012)
Cic1 (Nsa3)	R-protein L1 domain	27SA <sub>2</sub> , 27SA <sub>3</sub> , and 7S pre-rRNAs	Nop12, Pwp1, Drs1 (Y2H), Nop15 (Cryo- EM)	(Jäger et al. 2001; Fatica et al. 2003; McCann et al. 2015) (Dembowski et al. 2013b; Babiano et al. 2013; Sahasranaman et al. 2011; Dembowski et al. 2013a; Wu et al. 2016, submitted)
Rlp7	Similar to r-protein L7, but its role as place holder has been ruled out	35S, 27SA <sub>2</sub> , 27SA <sub>3</sub> , 7S pre-rRNAs	Cic1, Nop15, and Nop7 (Cryo-EM) CoIPs Erb1 and Nop15 after high salt wash, Has1, Nop15 (Y2H)	(Oeffinger and Tollervey 2003; Dembowski et al. 2013a; Wu et al. 2016, submitted)
Nop15	RNA recognition motif	27SA <sub>2</sub> , 27SA <sub>3</sub> , 27SB and 7S pre-rRNAs	Rlp7, Cic1, L8, Nop7 (cryo-EM), Has1 (Y2H)	(Pestov et al. 2001; Miles et al. 2005; McCann et al. 2015; Tang et al. 2008)
Erb1	WD40 repeats	35S, 27SA <sub>2</sub> , 27SA <sub>3</sub> , 27SB and 7S pre- rRNAs	Ytm1 (Y2H, <i>in vitro</i> pull down), Nop7 ( <i>in vitro</i> pull down), Has1 and Drs1 (yeast two-hybrid)	(Miles et al. 2005; Baßler et al. 2010; Sahasranaman et al. 2011; Thoms et al. 2015b; Tang et al. 2008)
Ytm1	WD40 repeats	35S, 27SA <sub>2</sub> , 27SA <sub>3</sub> , 27SB and 7S pre- rRNAs	Erb1 (Y2H, <i>in vitro</i> pull down), Rea1 (Y2H, genetic interactions)	(Ripmaster et al. 1993; Oeffinger et al. 2002; Adams et al. 2002a; Miles et al. 2005; Tang et al.
Nop7 (Yph1)	BRCT domains	35S, 27SA <sub>2</sub> , 27SA <sub>3</sub> , and 7S pre-rRNAs	Erb1, Rlp7, Cic1, L8 (cryo-EM), <i>nog1</i> (DR), <i>rlp25</i> ( <i>sl</i> )	

Has1	DEAD-box RNA helicase. Additional roles in 40S subunit assembly.	5S, 27SA <sub>2</sub> , 27SA <sub>3</sub> , 27SB, 7S pre-rRNAs	Rlp7, Nop15, Erb1, Nop7, Drs1 (Y2H)	2008; Granneman et al. 2011; Wu et al. 2016, submitted; Honma et al. 2006; Tang et al. 2008)
Drs1	DEAD-box RNA helicase	-	Nop7-subcomplex ( <i>in vitro</i> pull down), <i>nop7(sl)</i> Erb1 (Y2H), Cic1 (Y2H)	(Dembowski et al. 2013a; Kathleen L McCann 2013)
Rrp17, Rat1, Xrn1	5'-3' - RNA processing enzymes	-	-	(Adams et al. 2002b), Talkish J. (Personal Communication), (McCann et al. 2015) (Henry et al. 1994; Sahasranaman et al. 2011; Oeffinger et al. 2009)

Y2H – yeast two-hybrid

*sl* – synthetic lethal

DR – dosage rescue

Same color indicates subcomplex formation

### **1.2.3 Middle and late steps involving cleavage and processing of the ITS2 spacer**

#### **The removal of ITS2 spacer is performed in multiple steps**

ITS2 is the last spacer to be removed during 60S ribosomal subunit assembly. The cleavage and processing events required for removal of ITS2 are discussed in detail below, since my research focused on understanding the mechanistic details triggering these processes in the pre-ribosome (Figure 14).

#### **Cleavage of the ITS2 Spacer in 27SB pre-rRNA to generate 7S and 25.5S pre-rRNAs**

Removal of ITS2 begins with endonucleolytic cleavage at site C2 by Las1 (Castle et al. 2013; Gasse et al. 2015; Schillewaert et al. 2012). Fifteen assembly factors (referred to as 'B' factors) and 11 r-proteins are required for initiating the C2 cleavage (Woolford and Baserga 2013; Gamalinda et al. 2014). Upon depletion of any of these proteins, 27SB pre-rRNAs fail to undergo cleavage in ITS2 to form 25.5S and 7S pre-rRNAs. The 27SB pre-rRNA containing ITS2 is the longest-lived pre-rRNA, indicating that complex remodeling of RNP might be needed prior to ITS2 cleavage.

#### **The concerted action of multiple nucleases and the exosome remove the 5`- and 3`- ends of the ITS2 spacer during pre-rRNA processing**

Endonucleolytic cleavage at the C<sub>2</sub> site generates a 5`-OH at the end of 25.5S pre-rRNA and a 2`, 3`- cyclic phosphate at the 3`-end of 7S pre-rRNA. The 5`-OH on 25.5S pre-rRNA is phosphorylated by the Grc3 kinase, rendering it a proper substrate of the

Rat1-Rai1 exonuclease (Gasse et al. 2015; Schillewaert et al. 2012; Thomson and Tollervey 2010a). The 5'-end of 25.5S pre-rRNA then is processed by Rat1-Rai1 exonucleases (Fang et al. 2005; Gasse et al. 2015; Allmang et al. 2000). The exosomal components for 7S pre-rRNA processing are recruited to their site of action by assembly factors Nop53, Nop8, and Rix7, which are located close to ITS2 (Granato et al. 2008; Santos et al. 2011; Yoshikatsu et al. 2015; Hiraishi et al. 2015; Thoms et al. 2015c). Eleven assembly factors and four r-proteins are required for the processing of 3'-end of ITS2 to convert 7S pre-rRNA into 6S pre-rRNA (Woolford and Baserga 2013; Gamalinda et al. 2014). Depletion of any one of these proteins causes an accumulation of both 27SB and 7S pre-rRNAs, which indicates that they may also be important for ITS2 cleavage, and/or that these steps are somehow coupled to each other.

The final steps in ITS2 pre-rRNA processing are performed by the nucleases Rex1/Reh1 and Ngl2 in a two-step process (van Hoof et al. 2000; Thomson and Tollervey 2010a; Thoms et al. 2015c).

Figure 14

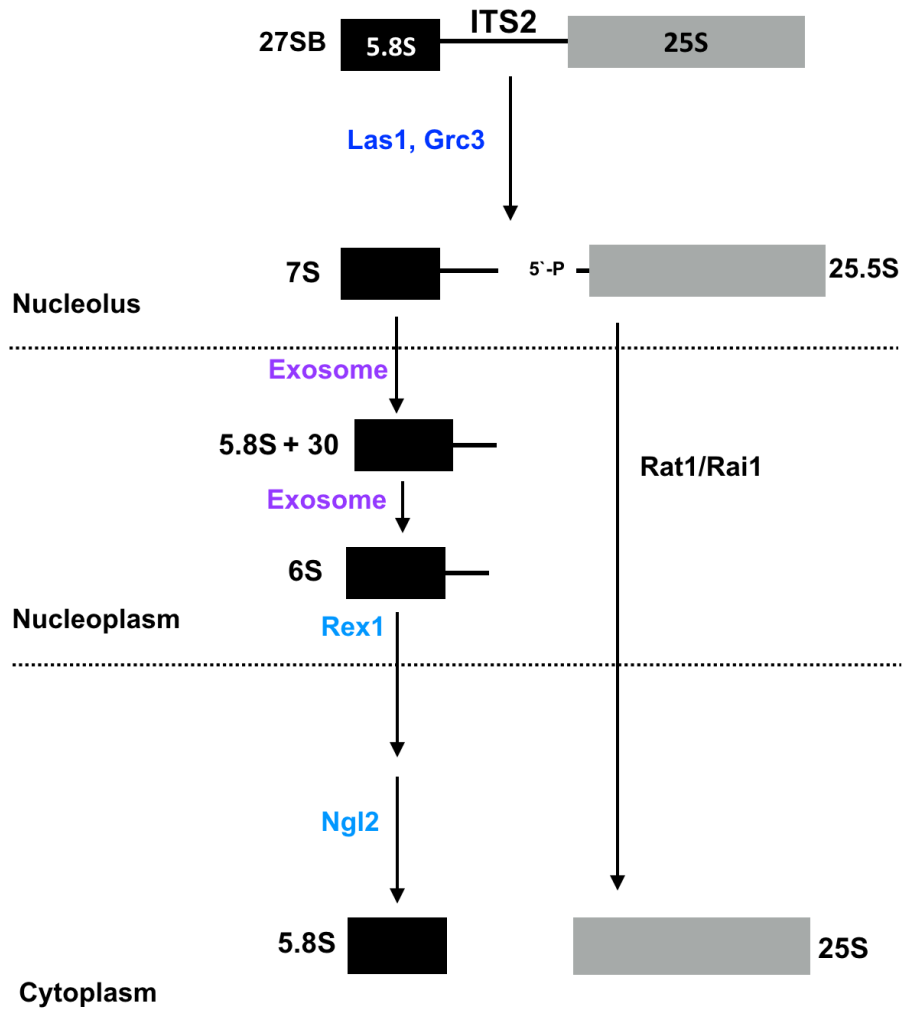
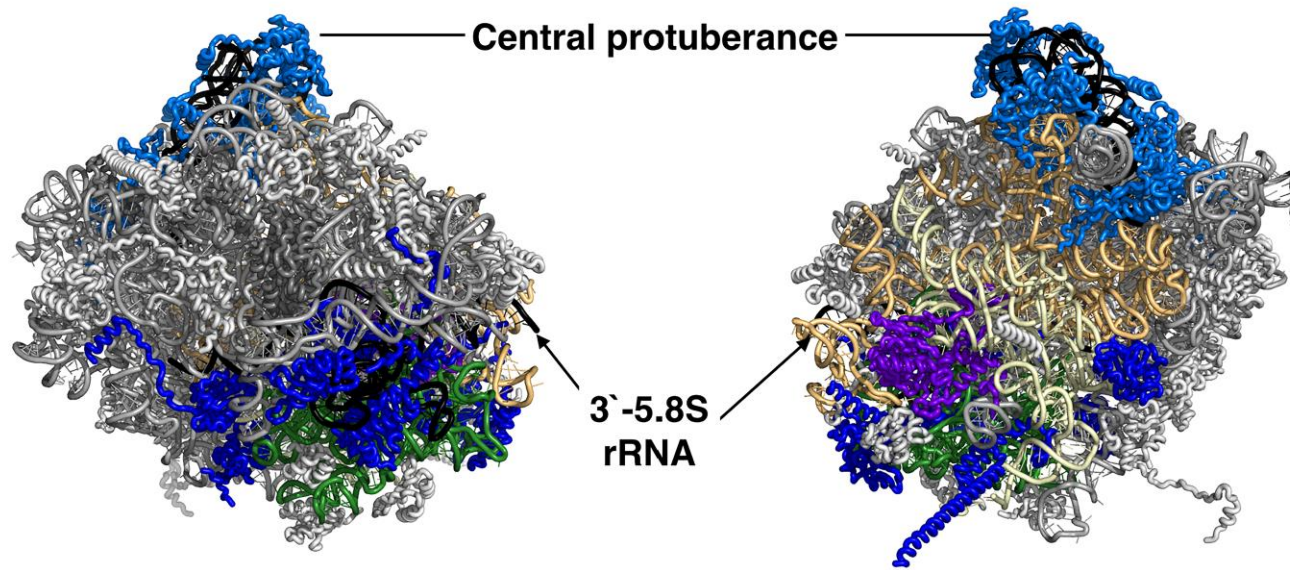


**Figure 14. Multistep process for removal of the ITS2 spacer during 60S ribosomal subunit assembly.** Removal of ITS2 is initiated by the cleavage at the C<sub>2</sub> site by the endonuclease Las1. The action of Las1 generates the 3'-end of 7S pre-rRNA and the 5'-OH end of 25.5S pre-rRNA. Multiple nucleases process the 5'- and 3'-ends of ITS2 to generate the 5'- and 3'-ends of mature 25S and 5.8S rRNAs, respectively.

### **R-proteins required for removal of ITS2 spacer**

The r-proteins required for ITS2 cleavage and processing localize to distinct neighborhoods in the structure of 60S subunits. (Figure 15) (A) The r-proteins required for ITS2 cleavage, namely L9, L17, L23, L25, L26, L27, L31, L34, L35, and L37, bind to domain III or the domain III/IV interface, with the exception of L9 and L23 that bind predominantly to domain V of 25S rRNA. Consequently, we believe that the RNA folding in domains III and V adjacent to ITS2 is required to initiate cleavage at ITS2. (B) The r-proteins L2 and L43 required for 7S pre-rRNA processing also bind to the interface of domains III/IV/V, indicating that the ITS2 processing steps require proper folding of 25S rRNA domains III, IV and V. The non-essential r-protein L39 that binds to 5.8S rRNA is also required for ITS2 pre-rRNA processing under restrictive conditions for cell growth. (C) In the nucleus, r-proteins L21 and L28 that are required for processing of 6S pre-rRNA bind to the domain II/V interface and adjacent to the central protuberance, along with r-proteins L5, and L11. Furthermore, 6S pre-rRNA processing events in the cytoplasm also require cytoplasmic r-proteins L40 and L10. (Pöll et al. 2009; Gamalinda et al. 2014; 2013; Babiano and la Cruz 2010)

Figure 15



Step	Phenotype	r-proteins
ITS2 Cleavage	27SB pre-rRNA accumulates and 7S pre-rRNA is not formed	L9, L17, L19, L23, L25, L26, L27, L31, L34, L35, and L37
ITS2 Processing (and cleavage??)	7S and 27SB pre-rRNA accumulates, 6S pre-rRNA is not formed	L2, L43
ITS2 Processing - Step 2	6S pre-rRNA accumulates	L21, L28, L5, L11, L10, L40

**Figure 15. Location of r-proteins required for ITS2 cleavage and processing in 60S subunits.** The r-proteins required for removal of the ITS2 spacer fall into three categories, as evidenced by effects of their depletion on the pre-rRNA processing pathway. The 3'-end of 5.8S rRNA formed by ITS2 processing is also shown. The r-proteins required for successive steps of ITS2 removal cluster in domain III (green) of 25S rRNA on the solvent interface (left side), at the domain IV/V interface (yellow/light orange) on the subunit interface (right side), or around the central protuberance (containing 5S rRNA) in mature 60S subunits (5S rRNA is in black). R-proteins are color coded according to the effects of their depletion on pre-rRNA processing.

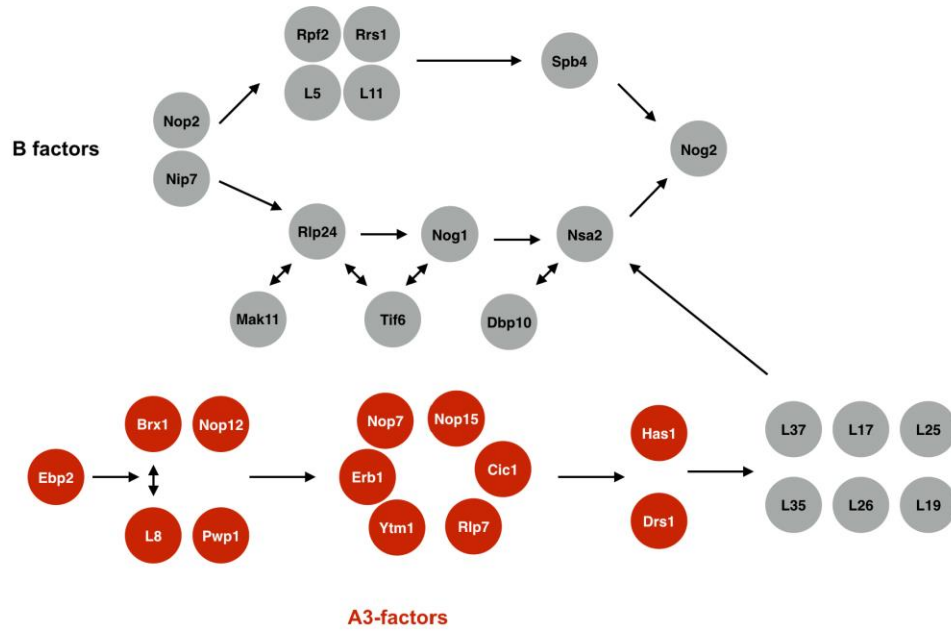
(PDB IDs: 3U5D, 3U5E)

### **Ribosome assembly events required for cleavage of the ITS2 spacer**

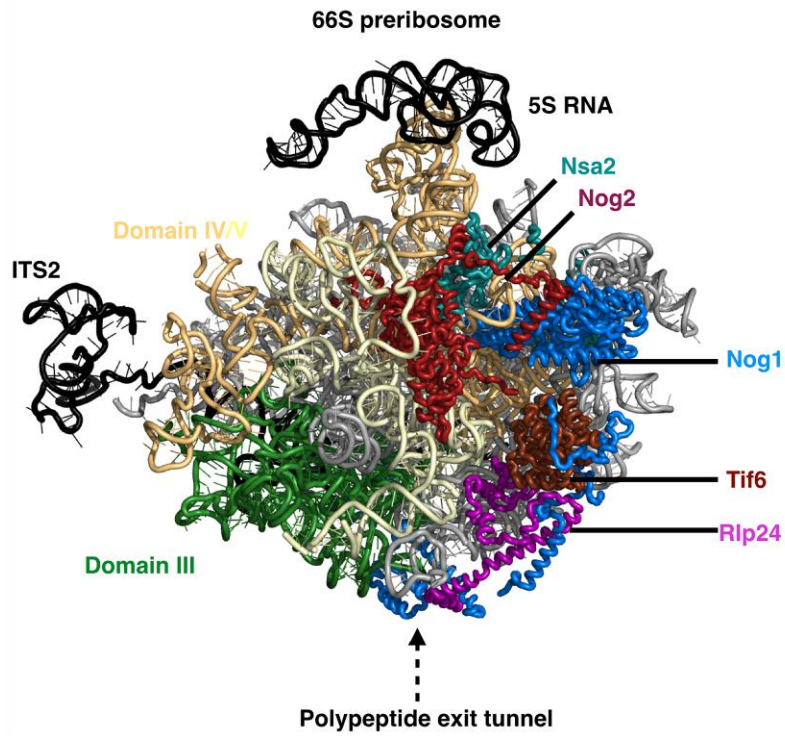
The concerted action of fifteen assembly factors and fifteen r-proteins is required to enable cleavage at the C<sub>2</sub> site on 27SB pre-rRNA (Table 4). The B assembly factors (B factors) enter early pre-ribosomal intermediates containing 27SA<sub>2</sub> pre-rRNA. Many B-factors form subcomplexes or exhibit direct physical or genetic interactions with each other. Previous work from our lab and the Fromont-Racine group showed that B-factors are recruited into preribosomes via two independent hierarchical recruitment pathways (Figure 16), converging in the recruitment of the GTPase Nog2 that binds to the peptidyl transferase center in domain V of 25S rRNA (Figure 16A). The recent determination of a cryo-EM structure revealed a structural basis for this hierarchical pattern in one part of the pathway (Figure 16). For example, assembly factors Nog1, Rlp24 and Tif6 form a tight complex in pre-ribosomes, thus explaining their interdependence (Figure 16B). Nsa2 and Nog2, downstream of Nog1, Rlp24 and Tif6, bind to domain V of 25S rRNA, thus suggesting a hierarchical restructuring of RNP architecture proceeding from domain III/polypeptide exit tunnel and domain V/peptidyl transferase center (Talkish et al. 2012; Saveanu et al. 2003).

Figure 16

A



B



**Figure 16. Hierarchy of association of B assembly factors with pre-ribosomes.** (A) Schematic of the hierarchical association of assembly factors required for 27B pre-rRNA processing. The hierarchical recruitment pathway for A<sub>3</sub> assembly factors (red) converges with the B-factor pathway at the Nsa2/Dbp10.node (B) This hierarchical recruitment is sequentially tightened from domain III (green) to the domain IV/V interface in 25S rRNA. Shown is the rRNA architecture of 66S pre-ribosomes, with a subset of the sequentially associating proteins, to highlight the parallels between the pathway shown in (A) and the organization of the binding sites of the assembly factors on pre-ribosomes (B).

(Structure: Wu et al. 2016, submitted)

We believe that the B assembly factors have an indirect role in ITS2 cleavage, because none of the known B factors binds directly to the ITS2 spacer RNA. Therefore, their role might be to establish an RNP architecture necessary to make the particles stable enough to get to this step, or to participate in a network of signaling within the macromolecular complex to initiate C2 cleavage (Figure 16). Interestingly, the A<sub>3</sub> factors Nop15, Cic1, Rlp7 and Nop12 bind directly or adjacent to the ITS2 spacer (Granneman et al. 2011; Dembowski et al. 2013a; Wu et al. 2016, submitted). Their roles in facilitating ITS2 cleavage are not yet fully understood.

Among the B-factors are a number of energy-dependent enzymes such as the GTPases Nog1 and Nog2, and DEAD-box helicases Spb4 and Dbp10 (Fuentes et al. 2007; Jensen et al. 2003; Kallstrom et al. 2003; CRUZ et al. 1998; Burger et al. 2000; Manikas 2014). The DEAD-box helicases Has1 and Drs1 that function in early steps are also required for ITS2 cleavage (Dembowski et al. 2013a; Biedka et al. 2016, submitted). Has1 is released from preribosomes prior to the entry of Nog2. In *has1* mutants defective in ATP hydrolysis, the B factors Nsa2 and Dbp10 that associate with domain V of 25S rRNA fail to stably associate with preribosomes (Bradatsch et al. 2012; Manikas 2014). Nsa2 and Dbp10 are required for the stable association of Nog2 with preribosomes (Talkish et al. 2012). This suggests that the association of Nog2 with preribosomes might require the action and exit of Has1. Depletion of r-proteins that bind to 5.8S rRNA/domain III of 25S rRNA also affect the stable association of Nsa2 with preribosomes, resulting in failure to cleave the ITS2 spacer (Figure 16A).

Collectively, the observations described above suggest that proper organization of domain III is required for the stable association of Nsa2, Dbp10 and other domain V binding assembly factors. The universally conserved GTPase Nog1 forms an interaction network starting near the 3'-end end of the 5.8S rRNA at the polypeptide exit tunnel and extends via the domain IV/V interface into the peptidyl transfer center. This network could potentially serve as the connecting link between domain III/IV organization and stable association of Nsa2. This model can be tested using mutagenesis to affect specific interactions or enzymatic activities of Nog1 (Figure 16B).

Cleavage at ITS2 also requires assembly of the 5S RNP to form the central protuberance. The 5S RNP contains 5S rRNA, r-proteins L5 and L11, and requires assembly factors Rrs1 and Rpf2 to associate with preribosomes (Zhang et al. 2007; Morita et al. 2002; Asano et al. 2015; Kharde et al. 2015; Asano et al. 2014). Depletion of any of the 5S RNP components blocks 27SB pre-rRNA processing (Dechampesme et al. 1999; Zhang et al. 2007). 5S RNP biogenesis begins with the interaction of a specialized importin called Syo1 with L5 and L11 in the cytoplasm to form a ternary complex. This ternary complex then binds to 5S rRNA (Calviño et al. 2015). Syo1 mimics the docking site of L11 on helix 84 of 25S rRNA. Thus, Syo1 might assess the folding of L11 before it is recruited into the nucleus. The Rpf2-Rrs1 complex interacts with 5S rRNA and recruits it to preribosomes. TFIIA associates with 5S rRNA at the same site as Rpf2 and potentially serves to block premature Rpf2-5S rRNA interaction (Madru et al. 2015). Interactions between Rpf2 and helices 80 and 87 of 25S rRNA are critical to recruitment of 5S RNP to preribosomes. Expression of the N-terminal portion of Rpf2 is dominant

negative, potentially because the 5S RNP fails to be integrated or stably associated with preribosomes. Further docking of the 5S RNP on domain V of 25S rRNA is mediated by contacts between L5, Rrs1 and Rpf2 and Rsa4, as well as the L11-helix 84 interaction. Cryo-EM of late pre-60S particles shows that the 5S RNA is assembled in a conformation that is rotated by 180° relative to its final conformation (Leidig et al. 2014) (Wu et al. 2016, submitted). We believe that this rearrangement happens after ITS2 cleavage, but before removal of ITS2, since preribosomal intermediates blocked at later stages of assembly contain 5S RNA in its pre-rotated state.

Las1 was recently identified as the endonuclease responsible for C2 cleavage. Las1 functions in concert with its interaction partner Grc3 kinase (Castle et al. 2013; Gasse et al. 2015; Schillewaert et al. 2012). How Las1 and Grc3 are recruited to the preribosomes and what triggers the cleavage at C2 site remain to be understood. Two potential candidates for the recruitment and activation of Las1 are the Ipi-subcomplex proteins and the exosome, since the mammalian homolog of Rix7 (Nvl2) shows direct interaction with the Ipi-subcomplex and Mrt4, an exosomal protein (Castle et al. 2012; 2013; Yoshikatsu et al. 2015; Nagahama et al. 2004; Hiraishi et al. 2015).

### **Processing of 7S pre-rRNA**

After the site C<sub>2</sub> is cleaved, the exosome removes ITS2 from 7S pre-rRNA to form the 5.8S + 30 pre-rRNA. 7S pre-rRNA is processed into 6S pre-rRNA by the enzymes Rex1 and Rex2 in the nucleus (Figure 14) (van Hoof et al. 2000; Allmang et al. 2000; FABER et al. 2002; Thomson and Tollervey 2010b; Dez et al. 2004b).

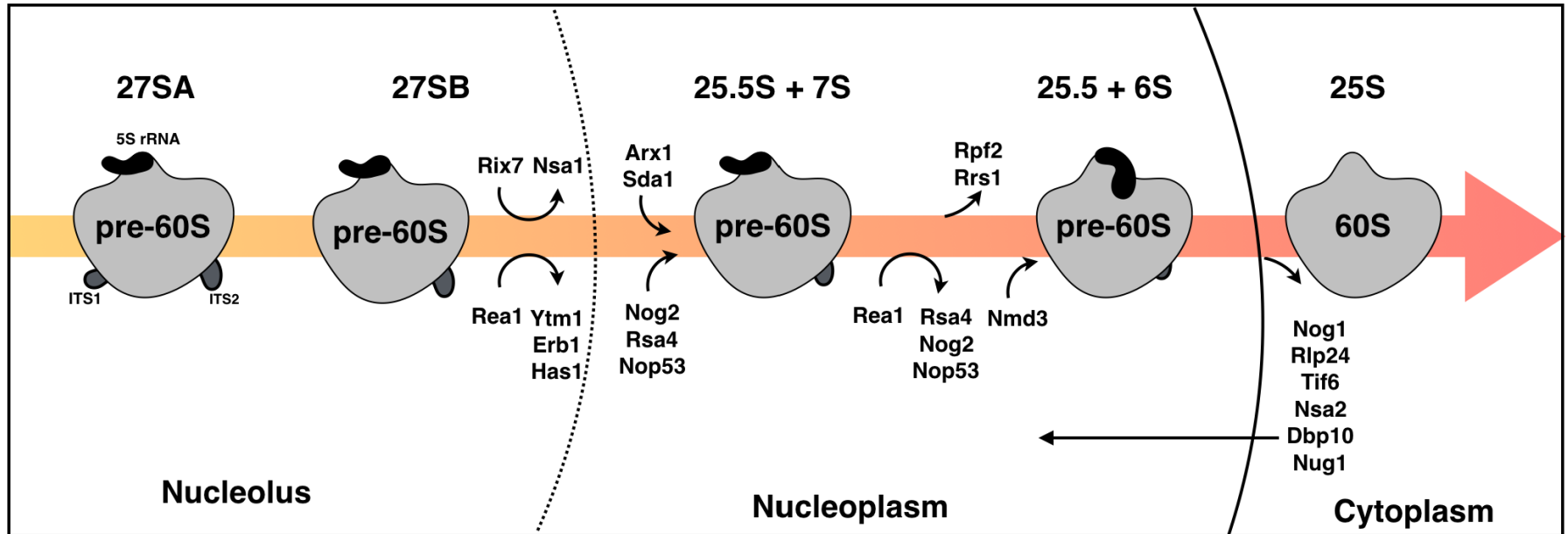
Preribosomes containing 6S pre-rRNA are then exported to the cytoplasm, where it is processed to mature 5.8S rRNA (FABER et al. 2002; Thomson and Tollervey 2010a).

Processing of 7S pre-rRNA requires nine assembly factors (Ipi1, Ipi2, Ipi3, Rsa4, Nog2, Nop53, Sda1, Nug1, and Rrp12) and six r-proteins (L5, L11, L2, L43, L21 and L28). The details of how the r-proteins facilitate late steps of 60S subunit assembly are discussed in Chapter 4.

### **Remodeling events during removal of the ITS2 spacer**

The 66S preribosomes undergo major changes in its composition or architecture during middle and late steps of 60S subunit assembly. These changes are initiated and/or mediated by the entry and exit of assembly factors at specific stages of ribosome maturation (Figure. 17).

Figure 17



Remodeling  
Events

Rea1-1  
Rix7

Rea1-2  
5S RNP Rotation

Drg1

**Figure 17. Remodeling events driving 60S subunit assembly**

### **Remodeling events facilitating cleavage at C2 site in the ITS2 spacer**

A major RNP remodeling event mediated by the AAA-ATPase Rea1 is required for ITS2 cleavage (Baßler et al. 2010). Mutants defective for interaction between Rea1 and Ytm1 cannot undergo cleavage of ITS2 (Baßler et al. 2010; Tang et al. 2008). Rea1-mediated removal of Erb1 and Ytm1 is accompanied by a marked reduction in the complexity of preribosomes (Baßler et al. 2010; Thoms et al. 2015b). Therefore, it is possible that the removal of other early acting assembly factors is initiated by the Rea1-mediated removal of Ytm1-Erb1. Association of assembly factors Nsa2, Dbp10, Nog2, Rsa4, Nop53 and Nug1 is most likely tightened after the Rea1-mediated release of Erb1 and Ytm1 (Salini Konikkat, unpublished). Nop53 binds at the domain I/III interface of 25S rRNA while the other five assembly factors bind to domain V of 25S rRNA (Manikas 2014; Wu et al. 2016, submitted) (2016), submitted) (2016), submitted). Collectively, these observations suggest that the Rea1-mediated removal of Erb1 and Ytm1 initiates a series of changes in preribosomes, culminating in cleavage of the ITS2 spacer in 27SB pre-rRNA.

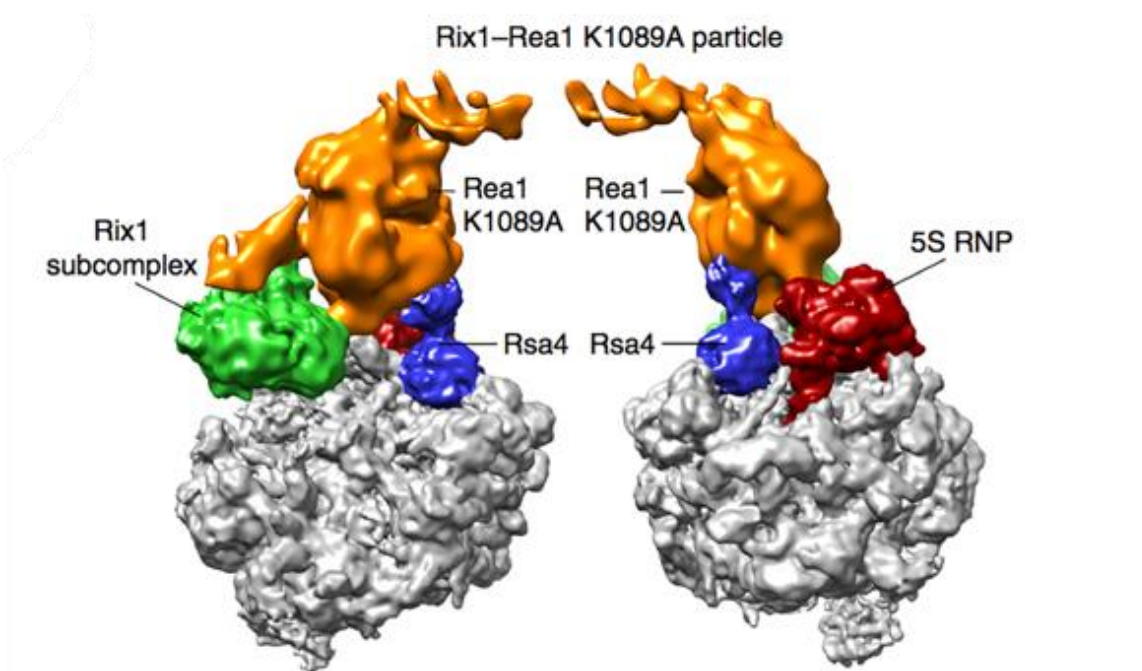
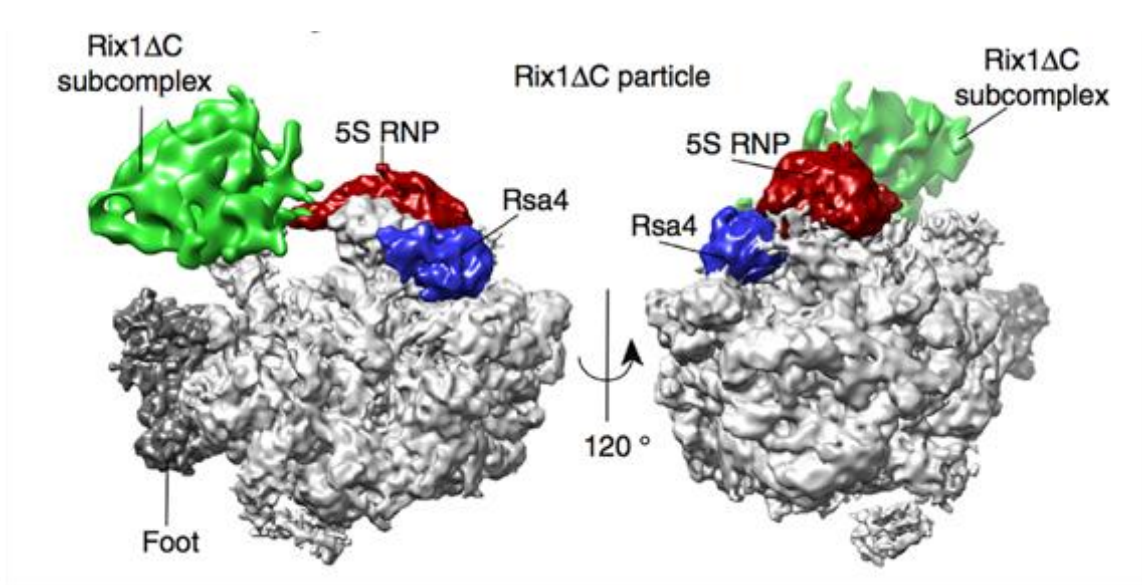
In addition to the above-mentioned NTPases, the AAA-ATPase Rix7 strips the assembly factor Nsa1 from preribosomes containing 27SB pre-rRNA (Kressler et al. 2008). The Rix7-Nsa1 interaction is necessary for removal of early assembly factors such as Rrp5, Noc1 and Rrp12. Rea1 and Rix7 mutants show a similar pre-rRNA processing phenotype as well as being unable to release early assembly factors (Gadal et al. 2001; Baßler et al. 2010). Therefore, it seems likely that the concerted action of these

two AAA-ATPases cannot be ignored. Further investigation is needed to understand the interaction network and roles of Rix7 in 60S subunit assembly.

### **Remodeling events during the processing of ITS2 spacer in 7S pre-rRNA**

Two major remodeling events are known to occur during the conversion of 7S pre-rRNA to 6S pre-rRNAs: (1) The 5S RNA undergoes a 180° rotation to attain its mature conformation (Leidig et al. 2014) and (2) the AAA-ATPase Rea1 mediates another remodeling event beginning with the stripping of Rsa4 from preribosomes. Rotation of 5S RNA to its mature conformation is blocked if Rea1 fails to associate with pre-ribosomes during late stages of assembly. ITS2 processing is also blocked in these mutants (Figure 18). In *real-* mutants that are defective in ATP binding and hydrolysis, 5S RNP undergoes rotation but fails to release Rsa4. (Galani et al. 2004; Barrio-Garcia et al. 2015). Our cryo-EM structures provide an excellent platform to design hypotheses for interaction networks driving late steps of 60S subunit assembly. There is an ongoing race between many ribosome biogenesis groups to dissect the players and mechanical underpinnings of these remodeling events.

Figure 18



(Barrio-Garcia et al. 2015)

**Figure 18. Two Roles of the AAA-ATPase Rea1 in late steps of 60S subunit assembly.** (A) Association of Rea1 with pre-ribosomes is required for 5S RNP rotation. In the *rix1ΔC* mutant, Rea1 fails to stably associate with pre-ribosomes and the 5S RNP remains in its premature unrotated conformation. (B) ATP binding and hydrolysis by Rea1 is required for removal of Rsa4 from pre-ribosomes, but not for 5S RNP rotation. Preribosomes in *real K1089A* mutants defective in ATP hydrolysis contain 5S RNP in its mature, rotated conformation, but also still contain Nog2 and Rsa4.

(PDB ID: 5FL8)

#### 1.2.4 Preparing for nuclear export

Preribosomes that have successfully completed assembly events in the nucleolus and the nucleoplasm are exported into the cytoplasm through the nuclear pore complex (NPC), in a RAN-GTP dependent fashion. (Kutay et al. 2003). Nuclear export of preribosomes is blocked when nuclear assembly is defective (Gleizes et al. 2001; Hurt et al. 1999; Stage-Zimmermann et al. 2000).

Preribosomes must be compact and bound to appropriate export factors to traverse the chemical milieu of the NPCs. Remodeling events prior to nuclear exit significantly reduce the complexity of pre-ribosomes, by releasing many nuclear assembly factors (reviewed in Nerurkar et al. 2015). Also, nuclear export requires association of the export factors Arx1-Alb1, Rrp12, Sda1, Bud20, Nmd3, Crm1, and MEx67/Mtr2 across the subunit interface of 66S preribosomes (Figure 19). These export factors coat the solvent-exposed RNA on the subunit interface (Greber et al. 2012; Bradatsch et al. 2007; Wu et al. 2016, submitted), and direct the preribosomes for nuclear export by direct or indirect interactions with the nucleoporins in the NPC. For example, Alb1/Arx1 and Mex67/Mrt2, Sda1 and Rrp12 direct the 66S preribosomes to the nuclear pore via direct interaction with FG-repeat containing nucleoporins lining the nuclear pores (Bradatsch et al. 2007; 2012; Oeffinger et al. 2004). Export factors do not associate with 66S preribosomes until late nucleoplasmic steps of maturation, preventing premature export into the cytoplasm (Altvater et al. 2012). In addition to the export factors, pre-ribosomes entering the cytoplasm also contain assembly factors Nog1, Rlp25, Tif6, Nug1, and Nsa2.

These assembly factors potentially aid to mask charges on pre-ribosomes, and are involved in functional proofreading steps in the cytoplasm.

Figure 19

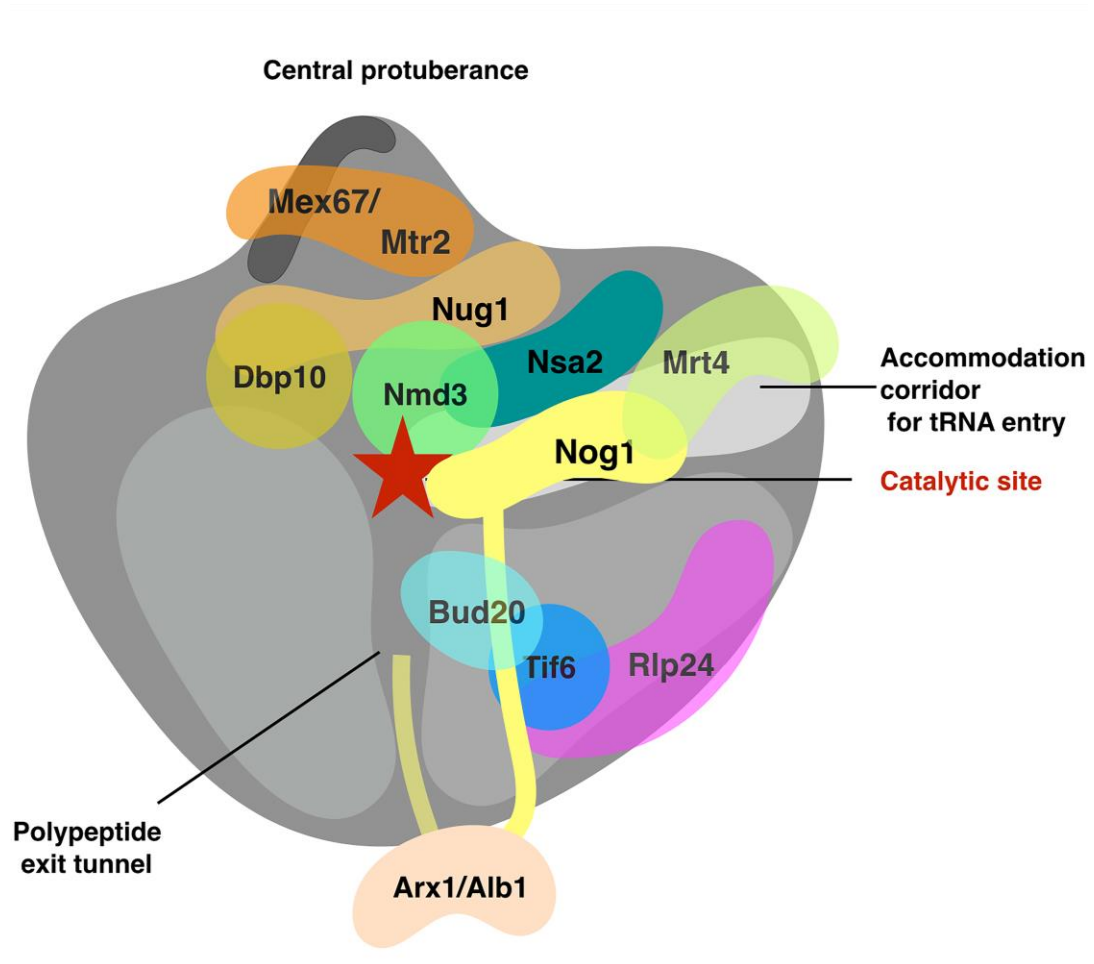


**Figure 19. Binding of export factors to the subunit interface on pre-ribosomes aids their transit into the cytoplasm.** Shown is schematic of the subunit interface of 66S pre-ribosomes, with export factors Bud20, Nmd3, Arx1/Alb1, and MEx67.Mtr2. The binding sites of export factors Rrp12 and Sda1 on the pre-ribosome are not known. Some nuclear factors (Nog1, Nog2, Nsa2, Dbp10, Nug1, Tif6, and Rlp24) are also present in the pre-ribosomes entering cytoplasm.

Curiously, Nmd3 (Sengupta et al. 2010) is the only essential protein among 60S subunit export factors. Nmd3 contains a leucine-rich nuclear export sequence recognized by Crm1 in a Ran-GTP dependent fashion. Blocking Crm1-mediated export using the leptomycin-sensitive allele of Crm1 (T539C) leads to nuclear accumulation of preribosomes (Ho et al. 2000). Nmd3 binds to the same site as Nog2 on preribosomes, but both assembly factors are not found in the same pre-ribosomal particles. Nog2 cross-link to the active site at PTC sharing common sites at H38, H69, and H89 of 25S rRNA. Since Nog2 and Nmd3 are mutually exclusive in their association to preribosomes, Nog2 is thought to prevent premature binding of Nmd3 to preribosomes (Sengupta et al. 2010; Matsuo et al. 2014). Hence, during late steps of 60S subunit assembly, the timely exit of Nog2 unmask the binding site of Nmd3 in preribosomes containing 6S pre-rRNA. However, in early and middle assembly mutants defective in association of Nog2, Nmd3 seems to bind prematurely with 66S particles (Sahasranaman et al. 2011).

Depletion/knock out of each of the other 60S export factors does not cause lethality (Bradatsch et al. 2007). Functional redundancy or negligible effects of RNA charge upon exposure of residues exposed due to the absence of export factors could account for why some of these export factors are not essential.

The export factors bind to functional centers on 60S subunits, along with other assembly factors that are exported into cytoplasm (Figure 19). (1) Arx1/Alb1 binds the surface surrounding polypeptide exit tunnel along with Nog1 inserting its C-terminal tail into the polypeptide exit tunnel (Greber et al. 2012; Bradatsch et al. 2012) (Wu et al.

2016, submitted) (2016). (2) Nmd3 and Nsa2 bind to the peptidyl transferase center adjacent to Nug1 and Mtr4, which binds to the tRNA binding sites (Matsuo et al. 2014; Bradatsch et al. 2012). (3) Mex67/Mtr2 bind to the central protuberance (Bradatsch et al. 2012). Hence, these proteins that bind to active centers of the ribosome could be involved in proofreading the functional competence of 66S preribosomes prior to their export into the cytoplasm.

### **1.2.5 Cytoplasmic maturation events release the nuclear assembly factors that enter the cytoplasm with 66S pre-ribosomes**

The cytoplasmic maturation steps are among the best-understood steps of ribosome assembly. Arlen Johnson and colleagues have successfully used clever genetic and biochemical experiments to decipher the sequential events driving the cytoplasmic maturation of 60S ribosomal subunits (Johnson 2014; Panse and Johnson 2010; Nerurkar et al. 2015). In this section, I outline the cytoplasmic maturation steps involving the release of nuclear assembly factors that are exported into the cytoplasm with 66S preribosomes, and the principles underlying these events.

In addition to export factors, pre-60S particles reaching the cytoplasm also contain Nug1, Nsa2, Nog1, Mrt4 and Rlp24, which are released in the cytoplasm (Altvater et al. 2012). These factors block the functional centers and intersubunit bridges in the pre-60S subunit, most likely preventing these immature ribosomes from poisoning the translation pool. They are released from cytoplasmic 66S preribosomes in a highly coordinated step-wise manner by energy-consuming enzymes. Failure to release these nuclear assembly factors in the cytoplasm perturbs their recycling into the nucleus. Thus, mutations affecting these cytoplasmic release steps result in nuclear assembly defects (Nerurkar et al. 2015; Panse and Johnson 2010; Gerhardy et al. 2014).

One of the earliest cytoplasmic maturation events is the replacement of Rpl24 by r-protein L24, mediated by the AAA-ATPase Drg1 (Loibl et al. 2014; Kressler et al. 2012). The release of Nug1, Nsa2, and Nog1 are also thought to follow this event. How

they are released, and if they have any cytoplasmic roles in 60S subunit assembly are not yet known. Release of Nog1 potentially facilitates the stable association of the cytoplasmic assembly factor Rei1, since both Nog1 and Rei1 are known to insert their C-terminal tails into the polypeptide exit tunnel (Greber et al. 2015; Wu et al. 2016, submitted). Structure-function analysis of Rei1 suggests that Rei1 assays the functional competency of the exit tunnel. The next step is the assembly of the P-stalk, which functions to recruit and activate translation elongation factors. . The protein phosphatase Yvh1 catalyzes removal of Mrt4, the placeholder for rpL10, from the P-stalk neighborhood (Lo et al. 2009). Binding of rpL10 facilitates folding of the P-stalk into its mature conformation, which then recruits the GTPase Efl1 to release Tif6 and Nmd3 (Senger et al. 2001). Mutations in a flexible loop of rpL10 that interacts with the P-site RNA block activation of Efl1 and subsequent release of Nmd3 and Tif6 (Bussiere et al. 2012; Lo et al. 2010). Molecular dynamics stimulations of Efl1 suggest a model in which Efl1 is activated by the P-site loop of L10 and the sarcin-ricin loop (SRL) on rRNA responsible for the activation of other GTPases involved in translation. Thus, Efl1, Tif6, and SRL test-drive translation-initiation competency before Nmd3 is finally released from the peptidyl transferase center. Gaps in our understanding of this process are reviewed in Nerurkar et al. 2015.

### **1.3 Concluding Remarks**

Development of mass spectrometric methods to analyze the global composition of preribosomes, and of new structural techniques to study the architecture of preribosomes and ribosomes (cryo-EM, CRAC and chemical probing of RNA structure), have transformed our field. It is an exciting period to study ribosome assembly (Ross et al.

2004; Bradatsch et al. 2007; Spitale et al. 2013; Granneman et al. 2010). Depletion mutants have been successfully used to authenticate the roles of *trans-acting* proteins in 60S subunit assembly, and to broadly identify the steps of their action. Preliminary data for changes in the protein-composition of preribosomes upon depletion of most of the assembly factors are available. In collaboration with structural information, these data provide platforms to generate functional interaction networks, and to hypothesize and test mechanisms driving 60S subunit assembly.

The studies discussed in Chapters 2-5 of this thesis utilized structural information from crystal structures of mature ribosomes, and known/predicted physical interaction networks, to generate hypotheses enabling the design of mutations affecting specific molecular interaction networks required for removal of the ITS2 spacer. I used proteomic, mass spectrometric, and RNA structure probing approaches to uncover a new role for the Nop7-subcomplex protein Erb1 in ITS2 cleavage. Furthermore, I used a comparative analysis of depletion of r-proteins L21 and L28 to further understand their roles in processing of the ITS2 spacer. My studies acquired a new dimension with the recently acquired cryo-EM structures of preribosomes containing the structure of ITS2 and the locations of assembly factors interesting to me (Barrio-Garcia et al. 2015; Wu et al. 2016, submitted). Further, my studies highlight the importance of targeted perturbation of molecular networks to decipher their functional significance.

## **CHAPTER 2. The Assembly Factor Erb1 Functions in a Molecular Interaction Network to Facilitate Cleavage of the ITS2 Spacer During 60S Subunit Assembly.**

### **2.1 Introduction**

Eukaryotic ribosome assembly is a multi-step process involving the intertwined processes of pre-rRNA processing and modification, RNA folding, and ribosomal protein binding, facilitated by more than 200 *trans*-acting proteins and small nucleolar RNPs. In recent years, a wealth of information has emerged about the nucleases performing most pre-rRNA processing and cleavage steps, and the dynamic nature of the pre-ribosomal complex. How molecular interactions in preribosomes drive decisions leading to each pre-rRNA processing or RNP remodeling event is not yet completely understood. My work discussed in this Chapter provides functional insights into the roles of the evolutionarily conserved Nop7-subcomplex in structuring the 5.8S pre-rRNA. I propose a model for how rRNA folding, r-protein binding and recruitment of assembly factors are coordinated to signal the cleavage at ITS2 spacer in 27SB pre-rRNA.

#### **The Nop7-subcomplex**

The Nop7-subcomplex, which is composed of the three assembly factors, Nop7, Erb1, and Ytm1, is essential for 60S ribosomal subunit assembly (Figure 20). In the absence of these proteins, exonucleolytic removal of the ITS1 spacer sequence in 27SA<sub>3</sub> pre-rRNA is perturbed, blocking formation of mature 60S subunits (Harnpicharnchai et al. 2001; Oeffinger et al. 2002; Adams et al. 2002a; Pestov et al. 2001; Miles et al. 2005;

Hölzel et al. 2005). In rapidly growing yeast cells, the majority of pre-rRNAs (~85%) of the 60S subunit undergo processing via this intermediate to generate the 5'-end of mature 5.8S<sub>s</sub> rRNA (Woolford and Baserga 2013).

The ability of the Nop7-subcomplex to form a heterotrimer has been demonstrated using yeast two-hybrid assays, *in vitro* GST pull-downs and various other biochemical assays (Miles et al. 2005; Rohmoser et al. 2007a). Erb1 is central to the formation of the subcomplex, since it interacts with both Nop7 and Ytm1 (Figure 20A). These proteins have no known intrinsic enzymatic activity, but all of them contain protein-protein interaction motifs. Even though Erb1 and Nop7 do not have conventional RNA binding motifs, they contact rRNA in domains I and III of 25S rRNA, respectively (Granneman et al. 2011).

Both Erb1 and Ytm1 contain the donut-shaped  $\beta$ -propeller structure formed by WD40 repeats (Figure 20B). WD40 repeats are composed of a repeating sequence of 40-60 amino acid residues containing variable regions of 11-24 amino acid residues, followed by a glycine-histidine dipeptide, and ends with a tryptophan (W)-aspartate (D) dipeptide. The WD40 domains are a common protein-protein interaction motif in eukaryotes. Three WD40 repeats fold into 4 anti-parallel  $\beta$ -strands that form each blade of the propeller (Figure 20B). Multiple WD40 repeats form a WD40 domain, which form the multi-bladed  $\beta$ -propeller. This organization enables intermolecular interactions via the top, the bottom, or the circumference of the propeller structure (Stirnemann et al. 2010; de la Cruz et al. 2005a; Baßler et al. 2014). The 60S ribosomal subunit assembly factors Rrb1, Rsa4, Ipi3, Pwp1, Mak11, and Sqt1 also contain WD40 repeats (Pausch et al. 2015; de la Cruz et al. 2005b; Merl et al. 2010; Talkish et al. 2014; Saveanu et al. 2007; Frénois

et al. 2016).

Recently multiple groups co-crystallized the WD40 domains of Erb1 and Ytm1, substantiating previous predictions that their WD40 domains interact with each other, based on mutational analysis of these proteins (Fig 20B) (Tang et al. 2008; Miles et al. 2005; Marcin et al. 2015; Romes et al. 2015; Thoms et al. 2015a; Wegrecki et al. 2015b). In addition to the WD40 repeats, Erb1 contains an equally long N-terminal domain. No group has successfully solved the crystal structure of this N-terminal half of Erb1 even when co-crystallized with Nop7 and Ytm1. The consensus is that this structure could be non-globular and extended, making it available for mediating other interactions. In fact, most proteins with WD40 domains also contain additional domains, increasing their ability to form molecular networks (Stirnemann et al. 2010). Several previous studies suggest that the Erb1-Nop7 interaction is potentially mediated by the N-terminal half of Erb1 (Tang et al. 2008; Thoms et al. 2015a; Strezoska et al. 2000). The domain architecture of Nop7 consists of an N-terminal conserved Pescadillo domain and a C-terminal BRCT domain flanked by two coiled-coils. Nop7 contacts preribosomes at the domain I/5.8S/domain III rRNA interface in the 66S preribosomes (Granneman et al. 2011; Wu et al. 2016, submitted). The BRCT-domain is also a protein-protein interaction domain. Thus, due to the prevalence of protein-protein interaction domains, the Nop7-subcomplex has the potential to serve as hub of protein-protein interactions providing platforms for complex assembly and regulation of macromolecular complexes. This is substantiated by the genetic and protein-protein interactions exhibited by the Nop7-subcomplex proteins (Figure 21) (McCann et al. 2015; Tarassov et al. 2008; Dembowski et al. 2013a; Talkish et al. 2012a; 2014; Honma et al. 2006; Miles et al. 2005; Saveanu et

al. 2003; Costanzo et al. 2010; Biedka et al. 2016, submitted) (Wu et al. 2016, submitted).

### **Moonlighting Functions of the Nop7-subcomplex proteins**

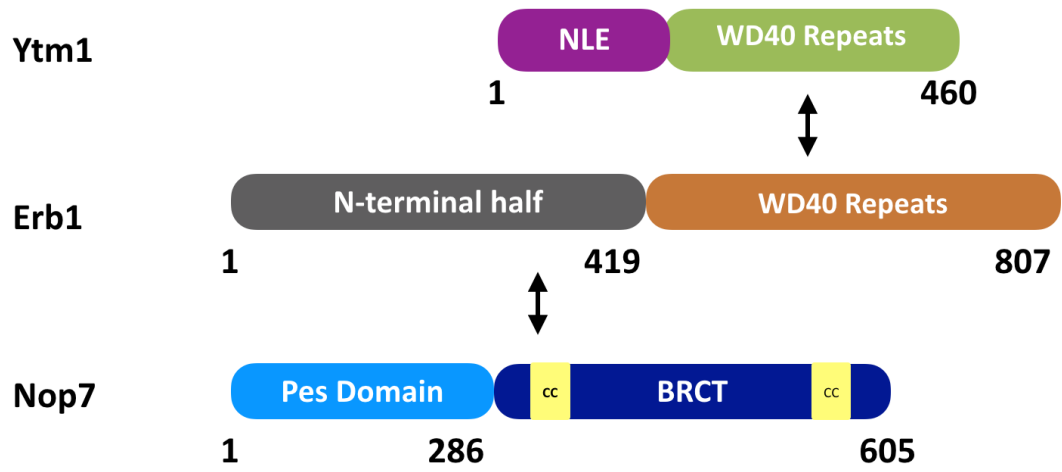
The roles of Nop7, Erb1, and Ytm1 in ribosome assembly have been established by (a) reduced levels of 60S subunits in their absence (by polysome analysis and pre-rRNA processing assays) and (b) their presence in preribosomes (CoIP of pre-rRNAs, other ribosome assembly factors, and interactions with other assembly factors) (Pestov et al. 2001; Adams et al. 2002; Oeffinger et al. 2002; Miles et al. 2005; Harnpicharnchai et al. 2002). In addition, there are additional known functions for these proteins in higher organisms:

- (1) Mutations in Bop1, the mammalian homolog of Erb1 causes p53-dependent cell cycle arrest (Pestov et al. 2001).
- (2) Yeast Ytm1 is implicated in mitosis and chromosome transmission (Oupenski et al. 1999)
- (3) Pes1 is known to interact with the origin replication complex, and is required for hyphal- to-yeast morphogenesis in *C. albicans* (Du et al. 2002; Shen et al. 2008). Pes1 also is implicated in normal development, and in regulating cancer progression and sensitivity of cancer cells to chemotherapeutic drugs (Tecza et al. 2011; Xie et al. 2013; Cheng et al. 2012).

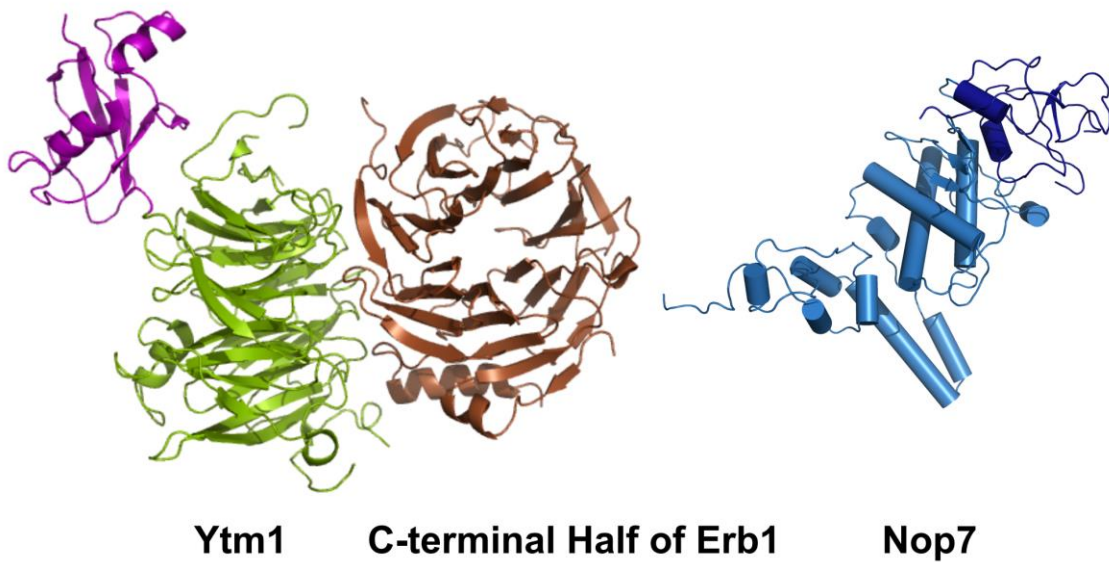
Therefore, the Nop7-subcomplex might serve as a link between ribosome assembly and the cell cycle. If and how Nop7, Erb1 and/or Ytm1 function as links between these processes remain to be understood.

Figure 20

A



B



**Figure 20. Molecular architecture of the Nop7-subcomplex** (A) A schematic representation of the domain architecture of Nop7, Erb1, and Ytm1 is shown. (B) A high-resolution structure of Ytm1 in complex with the C-terminal half of Erb1, and certain portions of Nop7 (Wegrecki et al. 2015a)(Wu et al. (2016), submitted), (PDB ID: 5CXC). The Notchless-like-element (Nle) of Ytm1 interacts with the AAA-ATPase Rea1 (Midasin or Mdn1); its WD40 (Romes et al. 2015; Thoms et al. 2015) domain repeats interact with Erb1 (Baßler et al. 2010b).

The Nop7-subcomplex proteins (Nop7, Erb1, Ytm1) are among the seven assembly factors (also Rlp7, Cic1, Nop15, and Pwp1) interdependent for their association with preribosomes (Figure 21). Their interdependence is partly contributed by direct protein-protein interactions between many of these proteins. (Miles et al. 2005; Sahasranaman et al. 2011). In addition to the interdependent A<sub>3</sub> factors, assembly factors Ebp2, Brx1, Nop12, Drs1, and Has1 are also required for processing of 27SA<sub>3</sub> pre-rRNA (Dembowski et al. 2013a; Talkish et al. 2014; Biedka et al. 2016, submitted). Even though depletion of these proteins blocks processing of the ITS1 spacer in 27SA<sub>3</sub> pre-rRNA, many of them bind 25S rRNA adjacent to the ITS2 spacer sequence (Figure 12) (Granneman et al. 2011; Wu et al. 2016, submitted). This suggested that the role of these A<sub>3</sub> factors in ITS1 processing is indirect. The A<sub>3</sub> protein-protein and protein-RNA interaction network may be necessary to create a preribosome structure stable enough to undergo 27SA<sub>3</sub> pre-rRNA processing. In their absence, preribosomes are turned over rapidly (Jakovljevic et al. 2012; Sahasranaman et al. 2011). Therefore, these A<sub>3</sub> factors could have more direct roles in the removal of the ITS2 spacer in 27SB pre-rRNA. Work in this thesis tested this hypothesis and provides evidence for a direct role of the A<sub>3</sub> factor Erb1 in removal of the ITS2 spacer in 27SB pre-rRNA.

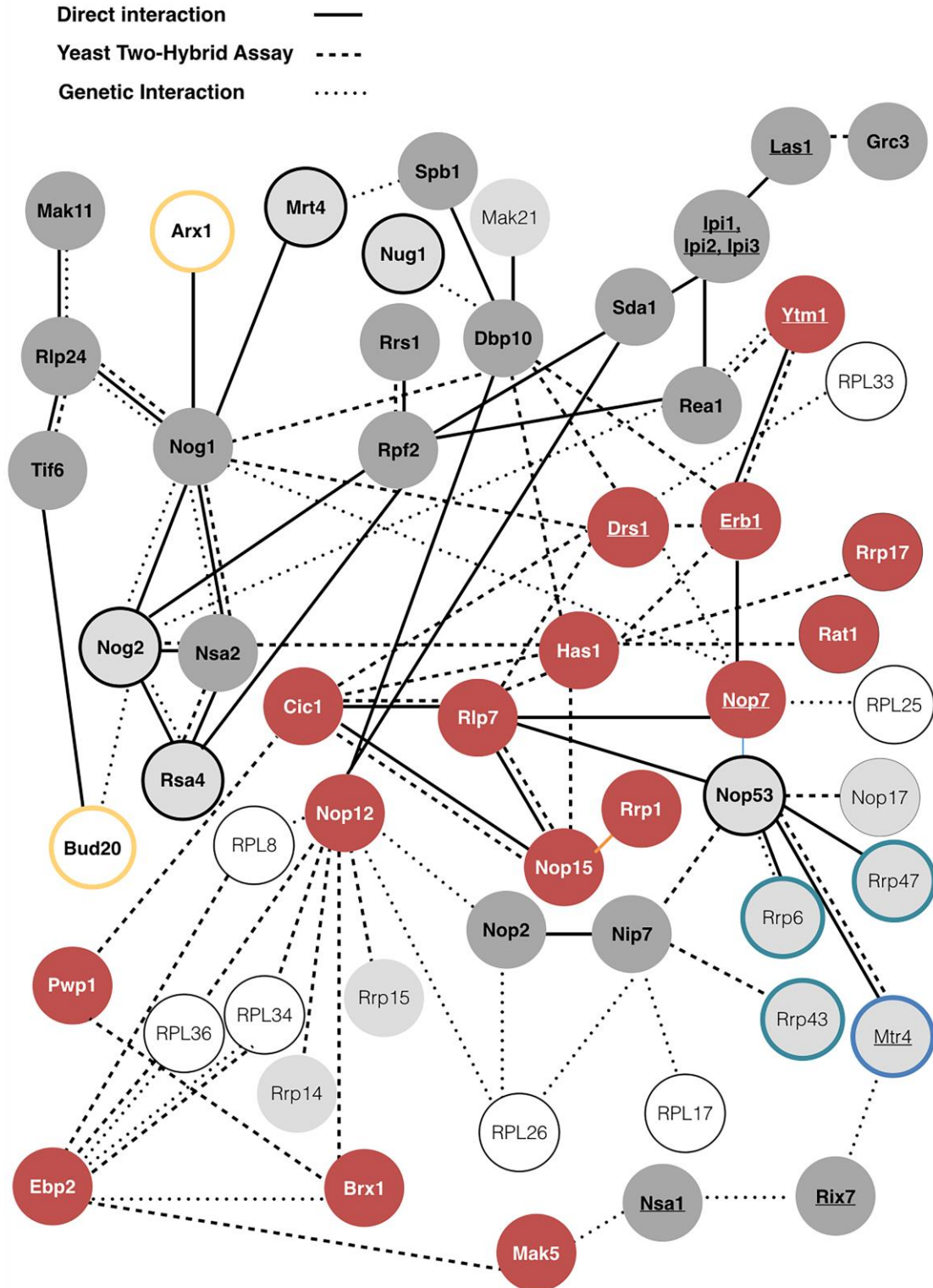
Nop7, Erb1, and Ytm1 enter 90S preribosomes, early in the assembly pathway, since they co-purify 35S pre-rRNA (Sahasranaman et al. 2011; Miles et al. 2005). The AAA-ATPase Rea1 drives the exit of Erb1 and Ytm1 from preribosomes (Baßler et al. 2010a; Thoms et al. 2015a; Wegrecki et al. 2015b) (Figure 22). Whether Nop7 exits preribosome with Erb1 and Ytm1 is not completely understood, since it co-purifies significantly higher amounts of the late intermediate 7S pre-rRNA compared to Erb1 and

Ytm1 (Granneman et al. 2011; Altvater et al. 2012). The *in vitro* assays showing remodeling activity of Rea1 on preribosomes provided evidence for only partial removal of Nop7 from preribosomes (Baßler et al. 2010a). Therefore, Nop7 might have sub-complex independent roles in ribosome biogenesis, about which nothing is known yet.

The mammalian homologs of the Nop7-subcomplex form the PeBoW subcomplex composed of Pes1, Bop1, and WDR12 (mammalian Nop7, Erb1, and Ytm1 homologs, respectively) (Moilanen et al. 2015; Rohrmoser et al. 2007b; Hölzel et al. 2005; Pestov et al. 2001; Strezoska et al. 2000; Hölzel et al. 2007a; Pestka 1968; Allende et al. 1996; Lapik et al. 2004; Hölzel et al. 2007b; Wang et al. 2014; Kellner et al. 2015b). Conditional shut down of Bop1 expression affects processing of the ITS1 spacer in mammalian cells, whereas an N-terminally truncated version of Bop1, namely Bop1 $\Delta$  blocked cleavage in the ITS2 spacer (Strezoska et al. 2000). The WDR12 $\Delta$ NLE (or N-terminal deletion of WDR12) causes an ITS2 cleavage defect (Hölzel et al. 2007a). Our hypothesis, as described previously, is that the yeast A<sub>3</sub> factors have direct roles in the cleavage of the ITS2 spacer. Hence, I decided to focus on the yeast homolog of Bop1, i.e. Erb1, to explore whether the Nop7-subcomplex has additional roles in the removal of the ITS2 spacer. I constructed eight internal deletion mutations in the relatively unexplored N-terminal half of Erb1 and assayed the effects of these mutations on pre-rRNA processing, preribosome composition, and the structure of the ITS2 spacer and 5.8S rRNA. Two of the *erb1*- internal deletion mutations blocked cleavage of the ITS2 spacer (referred to as *erb1*<sub>class 2</sub> mutations). Detailed analysis of these mutants revealed that Erb1 is required for proper folding of 5.8S rRNA, and association of specific r-proteins and assembly factors required for ITS2 cleavage. The 5.8S rRNA residues

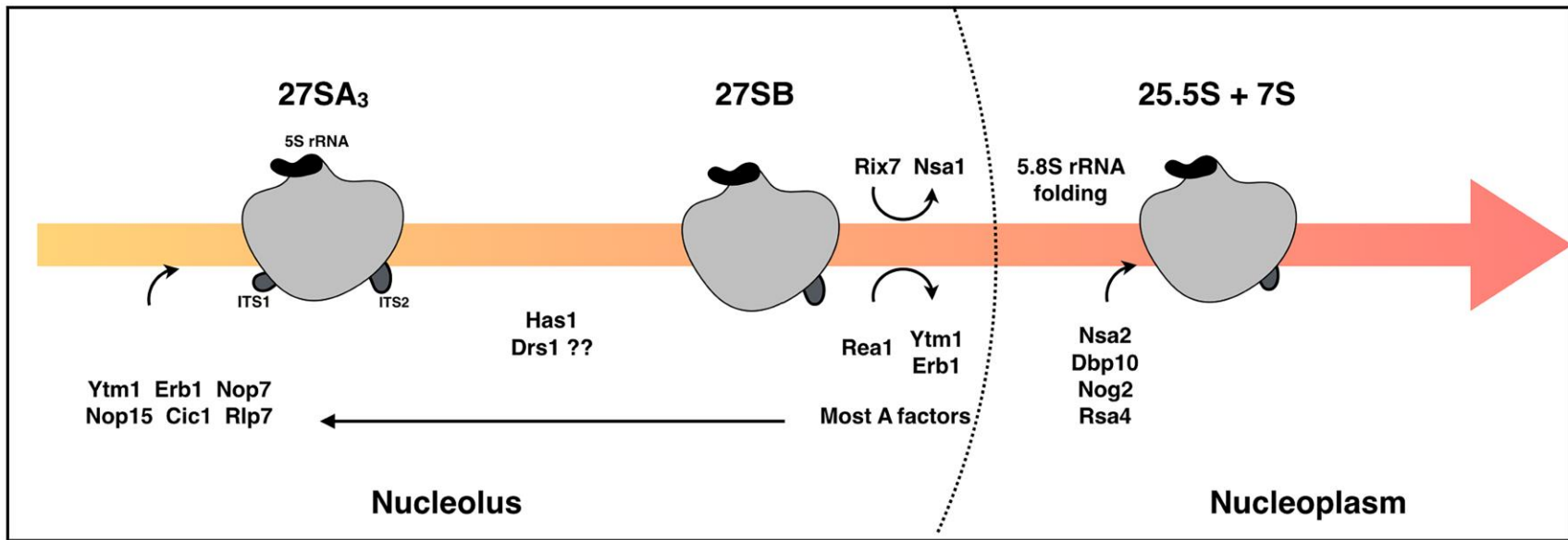
contacted by the interaction partner of Erb1, Nop7, showed increased protection to modification by the structure probing chemical NAI in *erb1<sub>class 2</sub>* mutants. This suggested that the timely removal of Erb1-Ytm1 by the AAA-ATPase may be perturbed in *erb1<sub>class 2</sub>* mutants (Figure 22). Based on our observations, we propose that the Rea1-mediated removal of Ytm1-Erb1 facilitates remodeling of the 5.8S rRNA, resulting in the release of ‘very early’ and ‘early’ acting assembly factors, and recruitment/stable association of assembly factors required for cleavage of the ITS2 spacer in 27SB pre-rRNA.

Figure 21



**Figure 21. Molecular interaction network of assembly factors involved in 27SA<sub>3</sub> (red), 27SB (dark grey), and 7S (light grey) pre-rRNA processing.** Direct physical interactions (yeast two-hybrid, pull downs *in vitro*, and cryo-EM observations), and genetic interactions between assembly factors involved in the early (red), middle (dark grey) and late (light grey/yellow) are shown. Proteins present in the exosome are shown in blue circles. Data for interactions with ribosomal proteins are included for approximation of locations of assembly factors whose locations on preribosomes have not been directly established. Molecular interactions identified or confirmed among the mammalian homologs of assembly factors are indicated by underlines. (Pratte et al. 2013; Wan et al. 2015; Shimoji et al. 2012; Yoshikatsu et al. 2015; Castle et al. 2013; 2012; Gasse et al. 2015; Leidig et al. 2014; Bradatsch et al. 2007; Thoms et al. 2015a; Wegrecki et al. 2015a; Dembowski et al. 2013b; 2013a; Costanzo et al. 2010; Talkish et al. 2012a; Honma et al. 2006; Santos et al. 2011; Goldfeder and Oliveira 2010; Luz et al. 2009; García-Gómez et al. 2011; Saveanu et al. 2007; Wilmes et al. 2008; McCann et al. 2015 Shimoji et al. 2012; Wan et al. 2015; Pratte et al. 2013; McCann et al. 2015; Saveanu et al. 2003).

Figure 22



**Figure 22. Molecular assembly events in early and middle preribosomal intermediates.**

## 2.2 Results

### 2.2.1 Conserved regions in the N-terminal half of Erb1 are essential for growth

Erb1 mediates the formation of the Nop7-subcomplex via its interaction with Nop7 and Ytm1 (Miles et al. 2005; Rohmoser et al. 2007b; Tang et al. 2008). The C-terminal half of Erb1 contains WD40 repeats, which are required for its interaction with Ytm1 (Tang et al. 2008; Thoms et al. 2015b; Wegrecki et al. 2015b) (Figure 20). The N-terminal half of Erb1 contains a stretch of highly conserved amino acids whose role in 60S subunit assembly is largely unexplored (Figure 23). To begin to explore the biological functions of the N-terminal half of Erb1, we constructed a series of eight internal deletions across the N-terminal half of Erb1 (residues 1-419) in the plasmid pOBD2-ERB1 (Figure 25A). Bioinformatic prediction of Erb1 secondary structure was used to avoid disruption of potential secondary structure elements (Figure 24). Plasmids containing these mutations were introduced into a yeast strain engineered to conditionally shut off the expression of wild-type *ERB1* by replacing the endogenous *ERB1* promoter with the *GAL1* promoter. When grown in glucose-containing medium, *GAL* promoter-driven WT *ERB1* expression is shut off, allowing us to assay the effects associated with *erb1*- internal deletions (Figure 25B). Plasmids expressing wild-type *ERB1* supported the growth of the *GAL-ERB1* strain in glucose-containing medium, while the empty vector did not. Mutations affecting the relatively poorly conserved N-terminal 150 amino acids (*erb1<sub>del3-50</sub>*, *erb1<sub>del51-100</sub>*, and *erb1<sub>del101-160</sub>*) had no effect on growth under standard laboratory conditions (Figure 25 and Figure 23). Of the three mutants, only *erb1<sub>Δ101-160</sub>* exhibited a temperature-sensitive growth defect at 37C (Figure 26A). Deletions of stretches of residues in the highly conserved interval of residues 161-419 (*erb1<sub>de161-200</sub>*,

*erb1<sub>del201-245</sub>*, *erb1<sub>del246-310</sub>*, *erb1<sub>del311-365</sub>*, *erb1<sub>del366-419</sub>*) failed to complement growth at 30°C (Figure 25B). These constructs also failed to support growth at 16°C as well as 37°C (data not shown). We did not observe any significant growth defects upon over-expression of any of these mutant constructs from pAG414-GAL-*ERBI*-TAP plasmid (Figure 26B).

Figure 23

```
S.cerevisiae  MMAKNNKT-T--EAKMSK-----KRAAS-----EESDV-EEDEDKLLSV 44
C.albicans    MARNSIKK-S--PVVKKKDTPIVRRKRPQQEAEDSND-EESEDEL-NV
D.erio       MSKLNK-----KRHLE-----ENEE---EQLPFDK
X.laevis     MKRGSKR-----ESGG-----PLTE---EPPLFSE
M.musculus   MAGACGKPH-MSPASLPG-----KRRLE-----PDQELQ-IQEPPLLS-
R.norvegicus MAGACGKHH-MSPGSLPG-----KRRLE-----PDQEPQ-IQEPPLLS-
H.sapiens    MAGSRGAGR-TAAPSVRPE-----KRRSE-----PELEPEPEPEPLLCT
*           .           :           :

S.cerevisiae  ---DGL--IDAEASESDEDDDEYESAVEEKESSSDKQAQDDSDSD--AE 79
C.albicans    ---EGL--IDASDDEDEEEQEQEQEENNSDDD-DDDDDDDD--NN
D.erio       DSGEDGHLDDGDEDPADLSDSEESVFSGLEDSGSDDE-DDDEDDE-DDD
X.laevis     ---ENRSLQD--GNPLDESDEESQYSGLEDSGTSS-DDEDHSSEEVQ
M.musculus   -----DPDSSLSDSEESVFSGLEDLGSDSS-EEDTEGVAGS--
R.norvegicus -----DPDSSLSDSEESVFSGLEDSGSDTS-DEDTTEVARA--
H.sapiens    ---SPL--SHSTGSDSGVSDSEESVFSGLEDSGSDSS-EDDDEGDEEG-E
           . : * .           : : * .           : : :

S.cerevisiae  LNKLLA-----EEEGDGEEDYDSSEF--SDD-TTS-LTD----RLS 113
C.albicans    SEADSEELNQLLGEDEEDPSDYNSEF--SDE-PK--DD--DL
D.erio       DKDGESEKSSDA-E---EDKADDDGDLKLSAKDDVKQVDSQNSKEKK
X.laevis     DPGKSPKEI-----IKVPHR-TSKSQAD-----
M.musculus   --S-GDEDNHRA-E-----ETSEE-LAQAAPL-----
R.norvegicus --G-CDKDN-RT-E-----KTSEE-QEQAVFP-----
H.sapiens    DGALDDEGHSGI-K-----KTEE-QVQASTP-----
           .

S.cerevisiae  GV--KLQITVDPNI---YSKYADGSDRIKIP-EINPVYSDSDSDAET-Q 154
C.albicans    RINIKLSLSDPSIQNSISKFSGDSIRILKP-EIEPKYSDSDSDAEN-F
D.erio       KKKRKGKSVLKDGE---EDVASGRDEALKITSQVDEYDHTSDEEDIR
X.laevis     -----SPADEEQP-NEIKKEYENDSDEEDIR
M.musculus   -----CSRTEEAGA-LAQDEYEDSDSDEEDIR
R.norvegicus -----CPRAEEAGA-LTRDEYEDSDSDEEDIR
H.sapiens    -----CPRTEMASA-RIGDEYEDSDSDEEDIR
           * * * * *

S.cerevisiae  NTIGNIPLSAYDEMPHIGYDINGKRIMRPAKG-SALDQLLDSIELPEGWT 203
C.albicans    NTIGNIPLSAYDEMPHIGYDINGKRIMRPAKG-SALDQLLESIDLPEGWT
D.erio       NTVGNIPMEWYKDYPHIGYDLGKIKFKPIRKNKDELDELKMNPDYWR
X.laevis     NTVGNIPMEWYKDLPHIGYDLGKIKFKPLRSKDQLEEFDLKMNPDYWR
M.musculus   NTVGNVPLAWYDEFFPHVGYDLGKRIYKPLRTRDELQFLDKMDDPFWR
R.norvegicus NTVGNVPLAWYDDFFPHVGYDLGKRIYKPLRTRDELQFLDKMDDPFWR
H.sapiens    NTVGNVPLEWYDDFFPHVGYDLGRRYKPLRTRDELQFLDKMDDPFWR
**:*:*:* * : * : * : * : * : * : * : * : * : * : * : *

S.cerevisiae  GLLDKNSGSSLNLTKEELISKIQRNEQTDSDSINPYEPLDWFTRHEEV 253
C.albicans    GLLDQNTGTSLKLTDELELIRKIQQENTDENINPYEPLDWFTRHEEV
D.erio       TVQDKMTGADIRLSDEQVLDVHRLQGGKFGDVNFNEYEPAVDFFSNEVMI
X.laevis     TVHDKKTGQDIKLTDEQVLDVRLQGGQFGDLNYPYQPAIDFFTHETMI
M.musculus   TVQDKMTGRDLRLTDEQVALVHRLQGGQFGDSGFNPEYPAVDFFSGDIMI
R.norvegicus TVQDKMTGSDLRLTDEQVALVHRLQGGQFGDSGFDPYEPVAVDFFSGDIMI
H.sapiens    TVQDPMTGRDLRLTDEQVALVRLQSGQFGDVGFNPEYPAVDFFSGDVMI
: * : * . : . : * : * : * : * : * : * : * : * : * :

S.cerevisiae  MPLTAVPEPKRRFVPSKNEAKRVMKIVRAIREGRIIPPKKLKEM-KEKEK 302
C.albicans    MPVTAVPEPKRRFVPSKHEAKRVMKIVKAIREGRIIPPKNVQQLTEEE
D.erio       HPVTNRPADKRSFIPSLIEKEKVKLVHAIKMGWIKPRRP-----K-E
X.laevis     HPVTNRPADKRSFIPSLIEKEKVSRLVHAIKMGWIKPRRP-----R-D
M.musculus   HPVTNRPADKRSFIPSLVEKEKVSRLVHAIKMGWIKPRRP-----H-D
R.norvegicus HPVTNRPADKRSFIPSLVEKEKVSRLVHAIKMGWIKPRRP-----P-D
H.sapiens    HPVTNRPADKRSFIPSLVEKEKVSRLVHAIKMGWIKPRRP-----R-D
* : * * * * * * : * : * : * : * * * .

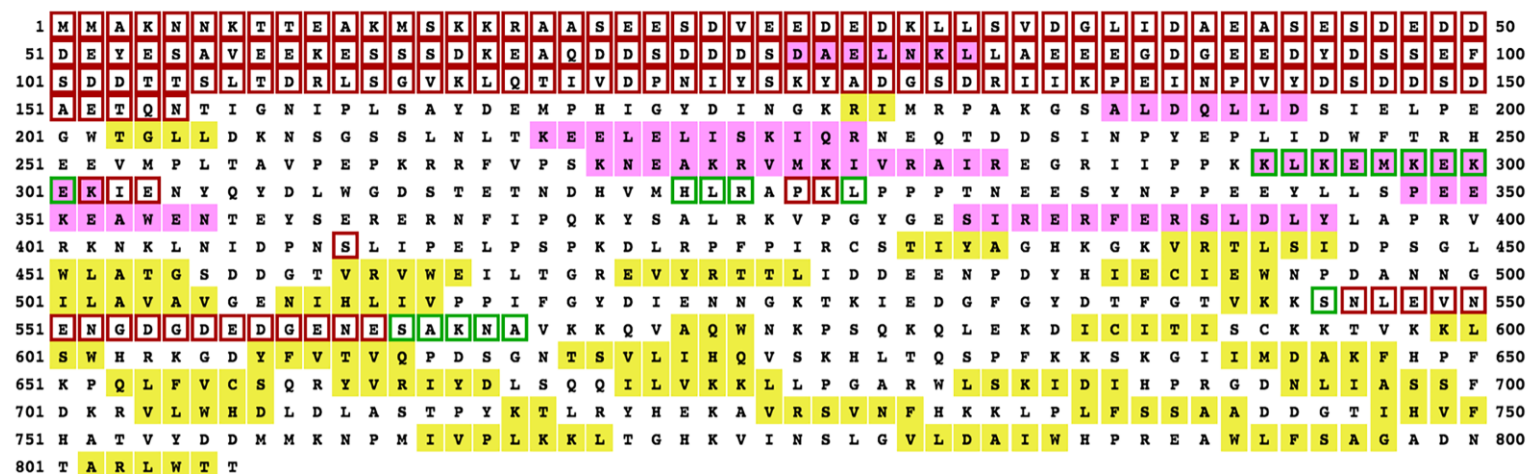
S.cerevisiae  IENYQYDLWGDST---ETNDHVMHLRAPKLPPPTNEESYNPPEYLLSPE 350
C.albicans    EDQFNFDLWQDEI---EISDHIMNLRAPKLPPPTNEESYNPPEYLLTTE
D.erio       TTPQYDLWAKEDPNILGRHKMHVPAPKMKLPGHEESYNPPEYLLSEE
X.laevis     DAPTYDLWAKEDPNAILGRHKMHVPAPKMLPLPGHEESYNPPEYLLMSEE
M.musculus   PTPSFYDLWAKEDPNAVLGRHKMHVPAPKMLPLPGHAESYNPPEYLLPTEE
R.norvegicus STPSFYDLWAKEDPNAVLGRHKMHVPAPKMLPLPGHAESYNPPEYLLPTEE
H.sapiens    PTPSFYDLWAKEDPNAVLGRHKMHVPAPKMLPLPGHAESYNPPEYLLSEE
:*** ..           * * : : * : * : * : * : * : * : * :

S.cerevisiae  EKEAWENTEYSERERNFIPQKYSALRKVPYGESIRERFERSLDLYLAPR 399
C.albicans    EKS KWLQESPIDRERNFLPQKYNLSRQVPGYQDSVRRERFERSLDLYLAPR
D.erio       ERLAWAQDPEDRKLSPFPQKFSCLRAVPFARFIERFERCLDLYLCP
X.laevis     ERLAWEQDPEDRKLSPFPQKFNCLRAVPGYARFIERFERCLDLYLCP
M.musculus   ERSAMWQEPVERKLNFLPQKFPSLRTVPAYGRFIQERFERCLDLYLCP
R.norvegicus ERLAWMQEPIERKLNFLPQKFPSLRTVPAYGRFIQERFERCLDLYLCP
H.sapiens    ERLAWEQEPGERKLSFLPKFPSLRAVPAYGRFIQERFERCLDLYLCP
* : * .           : : * : * : * : * : * : * : * : * : * :

S.cerevisiae  VRNKNLINDPNSLIPELPSP 419
C.albicans    VRHNKLNIDPDSLIPDLSP
D.erio       QRKMRVNVNPELIPKLPKP
X.laevis     QRKMRVNVNPELIPKLPKP
M.musculus   QRKMRVNVNPELIPKLPKP
R.norvegicus QRKMRVNVNPELIPKLPKP
H.sapiens    QRKMRVNVNPELIPKLPKP
* : : * : * : * : * * *
```

**Figure 23.** Erb1 sequences from seven phylogenetically diverse species were aligned using the web-based T-coffee server (<http://www.ebi.ac.uk/Tools/msa/tcoffee/>). Residues with conserved identities or biochemical properties across different phyla are indicated by ‘\*’ or ‘:’, respectively. The amino acids are color coded by the biochemical properties of their side chains: positively charged (magenta), negatively charged (blue), polar (green), and non-polar (red). Black and grey lines above the alignment indicate two stretches of highly conserved regions in the N-terminal half. Deletion of residues in these conserved stretches of *erb1* was lethal for *S. cerevisiae* (This study).

Figure 24A

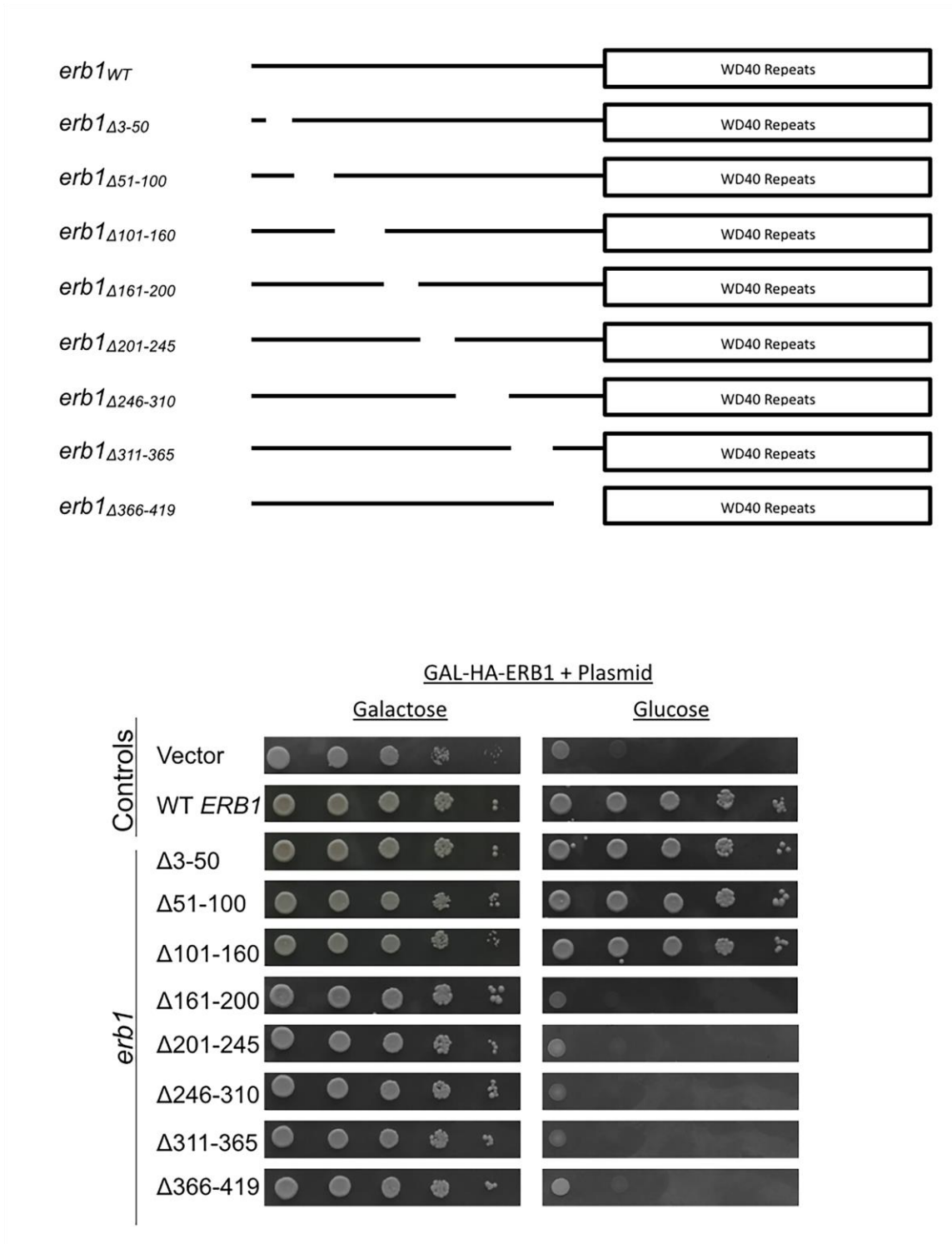


<b>KEY</b>	<b>Helix</b>	<b>Sheet</b>	<b>Disordered</b>	<b>Disordered protein binding</b>	<b>Dompred Boundary</b>	<b>DomSSEA Boundary</b>
<b>Annotations</b>	M	L	E	E	A	D



**Figure 24. Bioinformatic prediction of secondary structural elements in Erb1.** (A) Secondary structural elements in Erb1 were predicted using web-based PsiPRED software <http://bioinf.cs.ucl.ac.uk/psipred/>. (B) The confidence of the structure prediction for the N-terminal half of Erb1 is shown as blue bars.

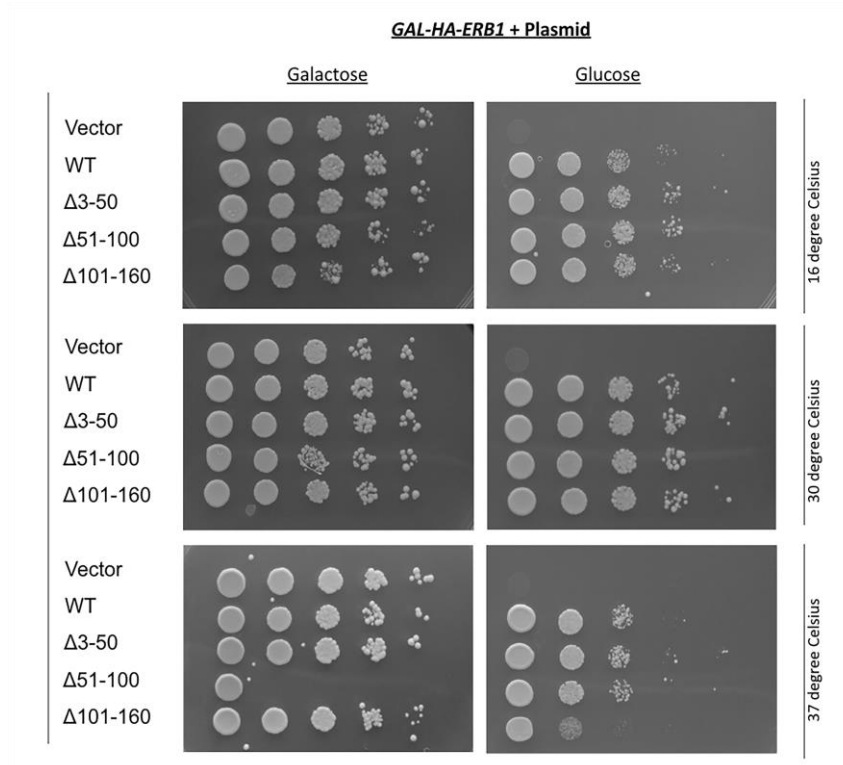
**Figure 25**



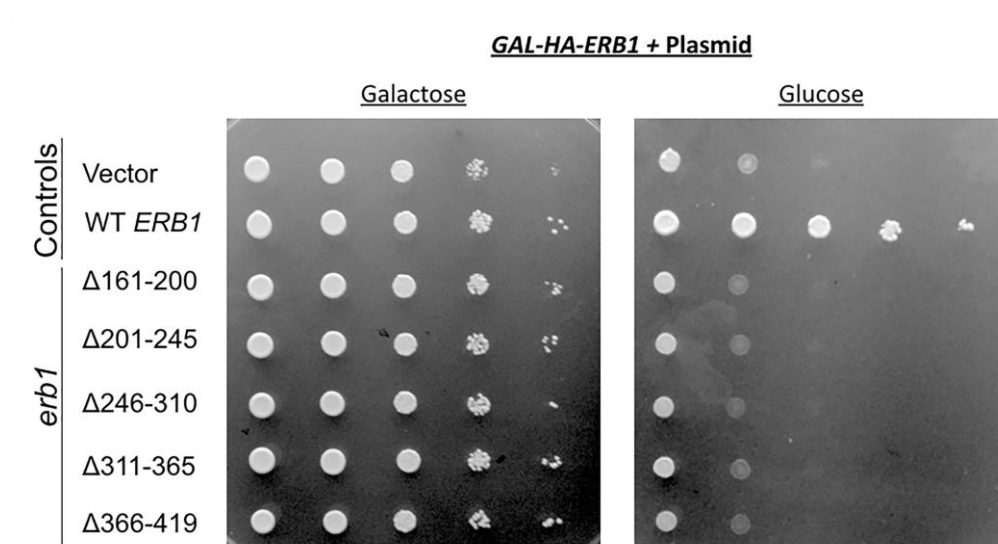
**Figure 25. Effects of deletions of discrete regions of Erb1 on growth of yeast.** (A) Schematic representation of amino acids removed by *erb1* internal deletion mutations. (B) Growth of *GAL-HA-ERB1* cells expressing WT or mutant *erb1* from pOBD2 plasmids on solid media containing galactose (left panel) or glucose (right panel). Tenfold serial dilutions of *GAL-HA-ERB1* cells containing plasmids were spotted on selective-media containing galactose (C-TRP+GAL) or glucose (C-TRP).

Figure 26

A



B



**Figure 26 (A) Effect of temperature on growth of *erb1* internal deletion mutants that have no growth defects at 30°C.** Growth of *GAL-HA-ERB1* cells expressing WT or mutant *erb1* from pOBD2 plasmids on solid media containing galactose (left panel) or glucose (right panel). Tenfold serial dilutions of *GAL-HA-ERB1* cells containing plasmids were spotted on selective-media containing galactose (C-TRP+GAL) or glucose (C-TRP). Plates were incubated at 16°C, 30°C, or 37°C. **(B) Effects of lethal *erb1* internal deletions expressed from the pAG415-GPD-EFGP-*ERB1* plasmid on growth of *GAL-3HA-ERB1*.** Tenfold serial dilutions of *GAL-HA-ERB1* cells containing plasmids were spotted on selective-media containing galactose (C-TRP+GAL) or glucose (C-TRP) and incubated at 30°C.

Figure 27

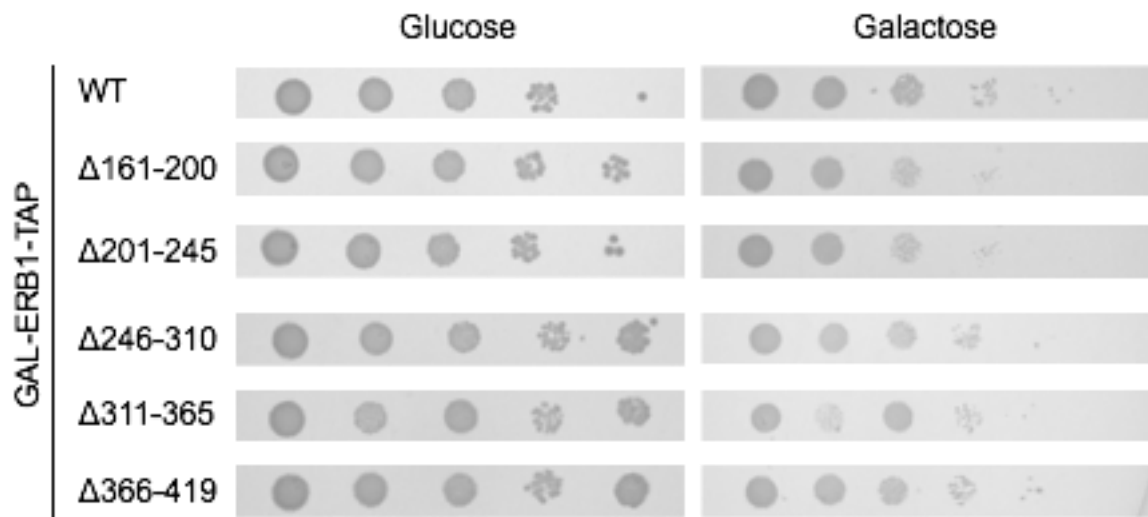


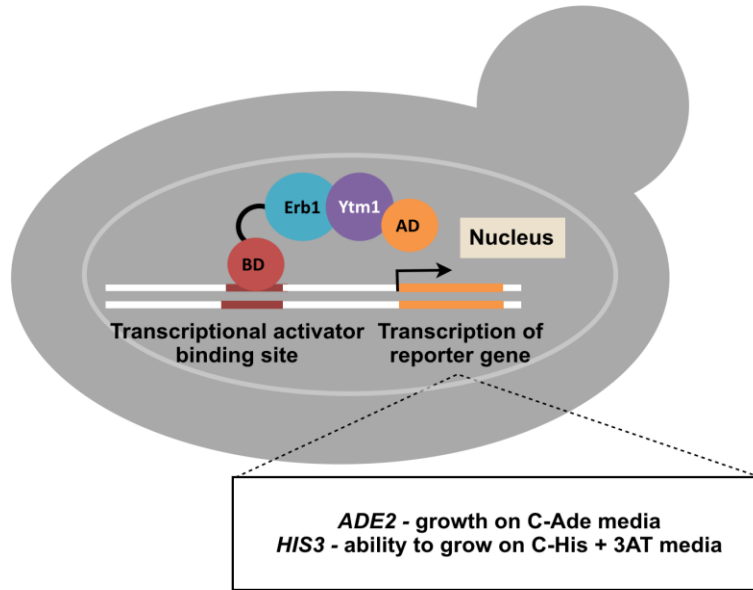
**Figure 27. Effects of overexpression of the lethal *erb1* internal deletion mutants on growth.** Wild type *S. cerevisiae* strains overexpressing lethal *erb1* internal deletions from the plasmid pAG414-GAL-*ERBI*-TAP were spotted as serial dilutions on selective solid-medium containing either glucose or galactose as the carbon source. The plates were incubated at 30°C for three days.

### **2.2.2 Most of the N-terminal Half of Erb1 is not required for its interaction with Ytm1**

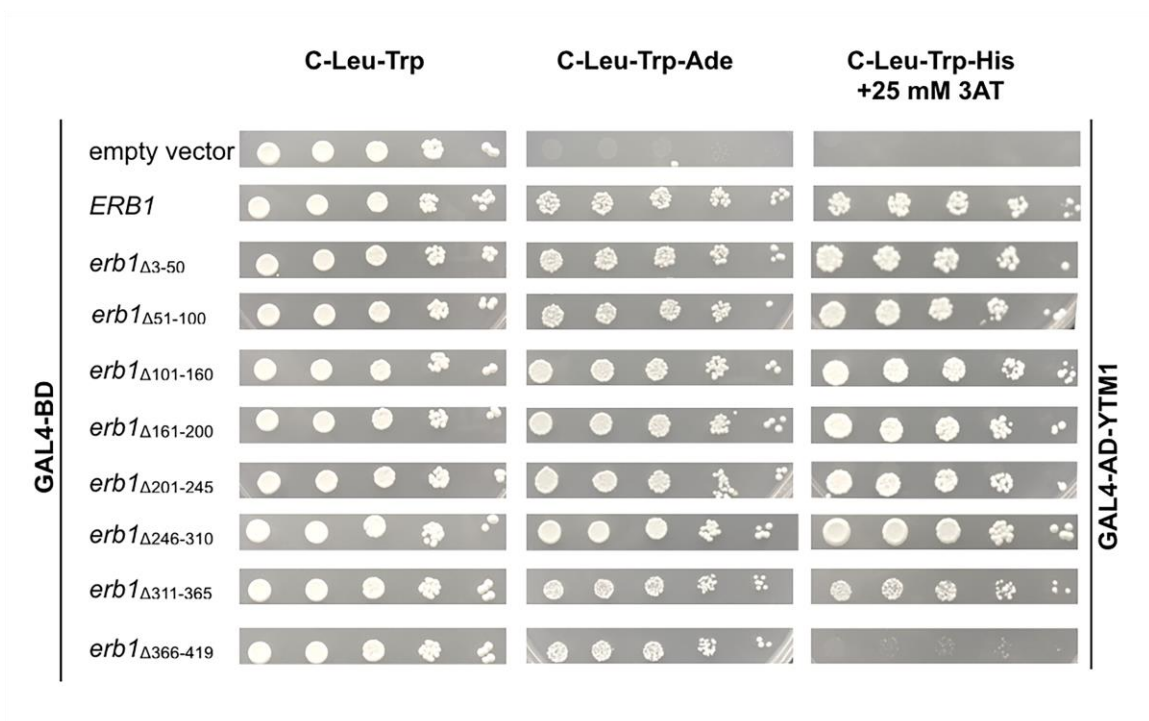
We performed yeast two-hybrid assays between *erb1* internal deletion mutant proteins and wildtype Ytm1, to assay Erb1-Ytm1 interactions and the stability of the mutant proteins (Figure 27A). Wild type Erb1 interacts strongly with Ytm1, allowing the cells to grow in the presence of the drug 3-aminotriazole up to a concentration of 25 mM (Figure 27B, row 2). All eight mutant constructs grew efficiently in C-Leu-Ade, indicating that the mutant proteins are stably expressed (Figure 2, lane 2, rows 3-10). Seven of the eight mutant constructs, except *erb1*<sub>del366-419</sub>, showed interaction in 25 mM AT, indicating strong interaction between the *erb1* internal deletion mutant proteins and Ytm1 (Figure 27, lane 3, rows 3-10). Thus, residues 366-419 in the N-terminal half of Erb1 are required for efficient interaction of Erb1 with Ytm1, in addition to its C-terminal WD40 motifs (Wegrecki et al. 2015b; Thoms et al. 2015b). The Nop7-Erb1 interaction assay could not be performed by yeast two-hybrid assay, since the Nop7 fusions do not work in yeast two-hybrid assay. Heterologous expression and purification of Erb1 mutant proteins and wild type Nop7 from *E. coli* to test Erb1 mutant- Nop7 interaction was not successful either.

Figure 28

A



B



**Figure 28. A major portion of the N-terminal half of Erb1 is not required for its interaction with Ytm1.** (A) Schematic of the two-hybrid analysis of the interaction between Erb1 mutant proteins and Ytm1. Positive interactions activate transcription of the reporter genes *ADE2* and *HIS3*, which allow yeast cells to grow in the absence of adenine (Ade) or histidine (His). (B) Tenfold serial dilutions of the two-hybrid reporter strains containing appropriate plasmids were spotted on control (C-Leu-Trp) or test (C-Leu-Trp-Ade or C-Leu-Trp-His + 25 mM 3AT) media. We used 3-aminotriazole, a competitive inhibitor of the *HIS3* gene, to assay the strength of interaction between Erb1 and Ytm1 (column 3). WT Erb1 and Ytm1 interact with each other at high strength, allowing cells to grow in medium containing up to 25mM 3AT (lane 3).

#### 2.2.4 Erb1 is required for the processing of both 27SA<sub>3</sub> and 27SB pre-rRNAs during 60S ribosomal subunit assembly

The effects of individual *erb1* internal deletions on pre-rRNA processing were assayed by primer extension (Figure 29). The levels of 27SA<sub>3</sub> pre-rRNA and 27SB pre-rRNA were quantified in relation to the control U2 snoRNA. Depletion of Erb1 resulted in accumulation of 27SA<sub>3</sub> pre-rRNA and a significant reduction in the level of its product, 27SB<sub>s</sub> pre-rRNA, as observed previously (Figure 29, lane 3) (Miles et al. 2005). We observed three classes of pre-rRNA processing phenotypes in the *erb1* internal deletion mutants:

- (a) Class 1, resembling WT *ERB1* (*erb1*<sub>del3-50</sub>, *erb1*<sub>del51-100</sub>, and *erb1*<sub>del101-160</sub>) (Figure 29, Lanes 4-6)
- (b) Class 2, showing accumulation or no change in levels of 27SB pre-rRNA (*erb1*<sub>del161-200</sub>, *erb1*<sub>del201-245</sub>). No change was observed in the levels of 27SA<sub>3</sub> pre-rRNA in these mutants, indicating they are blocked at a step later than 27SA<sub>3</sub> pre-rRNA processing (Figure 29, Lanes 7-8). Further assays show that these mutants are blocked in the formation of 7S pre-rRNA, consistent with a block in cleavage of ITS2 (Figure 30).
- (c) Class 3, exhibiting accumulation of 27SA<sub>3</sub> pre-rRNA (*erb1*<sub>del246-310</sub>, *erb1*<sub>del311-365</sub>, *erb1*<sub>del366-419</sub>) (Figure 29, Lanes 9-11).

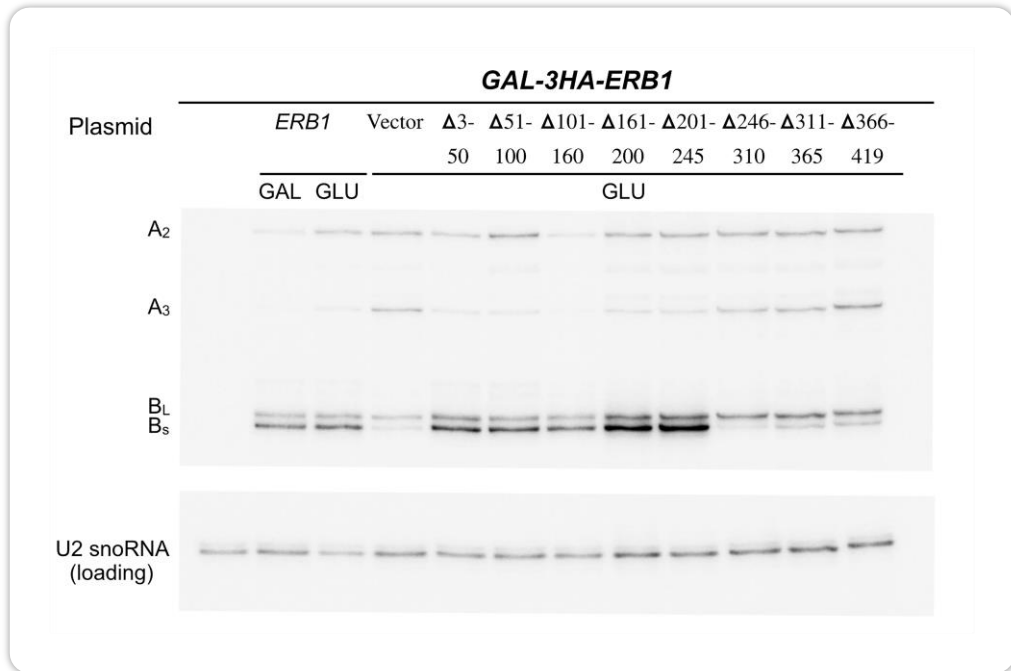
Steady-state levels of pre-rRNA processing intermediates in *erb1* internal deletion mutants were further assayed by northern blotting (Figure 30A). Depletion of Erb1

results in accumulation of 27SA<sub>3</sub> pre-rRNA. We also observe an increase in 35S pre-rRNA, as expected (row 3). This increase in 35S pre-rRNA is thought to be due to the slowing down of preceding pre-rRNA processing steps when 27SA<sub>3</sub> pre-rRNA processing is blocked. These pre-rRNA processing phenotypes of *erb1* internal deletion mutants were in agreement with the classification based on primer extension. (a) Class 1 mutants (*erb1<sub>del3-50</sub>*, *erb1<sub>del51-100</sub>*, and *erb1<sub>del101-160</sub>*) did not show any defects in pre-rRNA processing; (b) class 2 mutants (*erb1<sub>de161-200</sub>*, *erb1<sub>del201-245</sub>*) showed a marked increase in 27SA+B pre-rRNAs. The 27SA+B shows a slight shift in size towards lower molecular weight, indicating an accumulation of 27SB pre-rRNA(Figure 29A) We observe that formation of 7S pre-rRNA is blocked in the class 2 mutants (Figure 29B). (c) The class 3 mutants (*erb1<sub>del246-310</sub>*, *erb1<sub>del311-365</sub>*, *erb1<sub>del366-419</sub>*) were comparable to depletion of *erb1* (Figure 30B, lanes 9-11).

The plasmid pOBD2-*erb1* expresses *erb1* as an N-terminal fusion of GAL4-DNA binding domain. To rule out any bias in our observations due to the epitope-tag, we constructed the plasmid pAG414-GPD-EGFP-ERB1, which expresses *ERB1* with an N-terminal GFP tag fusion. The *erb1<sub>class 2</sub>* and *erb1<sub>class 3</sub>* mutants failed to support growth of the *GAL-ERB1* strain in glucose-containing solid media (Figure 26B). The pre-rRNA processing defects in the *GAL-3HA-ERB1* + pAG415-GPD-EGFP *erb1<sub>class 2</sub>* or *erb1<sub>class 3</sub>* mutants were similar to our previous observations (Figure 31).

**Figure 29**

A



B

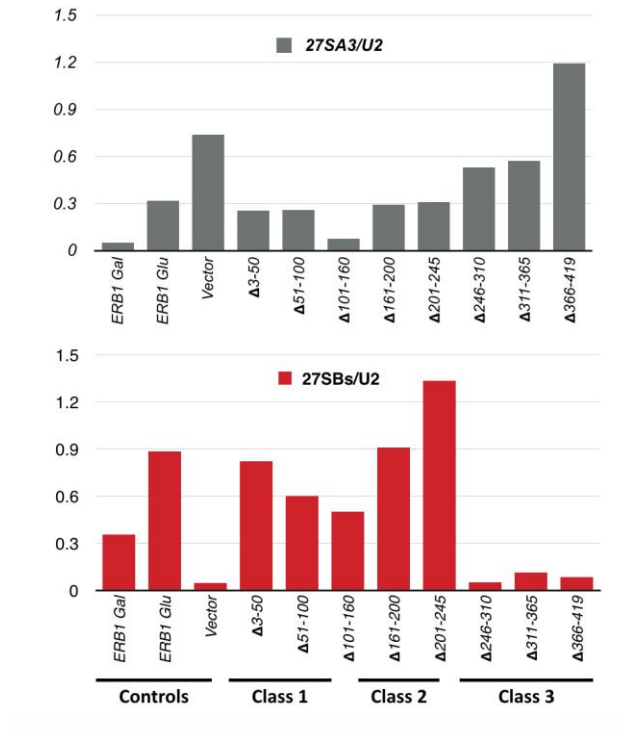


**Figure 29. *erb1*- internal deletion mutants are categorized into three classes based on pre-rRNA processing phenotypes (by primer extension).** (A) Steady-state levels of pre-rRNAs extracted from *GAL-3HA-ERB1* strains containing WT/mutant *erb1* plasmids were assayed by primer extension using an oligonucleotide primer that hybridizes to the ITS2 spacer (ITS2-B oligonucleotide). (B) Amounts of 27SA<sub>3</sub> and 27SB pre-rRNAs were quantified relative to U3 snoRNA. The *erb1* internal deletion mutations with WT-like pre-rRNA processing are categorized as class 1 (lanes 4-6), 27SB pre-rRNA processing defects as class 2 (lanes 7-8), and depletion-like accumulation of 27SA<sub>3</sub> as class 3 (lanes 9-11).



**Figure 30. *erb1*- internal deletion mutants can be categorized into three classes based on pre-rRNA processing phenotypes (by northern blotting).** (A) Steady-state levels of pre-rRNAs extracted from *GAL-3HA-ERBI* strains containing WT/mutant *erb1* plasmids were assayed by northern blotting using probes specific for the ITS2 spacer (ITSA for 27A+B and 35S pre-rRNA), 25S rRNA and 18S rRNA. (B) Steady-state levels of 7S pre-rRNA and 5S rRNA (probed with oligonucleotides binding to the ITS2A spacer and 5S rRNA) in *GAL-3HA-ERBI* strains containing *erb1*<sub>class 2</sub> mutants grown in galactose (control) or glucose (experiment). Consistent results were obtained in two or more independent experiments.

Figure 30C

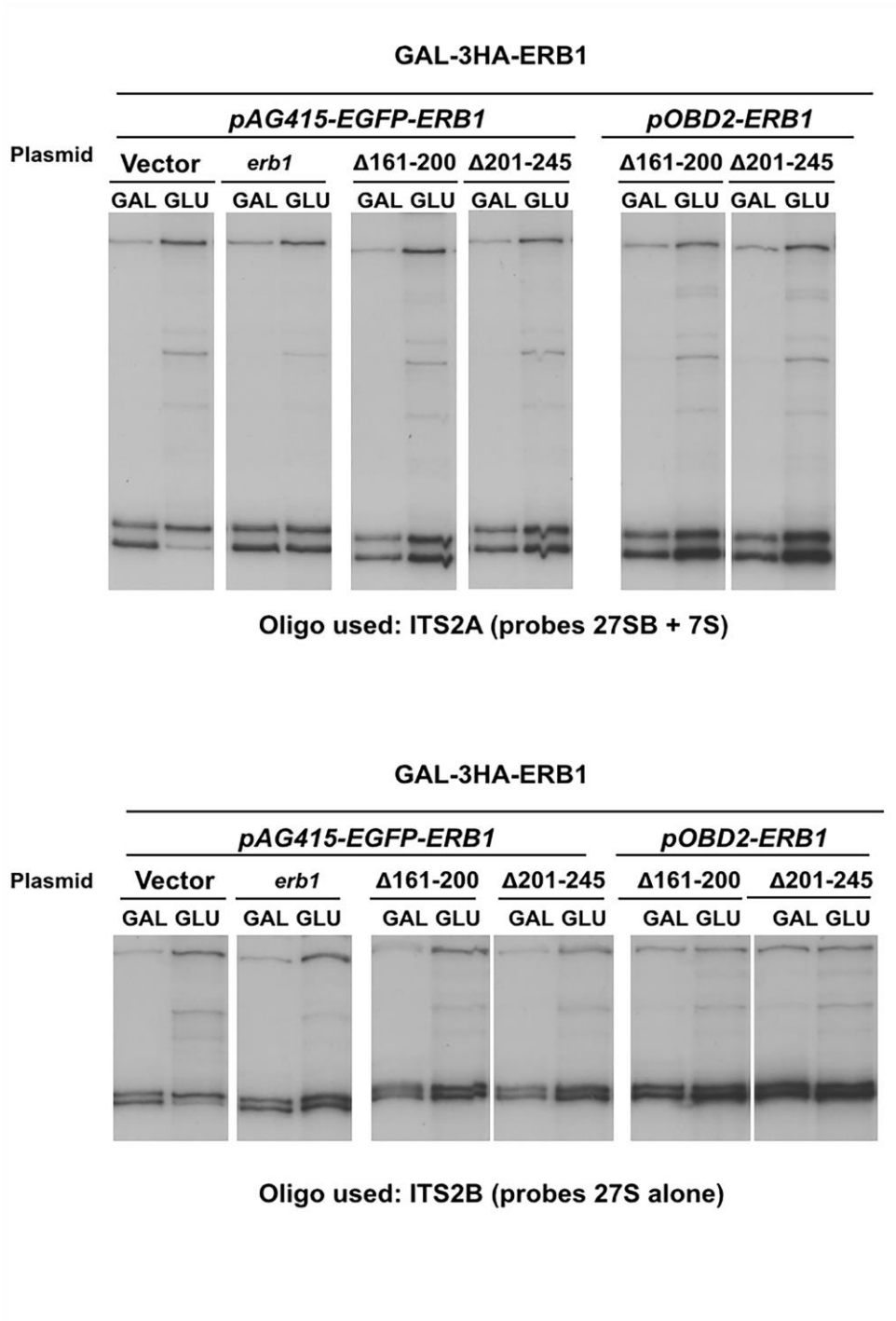


**Figure 30C. Pre-rRNA processing defects in cells expressing *erb1*<sub>class 2</sub> mutants from different plasmids.** The plasmid pOBD2-*ERB1* used in the previous experiment expresses WT/mutant Erb1 protein with a GAL4-DNA binding domain fused to its N-terminus. To rule out bias in the experimental observation, pAG414-GPD-EGFP-*ERB1* plasmids containing *erb1* internal deletion mutations were constructed and introduced into the *GAL-3HA-ERB1* strain. Steady-state levels of pre-rRNAs in total RNA extracted from these *GAL-3HA-ERB1* strains containing WT/mutant *erb1* plasmids were assayed by primer extension using the ITS2-A or ITS2-B oligonucleotide primers.

#### **2.2.4 The pre-ribosomal composition of the three classes of *erb1* mutants concurs with their pre-rRNA processing defects.**

To verify the classification of the *erb1* internal deletions, we purified preribosomes using the TAP-tagged assembly factor Rpf2 as bait. We resolved proteins in these preribosomes using SDS-PAGE and visualized the bands by silver staining. Many of proteins in these bands were previously identified by mass spectrometry (Zhang et al. 2007). Depletion of Erb1 affects stable association of the interdependent A<sub>3</sub>-cluster proteins Erb1, Nop7, Ytm1, Nop15, Cic1, Nop12, and Pwp1 (Figure 31A), as previously demonstrated (Sahasranaman et al. 2011; Miles et al. 2005; Tang et al. 2008). Changes in preribosome composition of the three classes of *erb1* internal deletion mutants are in agreement with the pre-rRNA processing phenotypes of these mutants.

- (1) The WT-like *erb1<sub>class 1</sub>* mutants did not show any significant changes in preribosome composition (Figure 31B).
- (2) The association of interdependent A<sub>3</sub> factors was not perturbed *erb1<sub>class 2</sub>* mutant preribosomes. Preribosomes are stable in these mutants compared to *erb1<sub>class 3</sub>* or *erb1* depletion mutants (Figure 31C).
- (3) The *erb1<sub>class 3</sub>* mutants displayed a silver-stained pattern similar to depletion of Erb1 (Figure 31D and 31A). We observe a significant decrease in the intensity of gel bands corresponding to the interdependent A<sub>3</sub>-cluster proteins Nop7, Ytm1, Cic1, Nop15, Nop12 and Has1.

To summarize, the preribosome composition of the three classes of *erb1* mutants is in agreement with their pre-rRNA processing phenotypes. The *erb1<sub>class 3</sub>* mutants were similar to depletion of *erb1*. The observed phenotype of the *erb1<sub>class 3</sub>* mutants is due to

the collective absence of the interdependent A<sub>3</sub>-factors. On the other hand, the *erb1<sub>class 2</sub>* mutants blocked 60S ribosomal subunit assembly at a later step of pre-rRNA processing than *erb1* depletion, and the preribosomes were more stable. But, the intensities of a few bands seemed to decrease by visual inspection. Therefore, changes in protein composition of these class 2 mutant preribosomes with respect to wild type were further assayed using a semi-quantitative mass spectrometric iTRAQ method (Ross et al. 2004)

Figure 31A

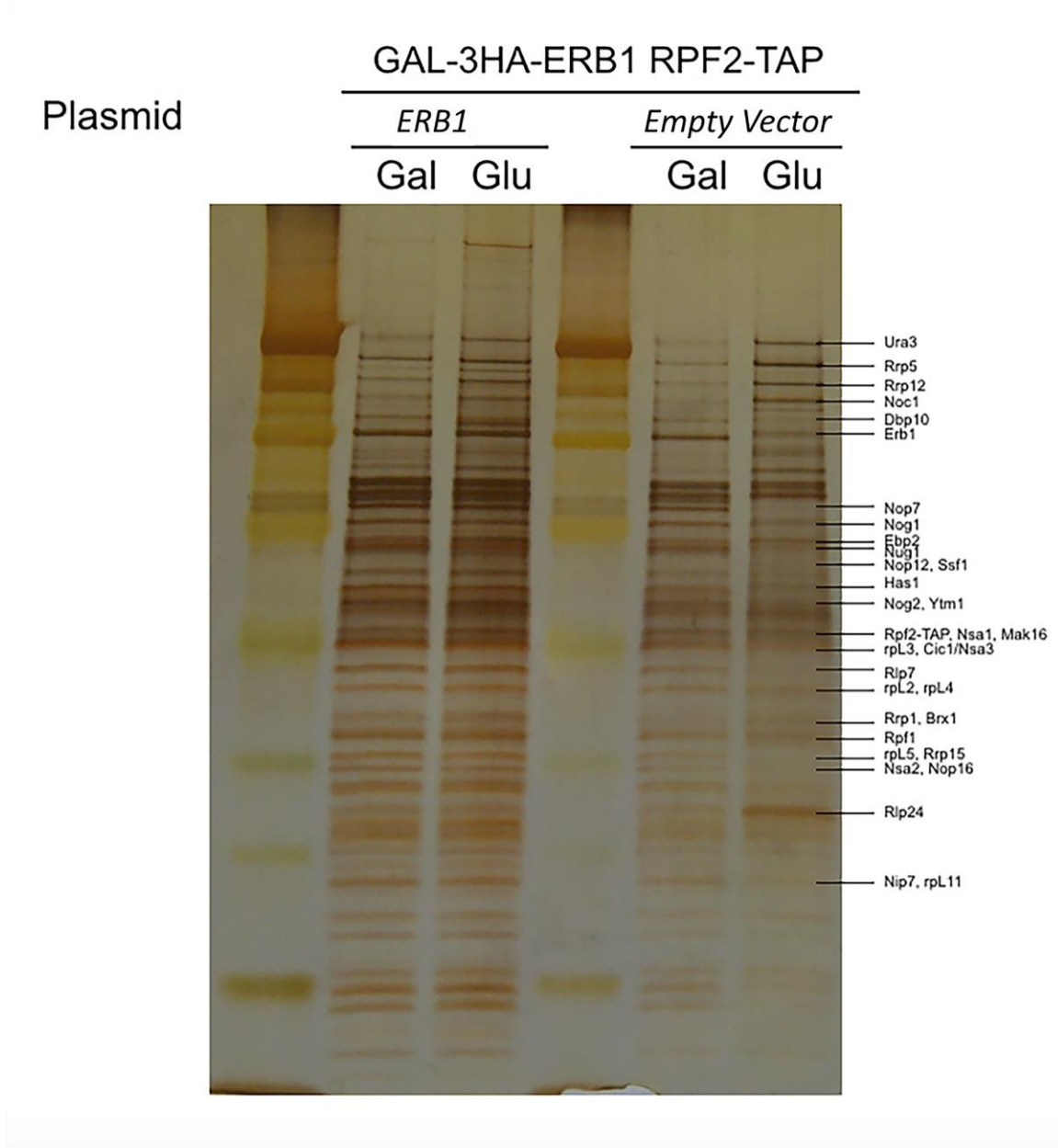


Figure 31B

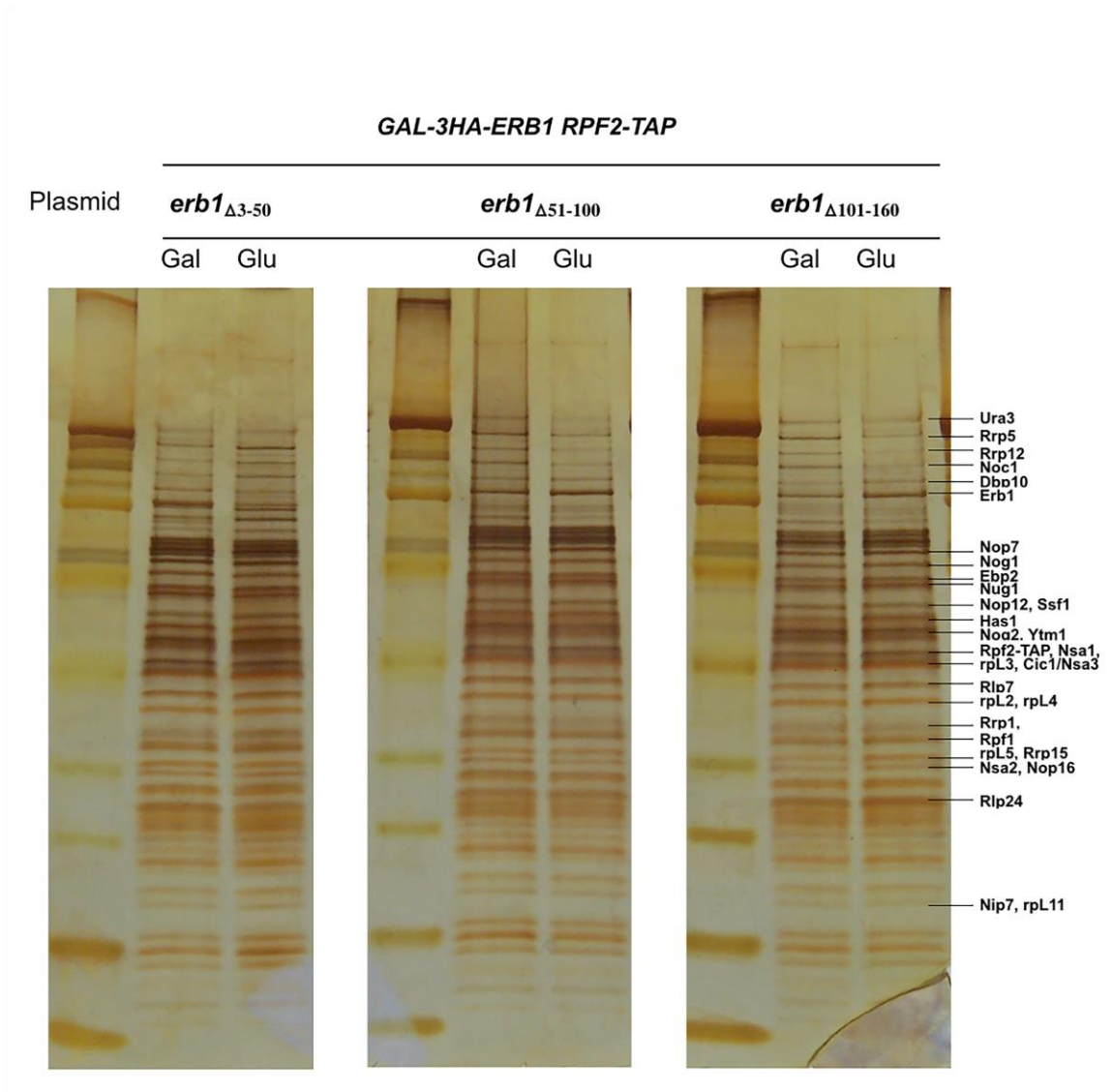


Figure 31C

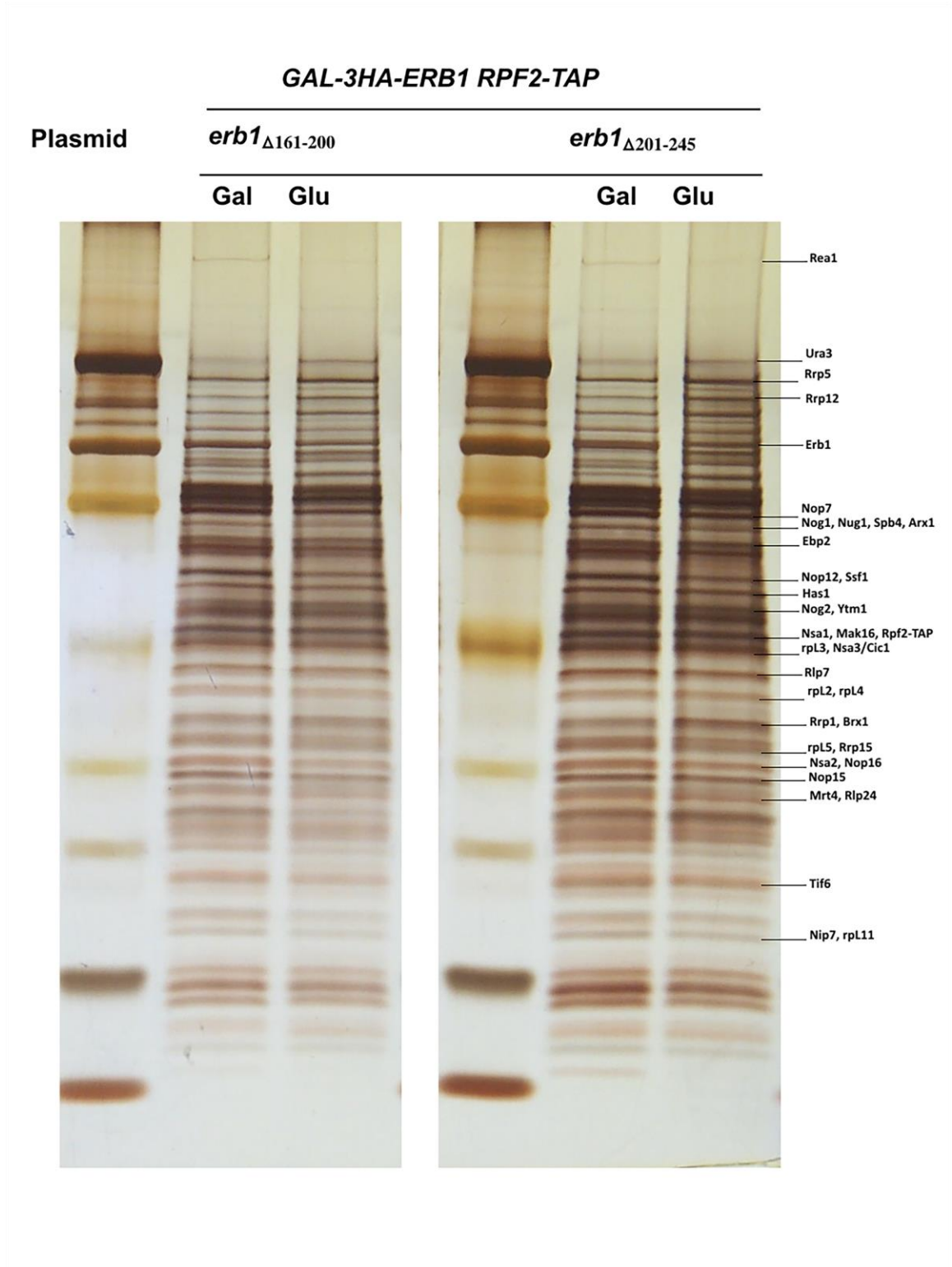
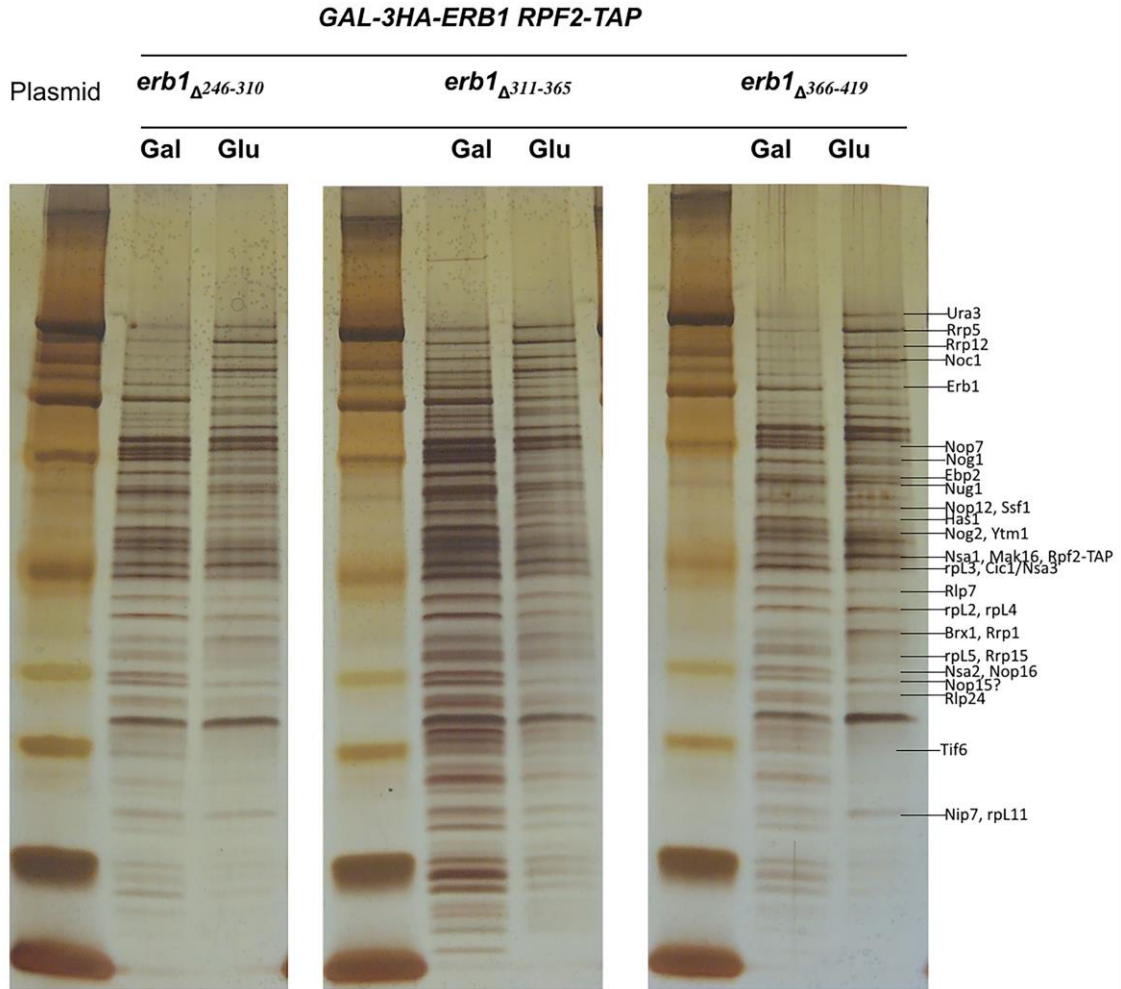


Figure 31D



**Figure 31. Preribosomes purified from *erb1<sub>class 2</sub>* mutants are more stable compared to depletion of Erb1.**

*GAL-3HA-ERB1* cells containing TAP-tagged assembly factor Rpf2 were used to purify 90S and 66S preribosomes from yeast cells grown in selective media containing galactose (Gal), or grown in galactose and then shifted to glucose (Glu) to deplete WT Erb1 protein. Proteins present in purified preribosomes were resolved on an SDS-PAGE gel and visualized by silver staining. Bands are marked as identified by mass spectrometry from previous experiments and this work. (A) Strains containing WT Erb1 or empty vector were used as controls. The A<sub>3</sub> factors (Erb1, Nop7, Ytm1, Nop15, Cic1, Nop12, and Has1) fail to stably associate with preribosomes when Erb1 is depleted. (B) Preribosomes purified from strains containing *erb1<sub>class 1</sub>* mutations are stable. (C) Preribosomes purified from strains containing *erb1<sub>class 2</sub>* plasmids contain bands corresponding to the interdependent A<sub>3</sub> factors. (D) *erb1<sub>class 3</sub>* mutations result in a depletion-like phenotype characterized by the absence of bands corresponding to the A<sub>3</sub> factors.

### **2.2.5 Stable association of specific assembly factors required for 27SB pre-rRNA processing is affected in *erb1<sub>class 2</sub>* mutants**

To determine global changes in protein-composition of preribosomes in the *erb1<sub>class 2</sub>* mutants, we performed semi-quantitative mass spectrometric iTRAQ analysis. We compared preribosomes purified from *GAL-ERB1 + erb1<sub>class 2</sub>* strains grown in galactose (WT *erb1* ON), or grown in galactose and then shifted to glucose (WT *erb1* OFF), using Rpf2-TAP as bait (Ross et al. 2004; Dembowski et al. 2013a; Ohmayer et al. 2013; Gamalinda et al. 2014; Sahasranaman et al. 2011). The mass spectrometric experiment was performed by Anne Stanley at the Stanley Lab, College of Medicine, Penn State University, Hershey, PA. We identified 450 proteins with  $\geq 95\%$  confidence. The data analysis was performed as described in Figure 32.

**Figure 32**

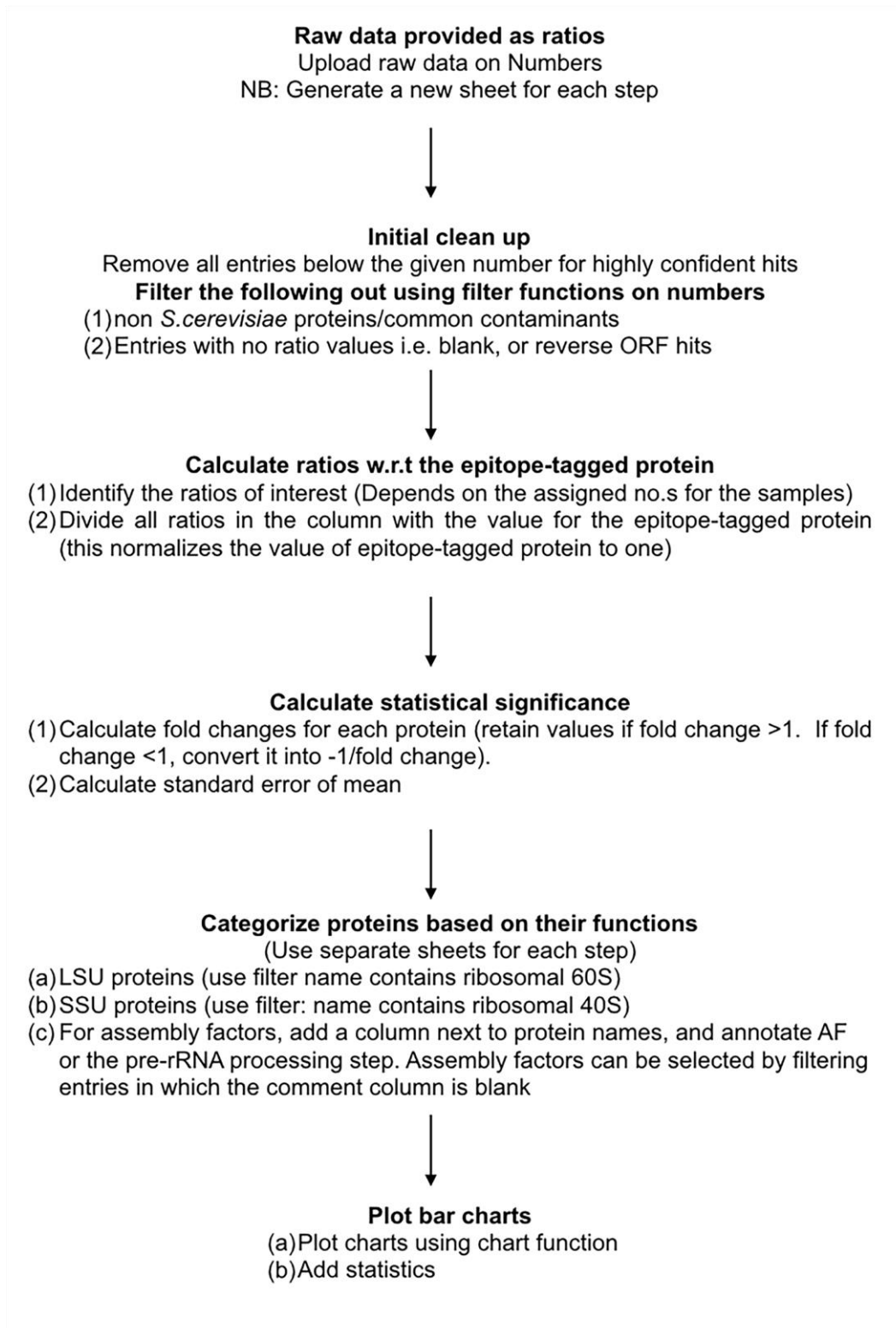


**Figure 32. Schematic flow chart for the analysis of iTRAQ data.**

The changes observed for assembly factors in *erb1<sub>class 2</sub>* largely correlate with their lifetime and function in pre-60S intermediates. The changes in the two *erb1<sub>class 2</sub>* mutants are qualitatively comparable and differed mostly in the magnitude of their change. This suggests that ribosome assembly is blocked in a very similar fashion in these two mutants (Figure 33). We observed an increase in the association of most early-acting assembly factors, which could be due to a failure to release them or due to a relative enrichment of early preribosomes when 27SB pre-rRNA processing is slowed down (Figure 33B, top panel). Consistent with the silver-stained SDS-PAGE gel (Figure 31C), the interdependent A<sub>3</sub> factors (Erb1, Ytm1, Nop7, Nop15, Rlp7, and Cic1) associate stably with preribosomes (Figure 2.13A). We also observe an increase in the levels of A<sub>3</sub> assembly factors Rpf1, Pwp1 and Nop12, which indicates a failure in their timely removal. Association of the DEAD-box helicases Drs1 and Has1, and the exonuclease Rat1 required for 27SA<sub>3</sub> pre-rRNA processing is not affected. These results are consistent with a block in C<sub>2</sub> cleavage, after the 27SA<sub>3</sub> pre-rRNA processing event.

Most assembly factors required for the C<sub>2</sub> cleavage in 27SB pre-rRNA were able to stably associate with preribosomes (Rrs1, Nop2, Nip7, Mak11, Dbp10, Rlp24, Tif6, and Nog1) in *erb1<sub>class 2</sub>* mutants, with the exception of Nsa2, Nog2, Spb4, Cgr1, and (Figure 33). Nsa2 and Nog2 bind the peptidyl transferase center in the domain V of 25S rRNA (Figure 15) (Shan *et al.*, (2016), submitted) (Leidig *et al.* 2014; Matsuo *et al.* 2014a; Bradatsch *et al.* 2012). The association of the endonuclease Las1 performing C<sub>2</sub> cleavage was not affected (Gasse *et al.* 2015). We observe two hits for the assembly factor Spb1 in our mass spec data, both of which show significant variation or error.

Hence, we did not consider these data while making any conclusions. The association of assembly factors involved in downstream processing of 7S pre-rRNA, i.e. Nog2, Rsa4, Nop53, Nug1, and Ipi1/Ipi2/Ipi3, is significantly reduced. We observe reduced association of the export factors Arx1 and Bud20 with preribosomes. Taken together, these results are consistent with a block in middle steps of 60S subunit assembly in the *erbI<sub>class2</sub>* mutants.

Interestingly, we observed fewer changes in the levels of large subunit ribosomal proteins in comparison to r-protein mutants blocked in ITS2 cleavage of 27SB pre-rRNA or processing of ITS1 in 27SA<sub>3</sub> pre-rRNA (Figure 33B, bottom panel) (Dembowski et al. 2013a; Sahasranaman et al. 2011; Gamalinda et al. 2013; Ohmayer et al. 2013; 2015; Gamalinda et al. 2014; Biedka et al. 2016, submitted). Specifically, the r-proteins L17, L35, L37, and L25 that bind to the 5.8S/domain I/domain III interface in 25S rRNA associated stably with the preribosomes. In the *erbI<sub>class 2</sub>* mutants, we observed slightly reduced levels of domain III binding r-protein L19B required for 27SB pre-rRNA processing (Gamalinda et al. 2014), suggesting that rRNA folding in domain III of 25S rRNA is affected in the *erbI<sub>class 2</sub>* mutants. We also observed reduction in the levels of the non-essential r-proteins L31 and L26 binding to domain III in the *erbI<sub>Δ161-200</sub>* mutant. L26 and L31 line the polypeptide exit tunnel and bind to the 5.8S/domain III/domain I interface, further strengthening our hypothesis that structuring of these regions is perturbed in *erbI<sub>class 2</sub>* mutants. These results indicate that the *erbI<sub>class 2</sub>* mutants are blocked at the recruitment of Dbp10, Nsa2, and r-protein L19 in the hierarchical recruitment pathway of assembly factors involved in 27SB pre-rRNA processing (Figure

34) (Dembowski et al. 2013a; Jakovljevic et al. 2012; Talkish et al. 2012a; Woolford and Baserga 2013).

Figure 33A

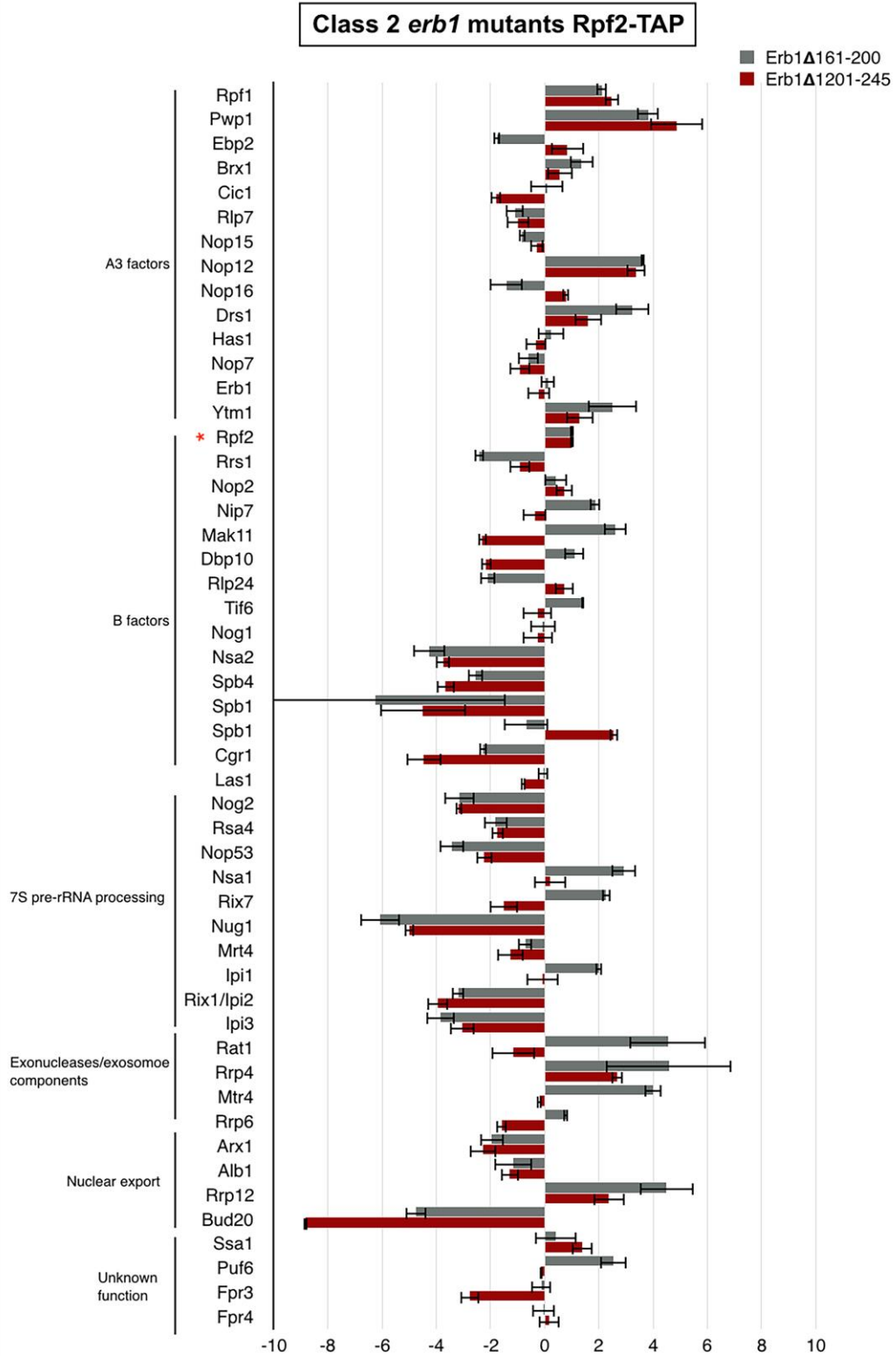
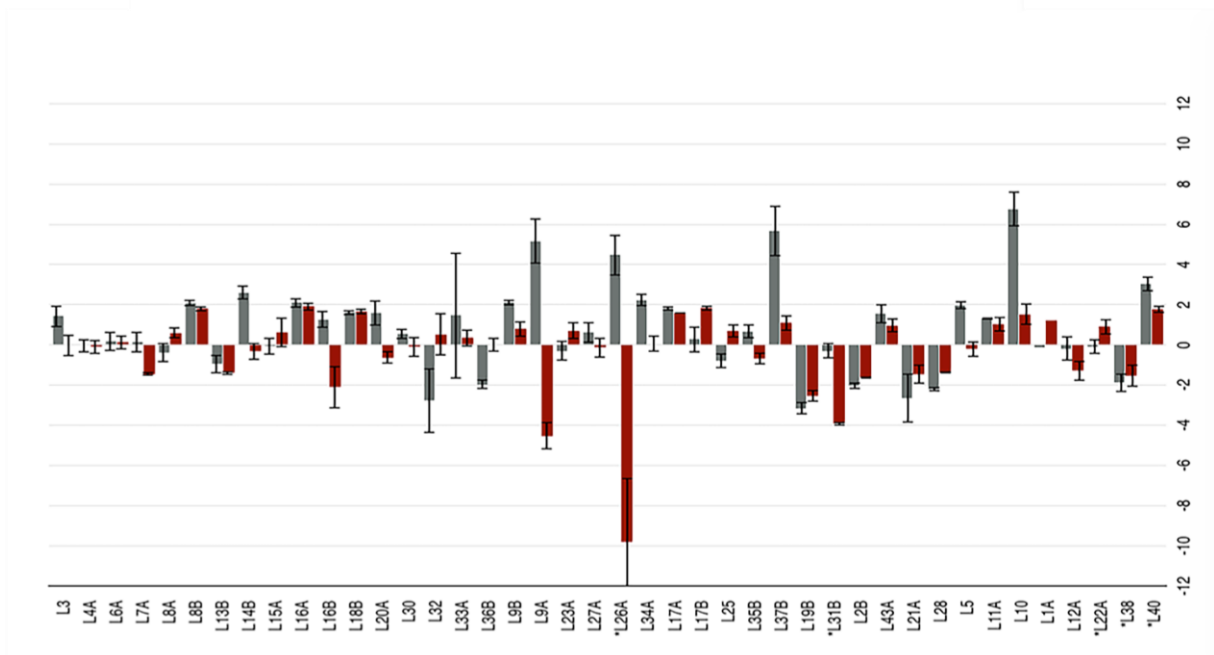
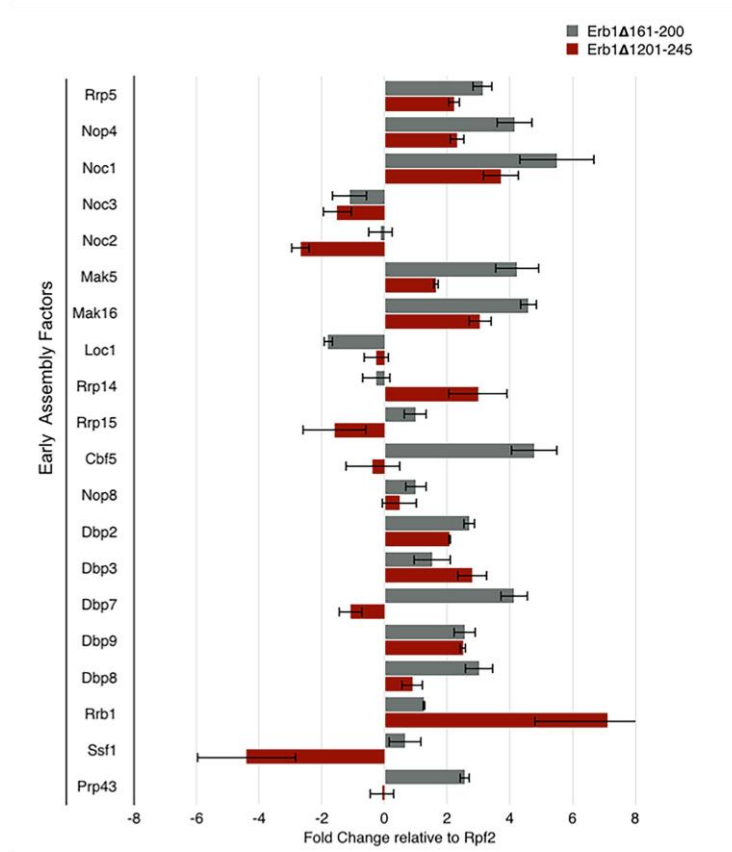
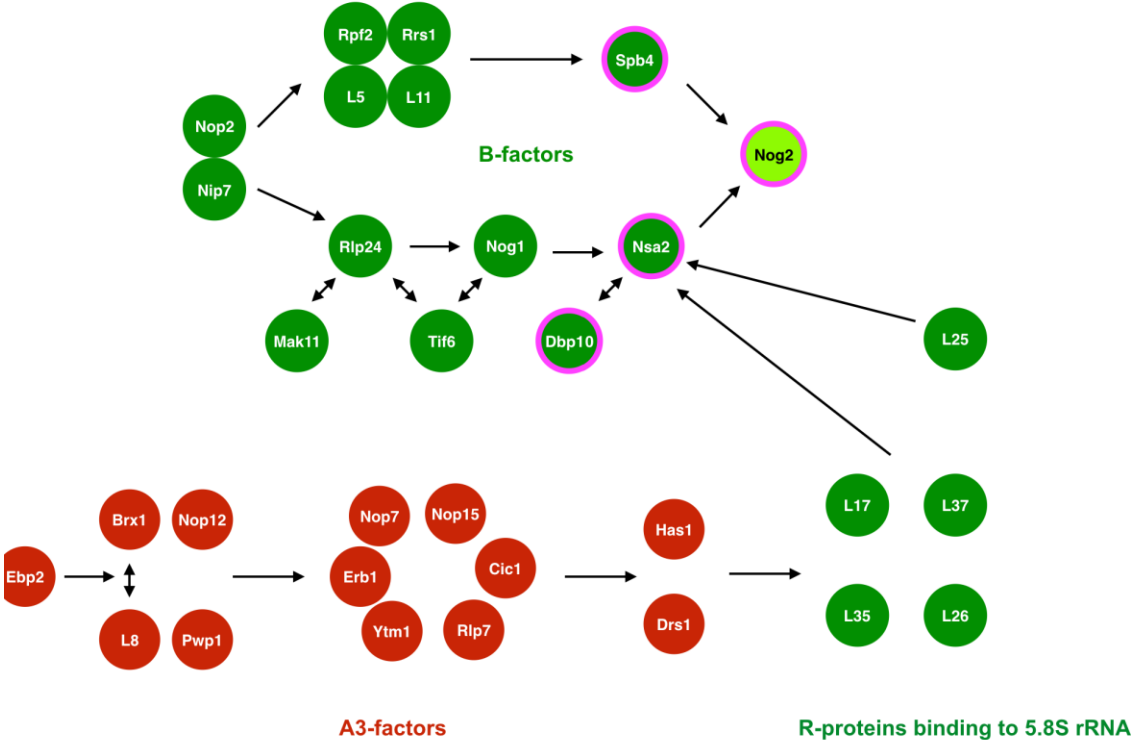


Figure 33B



**Figure 33. Erb1 is required for stable association of assembly factors involved in 27SB pre-rRNA processing.** Changes in the average relative ratios of assembly factors and r-proteins in 90S and 66S preribosomes in *erbI<sub>class 2</sub>* mutants were identified by iTRAQ of preribosomes purified using Rpf2-TAP (\*) as bait (average relative ratio of *erbI<sub>class 2</sub>* (Glu)/ *erbI<sub>class 2</sub>* (Gal)). Fold changes in the association of 66S assembly factors (A), early 90S assembly factors (B, top panel) and large subunit r-proteins (B, bottom panel) are shown. Data represent the average of four Glu/Gal ratios for each *erbI<sub>class 2</sub>* mutant, with the error bars representing the standard error of mean.

Figure 34



**Figure 34. *erb1<sub>class 2</sub>* mutants perturb the association of specific assembly factors involved in ITS2 cleavage and 27SB pre-rRNA processing.** Shown is a schematic representation of the hierarchical pathway for stable association of assembly factors and some r-proteins necessary for early and middle steps of 60S ribosomal subunit assembly. Proteins in the Pwp1-subcomplex, interdependent A<sub>3</sub> factors, and Has1 and Drs1 are required for 27SA<sub>3</sub> pre-rRNA processing (red). Stable association of the DEAD-box RNA helicases Drs1 and Spb4 depends on the preceding A<sub>3</sub> factors. These DEAD-Box proteins are, in turn, required for stable association of r-proteins that bind the 5.8S rRNA at the interface of domains I and III of 25S rRNA. The A<sub>3</sub> factors and 5.8S rRNA/domain III of 25S rRNA binding r-proteins are required for the stable association of a subset of assembly factors required for 27SB pre-rRNA processing (green). Stable association of assembly factors highlighted with the magenta outline is affected in *erb1<sub>class 2</sub>* mutants.

### **2.2.6 The structure of the bowtie region in 5.8S rRNA is affected in *erb1<sub>class 2</sub>* mutants**

Since the *erb1<sub>class 2</sub>* mutants prevent cleavage at the C2 site in pre-66S particles, we probed the structure of ITS2 and 5.8S rRNA by the Selective-2'-Hydroxyl Acylation analyzed by Primer Extension (SHAPE) method, using the chemical N-methylnicotinic acid imidazolide (NAI). SHAPE assays flexibility and solvent exposure of the 2'-OH group on the ribose sugar in both single- and double-stranded RNAs, providing information about base-pairing and tertiary interactions. Single-stranded or flexible regions react more with NAI, whereas RNA nucleotides engaged in intermolecular interactions exhibit low reactivity (Merino et al. 2005; Spitale et al. 2013). We analyzed the structure of ITS2 and 5.8S rRNA using oligonucleotide primers 5'-ITS2 and Oligo3140 that bind to different sequences in the ITS2. The 5.8S rRNA is sandwiched between domains I and domains III of 25S pre-rRNA. Therefore, folding of 5.8S rRNA was used as an assay to diagnose defects in rRNA folding of these regions.

Few modifications, except protection of two residues in ITS2 adjacent to the 5'-end of 5.8S rRNA, were observed in the ITS2 region, indicating that ITS2 structure is largely intact in *erb1<sub>class 2</sub>* mutants, after discounting the effects of loading (Figure 35). Observing only a few modifications in ITS2 is consistent with the stable association of the ITS2- associating A<sub>3</sub> factors Nop15, Rlp7, and Cic1 in *erb1<sub>class 2</sub>* mutants.

Figure 35

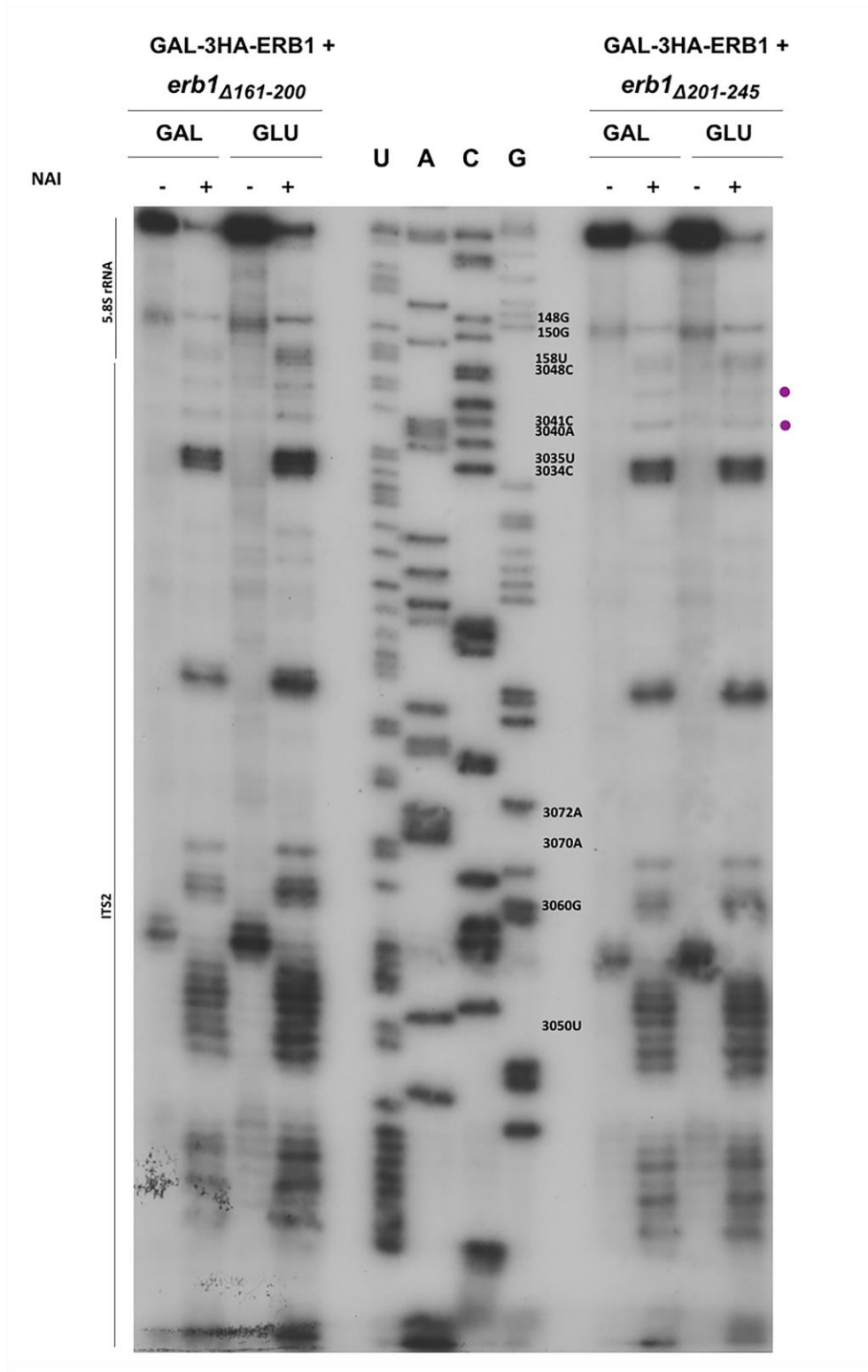


**Figure 35. The structure of ITS2 is largely intact in *erb1<sub>class 2</sub>* mutants.** The chemical NAI (indicated by +) was used to probe the structure of ITS2 in *GAL-3HA-ERB1 + erb1<sub>class 2</sub>* mutants grown in selective media containing galactose or shifted to glucose. Cells treated with DMSO alone (indicated by -) were used as controls. Total RNA extracted from NAI treated cells was used as substrate for primer extension (ITS2-3140). The locations of nucleotides that are protected are shown in magenta. The sequencing ladders are shown in lanes U, A, G and C. The nucleotide numbers in ITS2 are a continuation from the 5'-end of 25S rRNA.

The bowtie region in 5.8S rRNA was significantly modified in both *erb1<sub>class 2</sub>* mutants (Figures 36 and 37). We observe distinct changes in the modification pattern of the 5.8S rRNA helices in *erb<sub>class 2</sub>* mutants when compared to WT (Figure 36). The universal stop in 5.8S pre-rRNA (shown as a red circle) was used to assess loading-based changes in band intensities. The observed changes in primary sequence were then mapped onto the secondary structure of 5.8S rRNA (Figure 37A) and the tertiary structure of the 60S ribosomal subunit (Figure 2.17B) (Ben-Shem et al. 2011)(Shan *et. al* (2016), unpublished).

The contacts of L17, L35, L37, L39, L26 interacting with 5.8S rRNA are modified in our *erb1* class 2 mutants (Figure 37B). These r-proteins binding 5.8S rRNA are crucial to rRNA folding *in vivo* (Kwok et al. 2013). However, stable association of L17, L35, and L39 is not affected in the *erb1<sub>class 2</sub>* mutants (Figure 2.13B, bottom panel). Therefore, we conclude that the formation of the final, stabler conformation of weak helices h5-h9 in 5.8S rRNA and their r-protein contacts is perturbed in *erb1<sub>class 2</sub>* mutants. We observe selective protection or modification in 5.8S rRNA residues 75-85, protruding from helix 7. The GTPase Nog1 contacts residue 77, which is more modified in *erb1<sub>class 2</sub>* mutants (Figure 38C). Association of Nog1 to preribosomes is not affected in the *erb1<sub>class 2</sub>* mutants. Therefore, as it is the case with 5.8S rRNA binding r-proteins, the final contacts of Nog1 also seem to be perturbed in *erb1<sub>class 2</sub>* mutants.

Figure 36

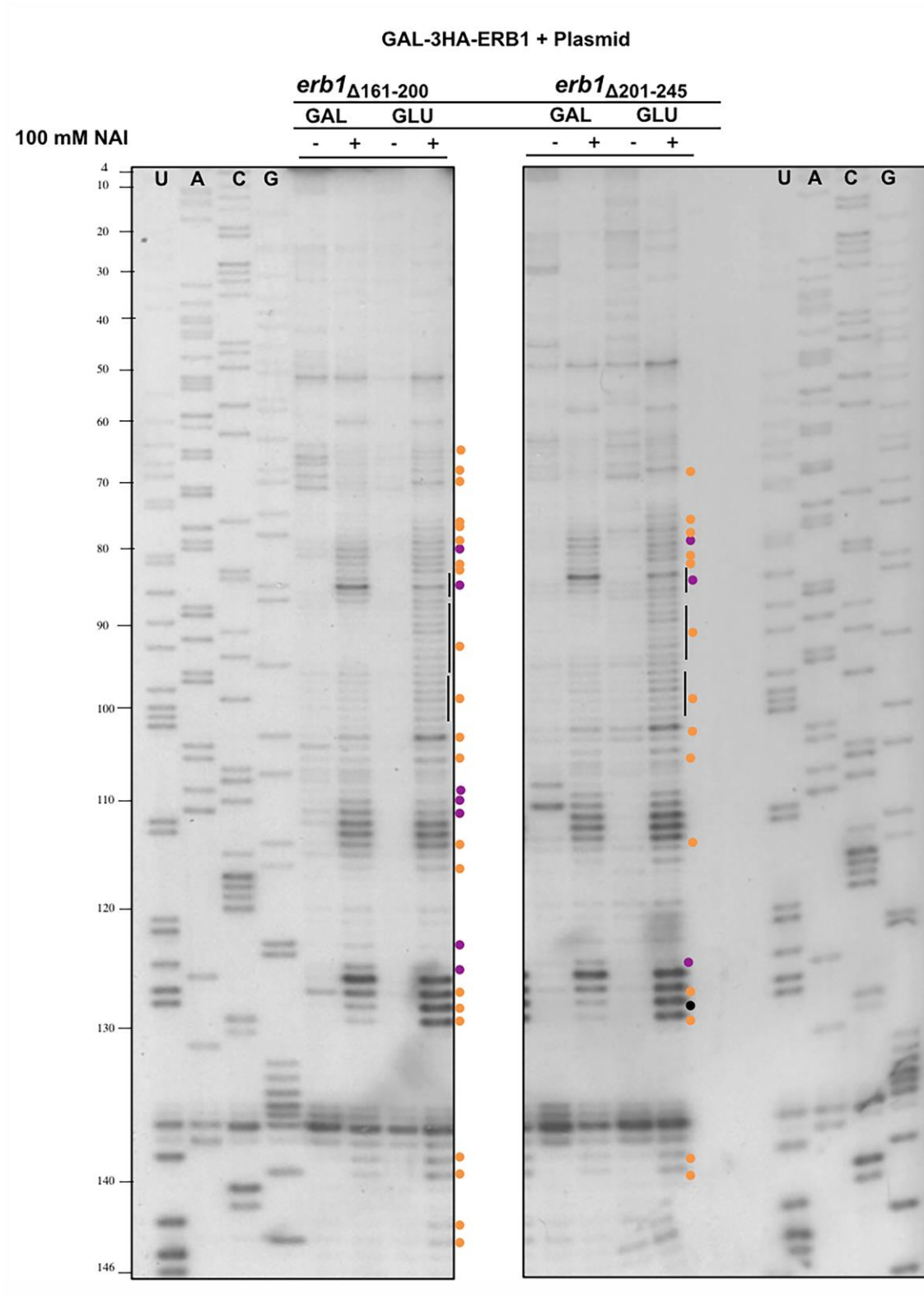


**Figure 36. The structure of 5.8S rRNA is perturbed in *erbI<sub>class 2</sub>* mutants.** The *in vivo* structure of 5.8S rRNA was probed using 100 mM NAI (indicated by +) in *GAL-3HA-ERB1* + *erbI<sub>class 2</sub>* mutants grown in selective media containing galactose, or grown in galactose and shifted to glucose. Cells treated with DMSO alone (indicated by -) were used as controls. Total RNA extracted from NAI treated cells was used as a substrate for primer extension (5'-ITS2 oligonucleotide primer). Locations of modified nucleotides are indicated in orange and protected residues are shown in magenta. The sequencing ladders are shown in lanes U, A, G and C.

Figure 37A

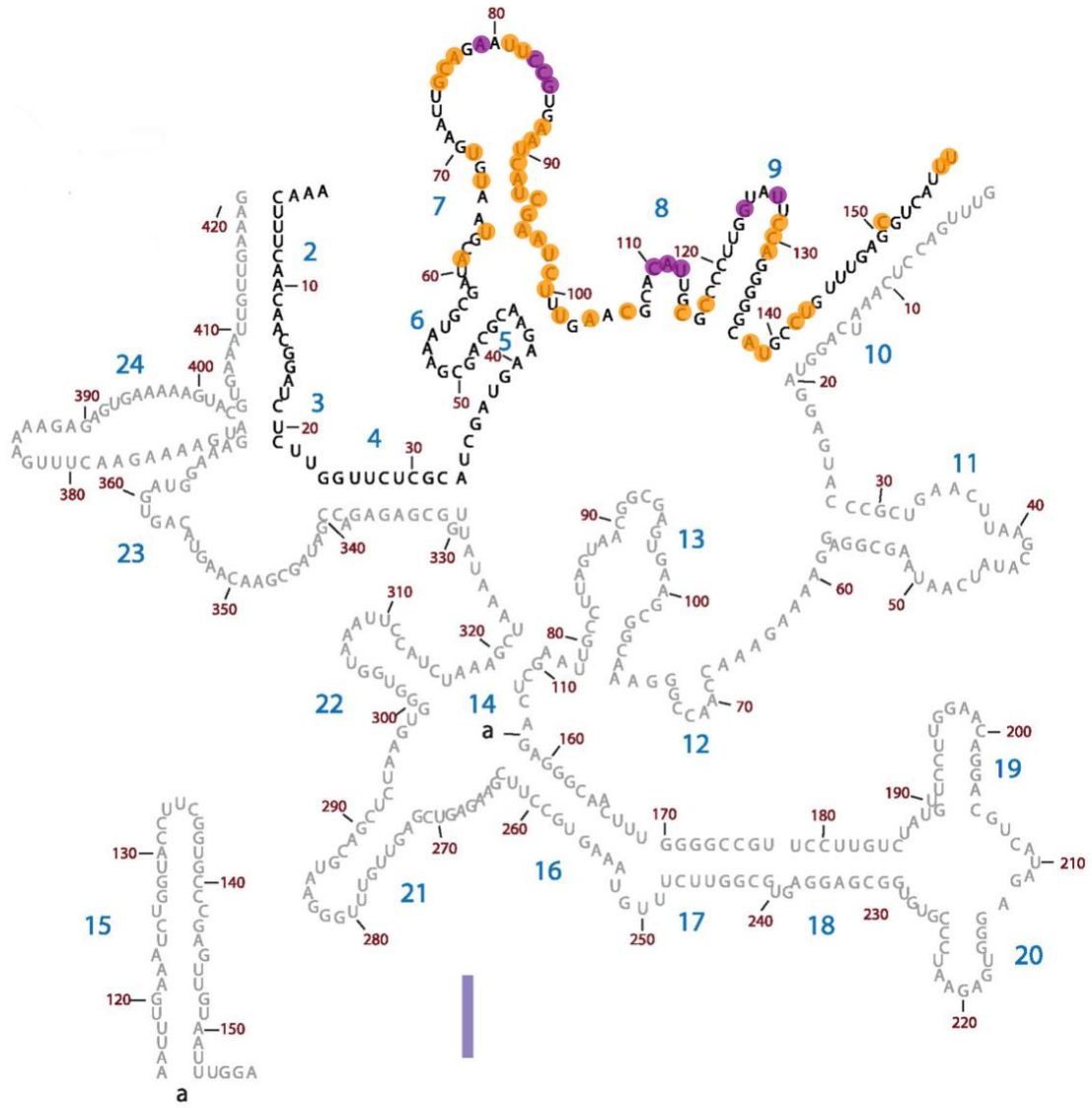
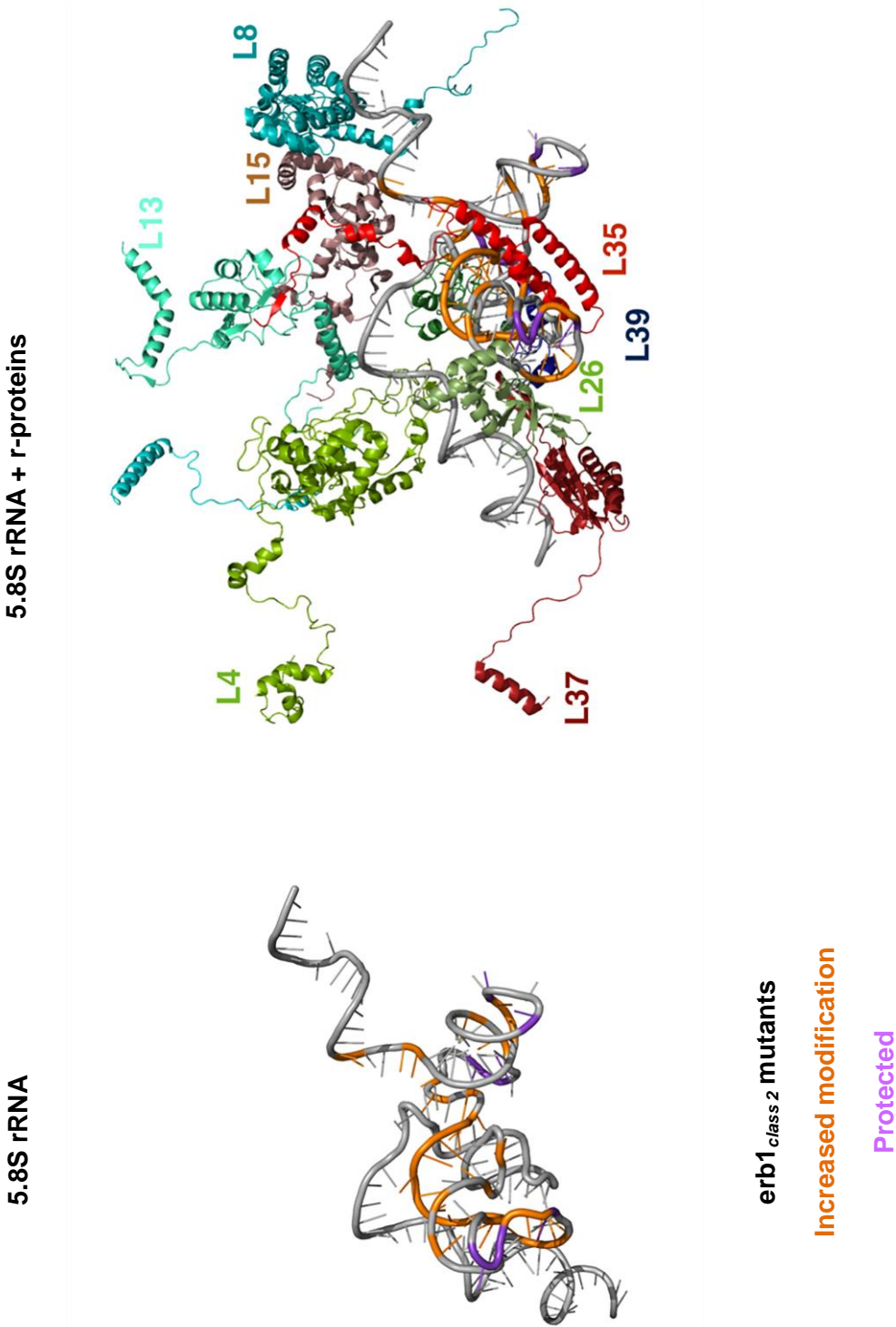


Figure 37B





## **CHAPTER 2. The Assembly Factor Erb1 Functions in a Molecular Interaction Network to Facilitate Cleavage of the ITS2 Spacer During 60S Subunit Assembly.**

### **2.1 Introduction**

Eukaryotic ribosome assembly is a multi-step process involving the intertwined processes of pre-rRNA processing and modification, RNA folding, and ribosomal protein binding, facilitated by more than 200 *trans*-acting proteins and small nucleolar RNPs. In recent years, a wealth of information has emerged about the nucleases performing most pre-rRNA processing and cleavage steps, and the dynamic nature of the pre-ribosomal complex. How molecular interactions in preribosomes drive decisions leading to each pre-rRNA processing or RNP remodeling event is not yet completely understood. My work discussed in this Chapter provides functional insights into the roles of the evolutionarily conserved Nop7-subcomplex in structuring the 5.8S pre-rRNA. I propose a model for how rRNA folding, r-protein binding and recruitment of assembly factors are coordinated to signal the cleavage at ITS2 spacer in 27SB pre-rRNA.

#### **The Nop7-subcomplex**

The Nop7-subcomplex, which is composed of the three assembly factors, Nop7, Erb1, and Ytm1, is essential for 60S ribosomal subunit assembly (Figure 20). In the absence of these proteins, exonucleolytic removal of the ITS1 spacer sequence in 27SA<sub>3</sub> pre-rRNA is perturbed, blocking formation of mature 60S subunits (Harnpicharnchai et al. 2001; Oeffinger et al. 2002; Adams et al. 2002a; Pestov et al. 2001; Miles et al. 2005;

Hölzel et al. 2005). In rapidly growing yeast cells, the majority of pre-rRNAs (~85%) of the 60S subunit undergo processing via this intermediate to generate the 5'-end of mature 5.8S<sub>s</sub> rRNA (Woolford and Baserga 2013).

The ability of the Nop7-subcomplex to form a heterotrimer has been demonstrated using yeast two-hybrid assays, *in vitro* GST pull-downs and various other biochemical assays (Miles et al. 2005; Rohmoser et al. 2007a). Erb1 is central to the formation of the subcomplex, since it interacts with both Nop7 and Ytm1 (Figure 20A). These proteins have no known intrinsic enzymatic activity, but all of them contain protein-protein interaction motifs. Even though Erb1 and Nop7 do not have conventional RNA binding motifs, they contact rRNA in domains I and III of 25S rRNA, respectively (Granneman et al. 2011).

Both Erb1 and Ytm1 contain the donut-shaped  $\beta$ -propeller structure formed by WD40 repeats (Figure 20B). WD40 repeats are composed of a repeating sequence of 40-60 amino acid residues containing variable regions of 11-24 amino acid residues, followed by a glycine-histidine dipeptide, and ends with a tryptophan (W)-aspartate (D) dipeptide. The WD40 domains are a common protein-protein interaction motif in eukaryotes. Three WD40 repeats fold into 4 anti-parallel  $\beta$ -strands that form each blade of the propeller (Figure 20B). Multiple WD40 repeats form a WD40 domain, which form the multi-bladed  $\beta$ -propeller. This organization enables intermolecular interactions via the top, the bottom, or the circumference of the propeller structure (Stirnemann et al. 2010; de la Cruz et al. 2005a; Baßler et al. 2014). The 60S ribosomal subunit assembly factors Rrb1, Rsa4, Ipi3, Pwp1, Mak11, and Sqt1 also contain WD40 repeats (Pausch et al. 2015; de la Cruz et al. 2005b; Merl et al. 2010; Talkish et al. 2014; Saveanu et al. 2007; Frénois

et al. 2016).

Recently multiple groups co-crystallized the WD40 domains of Erb1 and Ytm1, substantiating previous predictions that their WD40 domains interact with each other, based on mutational analysis of these proteins (Fig 20B) (Tang et al. 2008; Miles et al. 2005; Marcin et al. 2015; Romes et al. 2015; Thoms et al. 2015a; Wegrecki et al. 2015b). In addition to the WD40 repeats, Erb1 contains an equally long N-terminal domain. No group has successfully solved the crystal structure of this N-terminal half of Erb1 even when co-crystallized with Nop7 and Ytm1. The consensus is that this structure could be non-globular and extended, making it available for mediating other interactions. In fact, most proteins with WD40 domains also contain additional domains, increasing their ability to form molecular networks (Stirnemann et al. 2010). Several previous studies suggest that the Erb1-Nop7 interaction is potentially mediated by the N-terminal half of Erb1 (Tang et al. 2008; Thoms et al. 2015a; Strezoska et al. 2000). The domain architecture of Nop7 consists of an N-terminal conserved Pescadillo domain and a C-terminal BRCT domain flanked by two coiled-coils. Nop7 contacts preribosomes at the domain I/5.8S/domain III rRNA interface in the 66S preribosomes (Granneman et al. 2011; Wu et al. 2016, submitted). The BRCT-domain is also a protein-protein interaction domain. Thus, due to the prevalence of protein-protein interaction domains, the Nop7-subcomplex has the potential to serve as hub of protein-protein interactions providing platforms for complex assembly and regulation of macromolecular complexes. This is substantiated by the genetic and protein-protein interactions exhibited by the Nop7-subcomplex proteins (Figure 21) (McCann et al. 2015; Tarassov et al. 2008; Dembowski et al. 2013a; Talkish et al. 2012a; 2014; Honma et al. 2006; Miles et al. 2005; Saveanu et

al. 2003; Costanzo et al. 2010; Biedka et al. 2016, submitted) (Wu et al. 2016, submitted).

### **Moonlighting Functions of the Nop7-subcomplex proteins**

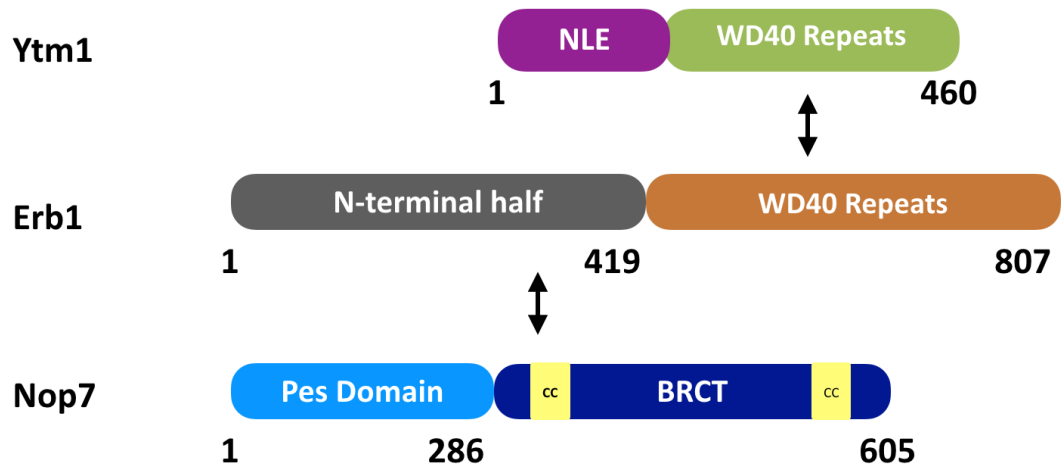
The roles of Nop7, Erb1, and Ytm1 in ribosome assembly have been established by (a) reduced levels of 60S subunits in their absence (by polysome analysis and pre-rRNA processing assays) and (b) their presence in preribosomes (CoIP of pre-rRNAs, other ribosome assembly factors, and interactions with other assembly factors) (Pestov et al. 2001; Adams et al. 2002; Oeffinger et al. 2002; Miles et al. 2005; Harnpicharnchai et al. 2002). In addition, there are additional known functions for these proteins in higher organisms:

- (1) Mutations in Bop1, the mammalian homolog of Erb1 causes p53-dependent cell cycle arrest (Pestov et al. 2001).
- (2) Yeast Ytm1 is implicated in mitosis and chromosome transmission (Oupenski et al. 1999)
- (3) Pes1 is known to interact with the origin replication complex, and is required for hyphal- to-yeast morphogenesis in *C. albicans* (Du et al. 2002; Shen et al. 2008). Pes1 also is implicated in normal development, and in regulating cancer progression and sensitivity of cancer cells to chemotherapeutic drugs (Tecza et al. 2011; Xie et al. 2013; Cheng et al. 2012).

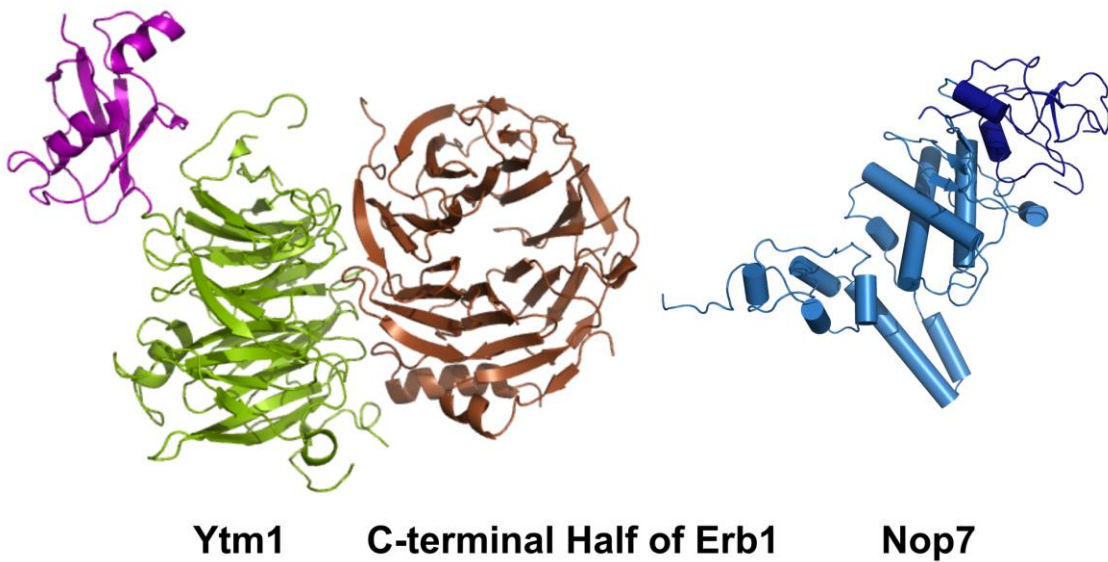
Therefore, the Nop7-subcomplex might serve as a link between ribosome assembly and the cell cycle. If and how Nop7, Erb1 and/or Ytm1 function as links between these processes remain to be understood.

Figure 20

A



B



**Figure 20. Molecular architecture of the Nop7-subcomplex** (A) A schematic representation of the domain architecture of Nop7, Erb1, and Ytm1 is shown. (B) A high-resolution structure of Ytm1 in complex with the C-terminal half of Erb1, and certain portions of Nop7 (Wegrecki et al. 2015a)(Wu et al. (2016), submitted), (PDB ID: 5CXC). The Notchless-like-element (Nle) of Ytm1 interacts with the AAA-ATPase Rea1 (Midasin or Mdn1); its WD40 (Romes et al. 2015; Thoms et al. 2015) domain repeats interact with Erb1 (Baßler et al. 2010b).

The Nop7-subcomplex proteins (Nop7, Erb1, Ytm1) are among the seven assembly factors (also Rlp7, Cic1, Nop15, and Pwp1) interdependent for their association with preribosomes (Figure 21). Their interdependence is partly contributed by direct protein-protein interactions between many of these proteins. (Miles et al. 2005; Sahasranaman et al. 2011). In addition to the interdependent A<sub>3</sub> factors, assembly factors Ebp2, Brx1, Nop12, Drs1, and Has1 are also required for processing of 27SA<sub>3</sub> pre-rRNA (Dembowski et al. 2013a; Talkish et al. 2014; Biedka et al. 2016, submitted). Even though depletion of these proteins blocks processing of the ITS1 spacer in 27SA<sub>3</sub> pre-rRNA, many of them bind 25S rRNA adjacent to the ITS2 spacer sequence (Figure 12) (Granneman et al. 2011; Wu et al. 2016, submitted). This suggested that the role of these A<sub>3</sub> factors in ITS1 processing is indirect. The A<sub>3</sub> protein-protein and protein-RNA interaction network may be necessary to create a preribosome structure stable enough to undergo 27SA<sub>3</sub> pre-rRNA processing. In their absence, preribosomes are turned over rapidly (Jakovljevic et al. 2012; Sahasranaman et al. 2011). Therefore, these A<sub>3</sub> factors could have more direct roles in the removal of the ITS2 spacer in 27SB pre-rRNA. Work in this thesis tested this hypothesis and provides evidence for a direct role of the A<sub>3</sub> factor Erb1 in removal of the ITS2 spacer in 27SB pre-rRNA.

Nop7, Erb1, and Ytm1 enter 90S preribosomes, early in the assembly pathway, since they co-purify 35S pre-rRNA (Sahasranaman et al. 2011; Miles et al. 2005). The AAA-ATPase Rea1 drives the exit of Erb1 and Ytm1 from preribosomes (Baßler et al. 2010a; Thoms et al. 2015a; Wegrecki et al. 2015b) (Figure 22). Whether Nop7 exits preribosome with Erb1 and Ytm1 is not completely understood, since it co-purifies significantly higher amounts of the late intermediate 7S pre-rRNA compared to Erb1 and

Ytm1 (Granneman et al. 2011; Altvater et al. 2012). The *in vitro* assays showing remodeling activity of Rea1 on preribosomes provided evidence for only partial removal of Nop7 from preribosomes (Baßler et al. 2010a). Therefore, Nop7 might have sub-complex independent roles in ribosome biogenesis, about which nothing is known yet.

The mammalian homologs of the Nop7-subcomplex form the PeBoW subcomplex composed of Pes1, Bop1, and WDR12 (mammalian Nop7, Erb1, and Ytm1 homologs, respectively) (Moilanen et al. 2015; Rohrmoser et al. 2007b; Hölzel et al. 2005; Pestov et al. 2001; Strezoska et al. 2000; Hölzel et al. 2007a; Pestka 1968; Allende et al. 1996; Lapik et al. 2004; Hölzel et al. 2007b; Wang et al. 2014; Kellner et al. 2015b). Conditional shut down of Bop1 expression affects processing of the ITS1 spacer in mammalian cells, whereas an N-terminally truncated version of Bop1, namely Bop1 $\Delta$  blocked cleavage in the ITS2 spacer (Strezoska et al. 2000). The WDR12 $\Delta$ NLE (or N-terminal deletion of WDR12) causes an ITS2 cleavage defect (Hölzel et al. 2007a). Our hypothesis, as described previously, is that the yeast A<sub>3</sub> factors have direct roles in the cleavage of the ITS2 spacer. Hence, I decided to focus on the yeast homolog of Bop1, i.e. Erb1, to explore whether the Nop7-subcomplex has additional roles in the removal of the ITS2 spacer. I constructed eight internal deletion mutations in the relatively unexplored N-terminal half of Erb1 and assayed the effects of these mutations on pre-rRNA processing, preribosome composition, and the structure of the ITS2 spacer and 5.8S rRNA. Two of the *erb1*- internal deletion mutations blocked cleavage of the ITS2 spacer (referred to as *erb1*<sub>class 2</sub> mutations). Detailed analysis of these mutants revealed that Erb1 is required for proper folding of 5.8S rRNA, and association of specific r-proteins and assembly factors required for ITS2 cleavage. The 5.8S rRNA residues

contacted by the interaction partner of Erb1, Nop7, showed increased protection to modification by the structure probing chemical NAI in *erb1<sub>class 2</sub>* mutants. This suggested that the timely removal of Erb1-Ytm1 by the AAA-ATPase may be perturbed in *erb1<sub>class 2</sub>* mutants (Figure 22). Based on our observations, we propose that the Rea1-mediated removal of Ytm1-Erb1 facilitates remodeling of the 5.8S rRNA, resulting in the release of ‘very early’ and ‘early’ acting assembly factors, and recruitment/stable association of assembly factors required for cleavage of the ITS2 spacer in 27SB pre-rRNA.



**Figure 21. Molecular interaction network of assembly factors involved in 27SA<sub>3</sub> (red), 27SB (dark grey), and 7S (light grey) pre-rRNA processing.** Direct physical interactions (yeast two-hybrid, pull downs *in vitro*, and cryo-EM observations), and genetic interactions between assembly factors involved in the early (red), middle (dark grey) and late (light grey/yellow) are shown. Proteins present in the exosome are shown in blue circles. Data for interactions with ribosomal proteins are included for approximation of locations of assembly factors whose locations on preribosomes have not been directly established. Molecular interactions identified or confirmed among the mammalian homologs of assembly factors are indicated by underlines. (Pratte et al. 2013; Wan et al. 2015; Shimoji et al. 2012; Yoshikatsu et al. 2015; Castle et al. 2013; 2012; Gasse et al. 2015; Leidig et al. 2014; Bradatsch et al. 2007; Thoms et al. 2015a; Wegrecki et al. 2015a; Dembowski et al. 2013b; 2013a; Costanzo et al. 2010; Talkish et al. 2012a; Honma et al. 2006; Santos et al. 2011; Goldfeder and Oliveira 2010; Luz et al. 2009; García-Gómez et al. 2011; Saveanu et al. 2007; Wilmes et al. 2008; McCann et al. 2015 Shimoji et al. 2012; Wan et al. 2015; Pratte et al. 2013; McCann et al. 2015; Saveanu et al. 2003).

Figure 22

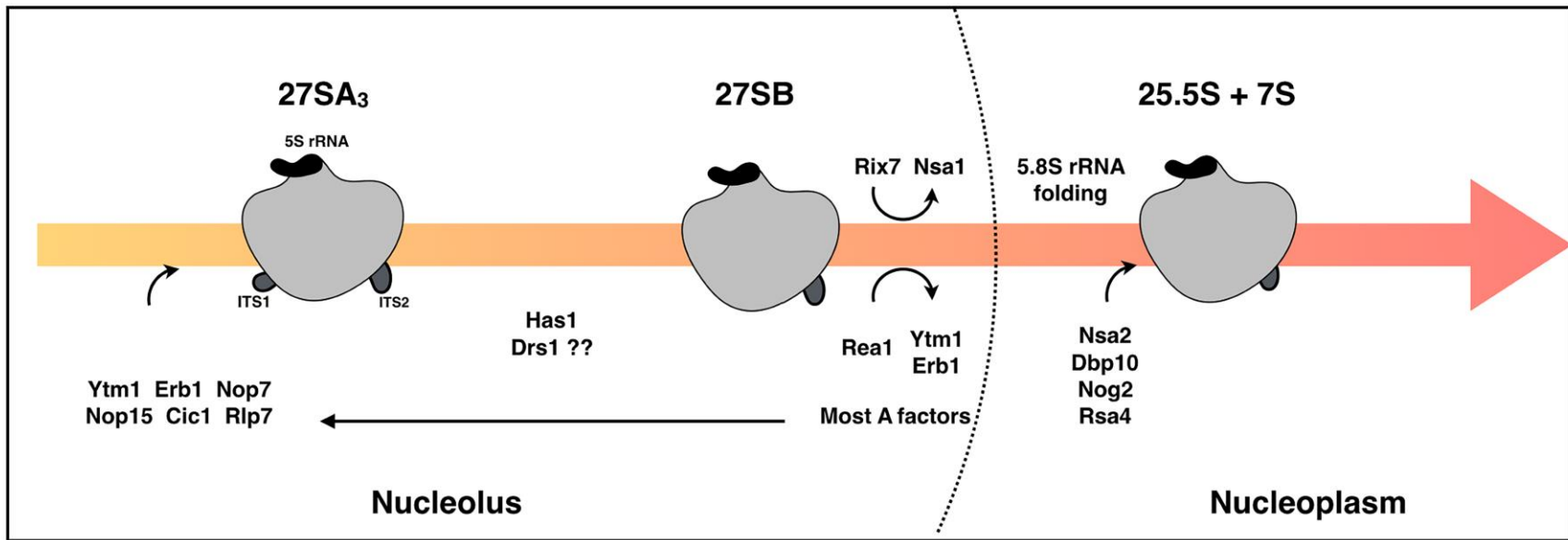


**Figure 22. Molecular assembly events in early and middle preribosomal intermediates.**

## 2.2 Results

### 2.2.1 Conserved regions in the N-terminal half of Erb1 are essential for growth

Erb1 mediates the formation of the Nop7-subcomplex via its interaction with Nop7 and Ytm1 (Miles et al. 2005; Rohrmoser et al. 2007b; Tang et al. 2008). The C-terminal half of Erb1 contains WD40 repeats, which are required for its interaction with Ytm1 (Tang et al. 2008; Thoms et al. 2015b; Wegrecki et al. 2015b) (Figure 20). The N-terminal half of Erb1 contains a stretch of highly conserved amino acids whose role in 60S subunit assembly is largely unexplored (Figure 23). To begin to explore the biological functions of the N-terminal half of Erb1, we constructed a series of eight internal deletions across the N-terminal half of Erb1 (residues 1-419) in the plasmid pOBD2-ERB1 (Figure 25A). Bioinformatic prediction of Erb1 secondary structure was used to avoid disruption of potential secondary structure elements (Figure 24). Plasmids containing these mutations were introduced into a yeast strain engineered to conditionally shut off the expression of wild-type *ERB1* by replacing the endogenous *ERB1* promoter with the *GAL1* promoter. When grown in glucose-containing medium, *GAL* promoter-driven WT *ERB1* expression is shut off, allowing us to assay the effects associated with *erb1*- internal deletions (Figure 25B). Plasmids expressing wild-type *ERB1* supported the growth of the *GAL-ERB1* strain in glucose-containing medium, while the empty vector did not. Mutations affecting the relatively poorly conserved N-terminal 150 amino acids (*erb1<sub>del3-50</sub>*, *erb1<sub>del51-100</sub>*, and *erb1<sub>del101-160</sub>*) had no effect on growth under standard laboratory conditions (Figure 25 and Figure 23). Of the three mutants, only *erb1<sub>Δ101-160</sub>* exhibited a temperature-sensitive growth defect at 37C (Figure 26A). Deletions of stretches of residues in the highly conserved interval of residues 161-419 (*erb1<sub>de161-200</sub>*,

*erb1<sub>del201-245</sub>*, *erb1<sub>del246-310</sub>*, *erb1<sub>del311-365</sub>*, *erb1<sub>del366-419</sub>*) failed to complement growth at 30°C (Figure 25B). These constructs also failed to support growth at 16°C as well as 37°C (data not shown). We did not observe any significant growth defects upon over-expression of any of these mutant constructs from pAG414-GAL-*ERBI*-TAP plasmid (Figure 26B).

Figure 23

```
S.cerevisiae  MMAKNNKT-T--EAKMSK-----KRAAS-----EESDV-EEDEDKLLSV 44
C.albicans    MARNSIKK-S--PVVKKKDTPIVRRKRPQQEAEDSND-EESEDEL-NV
D.erio       MSKLNK-----KRHLE-----ENEE-----EQLPFDK
X.laevis     MKRGSKR-----ESGG-----PLTE-----EPPLFSE
M.musculus   MAGACGKPH-MSPASLPG-----KRRLE-----PDQELQ-IQEPPLLS-
R.norvegicus MAGACGKHH-MSPGSLPG-----KRRLE-----PDQEPQ-IQEPPLLS-
H.sapiens    MAGSRGAGR-TAAPSVRPE-----KRRSE-----PELEPEPEPEPLLCT
*           .           :           :

S.cerevisiae  ---DGL--IDAEASESDEDDDEYESAVEEKESSSDKQAQDDSDSD--AE 79
C.albicans    ---EGL--IDASDDEDEEEEQEQQEENNSDDD-DDDDDDDD--NN
D.erio       DSGEDGHLDDGDEDPADLSDSEESVFSGLEDSGSDDE-DDDEDDE-DDD
X.laevis     ---ENRSLQD--GNPLDESDEESQYSGLEDSGTSS-DDEDHSSEEVQ
M.musculus   -----DPDSSLSDSEESVFSGLEDLGSDSS-EEDTEGVAGS--
R.norvegicus -----DPDSSLSDSEESVFSGLEDSGSDTS-DEDTTEVARA--
H.sapiens    ---SPL--SHSTGSDSGVSDSEESVFSGLEDSGSDSS-EDDDEGDEEG-E
           . : * .           : : * .           : : :

S.cerevisiae  LNKLLA-----EEEGDGEEDYDSSEF--SDD-TTS-LTD----RLS 113
C.albicans    SEADSEELNQLLGEDEEDPSDYNSEF--SDE-PK--DD--DL
D.erio       DKDGESEKSSDA-E---EDKADDDGDLKLSAKDDVKQVDSQNSKEKK
X.laevis     DPGKSPKEI-----IKVPHR-TSKSQAD-----
M.musculus   --S-GDEDNHRA-E-----ETSEE-LAQAAPL-----
R.norvegicus --G-CDKDN-RT-E-----KTSEE-QEQAVFP-----
H.sapiens    DGALDDEGHSGI-K-----KTEE-QVQASTP-----
           .

S.cerevisiae  GV--KLQITVDPNI---YSKYADGSDRIKIP-EINPVYSDSDSDAET-Q 154
C.albicans    RINIKLSLSDPSIQNSISKFSGDSIRILKP-EIEPKYSDSDSDAEN-F
D.erio       KKKRKGKSVLKDGE---EDVASGRDEALKITSQVDEYDHTSDEEDIR
X.laevis     -----SPADEEQP-NEIKKEYENDSDEEDIR
M.musculus   -----CSRTEEAGA-LAQDEYEDSDDEEDIR
R.norvegicus -----CPRAEAGA-LTRDEYEDSDDEEDIR
H.sapiens    -----CPRTEMASA-RIGDEYEDSDDEEDIR
           * * * * *

S.cerevisiae  NTIGNIPLSAYDEMPHIGYDINGKRIMRPAKG-SALDQLLDSIELPEGWT 203
C.albicans    NTIGNIPLSAYDEMPHIGYDINGKRIMRPAKG-SALDQLLESIDLPEGWT
D.erio       NTVGNIPMEWYKDYPHIGYDLGKIKFKPIRKNKDELDELKMNPDYWR
X.laevis     NTVGNIPMEWYKDLPHIGYDLGKIKFKPLRSKDQLEEFDLKMNPDYWR
M.musculus   NTVGNVPLAWYDEFFPHVGYDLGKRIYKPLRTRDELQFLDKMDDPFWR
R.norvegicus NTVGNVPLAWYDDFFPHVGYDLGKRIYKPLRTRDELQFLDKMDDPFWR
H.sapiens    NTVGNVPLEWYDDFFPHVGYDLGRRYKPLRTRDELQFLDKMDDPFWR
**:*:*:* * : * : * : * : * : * : * : * : * : * : * : *

S.cerevisiae  GLLDKNSGSSLNLTKEEELISKIQRNEQTDSDSINPYEPLDWFTRHEEV 253
C.albicans    GLLDQNTGTSKLTDEEELIRKIQQENTDENINPYEPLDWFTRHEEV
D.erio       TVQDKMTGADIRLSDEQVLDVHRLQGGKFGDVFNEYEPVDFFSNEVMI
X.laevis     TVHDKKTGQDIKLTDEQVLDVRLQGGQFGDNLNYPYQPAIDFFTHETMI
M.musculus   TVQDKMTGRDLRLTDEQVALVHRLQGGQFGDSGFNYPYEPVDFFSGDIMI
R.norvegicus TVQDKMTGSDLRLTDEQVALVHRLQGGQFGDSGFDPYEPVDFFSGDIMI
H.sapiens    TVQDPMTGRDLRLTDEQVALVRLQSGQFGDVGFNYPYEPVDFFSGDIMI
: * : * : * : * : * : * : * : * : * : * : * : * : * :

S.cerevisiae  MPLTAVPEPKRRFVPSKNEAKRVMKIVRAIREGRIIPPKKLEK-KEKEK 302
C.albicans    MPVTAVPEPKRRFVPSKHEAKRVMKIVKAIREGRIIPPKVQQLTEEE
D.erio       HPVTNRPDKRSFIPSLIEKEKVKLVHAIKMGWIKPRRP-----K-E
X.laevis     HPVTNRPADKRSFIPSLIEKEKVSRLVHAIKMGWIKPRRP-----R-D
M.musculus   HPVTNRPADKRSFIPSLVEKEKVSRLVHAIKMGWIKPRRP-----H-D
R.norvegicus HPVTNRPADKRSFIPSLVEKEKVSRLVHAIKMGWIKPRRP-----P-D
H.sapiens    HPVTNRPADKRSFIPSLVEKEKVSRLVHAIKMGWIKPRRP-----R-D
* : * * * * * * : * : * : * : * * * .

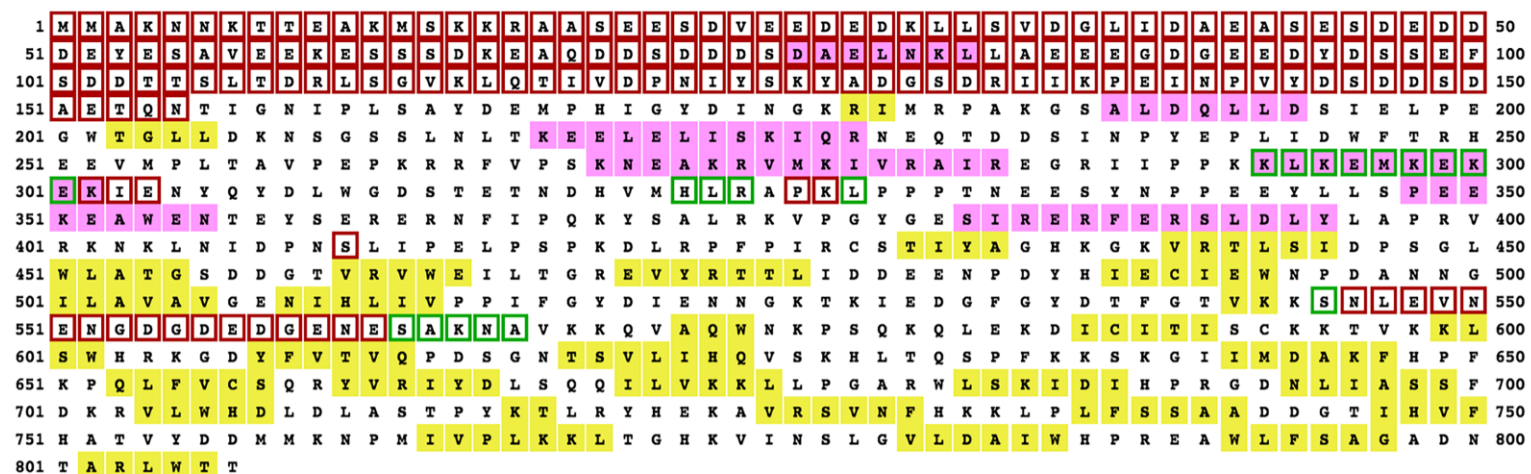
S.cerevisiae  IENYQYDLWGDST---ETNDHVMHLRAPKLPPPTNEESYNPPEYLLSPE 350
C.albicans    EDQFNFDLWQDEI---EISDHIMNLRAPKLPPPTNEESYNPPEYLLTEE
D.erio       TTPQYDLWAKEDPNSILGRHKMHVPAPKMKLPGHEESYNPPEYLLSEE
X.laevis     DAPTYDLWAKEDPNAILGRHKMHVPAPKMLPLPGHEESYNPPEYLLMSEE
M.musculus   PTPSFYDLWAKEDPNAVLGRHKMHVPAPKMLPLPGHAESYNPPEYLLPTEE
R.norvegicus STPSFYDLWAKEDPNAVLGRHKMHVPAPKMLPLPGHAESYNPPEYLLPTEE
H.sapiens    PTPSFYDLWAKEDPNAVLGRHKMHVPAPKMLPLPGHAESYNPPEYLLSEE
:*** ..           * * : : * : * : * : * : * : * : * : *

S.cerevisiae  EKEAWENTEYSERERNFIPQKYSALRKVPYGESIRERFERSLDLYLAPR 399
C.albicans    EKS KWLQESPIDRERNFLPQKYNLSRQVPGYQDSVREPERSLDLYLAPR
D.erio       ERLAWAQDPEDRKLSPFPQKFSCLRAVPFARFIERFERCLDLYLCP
X.laevis     ERLAWEQDPEDRKLSPFPQKFNCLRAVPGYARFIERFERCLDLYLCP
M.musculus   ERSAMWQEPVERKLNFLPQKFPSLRTPVAYSRFIQERFERCLDLYLCP
R.norvegicus ERLAWMQEPIERKLNFLPQKFPSLRTPVAYGRFIQERFERCLDLYLCP
H.sapiens    ERLAWEQEPGERKLSFLPKFPSLRAVPAYGRFIQERFERCLDLYLCP
* : * .           : : * : * : * : * : * : * : * : * : * : *

S.cerevisiae  VRNKNLIDPNSLIPELPSP 419
C.albicans    VRHNKLNIDPDSLIPDLSP
D.erio       QRKMRVNVNPELIPKLPKP
X.laevis     QRKMRVNVNPELIPKLPKP
M.musculus   QRKMRVNVNPELIPKLPKP
R.norvegicus QRKMRVNVNPELIPKLPKP
H.sapiens    QRKMRVNVNPELIPKLPKP
* : * : * : * : * * * *
```

**Figure 23.** Erb1 sequences from seven phylogenetically diverse species were aligned using the web-based T-coffee server (<http://www.ebi.ac.uk/Tools/msa/tcoffee/>). Residues with conserved identities or biochemical properties across different phyla are indicated by ‘\*’ or ‘:’, respectively. The amino acids are color coded by the biochemical properties of their side chains: positively charged (magenta), negatively charged (blue), polar (green), and non-polar (red). Black and grey lines above the alignment indicate two stretches of highly conserved regions in the N-terminal half. Deletion of residues in these conserved stretches of *erb1* was lethal for *S. cerevisiae* (This study).

Figure 24A



<b>KEY</b>	<b>Helix</b>	<b>Sheet</b>	<b>Disordered</b>	<b>Disordered protein binding</b>	<b>Dompred Boundary</b>	<b>DomSSEA Boundary</b>
<b>Annotations</b>	M	L	E	E	A	D



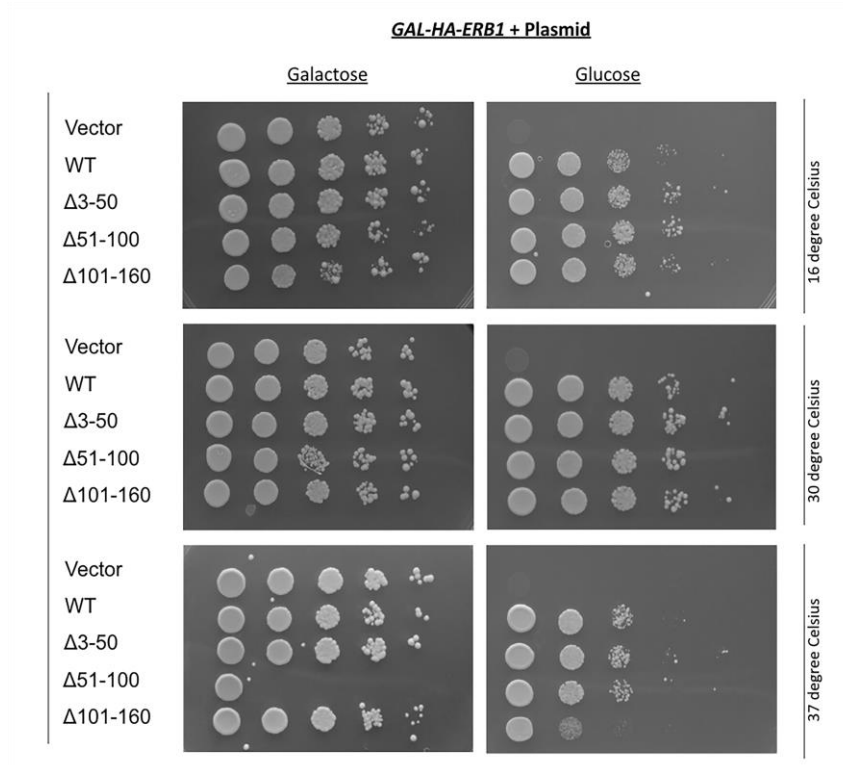
**Figure 24. Bioinformatic prediction of secondary structural elements in Erb1.** (A) Secondary structural elements in Erb1 were predicted using web-based PsiPRED software <http://bioinf.cs.ucl.ac.uk/psipred/>. (B) The confidence of the structure prediction for the N-terminal half of Erb1 is shown as blue bars.



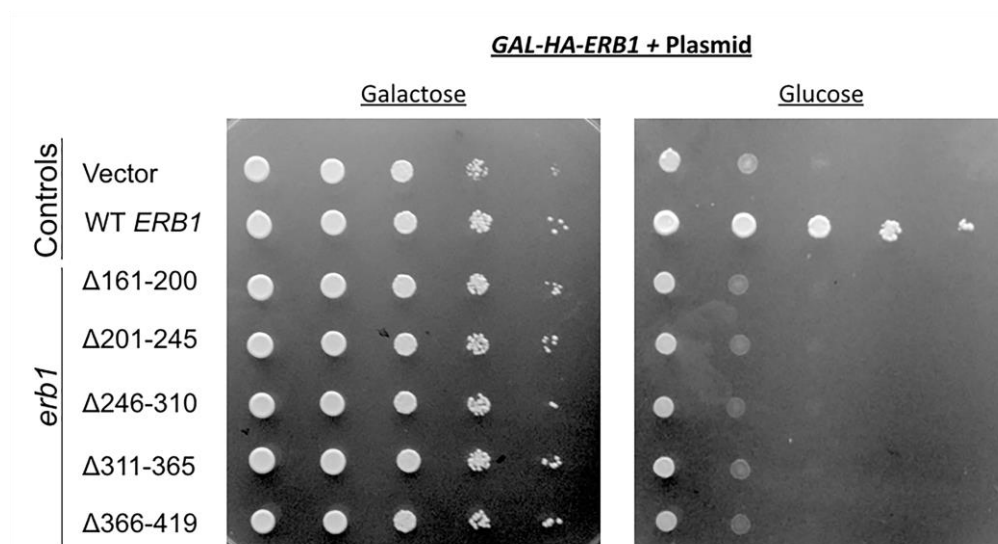
**Figure 25. Effects of deletions of discrete regions of Erb1 on growth of yeast.** (A) Schematic representation of amino acids removed by *erb1* internal deletion mutations. (B) Growth of *GAL-HA-ERB1* cells expressing WT or mutant *erb1* from pOBD2 plasmids on solid media containing galactose (left panel) or glucose (right panel). Tenfold serial dilutions of *GAL-HA-ERB1* cells containing plasmids were spotted on selective-media containing galactose (C-TRP+GAL) or glucose (C-TRP).

Figure 26

A



B



**Figure 26 (A) Effect of temperature on growth of *erb1* internal deletion mutants that have no growth defects at 30°C.** Growth of *GAL-HA-ERB1* cells expressing WT or mutant *erb1* from pOBD2 plasmids on solid media containing galactose (left panel) or glucose (right panel). Tenfold serial dilutions of *GAL-HA-ERB1* cells containing plasmids were spotted on selective-media containing galactose (C-TRP+GAL) or glucose (C-TRP). Plates were incubated at 16°C, 30°C, or 37°C. **(B) Effects of lethal *erb1* internal deletions expressed from the pAG415-GPD-EFGP-*ERB1* plasmid on growth of *GAL-3HA-ERB1*.** Tenfold serial dilutions of *GAL-HA-ERB1* cells containing plasmids were spotted on selective-media containing galactose (C-TRP+GAL) or glucose (C-TRP) and incubated at 30°C.

Figure 27

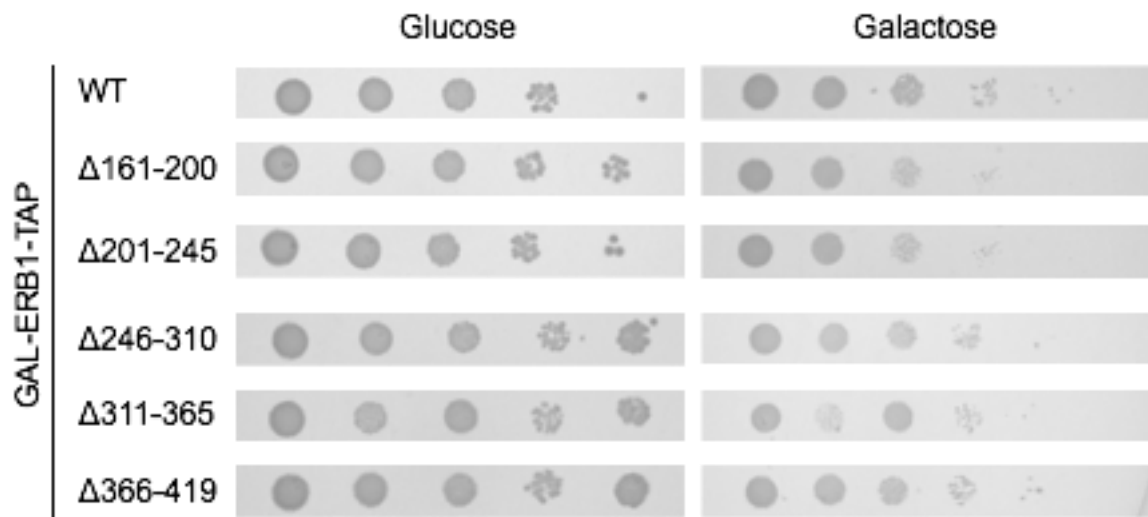


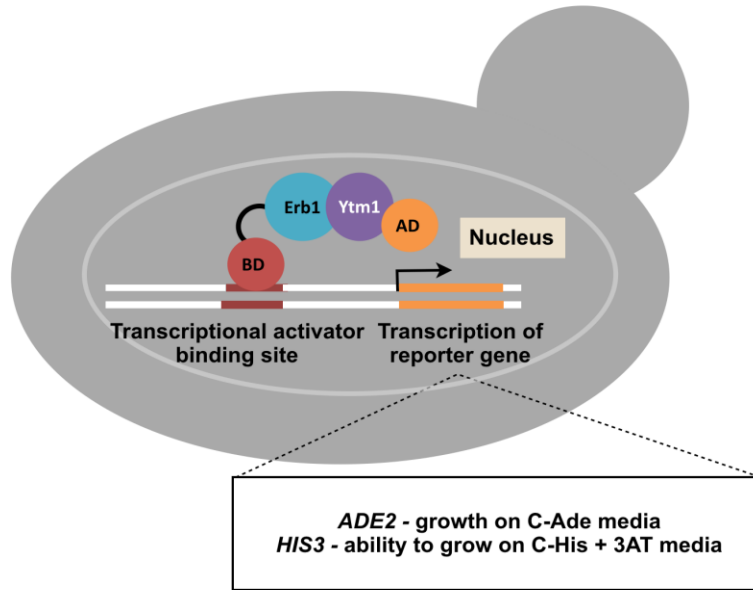
**Figure 27. Effects of overexpression of the lethal *erb1* internal deletion mutants on growth.** Wild type *S. cerevisiae* strains overexpressing lethal *erb1* internal deletions from the plasmid pAG414-GAL-*ERB1*-TAP were spotted as serial dilutions on selective solid-medium containing either glucose or galactose as the carbon source. The plates were incubated at 30°C for three days.

### **2.2.2 Most of the N-terminal Half of Erb1 is not required for its interaction with Ytm1**

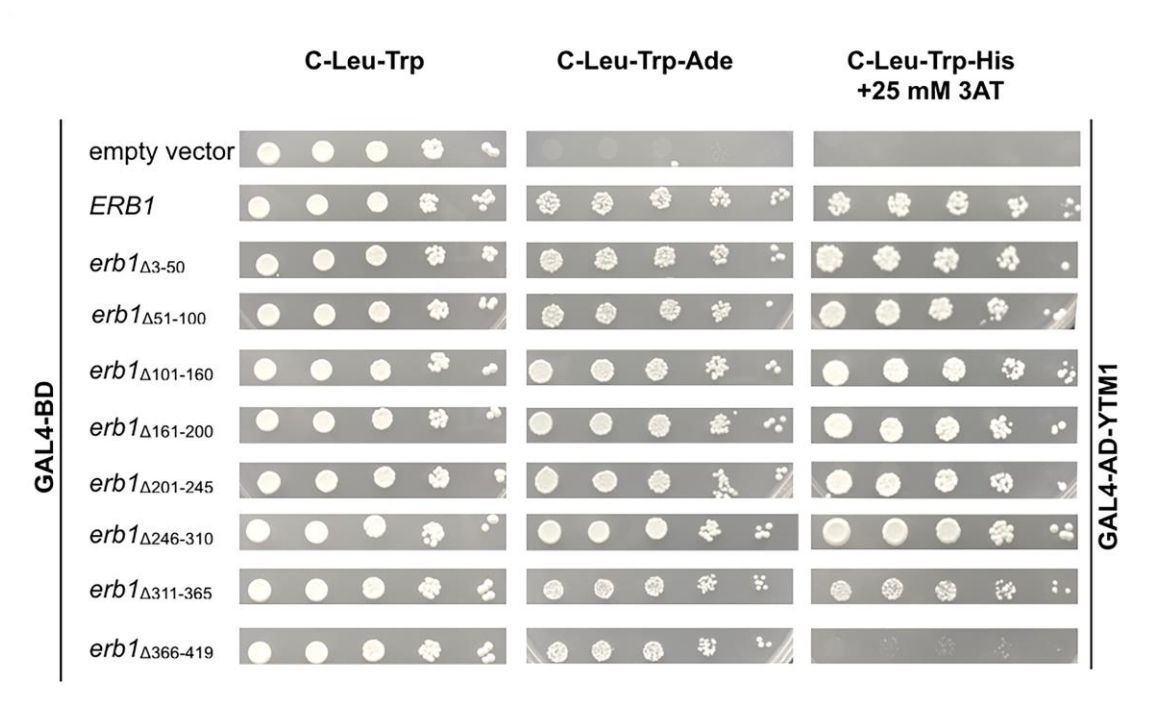
We performed yeast two-hybrid assays between *erb1* internal deletion mutant proteins and wildtype Ytm1, to assay Erb1-Ytm1 interactions and the stability of the mutant proteins (Figure 27A). Wild type Erb1 interacts strongly with Ytm1, allowing the cells to grow in the presence of the drug 3-aminotriazole up to a concentration of 25 mM (Figure 27B, row 2). All eight mutant constructs grew efficiently in C-Leu-Ade, indicating that the mutant proteins are stably expressed (Figure 2, lane 2, rows 3-10). Seven of the eight mutant constructs, except *erb1<sub>del366-419</sub>*, showed interaction in 25 mM AT, indicating strong interaction between the *erb1* internal deletion mutant proteins and Ytm1 (Figure 27, lane 3, rows 3-10). Thus, residues 366-419 in the N-terminal half of Erb1 are required for efficient interaction of Erb1 with Ytm1, in addition to its C-terminal WD40 motifs (Wegrecki et al. 2015b; Thoms et al. 2015b). The Nop7-Erb1 interaction assay could not be performed by yeast two-hybrid assay, since the Nop7 fusions do not work in yeast two-hybrid assay. Heterologous expression and purification of Erb1 mutant proteins and wild type Nop7 from *E. coli* to test Erb1 mutant- Nop7 interaction was not successful either.

Figure 28

A



B



**Figure 28. A major portion of the N-terminal half of Erb1 is not required for its interaction with Ytm1.** (A) Schematic of the two-hybrid analysis of the interaction between Erb1 mutant proteins and Ytm1. Positive interactions activate transcription of the reporter genes *ADE2* and *HIS3*, which allow yeast cells to grow in the absence of adenine (Ade) or histidine (His). (B) Tenfold serial dilutions of the two-hybrid reporter strains containing appropriate plasmids were spotted on control (C-Leu-Trp) or test (C-Leu-Trp-Ade or C-Leu-Trp-His + 25 mM 3AT) media. We used 3-aminotriazole, a competitive inhibitor of the *HIS3* gene, to assay the strength of interaction between Erb1 and Ytm1 (column 3). WT Erb1 and Ytm1 interact with each other at high strength, allowing cells to grow in medium containing up to 25mM 3AT (lane 3).

#### 2.2.4 Erb1 is required for the processing of both 27SA<sub>3</sub> and 27SB pre-rRNAs during 60S ribosomal subunit assembly

The effects of individual *erb1* internal deletions on pre-rRNA processing were assayed by primer extension (Figure 29). The levels of 27SA<sub>3</sub> pre-rRNA and 27SB pre-rRNA were quantified in relation to the control U2 snoRNA. Depletion of Erb1 resulted in accumulation of 27SA<sub>3</sub> pre-rRNA and a significant reduction in the level of its product, 27SB<sub>s</sub> pre-rRNA, as observed previously (Figure 29, lane 3) (Miles et al. 2005). We observed three classes of pre-rRNA processing phenotypes in the *erb1* internal deletion mutants:

- (a) Class 1, resembling WT *ERB1* (*erb1*<sub>del3-50</sub>, *erb1*<sub>del51-100</sub>, and *erb1*<sub>del101-160</sub>) (Figure 29, Lanes 4-6)
- (b) Class 2, showing accumulation or no change in levels of 27SB pre-rRNA (*erb1*<sub>del161-200</sub>, *erb1*<sub>del201-245</sub>). No change was observed in the levels of 27SA<sub>3</sub> pre-rRNA in these mutants, indicating they are blocked at a step later than 27SA<sub>3</sub> pre-rRNA processing (Figure 29, Lanes 7-8). Further assays show that these mutants are blocked in the formation of 7S pre-rRNA, consistent with a block in cleavage of ITS2 (Figure 30).
- (c) Class 3, exhibiting accumulation of 27SA<sub>3</sub> pre-rRNA (*erb1*<sub>del246-310</sub>, *erb1*<sub>del311-365</sub>, *erb1*<sub>del366-419</sub>) (Figure 29, Lanes 9-11).

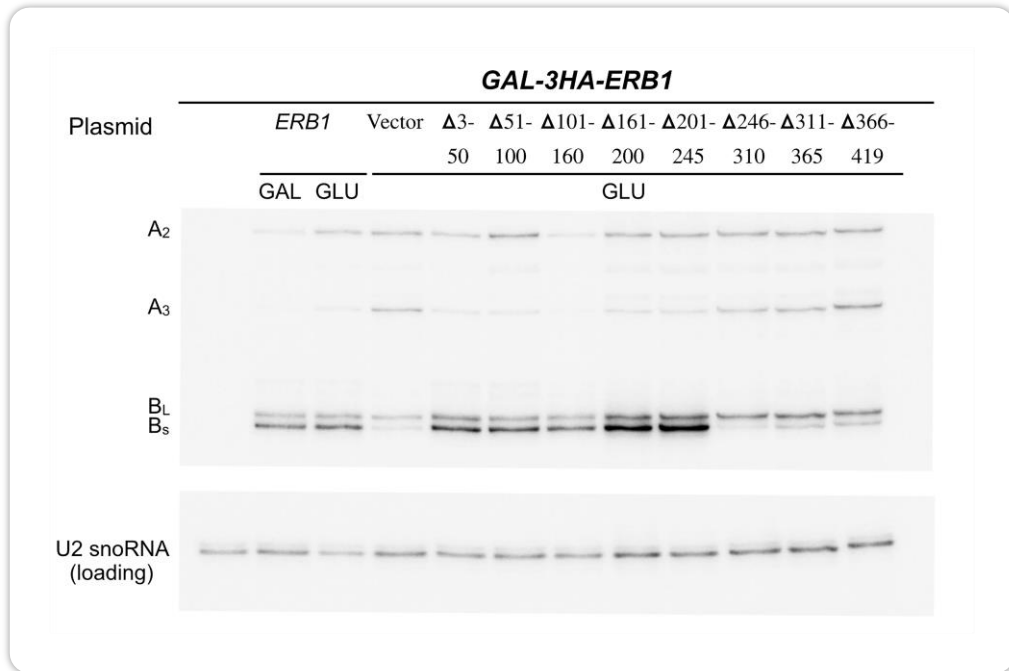
Steady-state levels of pre-rRNA processing intermediates in *erb1* internal deletion mutants were further assayed by northern blotting (Figure 30A). Depletion of Erb1

results in accumulation of 27SA<sub>3</sub> pre-rRNA. We also observe an increase in 35S pre-rRNA, as expected (row 3). This increase in 35S pre-rRNA is thought to be due to the slowing down of preceding pre-rRNA processing steps when 27SA<sub>3</sub> pre-rRNA processing is blocked. These pre-rRNA processing phenotypes of *erb1* internal deletion mutants were in agreement with the classification based on primer extension. (a) Class 1 mutants (*erb1<sub>del3-50</sub>*, *erb1<sub>del51-100</sub>*, and *erb1<sub>del101-160</sub>*) did not show any defects in pre-rRNA processing; (b) class 2 mutants (*erb1<sub>de161-200</sub>*, *erb1<sub>del201-245</sub>*) showed a marked increase in 27SA+B pre-rRNAs. The 27SA+B shows a slight shift in size towards lower molecular weight, indicating an accumulation of 27SB pre-rRNA (Figure 29A). We observe that formation of 7S pre-rRNA is blocked in the class 2 mutants (Figure 29B). (c) The class 3 mutants (*erb1<sub>del246-310</sub>*, *erb1<sub>del311-365</sub>*, *erb1<sub>del366-419</sub>*) were comparable to depletion of *erb1* (Figure 30B, lanes 9-11).

The plasmid pOBD2-*erb1* expresses *erb1* as an N-terminal fusion of GAL4-DNA binding domain. To rule out any bias in our observations due to the epitope-tag, we constructed the plasmid pAG414-GPD-EGFP-ERB1, which expresses *ERB1* with an N-terminal GFP tag fusion. The *erb1<sub>class 2</sub>* and *erb1<sub>class 3</sub>* mutants failed to support growth of the *GAL-ERB1* strain in glucose-containing solid media (Figure 26B). The pre-rRNA processing defects in the *GAL-3HA-ERB1* + pAG415-GPD-EGFP *erb1<sub>class 2</sub>* or *erb1<sub>class 3</sub>* mutants were similar to our previous observations (Figure 31).

**Figure 29**

A



B

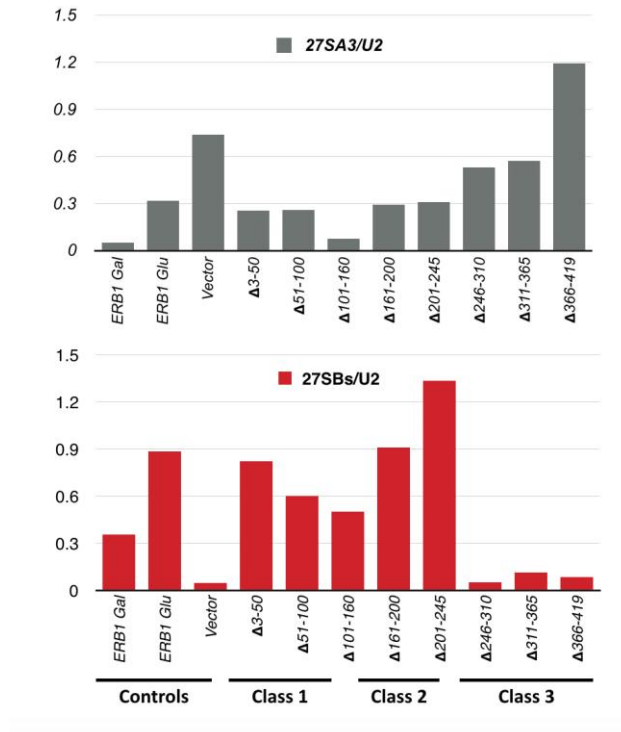


**Figure 29. *erb1*- internal deletion mutants are categorized into three classes based on pre-rRNA processing phenotypes (by primer extension).** (A) Steady-state levels of pre-rRNAs extracted from *GAL-3HA-ERB1* strains containing WT/mutant *erb1* plasmids were assayed by primer extension using an oligonucleotide primer that hybridizes to the ITS2 spacer (ITS2-B oligonucleotide). (B) Amounts of 27SA<sub>3</sub> and 27SB pre-rRNAs were quantified relative to U3 snoRNA. The *erb1* internal deletion mutations with WT-like pre-rRNA processing are categorized as class 1 (lanes 4-6), 27SB pre-rRNA processing defects as class 2 (lanes 7-8), and depletion-like accumulation of 27SA<sub>3</sub> as class 3 (lanes 9-11).



**Figure 30. *erb1*- internal deletion mutants can be categorized into three classes based on pre-rRNA processing phenotypes (by northern blotting).** (A) Steady-state levels of pre-rRNAs extracted from *GAL-3HA-ERBI* strains containing WT/mutant *erb1* plasmids were assayed by northern blotting using probes specific for the ITS2 spacer (ITSA for 27A+B and 35S pre-rRNA), 25S rRNA and 18S rRNA. (B) Steady-state levels of 7S pre-rRNA and 5S rRNA (probed with oligonucleotides binding to the ITS2A spacer and 5S rRNA) in *GAL-3HA-ERBI* strains containing *erb1*<sub>class 2</sub> mutants grown in galactose (control) or glucose (experiment). Consistent results were obtained in two or more independent experiments.

Figure 30C

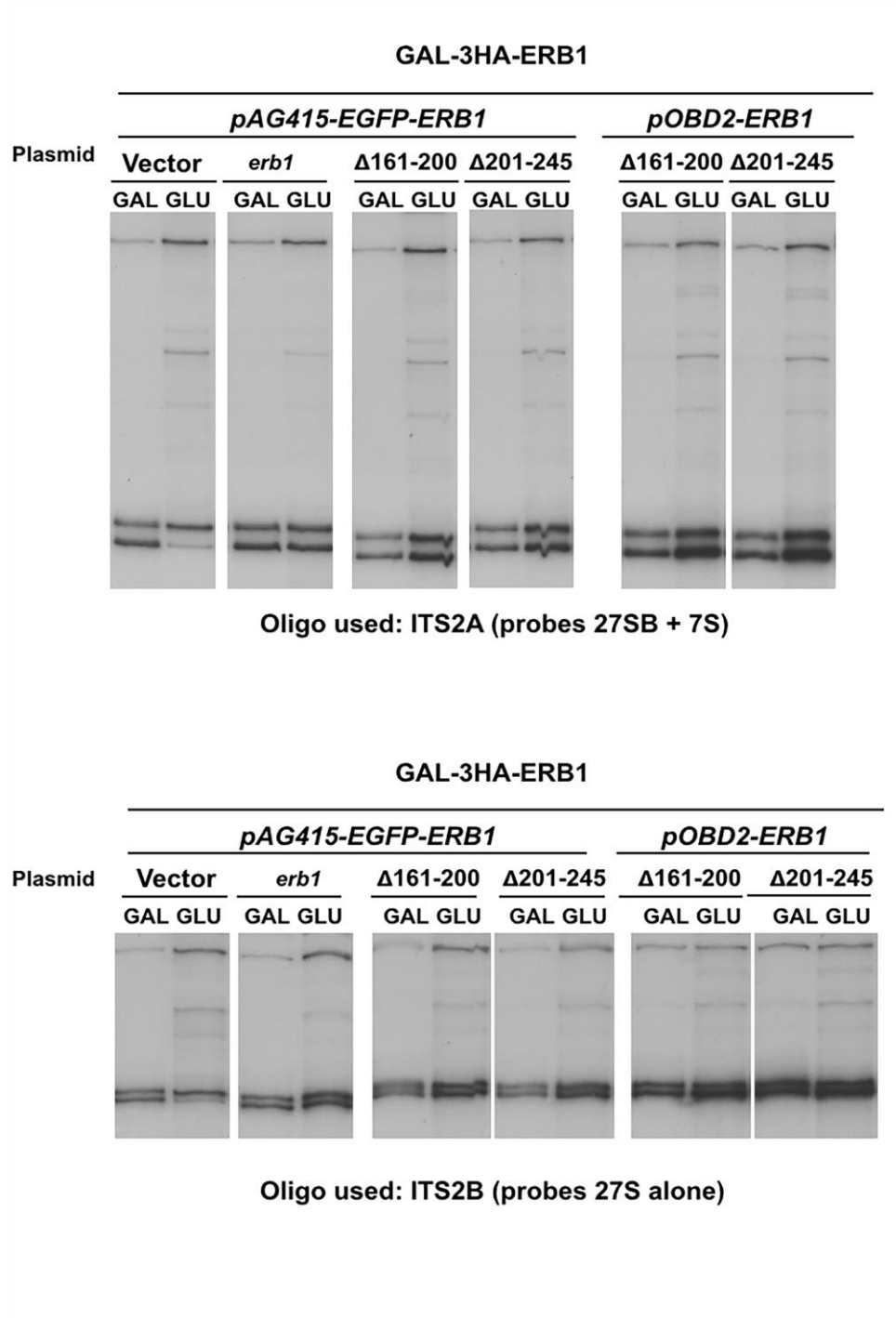


**Figure 30C. Pre-rRNA processing defects in cells expressing *erb1*<sub>class 2</sub> mutants from different plasmids.** The plasmid pOBD2-*ERB1* used in the previous experiment expresses WT/mutant Erb1 protein with a GAL4-DNA binding domain fused to its N-terminus. To rule out bias in the experimental observation, pAG414-GPD-EGFP-*ERB1* plasmids containing *erb1* internal deletion mutations were constructed and introduced into the *GAL-3HA-ERB1* strain. Steady-state levels of pre-rRNAs in total RNA extracted from these *GAL-3HA-ERB1* strains containing WT/mutant *erb1* plasmids were assayed by primer extension using the ITS2-A or ITS2-B oligonucleotide primers.

#### **2.2.4 The pre-ribosomal composition of the three classes of *erb1* mutants concurs with their pre-rRNA processing defects.**

To verify the classification of the *erb1* internal deletions, we purified preribosomes using the TAP-tagged assembly factor Rpf2 as bait. We resolved proteins in these preribosomes using SDS-PAGE and visualized the bands by silver staining. Many of proteins in these bands were previously identified by mass spectrometry (Zhang et al. 2007). Depletion of Erb1 affects stable association of the interdependent A<sub>3</sub>-cluster proteins Erb1, Nop7, Ytm1, Nop15, Cic1, Nop12, and Pwp1 (Figure 31A), as previously demonstrated (Sahasranaman et al. 2011; Miles et al. 2005; Tang et al. 2008). Changes in preribosome composition of the three classes of *erb1* internal deletion mutants are in agreement with the pre-rRNA processing phenotypes of these mutants.

- (1) The WT-like *erb1<sub>class 1</sub>* mutants did not show any significant changes in preribosome composition (Figure 31B).
- (2) The association of interdependent A<sub>3</sub> factors was not perturbed *erb1<sub>class 2</sub>* mutant preribosomes. Preribosomes are stable in these mutants compared to *erb1<sub>class 3</sub>* or *erb1* depletion mutants (Figure 31C).
- (3) The *erb1<sub>class 3</sub>* mutants displayed a silver-stained pattern similar to depletion of Erb1 (Figure 31D and 31A). We observe a significant decrease in the intensity of gel bands corresponding to the interdependent A<sub>3</sub>-cluster proteins Nop7, Ytm1, Cic1, Nop15, Nop12 and Has1.

To summarize, the preribosome composition of the three classes of *erb1* mutants is in agreement with their pre-rRNA processing phenotypes. The *erb1<sub>class 3</sub>* mutants were similar to depletion of *erb1*. The observed phenotype of the *erb1<sub>class 3</sub>* mutants is due to

the collective absence of the interdependent A<sub>3</sub>-factors. On the other hand, the *erb1<sub>class 2</sub>* mutants blocked 60S ribosomal subunit assembly at a later step of pre-rRNA processing than *erb1* depletion, and the preribosomes were more stable. But, the intensities of a few bands seemed to decrease by visual inspection. Therefore, changes in protein composition of these class 2 mutant preribosomes with respect to wild type were further assayed using a semi-quantitative mass spectrometric iTRAQ method (Ross et al. 2004)

Figure 31A

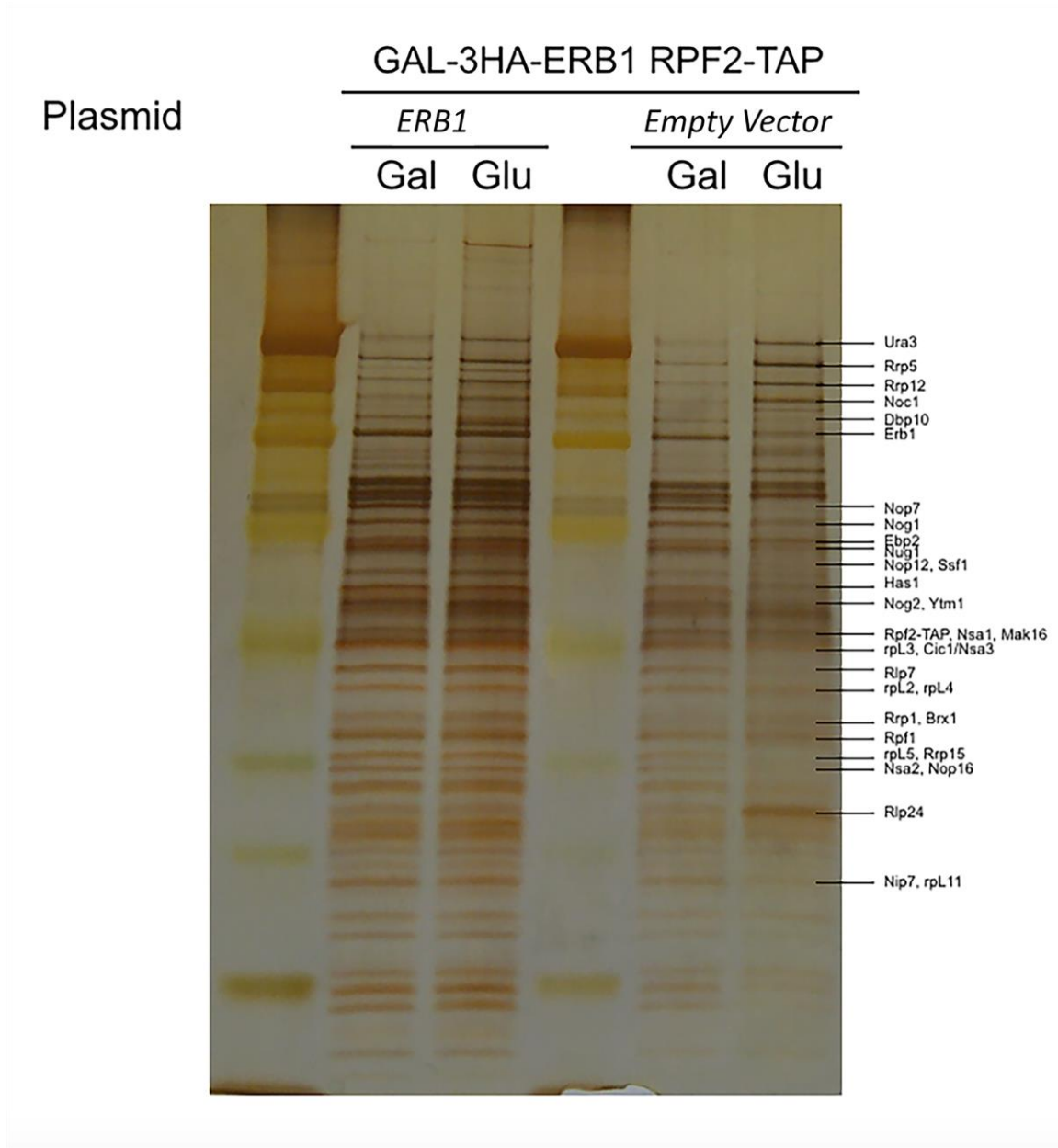


Figure 31B

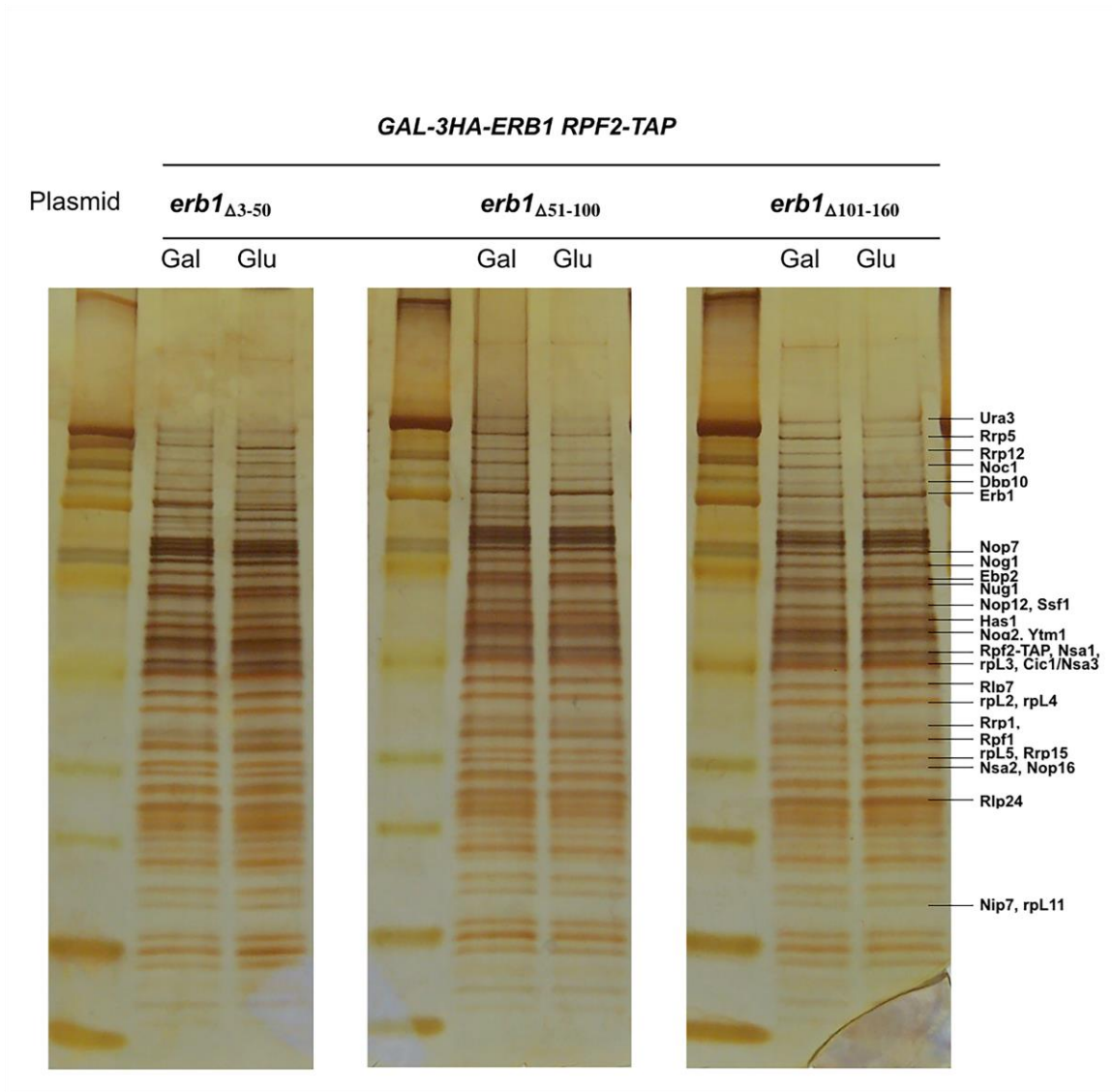


Figure 31C

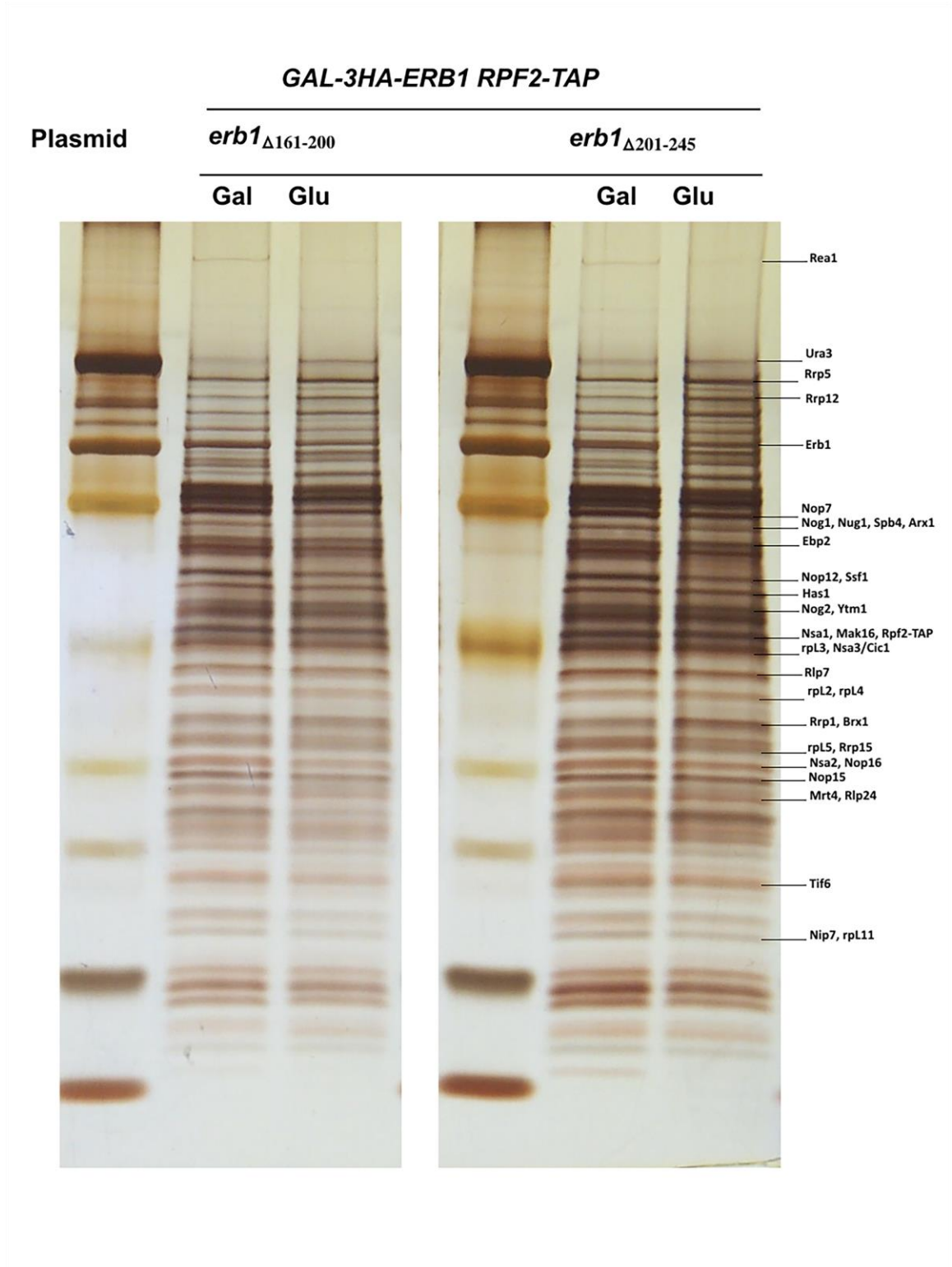
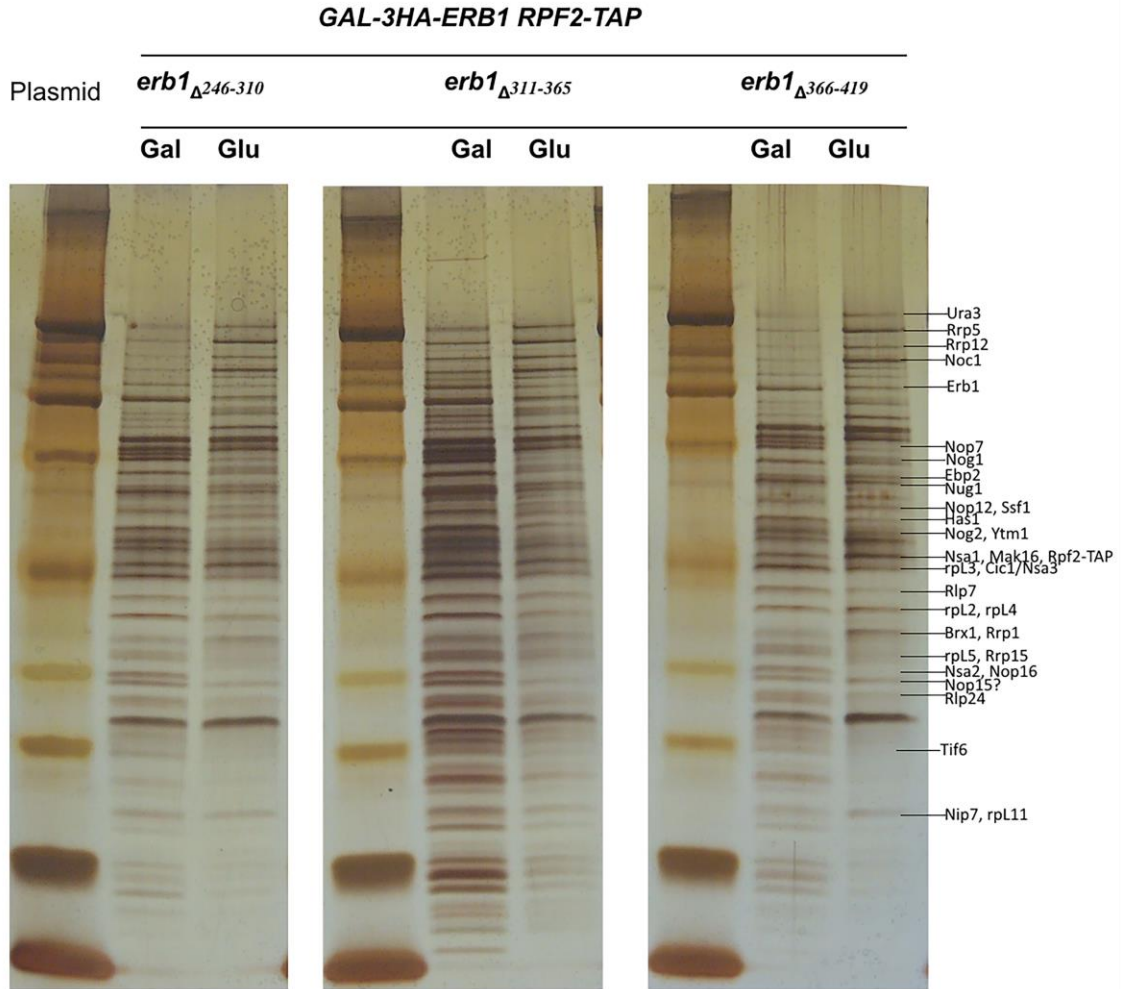


Figure 31D



**Figure 31. Preribosomes purified from *erb1<sub>class 2</sub>* mutants are more stable compared to depletion of Erb1.**

*GAL-3HA-ERB1* cells containing TAP-tagged assembly factor Rpf2 were used to purify 90S and 66S preribosomes from yeast cells grown in selective media containing galactose (Gal), or grown in galactose and then shifted to glucose (Glu) to deplete WT Erb1 protein. Proteins present in purified preribosomes were resolved on an SDS-PAGE gel and visualized by silver staining. Bands are marked as identified by mass spectrometry from previous experiments and this work. (A) Strains containing WT Erb1 or empty vector were used as controls. The A<sub>3</sub> factors (Erb1, Nop7, Ytm1, Nop15, Cic1, Nop12, and Has1) fail to stably associate with preribosomes when Erb1 is depleted. (B) Preribosomes purified from strains containing *erb1<sub>class 1</sub>* mutations are stable. (C) Preribosomes purified from strains containing *erb1<sub>class 2</sub>* plasmids contain bands corresponding to the interdependent A<sub>3</sub> factors. (D) *erb1<sub>class 3</sub>* mutations result in a depletion-like phenotype characterized by the absence of bands corresponding to the A<sub>3</sub> factors.

### **2.2.5 Stable association of specific assembly factors required for 27SB pre-rRNA processing is affected in *erb1<sub>class 2</sub>* mutants**

To determine global changes in protein-composition of preribosomes in the *erb1<sub>class 2</sub>* mutants, we performed semi-quantitative mass spectrometric iTRAQ analysis. We compared preribosomes purified from *GAL-ERB1 + erb1<sub>class 2</sub>* strains grown in galactose (WT *erb1* ON), or grown in galactose and then shifted to glucose (WT *erb1* OFF), using Rpf2-TAP as bait (Ross et al. 2004; Dembowski et al. 2013a; Ohmayer et al. 2013; Gamalinda et al. 2014; Sahasranaman et al. 2011). The mass spectrometric experiment was performed by Anne Stanley at the Stanley Lab, College of Medicine, Penn State University, Hershey, PA. We identified 450 proteins with  $\geq 95\%$  confidence. The data analysis was performed as described in Figure 32.

**Figure 32**

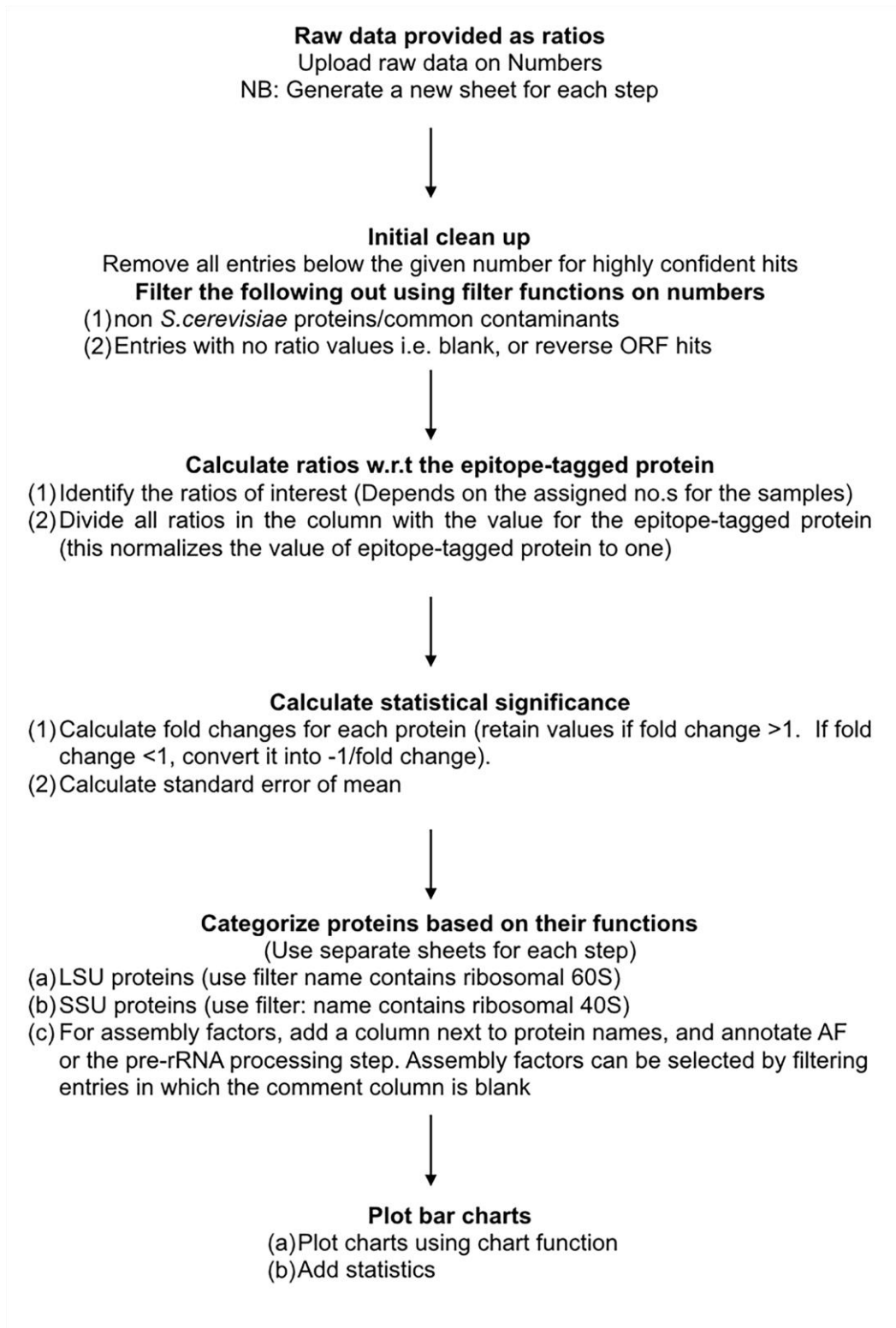


**Figure 32. Schematic flow chart for the analysis of iTRAQ data.**

The changes observed for assembly factors in *erb1<sub>class 2</sub>* largely correlate with their lifetime and function in pre-60S intermediates. The changes in the two *erb1<sub>class 2</sub>* mutants are qualitatively comparable and differed mostly in the magnitude of their change. This suggests that ribosome assembly is blocked in a very similar fashion in these two mutants (Figure 33). We observed an increase in the association of most early-acting assembly factors, which could be due to a failure to release them or due to a relative enrichment of early preribosomes when 27SB pre-rRNA processing is slowed down (Figure 33B, top panel). Consistent with the silver-stained SDS-PAGE gel (Figure 31C), the interdependent A<sub>3</sub> factors (Erb1, Ytm1, Nop7, Nop15, Rlp7, and Cic1) associate stably with preribosomes (Figure 2.13A). We also observe an increase in the levels of A<sub>3</sub> assembly factors Rpf1, Pwp1 and Nop12, which indicates a failure in their timely removal. Association of the DEAD-box helicases Drs1 and Has1, and the exonuclease Rat1 required for 27SA<sub>3</sub> pre-rRNA processing is not affected. These results are consistent with a block in C<sub>2</sub> cleavage, after the 27SA<sub>3</sub> pre-rRNA processing event.

Most assembly factors required for the C<sub>2</sub> cleavage in 27SB pre-rRNA were able to stably associate with preribosomes (Rrs1, Nop2, Nip7, Mak11, Dbp10, Rlp24, Tif6, and Nog1) in *erb1<sub>class 2</sub>* mutants, with the exception of Nsa2, Nog2, Spb4, Cgr1, and (Figure 33). Nsa2 and Nog2 bind the peptidyl transferase center in the domain V of 25S rRNA (Figure 15) (Shan *et al.*, (2016), submitted) (Leidig *et al.* 2014; Matsuo *et al.* 2014a; Bradatsch *et al.* 2012). The association of the endonuclease Las1 performing C<sub>2</sub> cleavage was not affected (Gasse *et al.* 2015). We observe two hits for the assembly factor Spb1 in our mass spec data, both of which show significant variation or error.

Hence, we did not consider these data while making any conclusions. The association of assembly factors involved in downstream processing of 7S pre-rRNA, i.e. Nog2, Rsa4, Nop53, Nug1, and Ipi1/Ipi2/Ipi3, is significantly reduced. We observe reduced association of the export factors Arx1 and Bud20 with preribosomes. Taken together, these results are consistent with a block in middle steps of 60S subunit assembly in the *erbI<sub>class2</sub>* mutants.

Interestingly, we observed fewer changes in the levels of large subunit ribosomal proteins in comparison to r-protein mutants blocked in ITS2 cleavage of 27SB pre-rRNA or processing of ITS1 in 27SA<sub>3</sub> pre-rRNA (Figure 33B, bottom panel) (Dembowski et al. 2013a; Sahasranaman et al. 2011; Gamalinda et al. 2013; Ohmayer et al. 2013; 2015; Gamalinda et al. 2014; Biedka et al. 2016, submitted). Specifically, the r-proteins L17, L35, L37, and L25 that bind to the 5.8S/domain I/domain III interface in 25S rRNA associated stably with the preribosomes. In the *erbI<sub>class 2</sub>* mutants, we observed slightly reduced levels of domain III binding r-protein L19B required for 27SB pre-rRNA processing (Gamalinda et al. 2014), suggesting that rRNA folding in domain III of 25S rRNA is affected in the *erbI<sub>class 2</sub>* mutants. We also observed reduction in the levels of the non-essential r-proteins L31 and L26 binding to domain III in the *erbI<sub>Δ161-200</sub>* mutant. L26 and L31 line the polypeptide exit tunnel and bind to the 5.8S/domain III/domain I interface, further strengthening our hypothesis that structuring of these regions is perturbed in *erbI<sub>class 2</sub>* mutants. These results indicate that the *erbI<sub>class 2</sub>* mutants are blocked at the recruitment of Dbp10, Nsa2, and r-protein L19 in the hierarchical recruitment pathway of assembly factors involved in 27SB pre-rRNA processing (Figure

34) (Dembowski et al. 2013a; Jakovljevic et al. 2012; Talkish et al. 2012a; Woolford and Baserga 2013).

Figure 33A

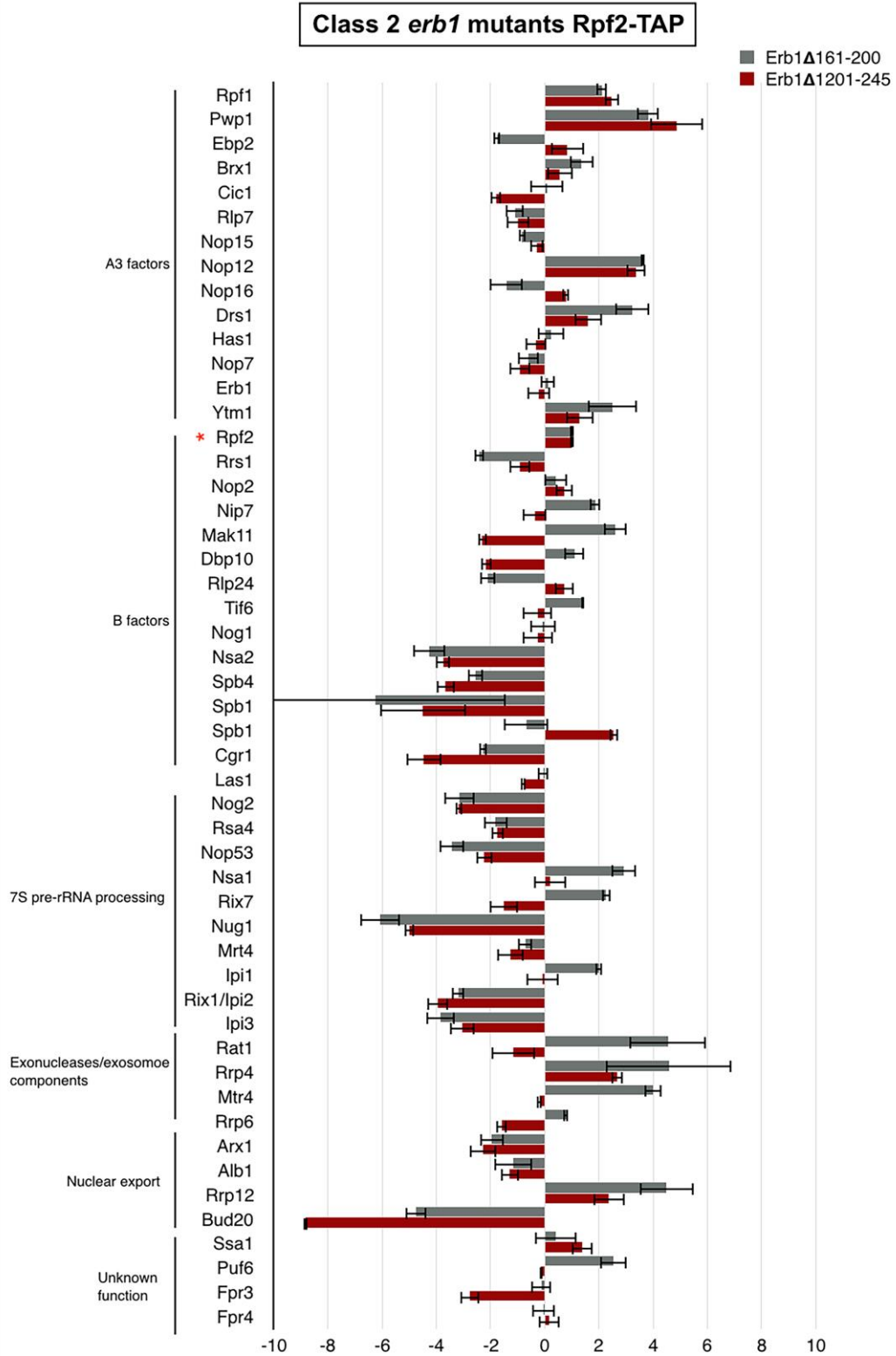
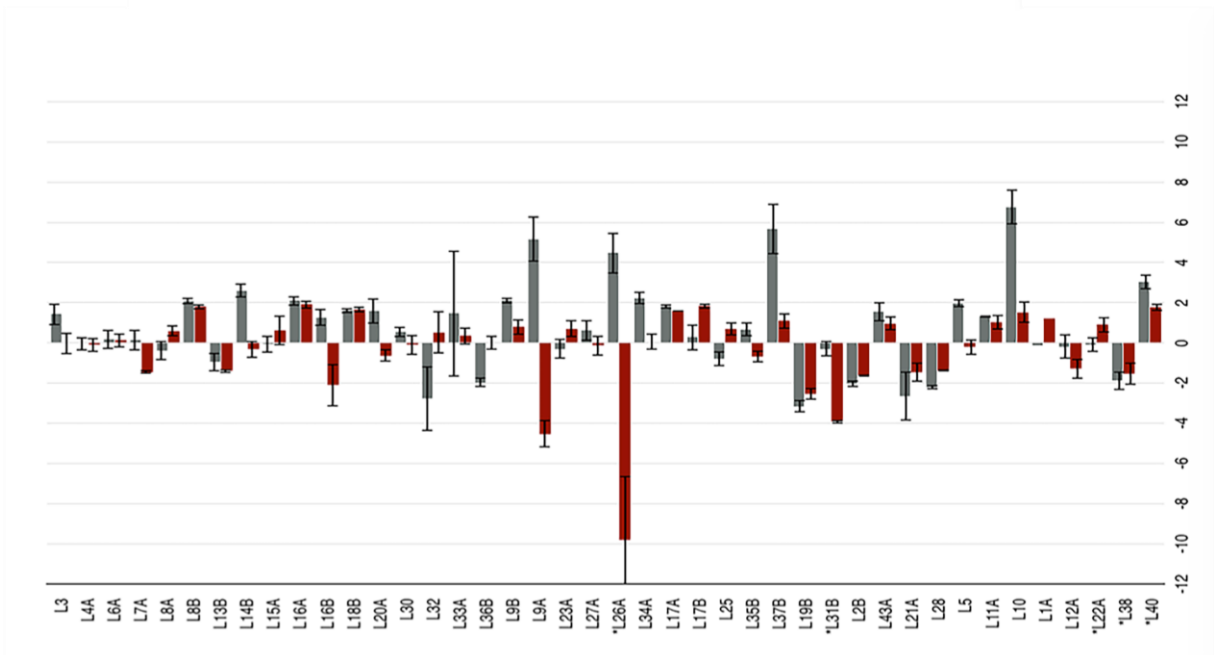
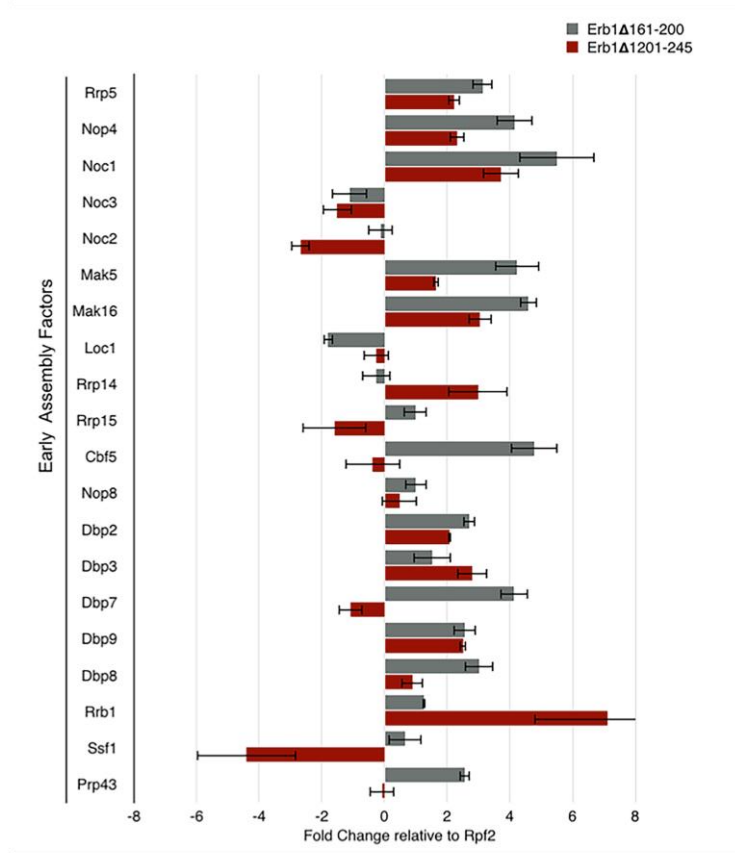


Figure 33B



**Figure 33. Erb1 is required for stable association of assembly factors involved in 27SB pre-rRNA processing.** Changes in the average relative ratios of assembly factors and r-proteins in 90S and 66S preribosomes in *erb1<sub>class 2</sub>* mutants were identified by iTRAQ of preribosomes purified using Rpf2-TAP (\*) as bait (average relative ratio of *erb1<sub>class 2</sub>* (Glu)/ *erb1<sub>class 2</sub>* (Gal)). Fold changes in the association of 66S assembly factors (A), early 90S assembly factors (B, top panel) and large subunit r-proteins (B, bottom panel) are shown. Data represent the average of four Glu/Gal ratios for each *erb1<sub>class 2</sub>* mutant, with the error bars representing the standard error of mean.



**Figure 34. *erb1<sub>class 2</sub>* mutants perturb the association of specific assembly factors involved in ITS2 cleavage and 27SB pre-rRNA processing.** Shown is a schematic representation of the hierarchical pathway for stable association of assembly factors and some r-proteins necessary for early and middle steps of 60S ribosomal subunit assembly. Proteins in the Pwp1-subcomplex, interdependent A<sub>3</sub> factors, and Has1 and Drs1 are required for 27SA<sub>3</sub> pre-rRNA processing (red). Stable association of the DEAD-box RNA helicases Drs1 and Spb4 depends on the preceding A<sub>3</sub> factors. These DEAD-Box proteins are, in turn, required for stable association of r-proteins that bind the 5.8S rRNA at the interface of domains I and III of 25S rRNA. The A<sub>3</sub> factors and 5.8S rRNA/domain III of 25S rRNA binding r-proteins are required for the stable association of a subset of assembly factors required for 27SB pre-rRNA processing (green). Stable association of assembly factors highlighted with the magenta outline is affected in *erb1<sub>class 2</sub>* mutants.

### **2.2.6 The structure of the bowtie region in 5.8S rRNA is affected in *erb1<sub>class 2</sub>* mutants**

Since the *erb1<sub>class 2</sub>* mutants prevent cleavage at the C2 site in pre-66S particles, we probed the structure of ITS2 and 5.8S rRNA by the Selective-2'-Hydroxyl Acylation analyzed by Primer Extension (SHAPE) method, using the chemical N-methylnicotinic acid imidazolide (NAI). SHAPE assays flexibility and solvent exposure of the 2'-OH group on the ribose sugar in both single- and double-stranded RNAs, providing information about base-pairing and tertiary interactions. Single-stranded or flexible regions react more with NAI, whereas RNA nucleotides engaged in intermolecular interactions exhibit low reactivity (Merino et al. 2005; Spitale et al. 2013). We analyzed the structure of ITS2 and 5.8S rRNA using oligonucleotide primers 5'-ITS2 and Oligo3140 that bind to different sequences in the ITS2. The 5.8S rRNA is sandwiched between domains I and domains III of 25S pre-rRNA. Therefore, folding of 5.8S rRNA was used as an assay to diagnose defects in rRNA folding of these regions.

Few modifications, except protection of two residues in ITS2 adjacent to the 5'-end of 5.8S rRNA, were observed in the ITS2 region, indicating that ITS2 structure is largely intact in *erb1<sub>class 2</sub>* mutants, after discounting the effects of loading (Figure 35). Observing only a few modifications in ITS2 is consistent with the stable association of the ITS2- associating A<sub>3</sub> factors Nop15, Rlp7, and Cic1 in *erb1<sub>class 2</sub>* mutants.



**Figure 35. The structure of ITS2 is largely intact in *erb1<sub>class 2</sub>* mutants.** The chemical NAI (indicated by +) was used to probe the structure of ITS2 in *GAL-3HA-ERB1 + erb1<sub>class 2</sub>* mutants grown in selective media containing galactose or shifted to glucose. Cells treated with DMSO alone (indicated by -) were used as controls. Total RNA extracted from NAI treated cells was used as substrate for primer extension (ITS2-3140). The locations of nucleotides that are protected are shown in magenta. The sequencing ladders are shown in lanes U, A, G and C. The nucleotide numbers in ITS2 are a continuation from the 5'-end of 25S rRNA.

The bowtie region in 5.8S rRNA was significantly modified in both *erb1<sub>class 2</sub>* mutants (Figures 36 and 37). We observe distinct changes in the modification pattern of the 5.8S rRNA helices in *erb<sub>class 2</sub>* mutants when compared to WT (Figure 36). The universal stop in 5.8S pre-rRNA (shown as a red circle) was used to assess loading-based changes in band intensities. The observed changes in primary sequence were then mapped onto the secondary structure of 5.8S rRNA (Figure 37A) and the tertiary structure of the 60S ribosomal subunit (Figure 2.17B) (Ben-Shem et al. 2011)(Shan *et. al* (2016), unpublished).

The contacts of L17, L35, L37, L39, L26 interacting with 5.8S rRNA are modified in our *erb1* class 2 mutants (Figure 37B). These r-proteins binding 5.8S rRNA are crucial to rRNA folding *in vivo* (Kwok et al. 2013). However, stable association of L17, L35, and L39 is not affected in the *erb1<sub>class 2</sub>* mutants (Figure 2.13B, bottom panel). Therefore, we conclude that the formation of the final, stabler conformation of weak helices h5-h9 in 5.8S rRNA and their r-protein contacts is perturbed in *erb1<sub>class 2</sub>* mutants. We observe selective protection or modification in 5.8S rRNA residues 75-85, protruding from helix 7. The GTPase Nog1 contacts residue 77, which is more modified in *erb1<sub>class 2</sub>* mutants (Figure 38C). Association of Nog1 to preribosomes is not affected in the *erb1<sub>class 2</sub>* mutants. Therefore, as it is the case with 5.8S rRNA binding r-proteins, the final contacts of Nog1 also seem to be perturbed in *erb1<sub>class 2</sub>* mutants.

Figure 36

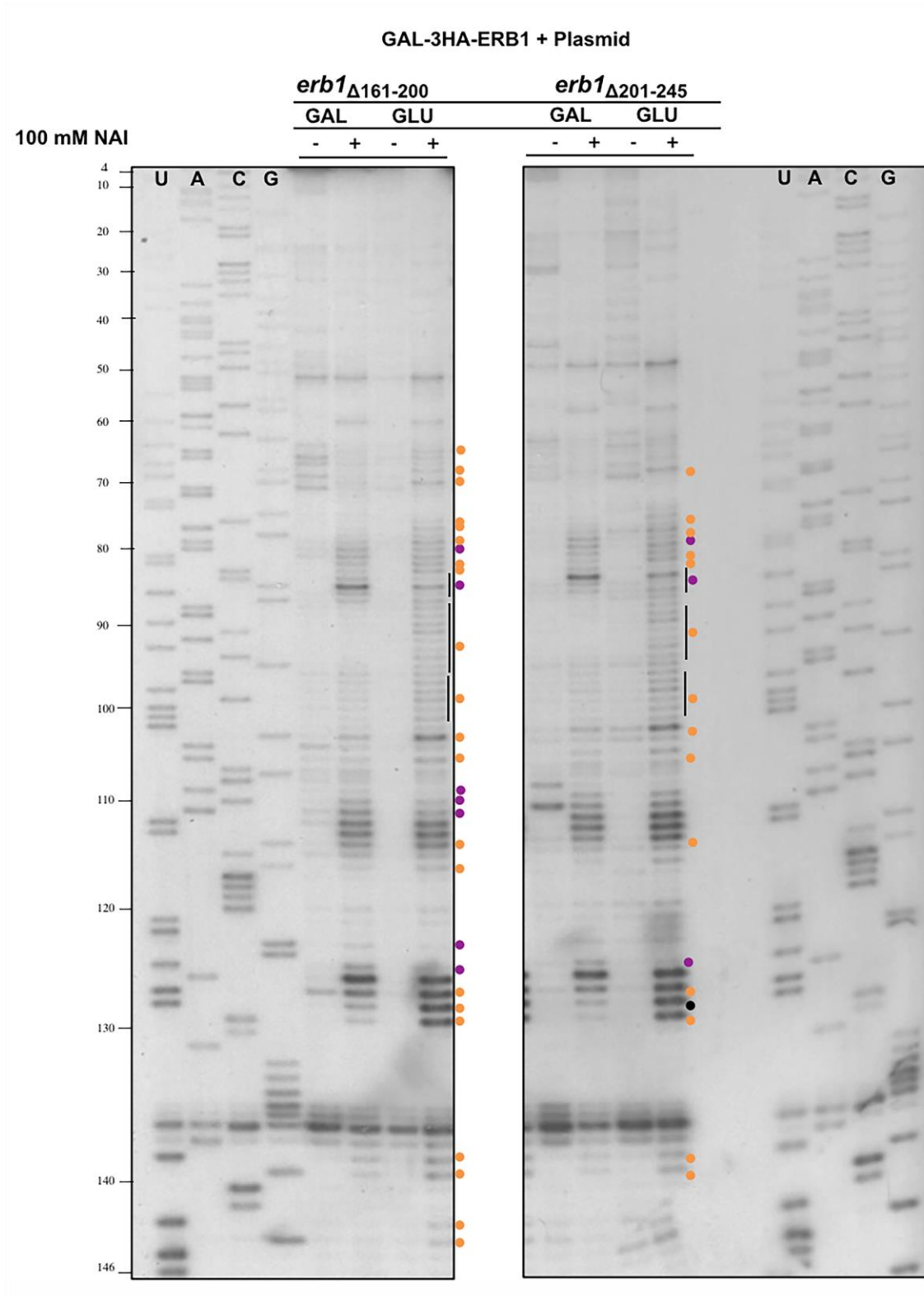
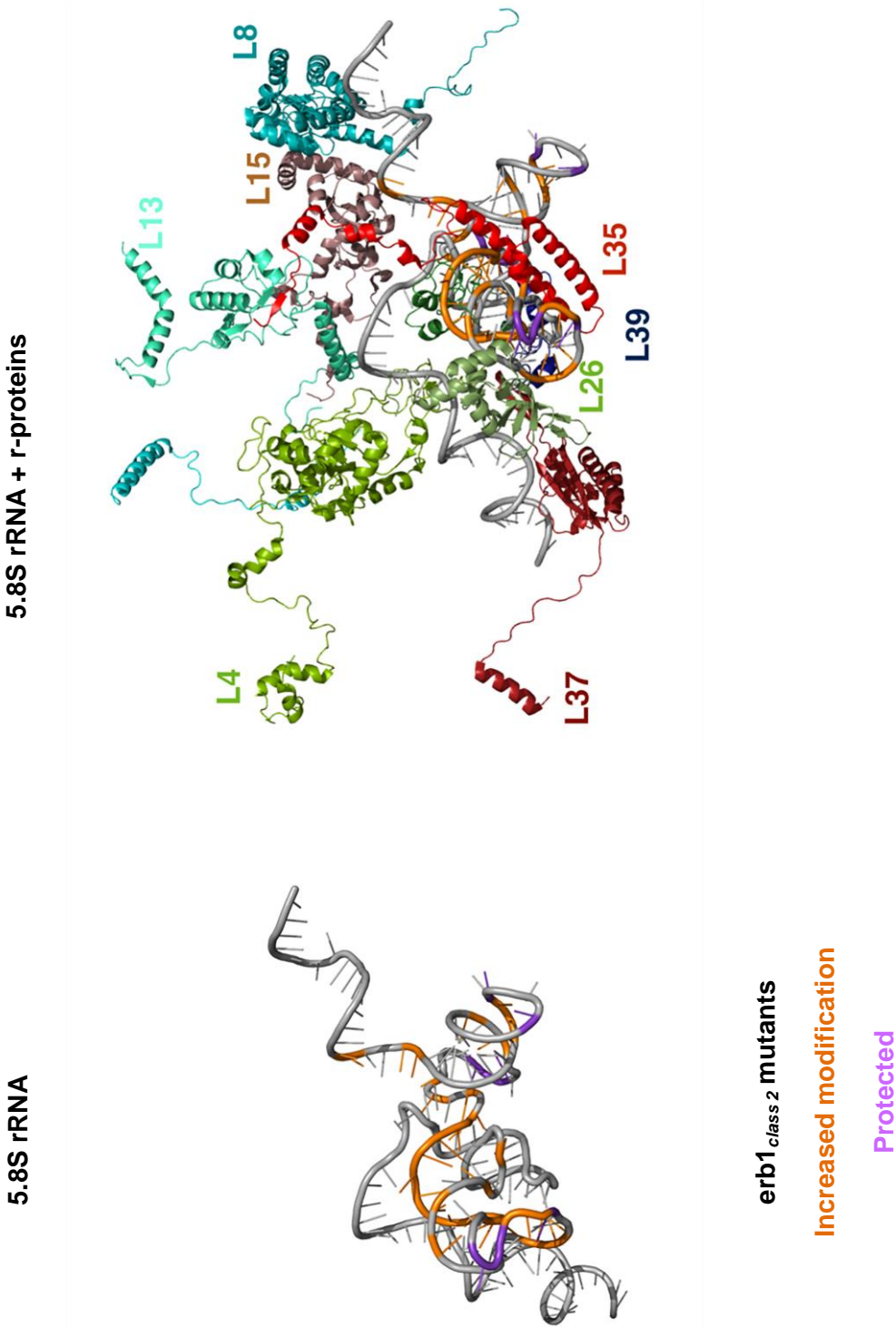


**Figure 36. The structure of 5.8S rRNA is perturbed in *erbI<sub>class 2</sub>* mutants.** The *in vivo* structure of 5.8S rRNA was probed using 100 mM NAI (indicated by +) in *GAL-3HA-ERB1* + *erbI<sub>class 2</sub>* mutants grown in selective media containing galactose, or grown in galactose and shifted to glucose. Cells treated with DMSO alone (indicated by -) were used as controls. Total RNA extracted from NAI treated cells was used as a substrate for primer extension (5'-ITS2 oligonucleotide primer). Locations of modified nucleotides are indicated in orange and protected residues are shown in magenta. The sequencing ladders are shown in lanes U, A, G and C.



Figure 37B





## **CHAPTER 3. Proper Structuring of Helices ES20 and ES26 in Domain III of 25S rRNA Is Required for 60S Ribosomal Subunit Assembly**

### **3.1 Introduction**

Ribosomal RNAs (rRNAs) form the core structure on which ribosomal proteins (r-proteins) are assembled to generate functional ribosomes. In eukaryotes, *trans*-acting proteins called assembly factors are required for folding of ribosomal RNAs and their assembly with r-proteins. Eukaryotic rRNAs contain regions that are not present in the core RNA secondary structure common to prokaryotes, archaea, and eukaryotes (Gerbi 1996; Melnikov et al. 2012). In the tertiary structure of mature 60S subunits, these regions referred to as expansion segments (ESs) are located on the solvent-exposed side of the 60S subunit (Figure 2). These expansion segments cluster at the central protuberance and the back of the P and L1 stalks. These two ESs are located adjacent to the ends formed after the removal of ITS1 and ITS2 spacer sequences in pre-rRNA (Ben-Shem et al. 2011). The eukaryote-specific r-proteins or eukaryote-specific r-protein extensions in the 60S subunit also localize close to these ESs (Figure 3). The ESs are thought to serve as docking sites for factors involved in regulation of translation, or processing and folding of the nascent transcript. It is becoming increasingly evident that these expansion segments also serve as the binding sites for assembly factors involved in 60S subunit assembly (Granneman et al. 2011; Dembowski et al. 2013; Bradatsch et al. 2012; Greber et al. 2012; Wu et al, 2016, submitted).

The assembly factor Nop7 binds to ES26 and helix 54 in domain III of 25S rRNA (Granneman et al. 2011) (Jill Dembowski, personal communication) (Wu et al. 2016, unpublished). ES26 and its base-pairing partner ES20 contain long, narrow, strongly bent loops that form many non-canonical base pairs and stacking interactions (Ben-Shem et al. 2011). In the tertiary structure of 25S rRNA, these ESs are located close to the proximal stem formed by the 3'-end of mature 5.8S rRNA and the 5'-end of mature 25S rRNA. The binding site of Nop7 is not occupied by any r-proteins in the mature 60S subunit, although ES20/ES26 and their adjacent helices (helix 54 and helix 55) closely contact the globular domains of r-proteins L34 (eL34) and L27 (eL27), and L2 (uL2), and the eukaryote-specific extension of the r-protein L8 (Ben-Shem et al. 2011). Analysis of high-resolution structures of pre-60S particles by cryo-EM revealed ES26 as the binding site of the 60S subunit assembly factor Nop53 (Wu et al. 2016, submitted) (Figure 45). The spacer sequence ITS2 emerges from third proximal stem adjacent to ES20/ES26 in pre-ribosomes (Figure 40).

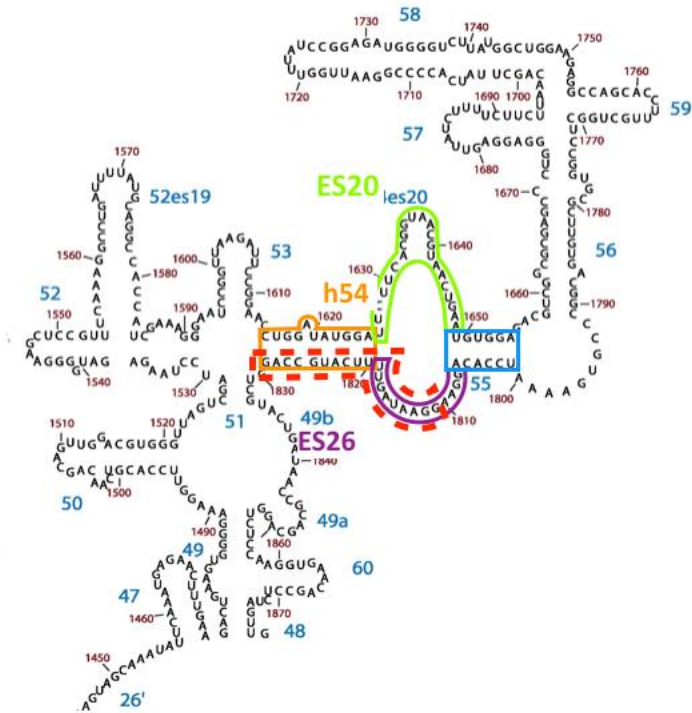
One of the main objectives of my thesis work was to dissect the roles of protein-protein and protein-RNA interactions of the Nop7-subcomplex in order to understand how the subcomplex components, namely Nop7, Erb1, and Ytm1, facilitate ribosome assembly. In order to do so, I generated six mutations perturbing the sequence and/or structure of ES20/ES26, thought to be important for the binding of Nop7 to pre-ribosomes (Granneman et al. 2011). Mutations perturbing ES20/ES26 structure are lethal, due to their effects on 60S subunit assembly (Figure 42 and Figure 43). Deletion of these expansion segments affects processing of the ITS2 spacer sequence adjacent to

it in 27SB pre-rRNA (Madhumitha Ramesh, Personal Communication). Depletion of the r-proteins L34, L27, or L2, or mutations in the extension of L8 contacting the ES20/ES26 neighborhood, also affect cleavage and /or processing of the ITS2 spacer (Figure 45) (Pöll et al. 2009; Ohmayer et al. 2013; Gamalinda et al. 2014). Collectively, these results indicate that proper structuring of ES26/ES20 is essential for processing of 27SB pre-rRNA during 60S subunit assembly. These results further strengthen my hypothesis that rRNA architecture in domain III is crucial for cleavage and processing of the ITS2 spacer in 27S pre-rRNA.

Figure 40

A

Secondary Structure of Domain III of 25S rRNA



B

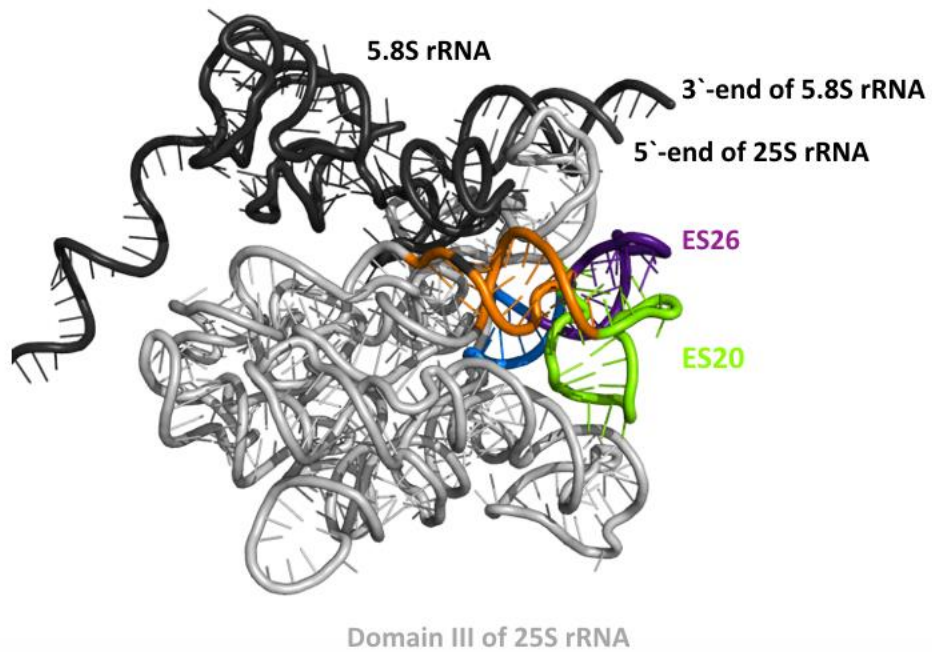


**Figure 40. Nop7 binds to ES26 and helix 54 in domain III of 25S rRNA.**

(A) Shown is the binding site of Nop7 (dotted red lines) on ES26 (purple) and helix 54 (orange)(Granneman et al. 2011). The secondary structure of domain III of 25S rRNA was obtained from the RiboVision website.

[http://apollo.chemistry.gatech.edu/RiboVision/#SC\\_LSU\\_Phylo](http://apollo.chemistry.gatech.edu/RiboVision/#SC_LSU_Phylo)

(B) ES26 (purple) forms intimate contact with ES20 (green), stabilized by helix 54 (orange) and helix 55 (blue) in 25S rRNA of mature 60S ribosomal subunits (Ben-Shem et al. 2011).

(PDB ID: 3U5D).

## 3.2 Results

### 3.2.1 The RNA polymerase I *Ts*<sup>-</sup> system to study rDNA mutants

The rRNAs are transcribed from ~200 copies of rDNA genes on chromosome XII in *S. cerevisiae*, making mutational analysis of chromosomally derived rRNA challenging. To circumvent this problem, several groups have generated RNA polymerase I 'pol1' temperature sensitive (*ts*) strains for conditionally expressing rRNA. For this study, we employed the NOY504 yeast strain which contains a mutant allele of the RNA polymerase I subunit A12.2 that results in *ts*- growth (Nogi et al. 1993). Since RNA polymerase I is responsible for transcription of rDNA genes, expression of endogenous rRNA can be shut off by shifting these pol I *ts* strains to 37°C (Figure 41). Growth defects and ribosome biogenesis defects in NOY504 can be rescued by a plasmid expressing rDNA genes under the control of RNA polymerase II-driven *GAL7* promoter (Fig. 3.2)(LaRiviere et al. 2006). Mutations affecting ES20/ES26 in the domain III of 25 rRNA were generated in this plasmid and introduced into the NOY504 strain.

Figure 41

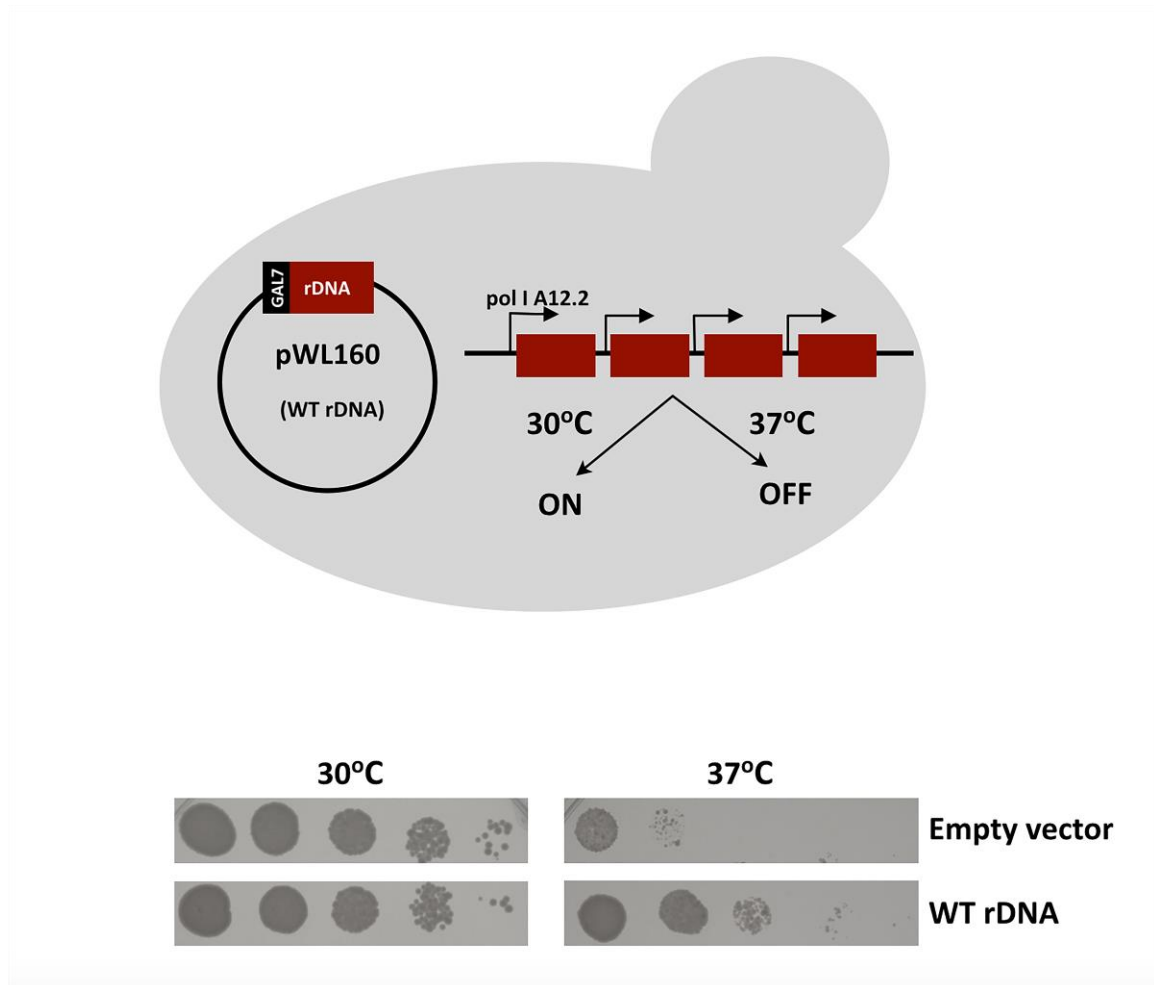


**Figure 41. The pol I *Ts*- system to study rDNA mutants.** (A) The yeast strain NOY504 containing temperature-sensitive (*Ts*-) mutations of RNA polymerase I subunit A12.2 fail to transcribe rRNA at 37°C. Plasmid-borne pWL160 expressing wild type 35S rDNA from the RNA polymerase II-driven *GAL7* promoter was introduced into NOY504 to study the effects of rDNA mutations on ribosome assembly. (B) NOY504 strains lacking wild type rDNA plasmid fail to grow at restrictive temperatures. Shown is the growth of the NOY504 strain containing either the empty vector or pWL160 (WT rDNA) on solid-media containing galactose.

### **3.2.2 Mutations affecting the structure of ES20/ES26 in domain III of 25S rRNA are lethal.**

To investigate the importance of the architecture of ES20/ES26, I designed mutations to affect either their sequence or structure, and assayed their effects on growth using the NOY504 yeast strain (Figure 42). NOY504 strains containing wild type or the A3DEL10 rDNA mutation were used as positive controls (Henry et al. 1994). Strains containing the empty vector pRS314 or the lethal H48 random mutation in domain III of 25S rRNA were used as negative controls for this assay (van Beekvelt et al. 2000). Deletions of nucleotides in the ES26 loop were lethal, whereas, a substitution mutation in the suspected cross-link site of Nop7 (1813-15 AAU-GGC) did not affect the growth of yeast cells at 37°C. In order to test if the unique architecture of ES26/ES20 was required for 60S subunit assembly, we designed a mutation to destabilize helix 54 that holds together ES26/ES20 (helix 54<sub>UG1622CA</sub>). This helix 54 mutation failed to complement growth defects of the pol I *ts* mutant. Re-establishing the helix architecture by constructing compensatory base pair changes suppressed the growth defect of the helix 54<sub>UG1622CA</sub> mutant. These results suggest that the structure of ES26 is crucial to 60S ribosomal subunit assembly or function.

Figure 42

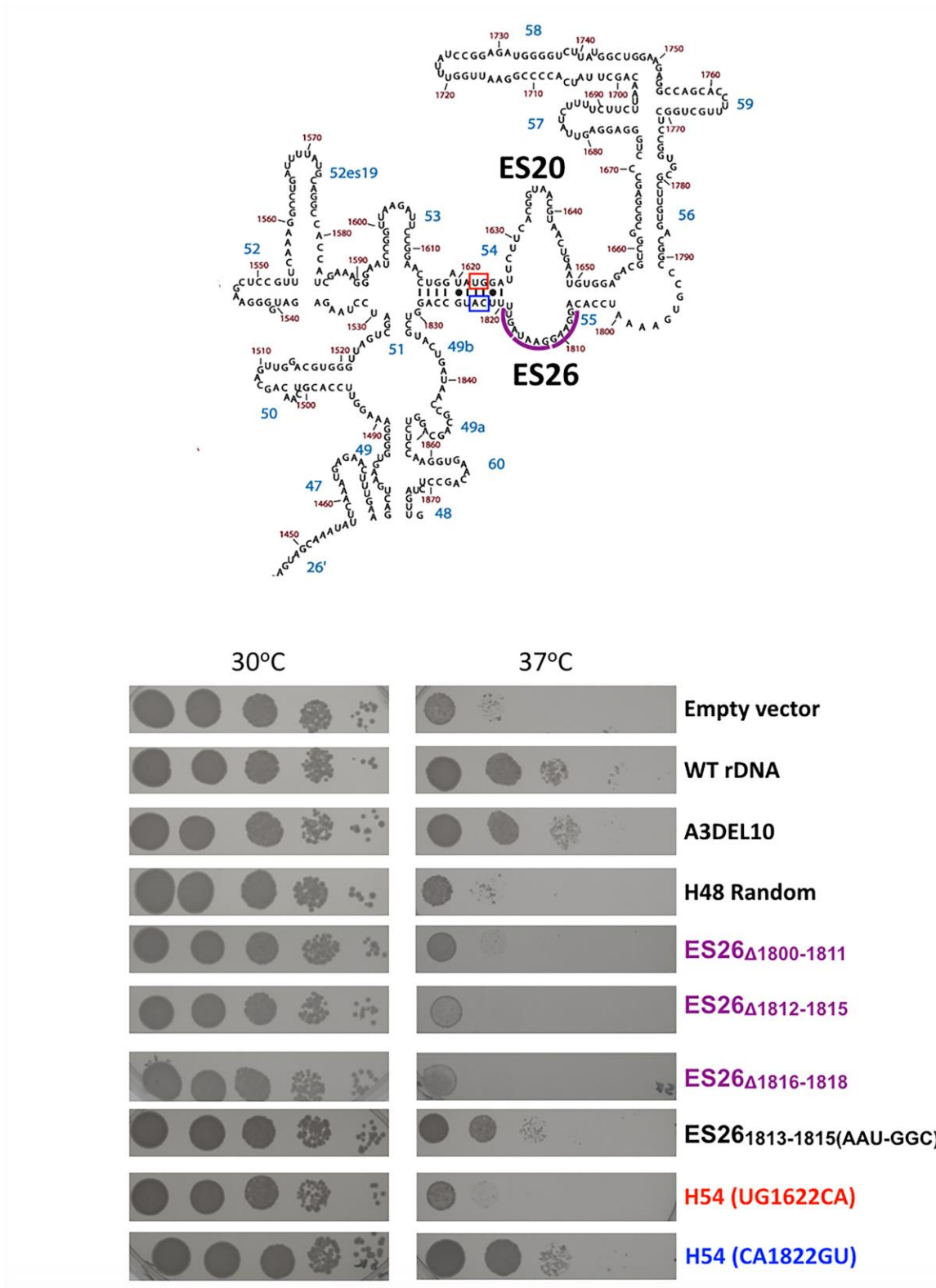


**Figure 42. Effects of ES20/ES26 mutations on cell viability.** (A) Shown are the locations of ES26 deletions (purple) and helix 54 mutations (red and blue) in domain III of 25S rRNA that were investigated in this study. The secondary structure of domain III of 25S rRNA was obtained from the RiboVision website ([http://apollo.chemistry.gatech.edu/RiboVision/#SC\\_LSU\\_Phylo](http://apollo.chemistry.gatech.edu/RiboVision/#SC_LSU_Phylo)). (B) Growth of the NOY504 pol I *ts* strain expressing mutations in ES26 or helix 54 at permissive (30°C) and restrictive temperatures (37°C), along with positive controls (Wild type rDNA and A3DEL10) and negative controls (empty vector and H48 random).

### **3.2.3 rRNA mutations perturbing the structure of the Nop7 cross-link site/ES26 affect ribosome biogenesis.**

To determine if the lethal mutations in ES26 or helix 54 of domain III affected 60S subunit assembly, we assayed the level of plasmid-derived 25S rRNAs in these mutants under restrictive conditions for expressing endogenous, wild type rRNA. The rDNA sequence in pWL160 contains two neutral tags inserted into 25S rRNA. Oligonucleotide probes base-pairing with the neutral tag sequence can be used to assay expression of plasmid-derived rRNA (Cole and LaRiviere 2008). We observed a significant reduction in the levels of 25S rRNA in strains containing lethal ES26/helix 54 mutants (Figure 43). The levels of endogenous 25S rRNA and 18S rRNA were used as loading controls, since their levels do not change after shifting NOY504 cells for 6 hours to 37°C (Kaempfer 1969). Thus, we conclude that ES0/ES26 architecture is important for 60S subunit assembly.

**Figure 43**

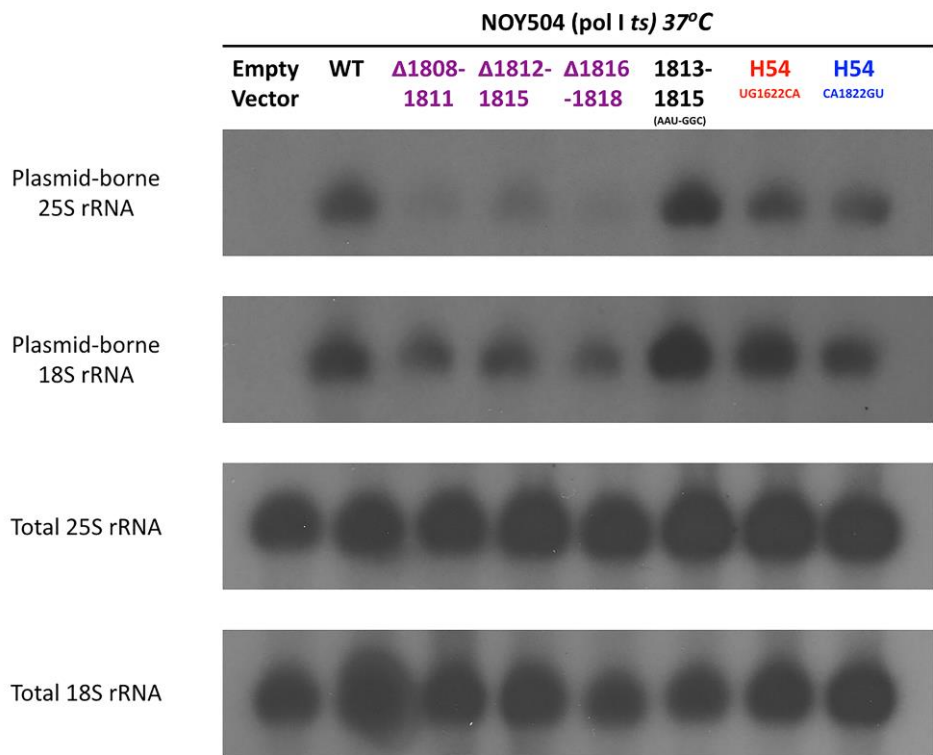


**Figure 43. Lethal mutations in ES26 and helix 54 of domain III of 25S rRNA perturb 60S subunit assembly.** Total rRNA was extracted from pol I *Ts*- strains containing WT /no/mutant plasmids grown at 37°C and assayed by northern blotting as previously described (Horsey et al. 2004; LaRiviere et al. 2006).

### 3.3 Discussion and Future Directions

My study demonstrates that the unique architecture of ES26/helix 54 is important for 60S ribosomal subunit assembly (Figure 41 and Figure 42). This rRNA expansion segment neighborhood forms the contact points for Nop7, Nop53, and r-proteins L34 and L27 (eukaryotic r-proteins), L8 (eukaryotic extension), and L2 (universal r-protein) (Figure 45). Deletion of ES20 or ES26 blocks formation of 7S pre-rRNA from the 27SB precursor (Madhumitha Ramesh, Personal Communication). Deletion of ES19 (also called V9 expansion segment) or point mutations in ES19 block processing of 7S pre-rRNAs. This helix is also contacted by Nop7 in 66S pre-ribosomes (Wu et al. 2016, submitted; van Beekvelt et al. 2000) (Fig.3.1 for location of ES19). Collectively, all of these studies implicate a crucial role for domain III architecture in the cleavage and processing of the ITS2 spacer sequence in 27SB and 7S pre-rRNAs.

The pol I *Ts*- strain is extremely challenging to work with for three reasons: (1) Depletion of WT rRNA is not complete, indicating leaky transcription from endogenous rDNA (lane 1, Figure 44). Therefore, we were not able to assay pre-rRNA processing defects in these mutants by primer extension. However, the strong growth defects and significant reduction of plasmid-borne 25S rRNA in the lethal ES26/helix 54 mutants accentuates the requirement of their proper structuring for 60S subunit biogenesis. (2) There is no existing method to purify pre-ribosomes from the rDNA mutant strains. I attempted to epitope-tag Nop7 (*NOP7-TAP*) in the pol I *Ts*- strain to purify pre-ribosomes from the mutants under restrictive conditions. The yield of pre-ribosomes that co-purify with Nop7-TAP was not sufficient for analysis, upon shifting to 37°C

(data not shown). (3) The pol I *Ts*- strains exhibit a high rate of suppressor formation, complicating the analysis using these strains (Yano and Nomura 1991).

Due to the inherent limitations of the NOY504 strain used in this study (discussed above), we were not able to pinpoint the molecular defects underlying 60S subunit assembly defects observed in the lethal mutants affecting ES20/ES26 architecture. However, since the atomic contacts of Nop7 and Nop53 with ES26 and helix 54 are now known, their role in 60S subunit assembly can now be explored by generating mutations in Nop7 or Nop53 to perturb their interactions with pre-rRNA. Additionally, we have established a system for *in vitro* transcription of domain III of *S. cerevisiae* 25S rRNA and heterologous expression of Nop7 in *E. coli* (data not shown). Domain III of 25S rRNA can fold to its near native architecture *in vitro* and also bind rpL25 *in vitro* ((van Beekvelt et al. 2000; Athavale et al. 2012)). Hence, it is possible to further develop and exploit *in vitro* binding systems with the above components to examine the effects of mutations in domain III of 25S rRNA on the binding of assembly factors such as Nop7 or Nop53, or its other interaction factors. Furthermore, the *in vitro* transcribed domain III of 25S rRNA can also be used to study the effects of protein binding or rRNA mutations on the global architecture of domain III of 25S rRNA (Athavale et al. 2012; Merino et al. 2005).

Figure 44

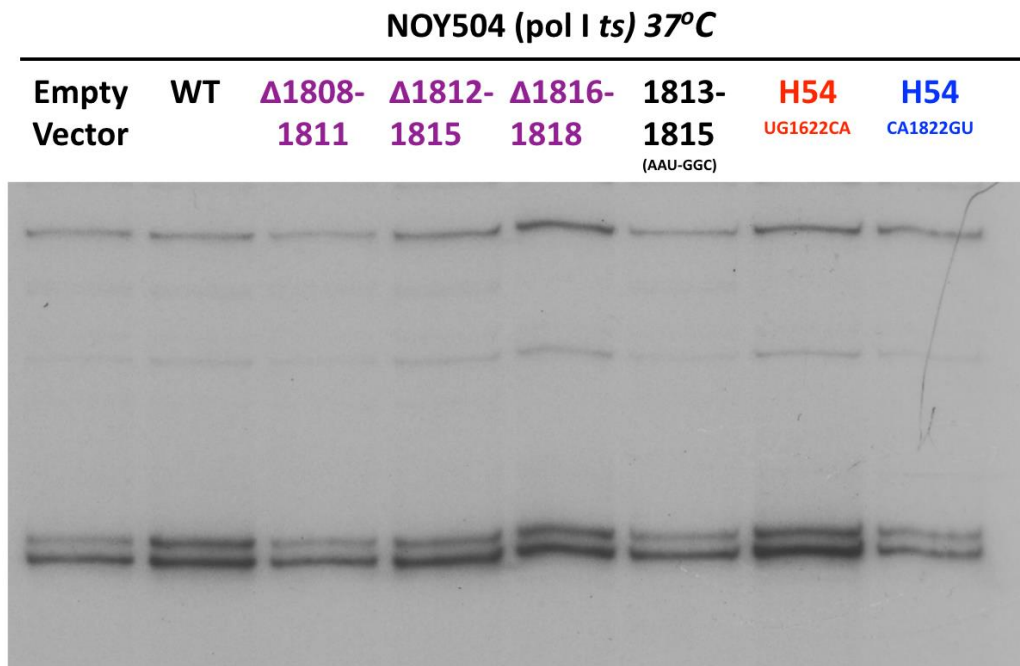


**Figure 44. Primer extension analysis of pre-rRNA processing in rDNA mutants.**

Total RNA was extracted from NOY504 strains containing WT/empty vector/mutated rDNA plasmids grown under restrictive conditions for endogenous rRNA expression. Primer extension revealed leaky transcription from the endogenous rDNA in the NOY504 strain (Lane 1). Therefore, this assay cannot be employed for pre-rRNA processing defect characterization in these mutant strains.

Figure 45

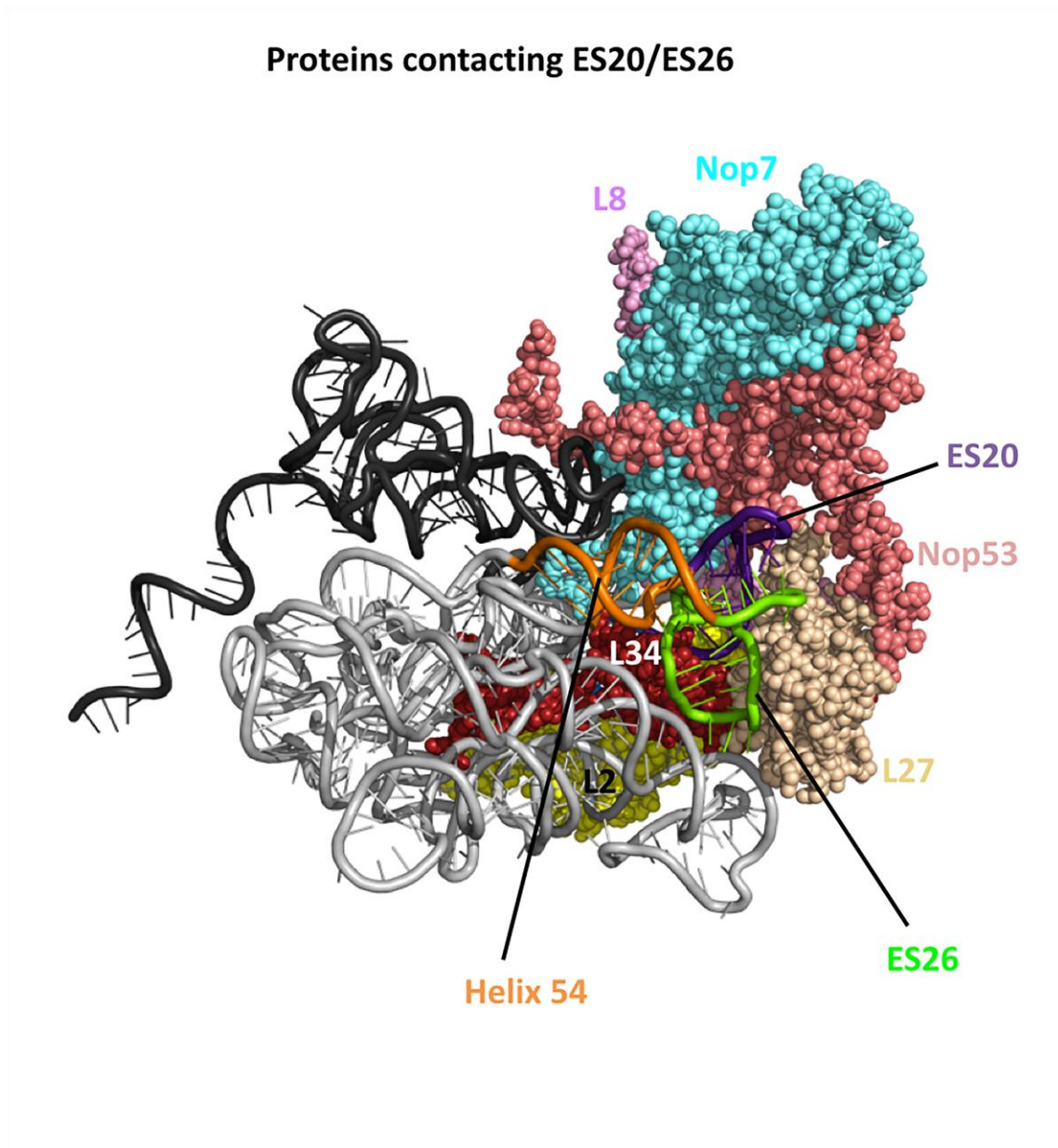


**Figure 45. The ES20/E26 neighborhood is a hub of interaction with assembly factors and r-proteins.** Nop7 (cyan) and Nop53 (light red) directly contact ES20 (purple) and helix 54 (orange) in domain III of 25S rRNA (light grey). 5.8S rRNA is shown in black for positional reference of domain III with respect to the 60S ribosomal subunit. In addition, ribosomal proteins L2 (yellow), L27 (wheat), L32 (brick red), and L8 (light violet) also contact the neighborhood of ES26/ES20.

### **3.4 Materials and Methods**

#### **Yeast strains and plasmids**

The pol I *Ts*- strain NOY504 was a generous gift from the Karbstein lab at the Scripps Research Institute, Florida. rDNA mutations were generated in the pWL160 plasmid containing rDNA gene under the control of the *GAL7* promoter. Mutagenesis was carried out using the QuikChange Lightning Site-directed Mutagenesis kit (Agilent). Mutagenesis was verified by sequencing (Genewiz) and plasmids were transformed into the NOY504 strain. Experiments were repeated at least twice using separate yeast transformations, due to a high tendency for suppressor mutations in this strain. For growth assays, ten-fold dilutions of yeast cultures beginning at O.D<sub>600</sub> of 0.8 were spotted on solid-media containing galactose at 30°C (control) and 37°C.

#### **Steady-state analyses of pre-rRNA processing**

NOY504 strains containing wild-type or mutant rRNA were grown overnight to O.D<sub>600</sub> of 0.2 in selective media containing galactose (C-TRP+GAL), and shifted to 37°C for 6 hours. Total RNA was isolated from whole-cell lysates as discussed previously (Horsey et al. 2004; Sahasranaman et al. 2011). Steady-state analyses of precursor and mature rRNAs were performed by northern blotting, as previously discussed (Horsey et al. 2004).

## **CHAPTER 4: The role of ribosomal proteins L21 and L28 in late nuclear steps of 60S ribosomal subunit assembly**

Ribosomal proteins L21 and L28 are required for generation of the 3'-end of mature 5.8S rRNA during late nuclear steps of 60S ribosomal subunit assembly. Previous studies revealed a defect in processing of 6S pre-rRNA upon their depletion. However, no significant defects were observed in pre-ribosome composition upon their depletion. In order to better understand how these proteins facilitate 60S subunit assembly, we conducted a comparative analysis of the location of these proteins on mature 60S subunits and 66S pre-ribosomal intermediates, and of the protein composition of pre-ribosomes upon their depletion.

### **4.1 Introduction**

Most r-proteins are essential to the assembly and function of ribosomes, and are hence indispensable to cell growth (Steffen et al. 2012). *In vitro* reconstitution studies of bacterial ribosomal subunits and *in vivo* analysis of eukaryotic ribosome assembly in *S. cerevisiae* provided valuable insights into the role of r-proteins in 60S subunit assembly. Pioneering work in the 1960s by Nomura, Nierhaus, and colleagues demonstrated that mature 50S subunits could be assembled *in vitro* from mature rRNAs and purified r-proteins (Nomura and Fahnestock 1973; Fahnestock et al. 1973) (Nierhaus and Dohme 1974). Along with the *in vitro* reconstitution of the small 30S subunit (Held et al. 1974) (Mizushima and Nomura 1970), these studies demonstrated that binding of r-proteins promoted productive conformers of rRNA, especially during tertiary structure formation.

They also showed that the r-proteins bound rRNA in a hierarchical fashion, with the early binding or primary r-proteins organizing binding sites for subsequent association of secondary and tertiary binding r-proteins. The overall assembly proceeded in a 5`-3` direction with respect to rRNA. Most importantly, the stringent chemical environment and slow kinetics of ribosome assembly from its mature components *in vitro* highlighted the necessity for more complex mechanisms required *in vivo* for the assembly of ribosomes from the pre-rRNAs and r-proteins at rates conducive to life (reviewed in detail in (Gamalinda and Woolford 2014; de la Cruz et al. 2015)).

Recent investigations of the effects of r-protein depletions on 60S ribosomal subunit assembly in yeast demonstrated a strong correlation between the locations of these r-proteins in the structure of 60S subunits and pre-rRNA processing defects caused by their depletion (van Beekvelt et al. 2001; Zhang et al. 2007; Babiano and de la Cruz 2010; Jakovljevic et al. 2012; Ohmayer et al. 2013; Gamalinda et al. 2013; 2014a; Pöll et al. 2009). This work provided valuable insights into the organizational hierarchy of the seemingly monolithic 60S subunits. The major conclusions from these studies are outline below:

- (1) Binding of r-protein L3 at both ends of 25S rRNA is required for early steps of pre-rRNA processing. Thus, the later stages of 60S subunit assembly can be assumed to be post-transcriptional.
- (2) R-proteins bound to domains I and II of 25S rRNA at its 3`-end resulted in early pre-rRNA processing defects affecting the processing of the ITS1 spacer sequence. These proteins are located across the equatorial region on the solvent interface, and hence

would be required to stabilize the initial compaction of domains I, II and III at the solvent interface.

- (3) Globular domains of r-proteins around the polypeptide exit tunnel contacting domain III/5.8S rRNA are necessary for middle-steps of pre-rRNA processing i.e., cleavage of the ITS2 spacer sequence.
- (4) R-proteins required for processing of 7S and 6S pre-rRNAs are located on the subunit interface and near the central protuberance of the 60S subunit contacting domains IV/V/and VI of 25S rRNA and the 5S rRNA. These r-proteins are required for nuclear export of pre-ribosomes.

Therefore, globally, 60S ribosomal subunit assembly proceeds in a 5`-3` direction, the solvent interface being assembled first before proceeding to the assembly of the subunit interface and the central protuberance, which host most functional centers of pre-60S ribosomes.

Until now, most detailed investigations into the mechanistic roles of r-proteins in assembly of the 60S ribosomal subunit focused on the early or middle acting r-proteins. Depletion of early and middle acting r-proteins causes large-scale changes in pre-ribosome composition, making it easier to observe changes in pre-rRNA processing and protein composition of pre-ribosomes. However, relatively few changes in protein composition of pre-ribosomes are observed upon depletion of late acting r-proteins, making their studies more challenging.

The r-proteins whose depletion affect late nuclear steps can be considered to be of

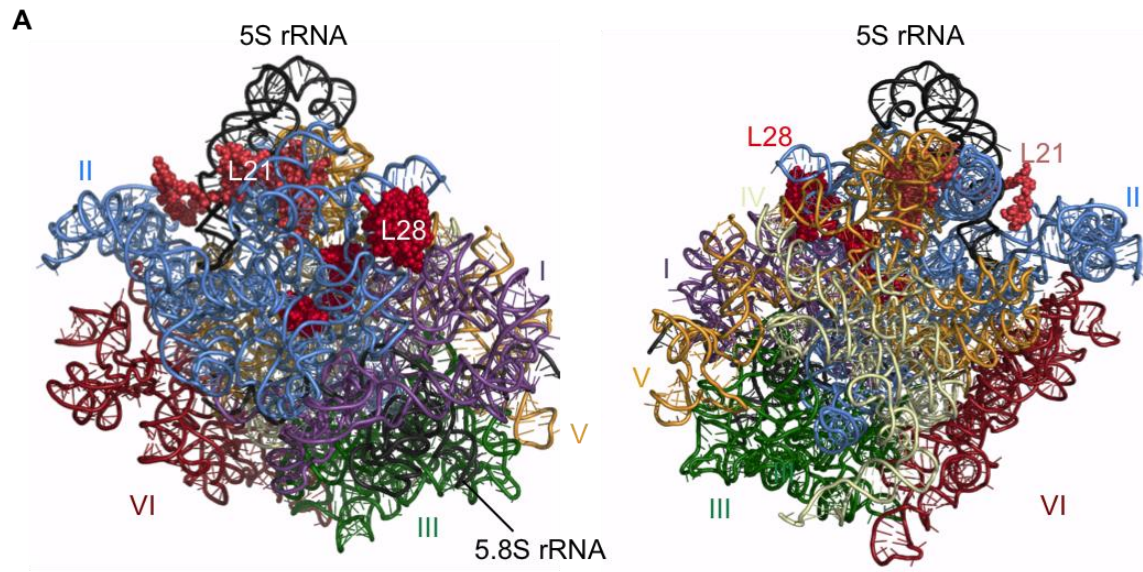
two groups based on their location in 60S subunits: (a) L2 and L43 located near the peptidyl transferase center, and (b) L28 and L21 located near the central protuberance of 60S subunit (Figure 46). Depletion/absence of these proteins affects processing of the ITS2 spacer causing accumulation of 7S pre-rRNA and 6S pre-rRNA, respectively. The misassembled pre-ribosomes are restricted to nucleus, safeguarding the translation pool (Ohmayer et al. 2013; Gamalinda et al. 2014a). How these proteins facilitate later steps of 60S subunit assembly is not well understood. Therefore, we focused on r-proteins L21 and L28 to understand their mechanistic roles during 60S ribosomal subunit assembly.

### **Comparative analysis of common features shared by L21 and L28 in 60S ribosomal subunits**

Most r-proteins form extensive contacts with rRNA. Hence, it has been proposed that these proteins facilitate rRNA folding and stabilization of RNP architecture during ribosome assembly and translation (Klein et al. 2004). Interestingly, binding sites of L21 and L28 cluster around multi-helical junctions on the secondary structure of rRNA (Figure 47), raising the possibility L21 and L28 acts as the scaffold to hold these helices together in their complex architecture. Both rpL28 and rpL21 contain globular domains that contact domains II and V of 25S rRNA. In addition, the extension of rpL21 contacts 5S rRNA in mature ribosomes, and rpL28 contacts domain I and the linker region between the six domains of 25S rRNA (Figure 46 and 47). Globular domains of r-proteins are known to mediate binding of r-proteins to the rRNA, and hence depletion phenotypes most likely reflect rRNA folding or assembly factor recruitment events mediated by these globular domains.

### **Prokaryotic homologs of L21 and L28**

L28 is the eukaryotic homolog of the universally conserved bacterial r-protein L15 (uL15). The bacterial homolog of L28 (uL15) contacts domains V and II, similar to the yeast r-protein. L21 is present in both archaea and eukaryotes and lacks a bacterial homolog. However, the bacterial r-protein L27 (bL27), which has no eukaryotic homolog, occupies a position similar to that of L21 in *E. coli* ribosomes (Figure 4.3). Therefore, in prokaryotes the role of L21 could be fulfilled by bL27. Both of these bacterial proteins are tertiary binding proteins *in vitro*, revealing that their association or tightening occurs late during large subunit assembly. Interestingly, the bacterial homolog of L28 is required for the assembly of rpL5 and 5S rRNA into 50S ribosomal subunits. The organization of 5S rRNA and helices around the central protuberance during 60S subunit assembly has been demonstrated recently (Leidig et al. 2014). It will be interesting to study if eukaryotic L28 is required for the events leading to 5S rRNA rotation.



Solvent interface view

Subunit interface view

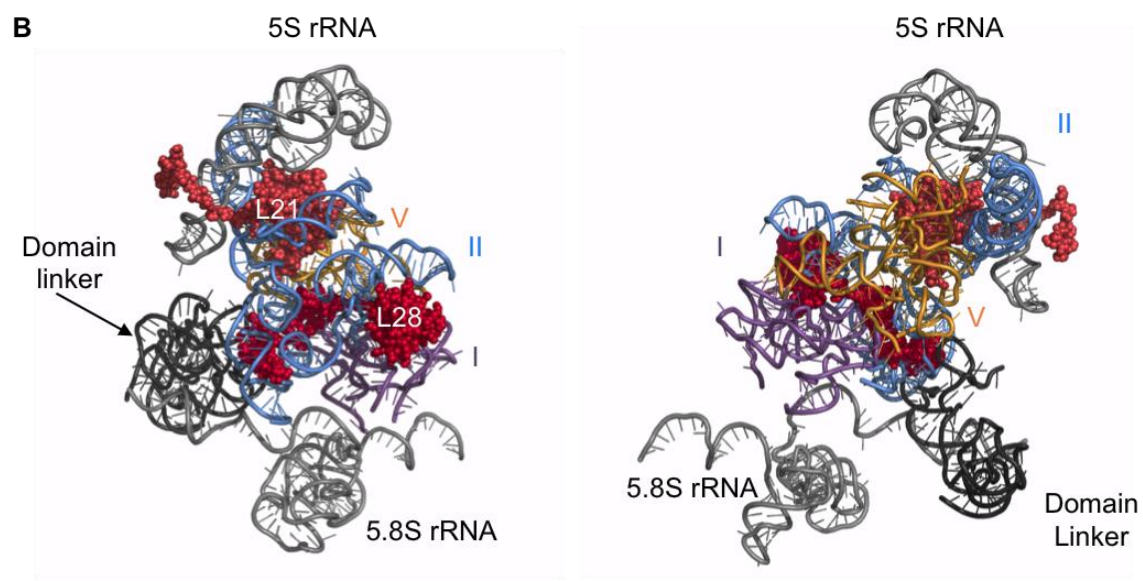


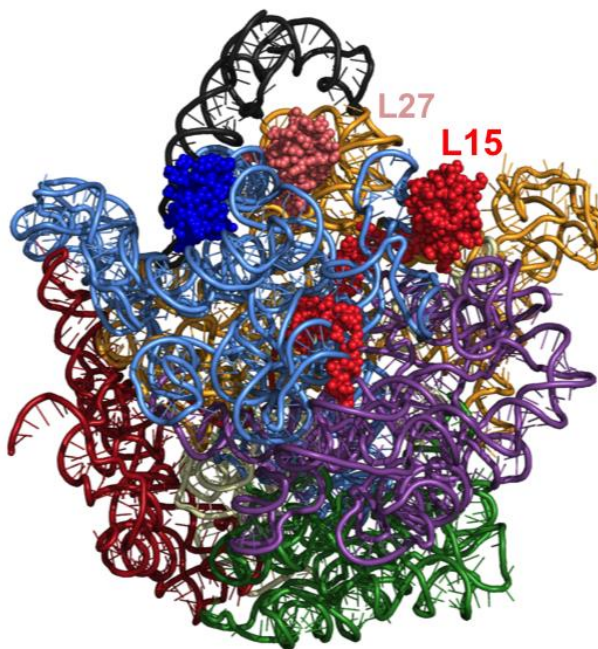
**Figure 46. A comparative analysis of interactions of L21 and L28 with rRNA in 60S ribosomal subunits** (a) The location of L28 and L21 on mature 60S subunits (PDB ID: 3U5D, 3U5E). The domain names are indicated in the same colors as in the crystal structure (Ben-Shem et al. 2011). (b) L28 contacts 25S rRNA domains I, II and V, and the domain linker region on which the six domains fold into the compact tertiary structure. L21 contacts domains II and V of 25S rRNA and 5S rRNA.

(PDB IDs: 3U5D, 3U5E).



**Figure 47. Direct contacts of L21 and L28 on 25S rRNA.** Direct rRNA contacts of L21 and L28 (Ben-Shem A., personal communication) were mapped on the secondary structure of rRNAs in the 60S ribosomal subunits, obtained from the RiboVision website. ([http://apollo.chemistry.gatech.edu/RiboVision/#SC\\_LSU\\_Phylo](http://apollo.chemistry.gatech.edu/RiboVision/#SC_LSU_Phylo)).

Solvent interface view



Subunit interface view

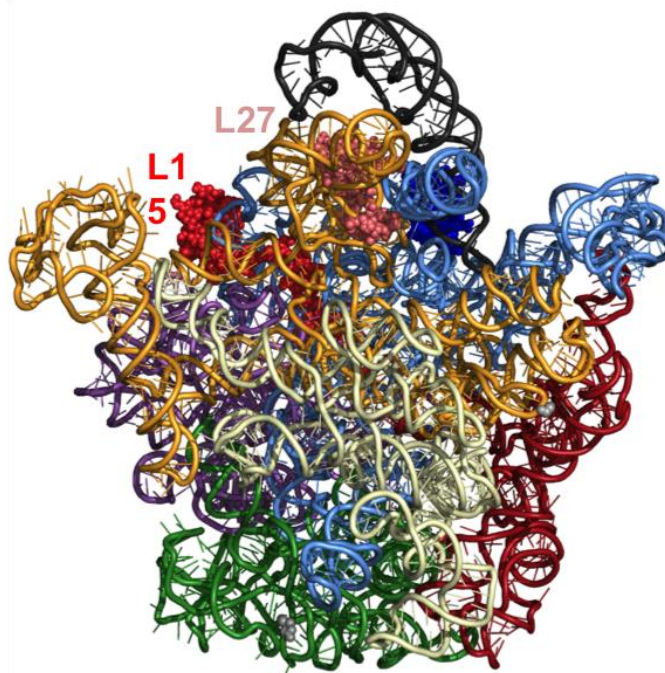


**Figure 48. L21 and L28 homologues in prokaryotic ribosomes.** Prokaryotic L15 (red) is a homolog of L28. There is no homolog for L21 in prokaryotes, but bacterial-specific r-protein L27 (light red) binds the region occupied by L21 in eukaryotes (Ban et al. 2014).

(PDB ID: 4V4V)

## **4.2 RESULTS**

### **L21 and L28 function in concert during 60S ribosomal subunit assembly**

To determine the effect of the absence of L28 on the composition of pre-ribosomes at different stages of 60S ribosomal subunit assembly, we purified and analyzed pre-ribosomal intermediates at different stages of nuclear maturation using a TAP-tag fusion at the C-terminus of assembly factors Rrp5 (very early to middle), Nop7 (very early to late), Rpf2 (very early to late), Nsa1 (middle to late), and Nog2 (middle to late) in the presence or absence of either L21 or L28. Purified pre-ribosome constituents were resolved on SDS-PAGE gels and visualized by silver staining. The bands were labeled as identified during this study and previous studies conducted in our lab ((Zhang et al. 2007), Hailey Brown (personal communication)). In contrast to previous studies, we observe distinct and comparable changes in the composition of pre-ribosomes upon depletion of L21 and L28 (Ohmayer et al. 2013; Gamalinda et al. 2014a).

#### **4.2.1 Depletion of L21 and L28 does not significantly alter the protein composition of early pre-ribosomal intermediates**

To assess the effect of depletion of late acting r-proteins L21 and L28 on early pre-ribosomal intermediates, we affinity-purified early pre-ribosomal intermediates using TAP-tagged assembly factor Rrp5 as bait. Rrp5 associates with 90S pre-ribosomes, containing 35S pre-rRNA, and leaves before 27SA<sub>3</sub> pre-rRNA processing occurs (Lebaron et al. 2013; Lebreton et al. 2008). Hence, Rrp5-containing preribosomes represents that portion of the assembly pathway before the formation of 27SB pre-rRNA, or early pre-66S particles. The band patterns of early pre-ribosomes in the presence or absence of Rrp5 look very similar, discounting the effects of loading (Figure 49). This observation makes sense, as depletion of L21 and L28 affect later steps of pre-rRNA processing, after Rrp5 exits pre-ribosomes. Hence, we concluded that Rrp5-TAP is not an appropriate bait to study the effects of L21 and L28 depletion on 60S subunit assembly.

**Figure 49**

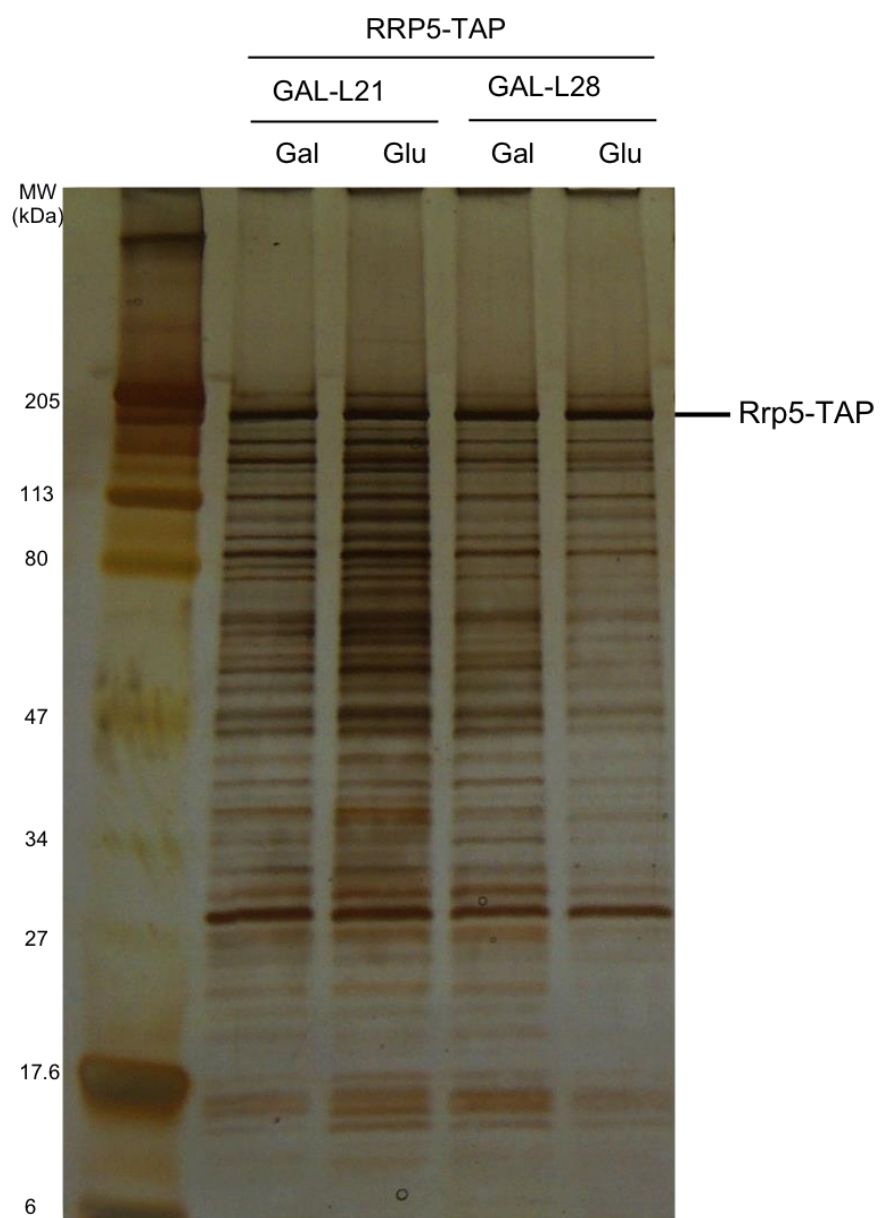


**Figure 49. The protein composition of pre-ribosomes is not altered at early stages of assembly upon depletion of L21 and L28.** TAP-tagged assembly factor Rrp5 was used as the bait to purify pre-ribosome in presence (GAL) or absence (GLU) of L21 or L28 from conditional null strains *GAL-RPL21* and *GAL-RPL28*. Bands that appear to increase or decrease in staining are indicated by orange dots. No significant changes are observed, if one discounts effect of loading with respect to the bait protein i.e., Rrp5-TAP.

#### **4.2.2 Association of late-acting assembly factors is affected upon depletion of L21 and L28.**

We probed the effects of depletion on early and middle pre-66S particles using pre-ribosomes purified with TAP-tagged assembly factors Rpf2 or Nop7 as baits (Figure 50). These assembly factors associate with pre-ribosomal intermediates containing 35S pre-rRNA and dissociate after the formation of 7S pre-rRNA (Dembowski et al. 2013; Granneman et al. 2011). Based on our gels, more changes in protein composition of pre-ribosomes were observed using Nop7 as bait (Figure 50B). We believe that the observed differences between Nop7-TAP and Rpf2-TAP purified preribosomes might arise from the close proximity of Rpf2 to L21 and L28 on preribosomes, thus biasing the observations in a manner that we do not yet understand. Since Rpf2 binds 5S rRNA (Zhang et al. 2007; Asano et al. 2015; Kharde et al. 2015; Madru et al. 2015) and less changes are visible when it was used as bait, we decided to use Nop7-TAP for further assays.

We observe an increase in the intensity of bands corresponding to assembly factors Drs1 and Rrp12, and a decrease in Nug1 (a GTPase), Rea1 (an AAA-ATPase), Ipi1 and Ipi3 (scaffolding proteins of the Ipi-subcomplex), and Mrt4 (an RNA helicase). The increased levels of Drs1 in preribosomes indicates that (a) its release is blocked in our mutants, or (b) Drs1, classified as an A<sub>3</sub> factor at present, may have later roles in 60S subunit assembly. The association of Ipi1, Ipi3, Nug1 and Rea1 are potentially affected since these factors bind to domain V of 25S rRNA, specifically close to the helices contacted by L21 and L28 (Barrio-Garcia et al. 2015; Manikas 2014) (Nissan et al.

2002). To quantitatively assay the relative changes in pre-ribosome composition upon depletion of L21 or L28, we have submitted Nop7-TAP purified pre-ribosomes for semi-quantitative iTRAQ analysis.

Figure 50A

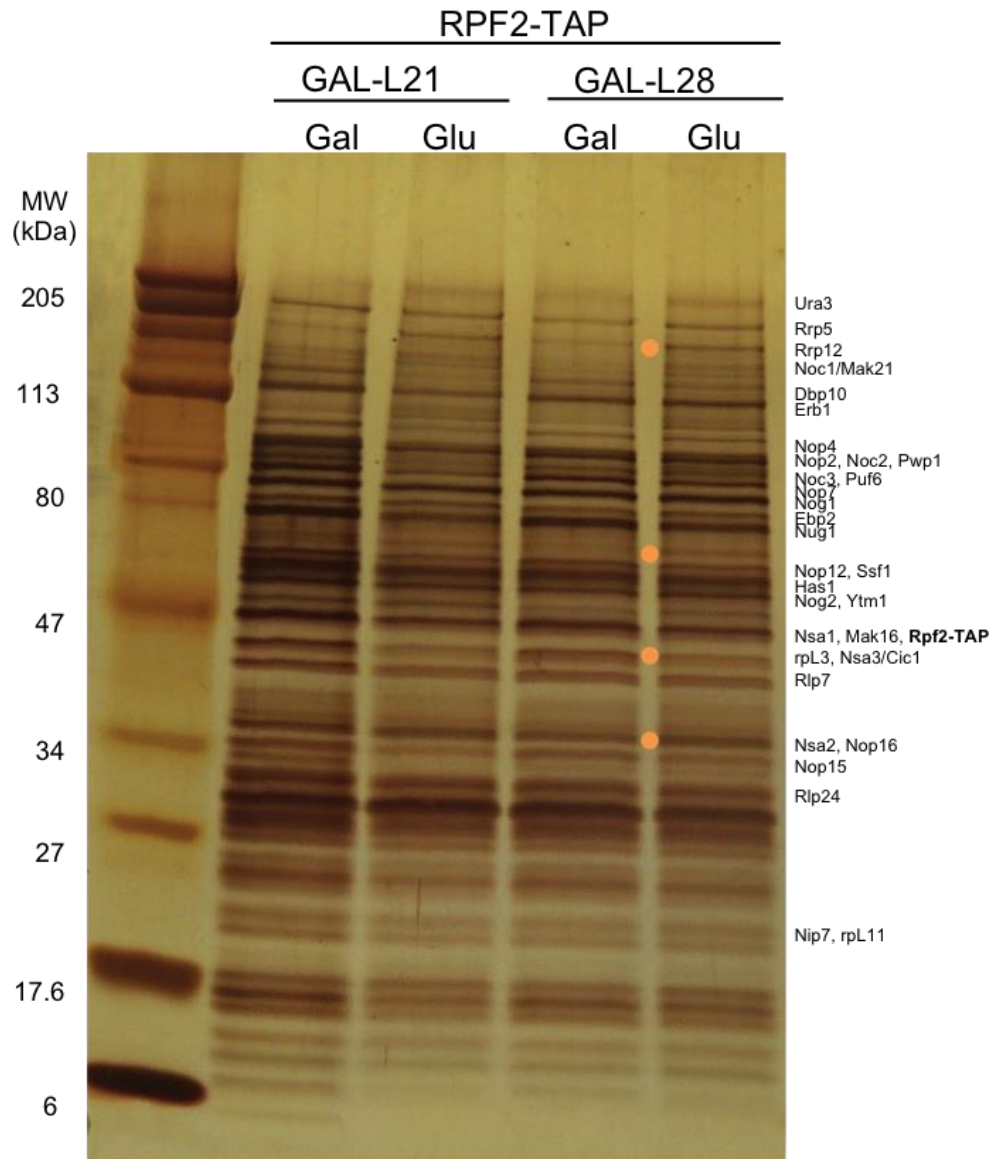


**Figure 50B**

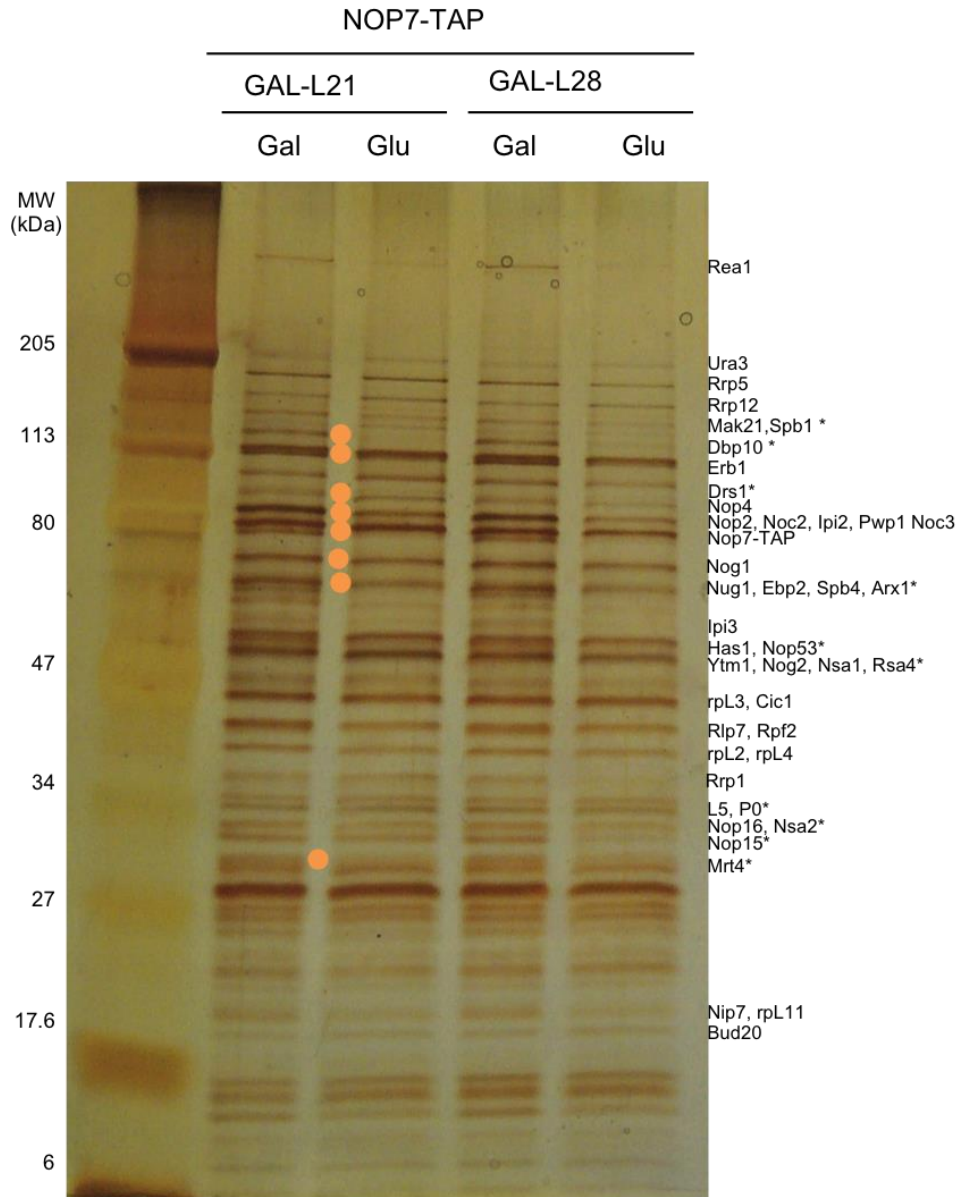


**Figure 50. The protein composition of pre-60S particles exhibits specific changes upon depletion of L21 and L28.** Pre-ribosomes purified using bait proteins Rpf2 and Nop7 in the presence (Gal) or absence (Glu) of L21 and L28 were resolved by SDS-PAGE and visualized by silver staining. These baits reveal changes in pre-ribosome composition from 90S pre-ribosomes to late stages of 60S maturation in nucleoplasm. Bands that appear to increase or decrease in staining are indicated by orange dots.

### **4.2.3 Depletion of L21 and L28 affects the stable association of proteins during middle and late events of 60S maturation.**

We used assembly factors Nsa1 and Nog2 as baits to purify pre-ribosomal intermediates during middle and late steps of 60S subunit, respectively. Nsa1 associates with pre-ribosomes containing 27SB pre-rRNA, and remains associated for a short intervals at the beginning of late nuclear steps of 60S subunit assembly (Kressler et al. 2008; Dembowski et al. 2013; Ohmayer et al. 2013).

Nsa1-TAP purified pre-ribosomes show relatively few changes in protein composition in the absence of L21 or L28 (Figure 51). Since we detect only minor changes in protein composition using Nsa1-TAP purified pre-ribosomes, we decided to focus on Nog2-TAP for further studies. We saw fewer changes in Nsa1-TAP purified pre-ribosomes in comparison to Nog2-TAP purified pre-ribosomes. This indicates that majority of the changes in preribosomes observed upon depletion of L21 or L28 are likely to happen after its exit, i.e., before ITS2 cleavage in 27SB pre-rRNA. This is in agreement with the pre-rRNA processing defect in 6S pre-rRNA upon depletion of L21 or L28.

We observe decreased intensity of bands corresponding to assembly factors Sda1, Rix1 and Rsa4, which bind near the central protuberance and the peptidyl transferase center (Figure 51B)(Barrio-Garcia et al. 2015). Since these proteins bind directly to the helices stabilized by L21 and L28, their binding sites might not be generated in the absence of L21 and L28 (Figure 50) We have sent the Nog2-TAP purified particles in presence or absence of L28 to our collaborators at Tsinghua University, China for analysis by cryo-EM.

Figure 51A

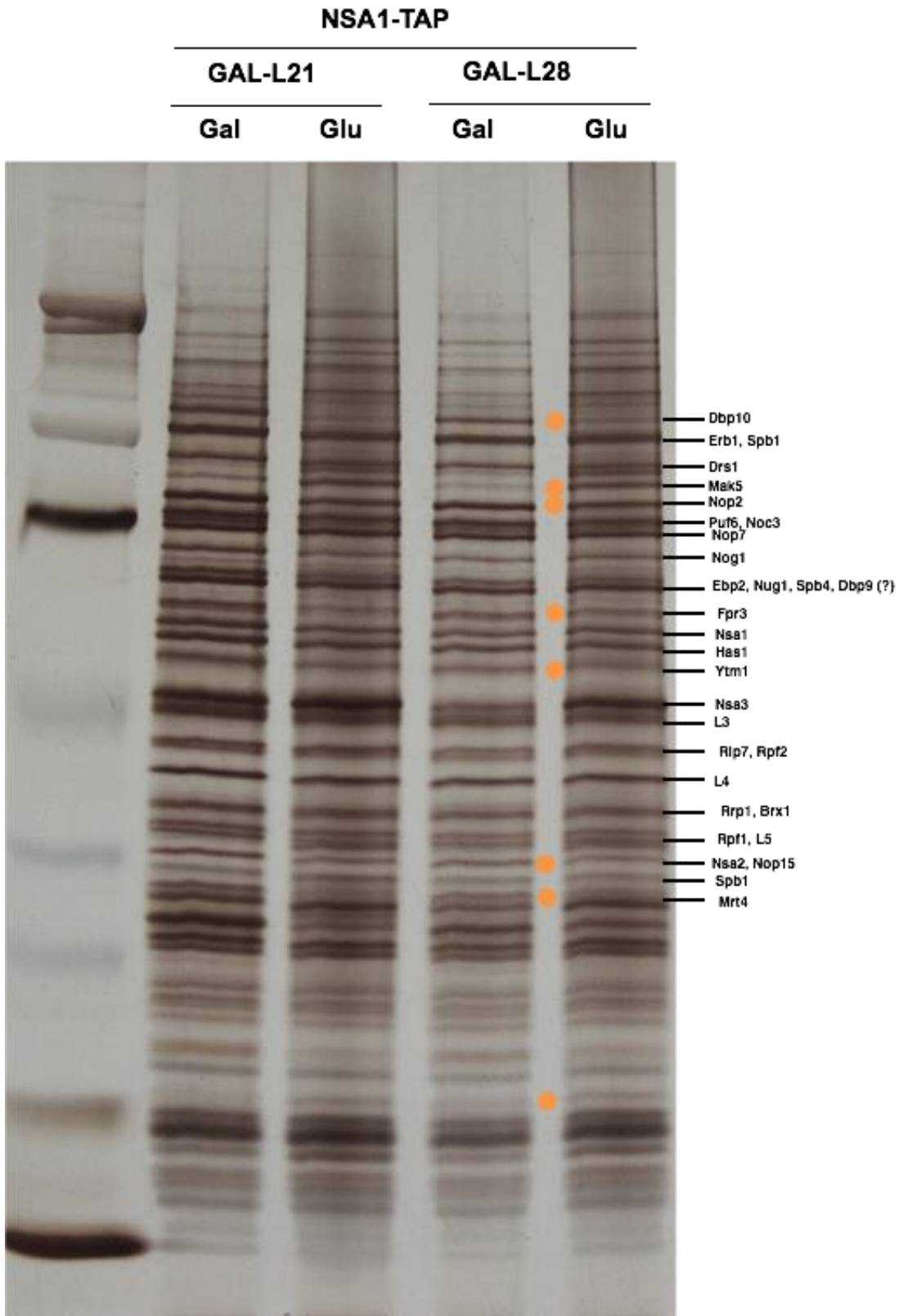
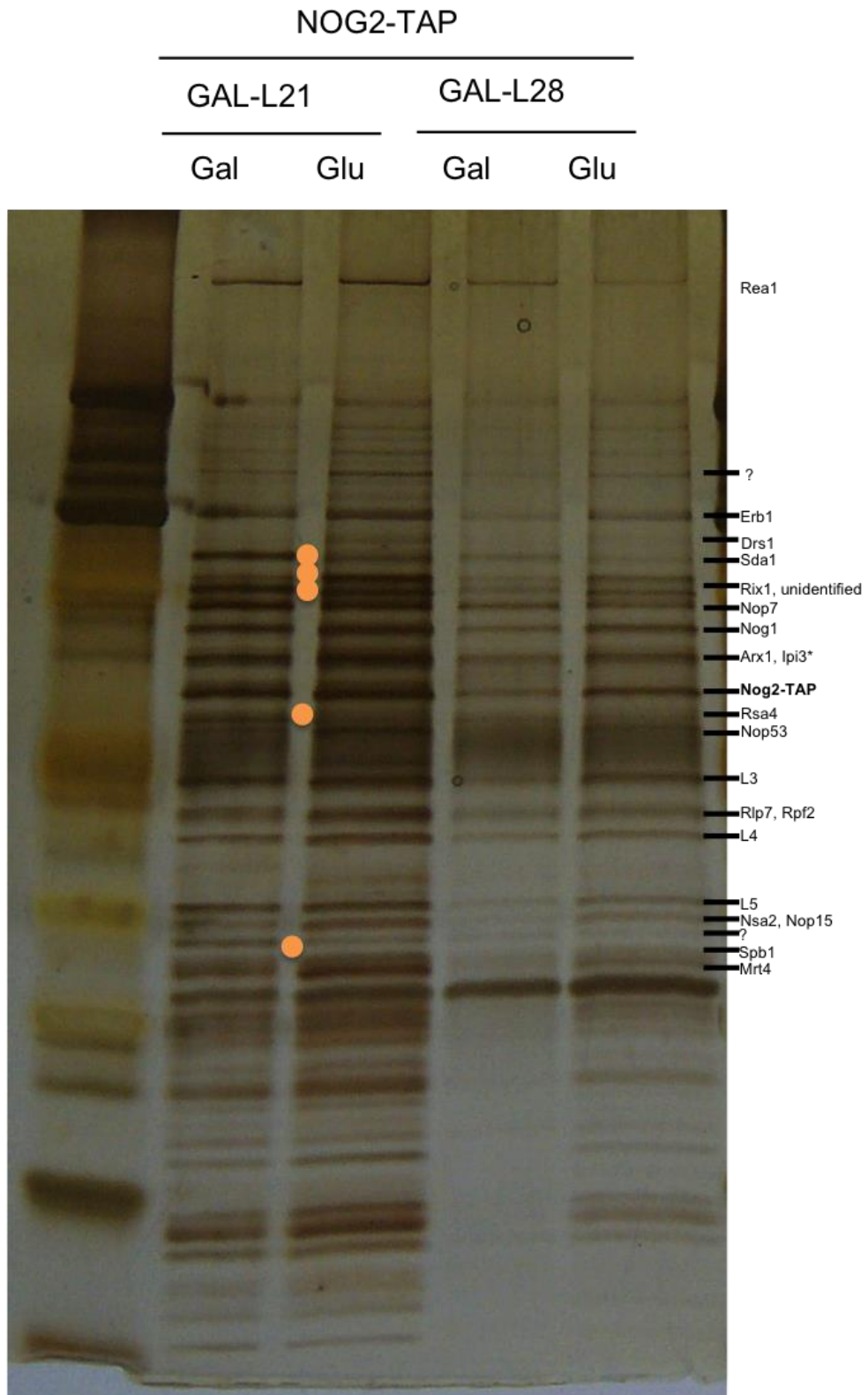


Figure 51B



**Figure 51. The association of assembly factors located in domain V of 25S pre-rRNA is affected upon depletion of L21 or L28.** Proteins in pre-ribosomes purified using bait proteins Nsa1 (A) and Nog2 (B) in the presence (Gal) or absence (Glu) of L21 and L28 were resolved by SDS-PAGE and visualized by silver staining. These baits reveal changes in pre-ribosome composition of middle and late 60S pre-ribosomal intermediates, respectively. Bands that appear to increase or decrease in staining are indicated by orange dots. For Nsa1-TAP, we have primarily focused on the bands whose intensity goes down, for reliable conclusions.

### **4.3. Discussion**

#### **Depletion of L21 or L28 affects association of assembly factors with rRNA domain V of 60S subunits.**

The conclusions from experiments discussed in sections 4.2. are outlined below.

- 1) We observe specific changes in the composition of pre-ribosomes upon depletion of L21 or L28. This is in contrast to previous studies by (Ohmayer et al. 2013) and (Gamalinda et al. 2014a). We used 16-hour shifts to restrictive conditions in contrast to 6 hours used in previous studies, thus facilitating characterization of protein composition of pre-ribosomes in these mutants.
- 2) We identified Nop7-TAP and Nog2-TAP as best baits to study pre-ribosome composition in L21 and L28 depletion mutants.
- 3) Analysis of our SDS-PAGE gels indicates that stable association of assembly factors Rsa4, Ipi2, Ipi3, Nug1, and Mrt4 is affected by L21 or L28 depletion. These assembly factors are localized to the domain II and/or V of 25S rRNA (Barrio-Garcia et al. 2015)(Wu et al., 2016, submitted).

#### **What are the effects of depletion of L28 on pre-rRNA folding?**

Since pre-rRNA processing and pre-ribosome composition defects in the absence of L21 or L28 are identical in all of the studies we conducted, we proposed that their concerted action would be required for 60S subunit assembly. To understand the structural dynamics of pre-ribosomes around L21 and L28 contact sites, we performed a detailed analysis of rRNA and protein contacts of L21 and L28 in mature and pre-60S particles using the crystal (Ben-Shem et al. 2011) and cryo-EM structures of *S. cerevisiae*

60S ribosomal subunits ((Barrio-Garcia et al. 2015)(Wu et al. 2016, submitted)). Here we focus on the shared contacts of L21 and L28.

L21 and L28 are required for the processing of the ITS2 spacer sequence in 6S pre-rRNA, required for the formation of the 3'-end of mature 5.8S rRNA(Ohmayer et al. 2013; Gamalinda et al. 2014b). With the recent discovery of the rotation of the 5S RNP during late steps of 60S maturation in the nucleus, we began to hypothesize that L21 could be required for 5S RNP rotation since it binds to the base of 5S RNA in its mature state. A large number of assembly factors, including NTPases (Nug1, Dbp10, Nog2, Nog1) and the large Rea1 AAA-ATPase are located adjacent to L21 in pre-ribosomes (Leidig et al. 2014; Matsuo et al. 2014; Barrio-Garcia et al. 2015). Since L28 is located apart from the CP, we reasoned that it could not be directly involved in structuring 5S rRNA or facilitating the activity of assembly factors contacting L21 during 60S subunit assembly. However, since L21 and L28 are located adjacent to each other, we carefully investigated the common features shared by these proteins on the 60S subunit.

As previously discussed, L21 and L28 contact domains II and V of 25S rRNA. We observe extensive changes in helices 80-88 in domain V and helices 27-29 in domain II of 25S rRNA (Figures 52-54). We observe perfect alignment of domain I rRNA in mature and pre-60S subunit structures in this solvent-exposed 60S subunit domain. This is in agreement with the model that domain I is organized early during 60S subunit assembly as the depletion of r-proteins contacting this domain aborts ribosome assembly at early

We then focused on the contacts of assembly factors affected by L21 and L28 depletion.

- Rsa4 contacts helices 86, 84, and 89 in domain V of 25S rRNA and Rea1. The contacts vary between pre-ribosomes purified using Rix1 and Nog2 as baits (Barrio-Garcia et al. 2015).
- Nug1 binds near the A-site finger in domain II and adjacent to helix 89 in domain V of 25S rRNA. The full structure of Nug1 has not yet been solved (Manikas, 2016).
- Mrt4 binds to the helices in and at the base of the A-site finger in domain II of 25S rRNA (Wu et al. 2016, submitted).
- Sda1 binds to helices h38a (Domain II), h78, h81, and h85 (Domain V) of 25S rRNA (Barrio-Garcia et al. 2015).
- The Rix1-subcomplex is located between Sda1 and Rix1 in the cryo-EM structures, making contacts in domains II (h38) and V of 25S rRNA (Barrio-Garcia et al. 2015).

None of these proteins makes direct contact with either L21 or L28, thus strengthening our hypothesis that rRNA folding induced by L21 and L28 is required for rearrangements of domains V and II in 25S rRNA, which are then required for 6S pre-rRNA processing. Therefore, we will next focus on analyzing changes in the rRNA structure of these helices upon depletion of these ribosomal proteins, using chemical structure probing of purified pre-ribosomes (Hector et al. 2014).

Figure 52

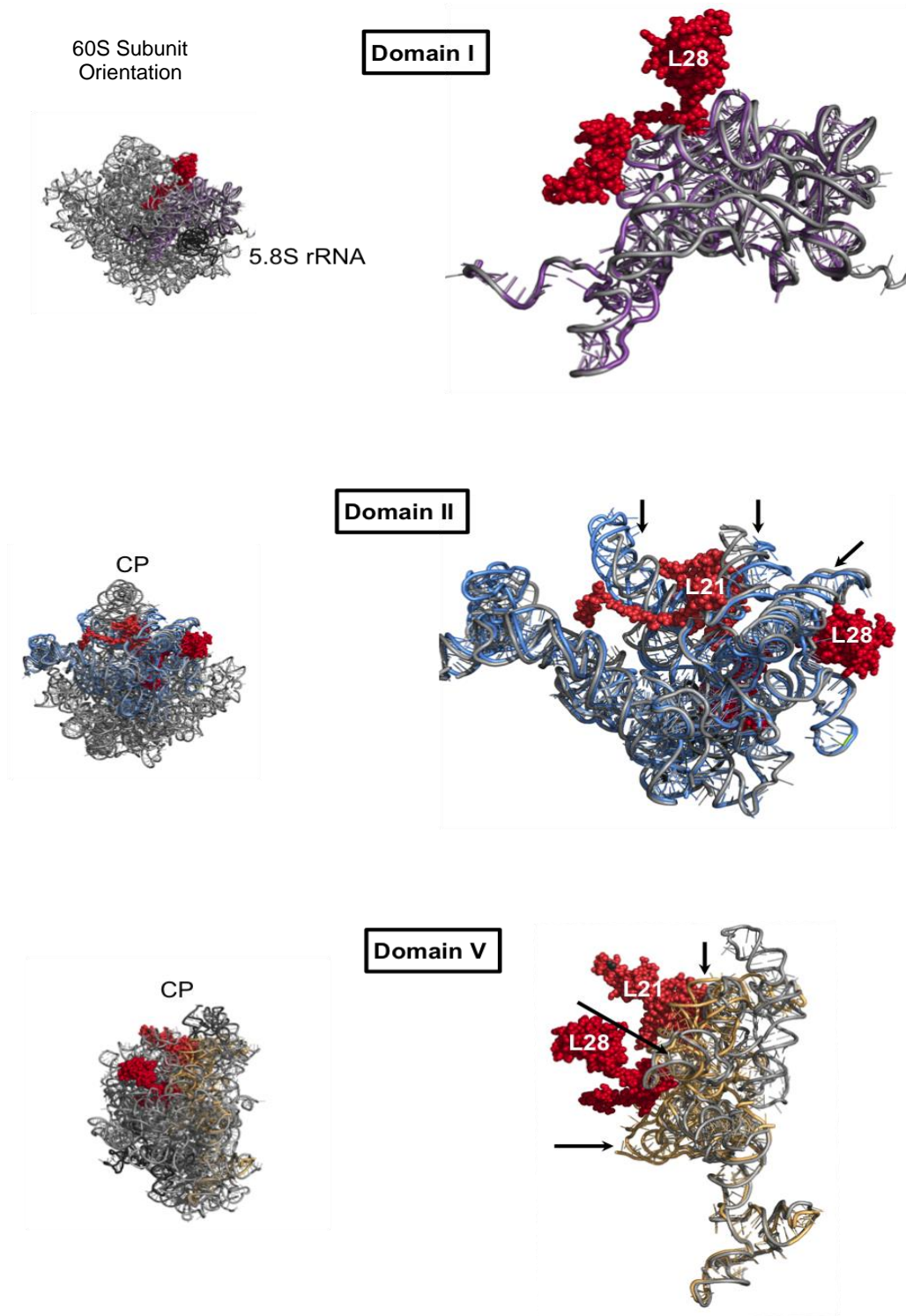


**Figure 52. Helices contacted by L21 and L28 in domains II and V are not in their mature conformations in pre-ribosomes.** Shown are the alignments of domains I, II, and V of 25 rRNA in mature 60S subunits (colored) and pre-ribosomes (grey) purified using **Nog2-TAP as bait**. The structures were aligned using PyMOL molecular visualization software. Locations of the highlighted domains on 60S subunits are shown on the left side. Significant changes in rRNA conformations were observed in domains II (light blue) and V (light orange) of 25S rRNA at regions contacted by L21 (light red) and L28 (red).

(PDB IDs: 3U5D, Wu et al. 2016, submitted)

Figure 53

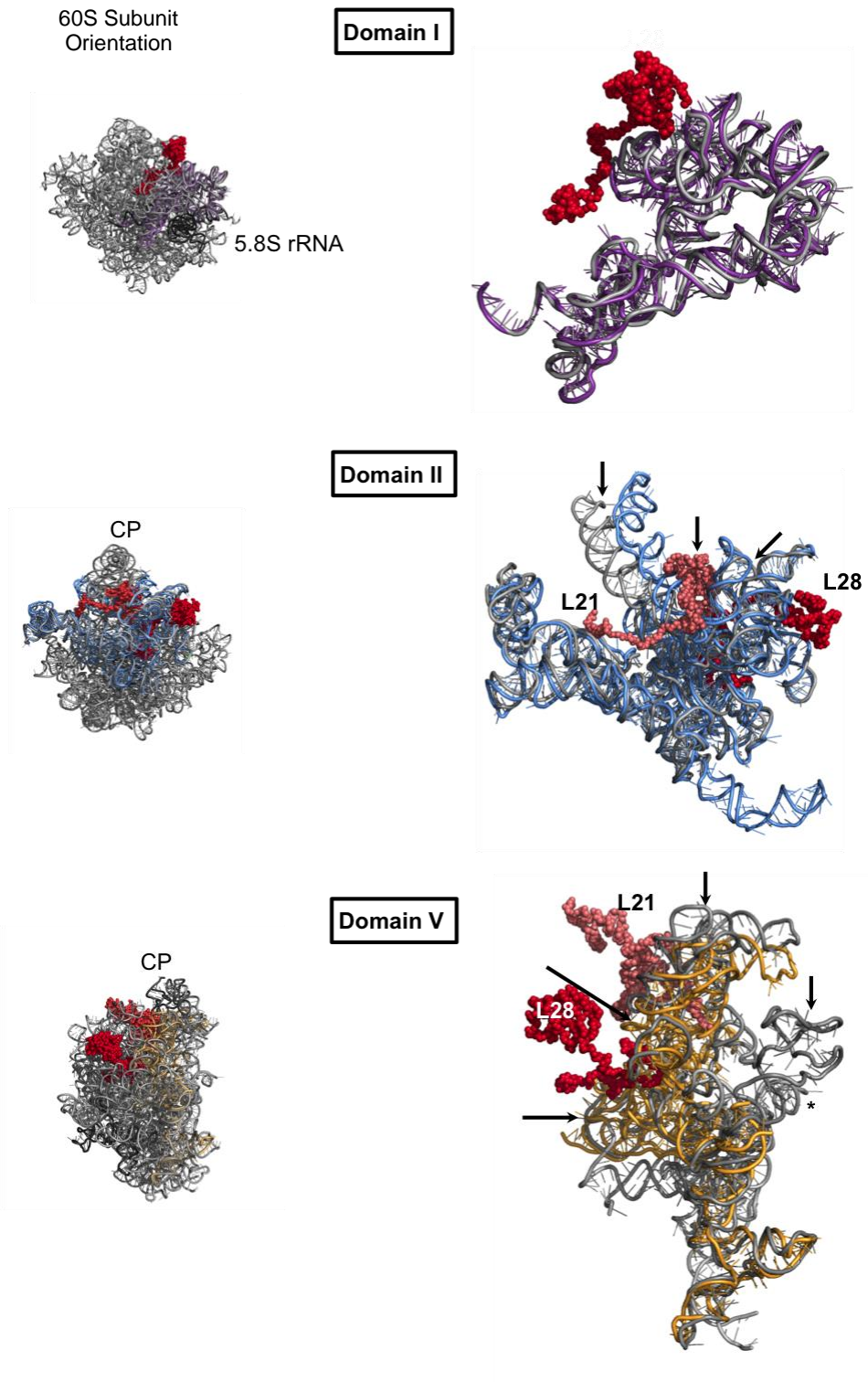


**Figure 53. Helices contacted by L21 and L28 in domains II and V are not in their mature conformations in pre-ribosomes.** Shown are the alignments of 25 rRNA in mature 60S subunits (colored) and pre-ribosomes (grey) (purified using **Rix1-FLAG as bait**) aligned using PyMOL molecular visualization software. The location of the highlighted domains on 60S subunits is shown on the left. Significant differences in rRNA conformations were observed in domains II (light blue) and V (light orange) of 25S rRNA at regions contacted by L21 (light red) and L28 (red). The structure of helices 77-79 missing in the mature 60S subunit structure is indicated with ‘\*’.

(PDB ID: 3U5D and 5FL8 (Rix1-FLAG affinity purified pre-ribosomes))

Figure 54

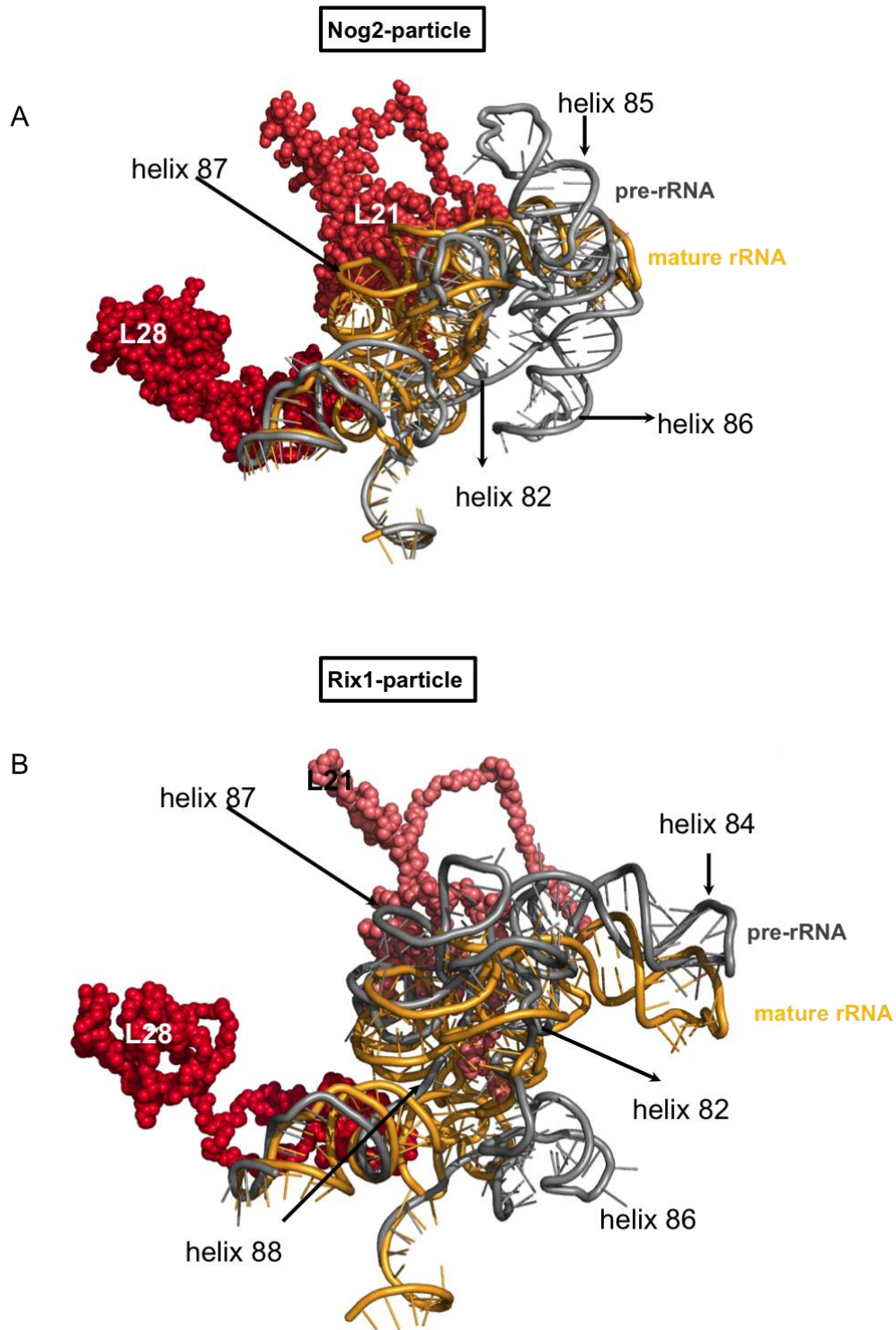


**Figure 54. Helices in domain V contacted by L21 and L28 undergo extensive changes during late steps of 60S ribosomal subunit maturation.** Shown are the alignments of domain V in the mature 60S subunit (colored) and in pre-ribosomes purified using Nog2-TAP (A) or Rix1-FLAG (B) as baits. Pre-rRNA is colored in grey. The structures were aligned using PyMOL molecular visualization software. Helices 80-88 contacted by L21 and L28 undergo significant rearrangements in pre-ribosomes.

(PDB IDs: 3U5D, 5FL8; Wu et al. 2016, unpublished)

## **4.4 Future directions**

### **Roles of specific domains of L21 and L28**

The extensions of rpL21 and rpL28 contact 5S rRNA and the linker domain upon which the six domains of 25S rRNA fold, respectively. Recent studies indicate that these r-protein extensions are also required for 60S ribosomal subunit assembly. For some r-proteins, deletions or mutations in these extensions affect pre-rRNA processing and ribosome assembly at later steps of pre-rRNA processing, allowing identification of the multiple roles of r-proteins in 60S subunit assembly (Beril Tutumcguolu, Jelena Jakovljevic, personal communication), (Gamalinda and Woolford 2014). Therefore, deletions or mutations of L28 or L21 in specific regions mediating their intermolecular interactions could deepen our understanding of the molecular networks driving 60S subunit assembly.

### **Role of L29 in late steps of nuclear assembly**

The eukaryote-specific ribosomal protein L29 is placed between ES12 and ES on the 60S ribosomal subunit, between L21 and L28. This protein is not essential for growth under standard laboratory conditions (Steffen et al. 2012). Sda1 shows negative genetic interactions with L29 (Costanzo et al. 2010). Hence, it would be interesting to examine whether this protein is required for growth and ribosome assembly under restrictive conditions and to screen for synthetic lethal alleles in *rpl29*- knockout strains.

## **4.5 Materials and methods**

### **Construction of yeast strains**

For depleting L21 and L28, cultures of *GAL-RPL21* or *GAL-RPL28*, strains were grown overnight (16 hours) to mid logarithmic phase ( $OD_{600}=0.4-0.6$  or  $3-5 \times 10^7$  cells/mL) at 30 degrees in YEPGal (1% yeast extract, 2% peptone and 2% galactose) medium or YEPD ((1% yeast extract, 2% peptone and 2% dextrose) medium using doubling times of 2.3 hours and 6.3 hours, respectively. C-terminal TAP tag fusions of Nog2 (in *GAL-RPL28*), Rrp5 (in *GAL-RPL21* and *GAL-RPL28*), and Nsa1-TAP (*GAL-RPL21* and *GAL-RPL28*) were constructed using PCR of the tag sequence and a selectable marker (*URA3*), as described previously (Puig et al. 2001). Transformants were screened by western blotting with anti-TAP antibody, to identify those expressing the tagged proteins. Positive controls of tagged strains were used whenever available. All tagged strains exhibited similar doubling-time as parent strains.

### **Affinity purification of pre-ribosomes**

Pre-ribosomes were purified from yeast cells grown as described above, using magnetic IgG-coated Dynabeads as described previously (Dembowski et al. 2013), with TNM150 buffer.

### **SDS-PAGE and western blot analysis of pre-ribosomes**

Purified pre-ribosomes were TCA precipitated and re-suspended in SDS sample buffer. The samples were resolved on 4-20% Novex precast gels (Life Technologies) and stained by standard silver staining methods. The bands whose identities were not

confirmed previously in Nop7-TAP purified pre-ribosomes were confirmed by mass spectrometry of bands isolated from SDS-PAGE gels stained with the Silver Quest silver staining kit (Invitrogen). The identity of bands on Nsa1-TAP and Nog2-TAP gels were also determined similarly (Hailey Brown, personal communication, this study).

## References

- Adams CC, Jakovljevic J, Roman J, Harnpicharnchai P, Woolford JL. 2002b. *Saccharomyces cerevisiae* nucleolar protein Nop7p is necessary for biogenesis of 60S ribosomal subunits. *RNA* 8: 150–165.
- Allmang C, Mitchell P, Petfalski E, Tollervey D. 2000. Degradation of ribosomal RNA precursors by the exosome. *Nucleic Acids Res* 28: 1684–1691.
- Altvater M, Chang Y, Melnik A, Occhipinti L, Schütz S, Rothenbusch U, Picotti P, Panse VG. 2012. Targeted proteomics reveals compositional dynamics of 60S pre-ribosomes after nuclear export. *Mol Syst Biol* 8: 628.
- Anger AM, Armache J-P, Berninghausen O, Habeck M, Subklewe M, Wilson DN, Beckmann R. 2013. Structures of the human and *Drosophila* 80S ribosome. *Nature* 497: 80–85.
- Armache J-P, Jarasch A, Anger AM, Villa E, Becker T, Bhushan S, Jossinet F, Habeck M, Dindar G, Franckenberg S, et al. 2010. Localization of eukaryote-specific ribosomal proteins in a 5.5-Å cryo-EM map of the 80S eukaryotic ribosome. *Proc Natl Acad Sci USA* 107: 19754–19759.
- Asano N, Kato K, Nakamura A, Komoda K, Tanaka I, Yao M. 2015. Structural and functional analysis of the Rpf2-Rrs1 complex in ribosome biogenesis. *Nucleic Acids Res* 43: 4746–4757.
- Asano N, Nakamura A, Komoda K, Kato K, Tanaka I, Yao M. 2014. Crystallization and preliminary X-ray crystallographic analysis of ribosome assembly factors: the Rpf2-Rrs1 complex. *Acta Crystallogr Struct Biol Commun* 70: 1649–1652.
- Athavale SS, Gossett JJ, Hsiao C, Bowman JC, O'Neill E, Hershkovitz E, Preeprem T, Hud NV, Wartell RM, Harvey SC, et al. 2012. Domain III of the *T. thermophilus* 23S rRNA folds independently to a near-native state. *RNA* 18: 752–758.

- Babiano R, Badis G, Saveanu C, Namane A, Doyen A, Diaz-Quintana A, Jacquier A, Fromont-Racine M, de la Cruz J. 2013. Yeast ribosomal protein L7 and its homologue Rlp7 are simultaneously present at distinct sites on pre-60S ribosomal particles. *Nucleic Acids Res* 41: 9461–9470.
- Babiano R, Gamalinda M, Woolford JL, la Cruz de J. 2012. *Saccharomyces cerevisiae* ribosomal protein L26 is not essential for ribosome assembly and function. *Mol Cell Biol* 32: 3228–3241.
- Babiano R, la Cruz de J. 2010. Ribosomal protein L35 is required for 27SB pre-rRNA processing in *Saccharomyces cerevisiae*. *Nucleic Acids Res* 38: 5177–5192.
- Ban N, Beckmann R, Cate JHD, Dinman JD, Dragon F, Ellis SR, Lafontaine DLJ, Lindahl L, Liljas A, Lipton JM, et al. 2014. A new system for naming ribosomal proteins. *Curr Opin Struct Biol* 24: 165–169.
- Barrio-Garcia C, Thoms M, Flemming D, Kater L, Berninghausen O, Baßler J, Beckmann R, Hurt E. 2015. Architecture of the Rix1-Real checkpoint machinery during pre-60S-ribosome remodeling. *Nat Struct Mol Biol*.
- Baßler J, Kallas M, Pertschy B, Ulbrich C, Thoms M, Hurt E. 2010. The AAA-ATPase Real drives removal of biogenesis factors during multiple stages of 60S ribosome assembly. *Molecular Cell* 38: 712–721.
- Baxter-Roshek JL, Petrov AN, Dinman JD. 2007. Optimization of Ribosome Structure and Function by rRNA Base Modification ed. T. Preiss. *PLoS ONE* 2: e174.
- Ben Liu, Liang X-H, Piekna-Przybylska D, Liu Q, Fournier MJ. 2008. Mis-targeted methylation in rRNA can severely impair ribosome synthesis and activity. *5*: 249–254.
- Ben-Shem A, Garreau de Loubresse N, Melnikov S, Jenner L, Yusupova G, Yusupov M. 2011. The structure of the eukaryotic ribosome at 3.0 Å resolution. *Science* 334: 1524–1529.
- Ben-Shem A, Jenner L, Yusupova G, Yusupov M. 2010. Crystal structure of the eukaryotic ribosome. *Science* 330: 1203–1209.

Bernstein KA, Granneman S, Lee AV, Manickam S, Baserga SJ. 2006. Comprehensive mutational analysis of yeast DEXD/H box RNA helicases involved in large ribosomal subunit biogenesis. *Mol Cell Biol* 26: 1195–1208.

Biedka S, Talkish J, Jakovljevic J, Zhang J, Tang L, Strahler JR, Andrews PC, Maddock JR, Woolford JL. 2016. Disruption of ribosome assembly in yeast blocks co-transcriptional pre-rRNA processing and affects the global hierarchy of ribosome biogenesis. (Submitted).

Bohnsack MT, Martin R, Granneman S, Ruprecht M, Schleiff E, Tollervey D. 2009. Prp43 Bound at Different Sites on the Pre-rRNA Performs Distinct Functions in Ribosome Synthesis. *Molecular Cell* 36: 583–592.

Bond AT, Mangus DA, He F, Jacobson A. 2001. Absence of Dbp2p Alters Both Nonsense-Mediated mRNA Decay and rRNA Processing. *Mol Cell Biol* 21: 7366–7379.

Bourgeois G, Ney M, Gaspar I, Aigueperse C, Schaefer M, Kellner S, Helm M, Motorin Y. 2015. Eukaryotic rRNA Modification by Yeast 5-Methylcytosine-Methyltransferases and Human Proliferation-Associated Antigen p120 ed. T. Preiss. *PLoS ONE* 10: e0133321.

Bradatsch B, Katahira J, Kowalinski E, Bange G, Yao W, Sekimoto T, Baumgärtel V, Boese G, Baßler J, Wild K, et al. 2007. Arx1 functions as an unorthodox nuclear export receptor for the 60S preribosomal subunit. *Molecular Cell* 27: 767–779.

Bradatsch B, Leidig C, Granneman S, Gnädig M, Tollervey D, Böttcher B, Beckmann R, Hurt E. 2012. Structure of the pre-60S ribosomal subunit with nuclear export factor Arx1 bound at the exit tunnel. *Nat Struct Mol Biol* 19: 1234–1241.

Burger F, Daugeron MC, Linder P. 2000. Dbp10p, a putative RNA helicase from *Saccharomyces cerevisiae*, is required for ribosome biogenesis. *Nucleic Acids Res* 28: 2315–2323.

Bussiere C, Hashem Y, Arora S, Frank J, Johnson AW. 2012. Integrity of the P-site is probed during maturation of the 60S ribosomal subunit. *J Cell Biol* 197: 747–759.

Butcher SE, Pyle AM. 2011. The Molecular Interactions That Stabilize RNA Tertiary Structure: RNA Motifs, Patterns, and Networks. *Acc Chem Res* 44: 1302–1311.

Byrgazov K, Vesper O, Moll I. 2013. Ribosome heterogeneity: another level of complexity in bacterial translation regulation. *Curr Opin Microbiol* 16: 133–139.

Calviño FR, Kharde S, Ori A, Hendricks A, Wild K, Kressler D, Bange G, Hurt E, Beck M, Sinning I. 2015. Symportin 1 chaperones 5S RNP assembly during ribosome biogenesis by occupying an essential rRNA-binding site. *Nat Commun* 6: 6510-6518.

Castle CD, Cassimere EK, Denicourt C. 2012. Las1L interacts with the mammalian Rix1 complex to regulate ribosome biogenesis. *Mol Biol Cell* 23: 716–728.

Castle CD, Cassimere EK, Lee J, Denicourt C. 2010. Las1L is a nucleolar protein required for cell proliferation and ribosome biogenesis. *Mol Cell Biol* 30: 4404–4414.

Castle CD, Sardana R, Dandekar V, Borgianini V, Johnson AW, Denicourt C. 2013. Las1 interacts with Grc3 polynucleotide kinase and is required for ribosome synthesis in *Saccharomyces cerevisiae*. *Nucleic Acids Res* 41: 1135–1150.

Cheng L, Li J, Han Y, Lin J, Niu C, Zhou Z, Yuan B, Huang K, Li J, Jiang K, et al. 2012. PES1 promotes breast cancer by differentially regulating ER $\alpha$  and ER $\beta$ . *J Clin Invest* 122: 2857–2870.

Cmarko D, Smigova J, Minichova L, Popov A. 2008. Nucleolus, The ribosome factory. *Histol Histopathol* 23: 1291-1298

Cole SE, LaRiviere FJ. 2008. Chapter 12. Analysis of nonfunctional ribosomal RNA decay in *Saccharomyces cerevisiae*. *Meth Enzymol* 449: 239–259.

Combs DJ, Nagel RJ, Ares M Jr, Stevens SW. 2006. Prp43p Is a DEAH-Box spliceosome disassembly factor essential for ribosome biogenesis. *Mol Cell Biol* 26: 523–534.

Costanzo M, Baryshnikova A, Bellay J, Kim Y, Spear ED, Sevier CS, Ding H, Koh JLY, Toufighi K, Mostafavi S, et al. 2010. The genetic landscape of a cell. *Science* 327: 425–431.

De la Cruz J, Kressler D, ROJO M, Tollervey D, Linder P. 1998. Spb4p, an essential putative RNA helicase, is required for a late step in the assembly of 60S ribosomal subunits in *Saccharomyces cerevisiae*. *RNA* 4: 1268–1281.

Daugeron M-C, Kressler D, Linder P. 2001. Dbp9p, a putative ATP-dependent RNA helicase involved in 60S-ribosomal subunit biogenesis, functionally interacts with Dbp6p. *RNA* 7: 1317–1334.

- Daugeron M-C, Linder P. 1998. Dbp7p, a putative ATP-dependent RNA helicase from *Saccharomyces cerevisiae*, is required for 60S ribosomal subunit assembly. *RNA* 4: 566–581.
- Dechampesme AM, Koroleva O, Léger-Silvestre I, Gas N, Camier S. 1999. Assembly of 5S ribosomal RNA is required at a specific step of the pre-rRNA processing pathway. *J Cell Biol* 145: 1369–1380.
- Del Campo M, Mohr S, Jiang Y, Jia H, Jankowsky E, Lambowitz AM. 2009. Unwinding by local strand separation is critical for the function of DEAD-Box proteins as RNA chaperones. *J Mol Biol* 389: 674–693.
- Dembowski JA, Kuo B, Woolford JL. 2013. Has1 regulates consecutive maturation and processing steps for assembly of 60S ribosomal subunits. *Nucleic Acids Res* 41: 7889–7904.
- Dembowski JA, Ramesh M, McManus CJ, Woolford JL. 2013b. Identification of the binding site of Rlp7 on assembling 60S ribosomal subunits in *Saccharomyces cerevisiae*. *RNA* 19: 1639–1647.
- Dez C, Froment C, Noaillic-Depeyre J, Monsarrat B, Caizergues-Ferrer M, Henry Y. 2004a. Npa1p, a component of very early pre-60S ribosomal particles, associates with a subset of small nucleolar RNPs required for peptidyl transferase center modification. *Mol Cell Biol* 24: 6324–6337.
- Du Y-CN, Stillman B. 2002. Yph1p, an ORC-interacting protein: potential links between cell proliferation control, DNA replication, and ribosome biogenesis. *Cell* 109: 835–848.
- Dutca LM, Gallagher JEG, Baserga SJ. 2011. The initial U3 snoRNA:pre-rRNA base pairing interaction required for pre-18S rRNA folding revealed by in vivo chemical probing. *Nucleic Acids Res* 39: 5164–5180.
- Eppens NA, Rensen S, Granneman S, Raué HA, Venema J. 1999. The roles of Rrp5p in the synthesis of yeast 18S and 5.8S rRNA can be functionally and physically separated. *RNA* 5: 779–793.
- Erzberger JP, Berger JM. 2006. Evolutionarily relationships and structural mechanisms of AAA+ proteins.. *Annu Rev Biophys Biomol Struct* 35: 93–114.

- Faber AW, van Dijk M, Rau HA, Vos JC. 2002. Ngl2p is a Ccr4p-like RNA nuclease essential for the final step in 3'-end processing of 5.8S rRNA in *Saccharomyces cerevisiae*. *RNA* 8: 1095–1101.
- Fabian GR, Hopper AK. 1987. RRP1, a *Saccharomyces cerevisiae* gene affecting rRNA processing and production of mature ribosomal subunits. *J Bacteriol* 169: 1571–1578.
- Fahnestock S, Erdmann V, Nomura M. 1973. Reconstitution of 50S ribosomal subunits from protein-free ribonucleic acid. *Biochemistry* 12: 220–224.
- Fang F, Phillips S, Butler JS. 2005. Rat1p and Rai1p function with the nuclear exosome in the processing and degradation of rRNA precursors. *RNA* 11: 1571–1578.
- Fatica A, Cronshaw AD, Dlakić M, Tollervey D. 2002. Ssf1p prevents premature processing of an early pre-60S ribosomal particle. *Molecular Cell* 9: 341–351.
- Fatica A, Oeffinger M, Tollervey D, Bozzoni I. 2003. Cic1p/Nsa3p is required for synthesis and nuclear export of 60S ribosomal subunits. *RNA* 9: 1431–1436.
- Fedorova O, Solem A, Pyle AM. 2010. Protein-facilitated folding of group II intron ribozymes. *J Mol Biol* 397: 799–813.
- Fernández-Pevida A, Kressler D, la Cruz de J. 2015. Processing of preribosomal RNA in *Saccharomyces cerevisiae*. *Wiley Interdisciplinary Reviews: RNA* 6: 191–209.
- Freed EF, Bleichert F, Dutca LM, Baserga SJ. 2010. When ribosomes go bad: diseases of ribosome biogenesis. *Molecular BioSystems* 6: 481–493.
- Fuentes JL, Datta K, Sullivan SM, Walker A, Maddock JR. 2007. In vivo functional characterization of the *Saccharomyces cerevisiae* 60S biogenesis GTPase Nog1. *Mol Genet Genomics* 278: 105–123.
- Gadal O, Strauß D, Braspenning J, Hoepfner D, Petfalski E, Philippsen P, Tollervey D, Hurt E. 2001. A nuclear AAA-type ATPase (Rix7p) is required for biogenesis and nuclear export of 60S ribosomal subunits. *EMBO J* 20: 3695–3704.

- Galani K, Nissan TA, Petfalski E, Tollervey D, Hurt E. 2004. Rea1, a dynein-related nuclear AAA-ATPase, is involved in late rRNA processing and nuclear export of 60 S subunits. *J Biol Chem* 279: 55411–55418.
- Gamalinda M, Jakovljevic J, Babiano R, Talkish J, la Cruz de J, Woolford JL. 2013. Yeast polypeptide exit tunnel ribosomal proteins L17, L35 and L37 are necessary to recruit late-assembling factors required for 27SB pre-rRNA processing. *Nucleic Acids Res* 41: 1965–1983.
- Gamalinda M, John L Woolford J. 2014. Deletion of L4 domains reveals insights into the importance of ribosomal protein extensions in eukaryotic ribosome assembly. *RNA* 20: 1725–1731.
- Gamalinda M, Ohmayer U, Jakovljevic J, Kumcuoglu B, Woolford J, Mbom B, Lin L, Woolford JL. 2014. A hierarchical model for assembly of eukaryotic 60S ribosomal subunit domains. *Genes Dev* 28: 198–210.
- Gamalinda M, Woolford JL Jr. 2014. Paradigms of ribosome synthesis: Lessons learned from ribosomal proteins. *Translation* 3: e975018.
- García-Gómez JJ, Fernandez-Pevida A, Lebaron S, Rosado IV, Tollervey D, Kressler D, de la Cruz J. 2014 . Final pre-40S maturation depends on the functional integrity of the 60S subunit ribosomal protein L3. *PLoS Genet.* 10, e1004205.
- Gasse L, Flemming D, Hurt E. 2015. Coordinated Ribosomal ITS2 RNA Processing by the Las1 Complex Integrating Endonuclease, Polynucleotide Kinase, and Exonuclease Activities. *Molecular Cell* 60: 808–815.
- Gerbi, S. A. 1996. Expansion segments: regions of variable size that interrupt the universal core secondary structure of ribosomal RNA. *Ribosomal RNA structure, evolution, processing, and function in protein biosynthesis*: 87.
- Gerhardy S, Menet AM, Peña C, Petkowski JJ, Panse VG. 2014. Assembly and nuclear export of pre-ribosomal particles in budding yeast. *Chromosoma* 123: 327–344.

- Gilbert WV. 2011. Functional specialization of ribosomes? *Trends in Biochemical Sciences* 36: 127–132.
- Gleizes PE, Noaillac-Depeyre J, Léger-Silvestre I, Teulières F, Dauxois JY, Pommet D, Azum-Gelade MC, Gas N. 2001. Ultrastructural localization of rRNA shows defective nuclear export of preribosomes in mutants of the Nup82p complex. *J Cell Biol* 155: 923–936.
- Gluick TC, Draper DE. 1994. Thermodynamics of folding a pseudoknotted mRNA fragment. *J Mol Biol* 241: 246–262.
- Granato DC, Machado Santelli GM, Oliveira CC. 2008. Nop53p interacts with 5.8S rRNA co-transcriptionally, and regulates processing of pre-rRNA by the exosome. *FEBS J* 275: 4164–4178.
- Granneman S, Petfalski E, Swiatkowska A, Tollervey D. 2010. Cracking pre-40S ribosomal subunit structure by systematic analyses of RNA–protein cross-linking. *EMBO J* 29: 2026–2036.
- Granneman S, Petfalski E, Tollervey D. 2011. A cluster of ribosome synthesis factors regulate pre-rRNA folding and 5.8S rRNA maturation by the Rat1 exonuclease. *EMBO J* 30: 4006–4019.
- Greber BJ, Boehringer D, Montellese C, Ban N. 2012. Cryo-EM structures of Arx1 and maturation factors Rei1 and Jjj1 bound to the 60S ribosomal subunit. *Nat Struct Mol Biol* 19: 1228–1233.
- Greber BJ, Gerhardy S, Leitner A, Leibundgut M, Salem M, Boehringer D, Leulliot N, Aebersold R, Panse VG, Ban N. 2015. Insertion of the Biogenesis Factor Rei1 Probes the Ribosomal Tunnel during 60S Maturation. *Cell* 164:1-12.
- Guenther U-P, Jankowsky E. 2009. Helicase multitasking in ribosome assembly. *Molecular Cell* 36: 537–538.
- Hector RD, Burlacu E, Aitken S, Le Bihan T, Tuijtel M, Zaplatina A, Cook AG, Granneman S. 2014. Snapshots of pre-rRNA structural flexibility reveal eukaryotic 40S assembly dynamics at nucleotide resolution. *Nucleic Acids Res* 42: 12138–12154.

- Henry Y, Wood H, Morrissey JP, Petfalski E, Kearsey S, Tollervey D. 1994. The 5' end of yeast 5.8S rRNA is generated by exonucleases from an upstream cleavage site. *EMBO J* 13: 2452–2463.
- Herschlag D. 1995. RNA chaperones and the RNA folding problem. *J Biol Chem* 270: 20871–20874.
- Hierlmeier T, Merl J, Sauert M, Perez-Fernandez J, Schultz P, Bruckmann A, Hamperl S, Ohmayer U, Rachel R, Jacob A, et al. 2013. Rrp5p, Noc1p and Noc2p form a protein module which is part of early large ribosomal subunit precursors in *S. cerevisiae*. *Nucleic Acids Res* 41: 1191–1210.
- Hiraishi N, Ishida Y-I, Nagahama M. 2015. AAA-ATPase NVL2 acts on MTR4-exosome complex to dissociate the nucleolar protein WDR74. *Biochem Biophys Res Commun* 467: 534–540.
- Ho JH, Kallstrom G, Johnson AW. 2000. Nmd3p is a Crm1p-dependent adapter protein for nuclear export of the large ribosomal subunit. *J Cell Biol* 151: 1057–1066.
- Holbrook SR. 2005. RNA structure: the long and the short of it. *Curr Opin Struct Biol* 15: 302–308.
- Hong B, Brockenbrough JS, Wu P, Aris JP. 1997. Nop2p is required for pre-rRNA processing and 60S ribosome subunit synthesis in yeast. *Mol Cell Biol* 17: 378–388.
- Hong B, Wu K, Brockenbrough JS, Wu P, Aris JP. 2001. Temperature sensitive nop2 alleles defective in synthesis of 25S rRNA and large ribosomal subunits in *Saccharomyces cerevisiae*. *Nucleic Acids Res* 29: 2927–2937.
- Honma Y, Kitamura A, Shioda R, Maruyama H, Ozaki K, Oda Y, Mini T, Jenö P, Maki Y, Yonezawa K, et al. 2006. TOR regulates late steps of ribosome maturation in the nucleoplasm via Nog1 in response to nutrients. *EMBO J* 25: 3832–3842.
- Horn DM, Mason SL, Karbstein K. 2011. Rcl1 protein, a novel nuclease for 18 S ribosomal RNA production. *J Biol Chem* 286: 34082–34087.

- Horseley EW, Jakovljevic J, Miles TD, Harnpicharnchai P, Woolford JL. 2004. Role of the yeast Rrp1 protein in the dynamics of pre-ribosome maturation. *RNA* 10: 813–827.
- Hurt E, Hannus S, Schmelzl B, Lau D, Tollervey D, Simos G. 1999. A novel in vivo assay reveals inhibition of ribosomal nuclear export in ran-cycle and nucleoporin mutants. *J Cell Biol* 144: 389–401.
- Jack K, Bellodi C, Landry DM, Niederer RO, Meskauskas A, Musalgaonkar S, Kopmar N, Krasnykh O, Dean AM, Thompson SR, et al. 2011. rRNA Pseudouridylation Defects Affect Ribosomal Ligand Binding and Translational Fidelity from Yeast to Human Cells. *Molecular Cell* 44: 660–666.
- Jäger S, Strayle J, Heinemeyer W, Wolf DH. 2001. Cic1, an adaptor protein specifically linking the 26S proteasome to its substrate, the SCF component Cdc4. *EMBO J* 20: 4423–4431.
- Jakovljevic J, Ohmayer U, Gamalinda M, Talkish J, Alexander L, Linnemann J, Milkereit P, Woolford JL. 2012. Ribosomal proteins L7 and L8 function in concert with six A<sub>3</sub> assembly factors to propagate assembly of domains I and II of 25S rRNA in yeast 60S ribosomal subunits. *RNA* 18: 1805–1822.
- Jankowsky E. 2011. RNA helicases at work: binding and rearranging. *Trends in Biochemical Sciences* 36:19-29.
- Jensen BC, Wang Q, Kifer CT, Parsons M. 2003. The NOG1 GTP-binding Protein Is Required for Biogenesis of the 60 S Ribosomal Subunit. *J Biol Chem* 278: 32204–32211.
- Johnson AW. 2014. Ribosomes: lifting the nuclear export ban. *Curr Biol* 24: 127–129.
- Kaempfer R. 1969. Ribosomal Subunit Exchange in the Cytoplasm of a Eukaryote. *Nature* 222: 950–953.
- Kallstrom G, Hedges J, Johnson A. 2003. The putative GTPases Nog1p and Lsg1p are required for 60S ribosomal subunit biogenesis and are localized to the nucleus and cytoplasm, respectively. *Mol Cell Biol* 23: 4344–4355.
- Kathleen L McCann SJB. 2013. Mysterious Ribosomopathies. *Science* 341: 849–850.

- Kellner M, Rohrmoser M, Forné I, Voss K, Burger K, Mühl B, Gruber-Eber A, Kremmer E, Imhof A, Eick D. 2015. DEAD-box helicase DDX27 regulates 3' end formation of ribosomal 47S RNA and stably associates with the PeBoW-complex. *Exp Cell Res* 334: 146–159.
- Kharde S, Calviño FR, Gumiero A, Wild K, Sinning I. 2015. The structure of Rpf2-Rrs1 explains its role in ribosome biogenesis. *Nucleic Acids Res* 43: 7083–7095.
- Kiss T, Fayet-Lebaron E, Jády BE. 2010. Box H/ACA small ribonucleoproteins. *Molecular Cell* 37: 597–606.
- Klein DJ, Moore PB, Steitz TA. 2004. The roles of ribosomal proteins in the structure assembly, and evolution of the large ribosomal subunit. *J Mol Biol* 340: 141–177.
- Kondrashov N, Pusic A, Stumpf CR, Shimizu K, Hsieh AC, Xue S, Ishijima J, Shiroishi T, Barna M. 2011. Ribosome-mediated specificity in Hox mRNA translation and vertebrate tissue patterning. *Cell* 145: 383–397.
- Koš M, Tollervey D. 2010. Yeast pre-rRNA processing and modification occur cotranscriptionally. *Molecular Cell* 37: 809–820.
- Kressler D, Hurt E, Bergler H, Baßler J. 2012. The power of AAA-ATPases on the road of pre-60S ribosome maturation--molecular machines that strip pre-ribosomal particles. *Biochim Biophys Acta* 1823: 92–100.
- Kressler D, Roser D, Pertschy B, Hurt E. 2008. The AAA ATPase Rix7 powers progression of ribosome biogenesis by stripping Nsa1 from pre-60S particles. *J Cell Biol* 181: 935–944.
- Kressler D. 1999. Spb1p is a putative methyltransferase required for 60S ribosomal subunit biogenesis in *Saccharomyces cerevisiae*. *Nucleic Acids Res* 27: 4598–4608.
- De la Cruz J, Karbstein K, Woolford JL. 2015. Functions of ribosomal proteins in assembly of eukaryotic ribosomes in vivo. *Annu Rev Biochem* 84: 93–129.
- De la Cruz J, Lacombe T, Deloche O, Linder P, Kressler D. 2004. The Putative RNA Helicase Dbp6p Functionally Interacts With Rpl3p, Nop8p and the Novel trans-acting Factor Rsa3p

During Biogenesis of 60S Ribosomal Subunits in *Saccharomyces cerevisiae*. *Genetics* 166: 1687–1699.

Lafontaine DL, Bousquet-Antonelli C, Henry Y, Caizergues-Ferrer M, Tollervey D. 1998. The box H + ACA snoRNAs carry Cbf5p, the putative rRNA pseudouridine synthase. *Genes Dev* 12: 527–537.

Lafontaine DL, Tollervey D. 1999. Nop58p is a common component of the box C+D snoRNPs that is required for snoRNA stability. *RNA* 5: 455–467.

Lafontaine DL, Tollervey D. 2001. The function and synthesis of ribosomes. *Nat Rev Mol Cell Biol* 2: 514–520.

Lafontaine DLJ. 2015. Noncoding RNAs in eukaryotic ribosome biogenesis and function. *Nat Struct Mol Biol* 22: 11–19.

Lamanna AC, Karbstein K. 2011. An RNA conformational switch regulates pre-18S rRNA cleavage. *J Mol Biol* 405: 3–17.

Lapeyre B, Purushothaman SK. 2004. Spb1p-directed formation of Gm2922 in the ribosome catalytic center occurs at a late processing stage. *Molecular Cell* 16: 663–669.

LaRiviere FJ, Cole SE, Ferullo DJ, Moore MJ. 2006. A late-acting quality control process for mature eukaryotic rRNAs. *Molecular Cell* 24: 619–626.

Lebaron S, Segerstolpe Å, French SL, Dudnakova T, de lima Alves F, Granneman S, Rappsilber J, Beyer AL, Wieslander L, Tollervey D. 2013. Rrp5 Binding at Multiple Sites Coordinates Pre-rRNA Processing and Assembly. *Molecular Cell* 52: 707–719.

Lebaron S, Schneider C, van Nues RW, Swiatkowska A, Walsh D, Böttcher B, Granneman S, Watkins NJ, Tollervey D. 2012. Proofreading of pre-40S ribosome maturation by a translation initiation factor and 60S subunits. *Nat. Struct. Mol. Biol.* 19, 744–753.

Lebreton A, Rousselle J-C, Lenormand P, Namane A, Jacquier A, Fromont-Racine M, Saveanu C. 2008. 60S ribosomal subunit assembly dynamics defined by semi-quantitative mass spectrometry of purified complexes. *Nucleic Acids Res* 36: 4988–4999.

- Leeds NB, Small EC, Hiley SL, Hughes TR, Staley JP. 2006. The splicing factor Prp43p, a DEAH Box ATPase, functions in ribosome biogenesis. *Mol Cell Biol* 26: 513–522.
- Leidig C, Thoms M, Holdermann I, Bradatsch B, Berninghausen O, Bange G, Sinning I, Hurt E, Beckmann R. 2014. 60S ribosome biogenesis requires rotation of the 5S ribonucleoprotein particle. *Nat Commun* 5: 3491-3498.
- Leitão AL, Costa MC, Enguita FJ. 2015. Unzippers, resolvers and sensors: a structural and functional biochemistry tale of RNA helicases. *Int J Mol Sci* 16: 2269–2293.
- Leontis NB, Lescoute A, Westhof E. 2006. The building blocks and motifs of RNA architecture. *Curr Opin Struct Biol* 16: 279–287.
- Liang X-H, Liu Q, Fournier MJ. 2007. rRNA modifications in an intersubunit bridge of the ribosome strongly affect both ribosome biogenesis and activity. *Molecular Cell* 28: 965–977.
- Lo K-Y, Li Z, Bussiere C, Bresson S, Marcotte EM, Johnson AW. 2010. Defining the pathway of cytoplasmic maturation of the 60S ribosomal subunit. *Molecular Cell* 39: 196–208.
- Lo K-Y, Li Z, Wang F, Marcotte EM, Johnson AW. 2009. Ribosome stalk assembly requires the dual-specificity phosphatase Yvh1 for the exchange of Mrt4 with P0. *J Cell Biol* 186: 849–862.
- Loibl M, Klein I, Prattes M, Schmidt C, Kappel L, Zisser G, Gungl A, Krieger E, Pertschy B, Bergler H. 2014. The drug diazaborine blocks ribosome biogenesis by inhibiting the AAA-ATPase Drg1. *J Biol Chem* 289: 3913–3922.
- Longtine MS, McKenzie A, Demarini DJ, Shah NG, Wach A, Brachet A, Philippsen P, Pringle JR. 1998. Additional modules for versatile and economical PCR-based gene deletion and modification in *Saccharomyces cerevisiae*. *Yeast* 14: 953–961.
- Lorsch JR. 2002. RNA Chaperones Exist and DEAD Box Proteins Get a Life. *Cell* 109: 797–800.
- Madru C, Lebaron S, Blaud M, Delbos L, Pipoli J, Pasmant E, Réty S, Leulliot N. 2015. Chaperoning 5S RNA assembly. *Genes Dev* 29: 1432–1446.

- Madru C, Lebaron S, Blaud M, Delbos L, Pipoli J, Pasmant E, Réty S, Leulliot N. 2015. Chaperoning 5S RNA assembly. *Genes Dev* 29: 1432–1446.
- Manikas R-G. 2014. Nug1 is a potassium-stimulated GTPase affecting the association of early 60S assembly factors in ribosome biogenesis (Dissertation, Univ. of Heidelberg, Germany).
- Marchis MLD, Giorgi A, Schinnia ME, Bozzoni I, Fatica A. 2005. Rrp15p, a novel component of pre-ribosomal particles required for 60S ribosome subunit maturation. *RNA* 11: 495–502.
- Martin R, Straub AU, Doebele C, Bohnsack MT. 2013. DExD/H-box RNA helicases in ribosome biogenesis. *10*: 4–18.
- Matsuo Y, Granneman S, Thoms M, Manikas R-G, Tollervey D, Hurt E. 2014. Coupled GTPase and remodelling ATPase activities form a checkpoint for ribosome export. *Nature* 505: 112–116.
- Merino EJ, Wilkinson KA, Coughlan JL, Weeks KM. 2005. RNA Structure Analysis at Single Nucleotide Resolution by Selective 2'-Hydroxyl Acylation and Primer Extension (SHAPE). *J Am Chem Soc.* 127: 4223-4231.
- McCann KL, Charette JM, Vincent NG, Baserga SJ. 2015. A protein interaction map of the LSU processome. *Genes Dev* 29: 862–875.
- Melnikov S, Ben-Shem A, de Loubresse NG, Jenner L, Yusupova G, Yusupov M. 2012. One core, two shells: bacterial and eukaryotic ribosomes. *Nat Struct Mol Biol* 19: 560–567.
- Merl J, Jakob S, Ridinger K, Hierlmeier T, Deutzmann R, Milkereit P, Tschochner H. 2010. Analysis of ribosome biogenesis factor-modules in yeast cells depleted from pre-ribosomes. *Nucleic Acids Res* 38: 3068–3080.
- Miles TD, Jakovljevic J, Horsey EW, Harnpicharnchai P, Tang L, Woolford JL. 2005. Ytm1, Nop7, and Erb1 form a complex necessary for maturation of yeast 66S preribosomes. *Mol Cell Biol* 25: 10419–10432.
- Milkereit P, Gadal O, Podtelejnikov A, Trumtel S, Gas N, Petfalski E, Tollervey D, Mann M, Hurt E, Tschochner H. 2001. Maturation and Intranuclear Transport of Pre-Ribosomes Requires Noc Proteins. *Cell* 105: 499–509.

- Milkereit P, Griesenbeck J, Tschochner H, Ohmayer U, Gil-Hernández Á, Sauert M, Martín-Marcos P, Tamame M. 2015. Studies on the Coordination of Ribosomal Protein Assembly Events Involved in Processing and Stabilization. S. Granneman. PLoS ONE 10: e0143768.
- Miller SA, Brown AJ, Farach Carson MC, Kirn Safran CB. 2003. HIP/RPL29 down-regulation accompanies terminal chondrocyte differentiation. Differentiation 71: 322–336.
- Mizushima S, Nomura M. 1970. Assembly mapping of 30S ribosomal proteins from *E. coli*. Nature 226: 1214-1218.
- Morita D, Miyoshi K, Matsui Y, Toh-E A, Shinkawa H, Miyakawa T, Mizuta K. 2002. Rpf2p, an evolutionarily conserved protein, interacts with ribosomal protein L11 and is essential for the processing of 27 SB Pre-rRNA to 25 S rRNA and the 60 S ribosomal subunit assembly in *Saccharomyces cerevisiae*. J Biol Chem 277: 28780–28786.
- Nagahama M, Hara Y, Seki A, Yamazoe T, Kawate Y, Shinohara T, Hatsuzawa K, Tani K, Tagaya M. 2004. NVL2 Is a Nucleolar AAA-ATPase that interacts with ribosomal protein L5 through Its nucleolar localization sequence. Mol Biol Cell 15: 5712–5723.
- Nerurkar P, Altvater M, Gerhardy S, Schütz S, Fischer U, Weirich C, Panse VG. 2015. Eukaryotic ribosome assembly and nuclear export. Int Rev Cell Mol Biol 319: 107–140.
- Nierhaus KH, Dohme F. 1974. Total reconstitution of functionally active 50S ribosomal subunits from *Escherichia coli*. PNAS 71: 4713–4717.
- Nissan TA, Baßler J, Petfalski E, Tollervey D, Hurt E. 2002. 60S pre-ribosome formation viewed from assembly in the nucleolus until export to the cytoplasm. EMBO J 21: 5539–5547.
- Nogi Y, Yano R, Dodd J, Carles C, Nomura M. 1993. Gene RRN4 in *Saccharomyces cerevisiae* encodes the A12.2 subunit of RNA polymerase I and is essential only at high temperatures. Mol Cell Biol 13: 114–122.
- Nomura M, Fahnestock S. 1973. Reconstitution of 50S ribosomal subunits and the role of 5S RNA. Basic Life Sci 1: 241–250.

- Oeffinger M, Dlakić M, Tollervey D. 2004. A pre-ribosome-associated HEAT-repeat protein is required for export of both ribosomal subunits. *Genes Dev* 18: 196-209.
- Oeffinger M, Leung A, Lamond A, Tollervey D, Lueng A. 2002. Yeast Pescadillo is required for multiple activities during 60S ribosomal subunit synthesis. *RNA* 8: 626–636.
- Oeffinger M, Tollervey D. 2003. Yeast Nop15p is an RNA-binding protein required for pre-rRNA processing and cytokinesis. *EMBO J* 22: 6573–6583.
- Oeffinger M, Wei KE, Rogers R, DeGrasse JA, Chait BT, Aitchison JD, Rout MP. 2007. Comprehensive analysis of diverse ribonucleoprotein complexes. *Nat Methods* 4: 951–956.
- Oeffinger M, Zenklusen D, Ferguson A, Wei KE, Hage El A, Tollervey D, Chait BT, Singer RH, Rout MP. 2009. Rrp17p is a eukaryotic exonuclease required for 5' end processing of Pre-60S ribosomal RNA. *Molecular Cell* 36: 768–781.
- Ohmayer U, Gamalinda M, Sauert M, Ossowski J, Pöll G, Linnemann J, Hierlmeier T, Perez-Fernandez J, Kumcuoglu B, Leger-Silvestre I, et al. 2013. Studies on the Assembly Characteristics of Large Subunit Ribosomal Proteins in *S. cerevisiae* ed. S.R. Ellis. *PLoS ONE* 8: e68412.
- Ohmayer U, Gil-Hernández Á, Sauert M, Martín-Marcos P, Tamame M, Tschochner H, Griesenbeck J, Milkereit P. 2015. Studies on the Coordination of Ribosomal Protein Assembly Events Involved in Processing and Stabilization of Yeast Early Large Ribosomal Subunit Precursors ed. S. Granneman. *PLoS ONE* 10: e0143768.
- Osheim YN, French SL, Keck KM, Champion EA, Spasov K, Dragon F, Baserga SJ, Beyer AL. 2004. Pre-18S Ribosomal RNA Is Structurally Compacted into the SSU Processome Prior to Being Cleaved from Nascent Transcripts in *Saccharomyces cerevisiae*. *Molecular Cell* 16: 943–954.
- Ouspenski II, Elledge SJ, Brinkley BR. 1999. New yeast genes important for chromosome integrity and segregation identified by dosage effects on genome stability. *Nucleic Acids Res* 27: 3001–3008.

- Panse VG, Johnson AW. 2010. Maturation of eukaryotic ribosomes: acquisition of functionality. *Trends in Biochemical Sciences* 35: 260–266.
- Pausch P, Singh U, Ahmed YL, Pillet B, Murat G, Altegoer F, Stier G, Thoms M, Hurt E, Sinning I, et al. 2015. Co-translational capturing of nascent ribosomal proteins by their dedicated chaperones. *Nat Commun* 6: 7494.
- Pellett S, Tracy JW. 2006. Mak16p is required for the maturation of 25S and 5.8S rRNAs in the yeast *Saccharomyces cerevisiae*. *Yeast* 23: 495–506.
- Peng Z, Oldfield CJ, Bin Xue, Mizianty MJ, Dunker AK, Kurgan L, Uversky VN. 2014. A creature with a hundred waggly tails: intrinsically disordered proteins in the ribosome. *Cell Mol Life Sci* 71: 1477–1504.
- Pestov DG, Stockelman MG, Strezoska Ž, Lau LF. 2001. ERB1, the yeast homolog of mammalian Bop1, is an essential gene required for maturation of the 25S and 5.8S ribosomal RNAs. *Nucleic Acids Res* 29: 3621–3630.
- Pöll G, Braun T, Jakovljevic J, Neueder A, Jakob S, Woolford JL Jr, Tschochner H, Milkereit P. 2009. rRNA Maturation in yeast cells depleted of large ribosomal subunit proteins. *PLoS ONE* 4: e8249.
- Pratte D, Singh U, Murat G, Kressler D. 2013. Mak5 and Ebp2 act together on early pre-60S particles and their reduced functionality bypasses the requirement for the essential pre-60S factor Nsa1. *PLoS ONE* 8: e82741.
- Puig O, Caspary F, Rigaut G, Rutz B, Bouveret E, Bragado-Nilsson E, Wilm M, Séraphin B. 2001. The Tandem Affinity Purification (TAP) Method: A General Procedure of Protein Complex Purification. *Methods* 24: 218–229.
- Pyle AM, Green JB. 1995. RNA folding. *Curr Opin Struct Biol* 5: 303–310.
- Ripmaster TL, Vaughn GP, Woolford JL. 1993. DRS1 to DRS7, novel genes required for ribosome assembly and function in *Saccharomyces cerevisiae*. *Mol Cell Biol* 13: 7901–7912.

- Rodríguez-Galán O, García-Gómez JJ, la Cruz de J. 2013. Yeast and human RNA helicases involved in ribosome biogenesis: Current status and perspectives. *Biochimica et Biophysica Acta- Gene Regulatory Mechanisms* 1829: 775–790.
- Romes EM, Sobhany M, Stanley RE. 2016. The Crystal Structure of the Ubiquitin-Like Domain of Ribosome Assembly Factor Ytm1 and Characterization of its Interaction with the AAA-ATPase Midasin. *J Biol Chem* 291: 882-293.
- Rosado IV, Dez C, Lebaron S, Caizergues-Ferrer M, Henry Y, la Cruz de J. 2007. Characterization of *Saccharomyces cerevisiae* Npa2p (Urb2p) reveals a low-molecular-mass complex containing Dbp6p, Npa1p (Urb1p), Nop8p, and Rsa3p involved in early steps of 60S ribosomal subunit biogenesis. *Mol Cell Biol* 27: 1207–1221.
- Ross PL, Huang YN, Marchese JN, Williamson B, Parker K, Hattan S, Khainovski N, Pillai S, Dey S, Daniels S, et al. 2004. Multiplexed protein quantitation in *Saccharomyces cerevisiae* using amine-reactive isobaric tagging reagents. *Mol Cell Proteomics* 3: 1154–1169.
- Sahasranaman A, Dembowski J, Strahler J, Andrews P, Maddock J, Woolford JL. 2011. Assembly of *Saccharomyces cerevisiae* 60S ribosomal subunits: role of factors required for 27S pre-rRNA processing. *EMBO J* 30: 4020–4032.
- Santos MCT, Goldfeder MB, Zanchin NIT, Oliveira CC. 2011. The essential nucleolar yeast protein Nop8p controls the exosome function during 60S ribosomal subunit maturation. *PLoS ONE* 6: e21686.
- Saveanu C, Bienvenu D, Namane A, Gleizes PE, Gas N, Jacquier A, Fromont-Racine M. 2001. Nog2p, a putative GTPase associated with pre-60S subunits and required for late 60S maturation steps. *EMBO J* 20: 6475–6484.
- Saveanu C, Namane A, Gleizes P-E, Lebreton A, Rousselle J-C, Noaillac-Depeyre J, Gas N, Jacquier A, Fromont-Racine M. 2003. Sequential protein association with nascent 60S ribosomal particles. *Mol Cell Biol* 23: 4449–4460.

- Saveanu C, Rousselle J-C, Lenormand P, Namane A, Jacquier A, Fromont-Racine M. 2007. The p21-activated protein kinase inhibitor Skb15 and its budding yeast homologue are 60S ribosome assembly factors. *Mol Cell Biol* 27: 2897–2909.
- Schillewaert S, Wacheul L, Lhomme F, Lafontaine DLJ. 2012. The evolutionarily conserved protein Las1 is required for pre-rRNA processing at both ends of ITS2. *Mol Cell Biol* 32: 430–444.
- Senger B, Lafontaine DLJ, Graindorge J-S, Gadai O, Camasses A, Sanni A, Garnier J-M, Breitenbach M, Hurt E, Fasiolo F. 2001. The Nucleolar Tif6p and Efl1p Are Required for a Late Cytoplasmic Step of Ribosome Synthesis. *Molecular Cell* 8: 1363–1373.
- Sengupta J, Bussiere C, Pallesen J, West M, Johnson AW, Frank J. 2010. Characterization of the nuclear export adaptor protein Nmd3 in association with the 60S ribosomal subunit. *J Cell Biol* 189: 1079–1086.
- Sharma S, Lafontaine DLJ. 2015. “View From A Bridge”: A New Perspective on Eukaryotic rRNA Base Modification. *Trends in Biochemical Sciences* 40: 560–575.
- Sharma S, Yang J, Watzinger P, Kötter P, Entian K-D. 2013. Yeast Nop2 and Rcm1 methylate C2870 and C2278 of the 25S rRNA, respectively. *Nucleic Acids Res* 41: 9062–9076.
- Shen J, Cowen LE, Griffin AM, Chan L, Köhler JR. 2008. The *Candida albicans* pescadillo homolog is required for normal hypha-to-yeast morphogenesis and yeast proliferation. *Proc Natl Acad Sci* 105: 20918–20923.
- Shimoji K, Jakovljevic J, Tsuchihashi K, Umeki Y, Wan K, Kawasaki S, Talkish J, Woolford JL, Mizuta K. 2012. Ebp2 and Brx1 function cooperatively in 60S ribosomal subunit assembly in *Saccharomyces cerevisiae*. *Nucleic Acids Res* 40: 4574–4588.
- Spitale RC, Crisalli P, Flynn RA, Torre EA, Kool ET, Chang HY. 2013. RNA SHAPE analysis in living cells. *Nat Chem Biol* 9: 18–20.
- Stage-Zimmermann T, Schmidt U, Silver PA. 2000. Factors affecting nuclear export of the 60S ribosomal subunit in vivo. *Mol Biol Cell* 11: 3777–3789.

- Steffen KK, McCormick MA, Pham KM, MacKay VL, Delaney JR, Murakami CJ, Kaeberlein M, Kennedy BK. 2012. Ribosome deficiency protects against ER stress in *Saccharomyces cerevisiae*. *Genetics* 191: 107–118.
- Steitz JA, Tycowski KT. 1995. Small RNA chaperones for ribosome biogenesis. *Science* 270: 1626–1627.
- Stelter P, Huber FM, Kunze R, Flemming D, Hoelz A, Hurt E. 2015. Coordinated ribosomal L4 protein assembly into the pre-ribosome is regulated by its eukaryote-specific extension. *Molecular Cell* 58: 854–862.
- Stirnemann CU, Petsalaki E, Russell RB, Müller CW. 2010. WD40 proteins propel cellular networks. *Trends in Biochemical Sciences* 35: 565–574.
- Strezoska Ž, Pestov DG, Lau LF. 2000. Bop1 is a mouse WD40 repeat nucleolar protein involved in 28S and 5.8S rRNA processing and 60S ribosome biogenesis. *Mol Cell Biol* 20: 5516–5528.
- Strunk BS, Novak MN, Young CL, Karbstein K. 2012. A translation-like cycle is a quality control checkpoint for maturing 40S ribosome subunits. *Cell* **150**, 111–121.
- Sulima SO, Patchett S, Advani VM, De Keersmaecker K, Johnson AW, Dinman JD. 2014. Bypass of the pre-60S ribosomal quality control as a pathway to oncogenesis. *111*: 5640–5645.
- Sun C, John L, Woolford J. 1997. The yeast nucleolar protein Nop4p contains four RNA recognition motifs necessary for ribosome biogenesis. *J Biol Chem* 272: 25345–25352.
- Talkish J, Campbell IW, Sahasranaman A, Jakovljevic J, Woolford JL. 2014. Ribosome assembly factors Pwp1 and Nop12 are important for folding of 5.8S rRNA during ribosome biogenesis in *Saccharomyces cerevisiae*. *Mol Cell Biol* 34: 1863–1877.
- Talkish J, Zhang J, Jakovljevic J, Horsey EW, Woolford JL. 2012. Hierarchical recruitment into nascent ribosomes of assembly factors required for 27SB pre-rRNA processing in *Saccharomyces cerevisiae*. *Nucleic Acids Res* 40: 8646–8661.

Tang L, Sahasranaman A, Jakovljevic J, Schleifman E, Woolford JL. 2008. Interactions among Ytm1, Erb1, and Nop7 required for assembly of the Nop7-subcomplex in yeast preribosomes. *Mol Biol Cell* 19: 2844–2856.

Tarassov K, Messier V, Landry CR, Radinovic S, Serna Molina MM, Shames I, Malitskaya Y, Vogel J, Bussey H, Michnick SW. 2008. An in vivo map of the yeast protein interactome. *Science* 320: 1465–1470.

Tecza A, Bugner V, Köhl M, Köhl SJ. 2011. Pescadillo homologue 1 and Peter Pan function during *Xenopus laevis* pronephros development. *Biol Cell* 103: 483–498.

Thoms M, Thomson E, Baßler J, Gnädig M, Griesel S, Hurt E. 2015c. The Exosome Is Recruited to RNA Substrates through Specific Adaptor Proteins. *Cell* 162: 1029–1038.

Thomson E, Tollervey D. 2010b. The final step in 5.8S rRNA processing is cytoplasmic in *Saccharomyces cerevisiae*. *Mol Cell Biol* 30: 976–984.

van Beekvelt CA, de Graaff-Vincent M, Faber AW, van't Riet J, Venema J, Raué HA. 2001. All three functional domains of the large ribosomal subunit protein L25 are required for both early and late pre-rRNA processing steps in *Saccharomyces cerevisiae*. *Nucleic Acids Res* 29: 5001–5008.

van Beekvelt CA, Kooi EA, de Graaff-Vincent M, Riet J, Venema J, Raué HA. 2000. Domain III of *Saccharomyces cerevisiae* 25 S ribosomal RNA: its role in binding of ribosomal protein L25 and 60 S subunit formation. *J Mol Biol* 296: 7–17.

van Hoof A, Lennertz P, Parker R. 2000. Three conserved members of the RNase D family have unique and overlapping functions in the processing of 5S, 5.8S, U4, U5, RNase MRP and RNase P RNAs in yeast. *EMBO J* 19: 1357–1365.

Wan K, Tsuchihashi K, KANDA K, Shimoji K, Mizuta K. 2014. N $\alpha$ -Acetyltransferase NatA Is involved in ribosome synthesis in *Saccharomyces cerevisiae*. *Bioscience, Biotechnology and Biochemistry* 77: 631–638.

Wan K, Yabuki Y, Mizuta K. 2015. Roles of Ebp2 and ribosomal protein L36 in ribosome biogenesis in *Saccharomyces cerevisiae*. *Curr Genet* 61: 31–41.

- Warner JR. 1999. The economics of ribosome biosynthesis in yeast. *Trends in Biochemical Sciences* 24: 437–440.
- Weaver PL, Sun C, Chang TH. 1997. Dbp3p, a putative RNA helicase in *Saccharomyces cerevisiae*, is required for efficient pre-rRNA processing predominantly at site A3. *Mol Cell Biol* 17: 1354–1365.
- Wegrecki M, Rodríguez-Galán O, la Cruz de J, Bravo J. 2015. The structure of Erb1-Ytm1 complex reveals the functional importance of a high-affinity binding between two  $\beta$ -propellers during the assembly of large ribosomal subunits in eukaryotes. *Nucleic Acids Res* 43: 11017–11030.
- Woodson SA. 2008. RNA folding and ribosome assembly. *Current Opinion in Chemical Biology* 12: 667–673.
- Woodson SA. 2010. Compact intermediates in RNA folding. *Annu Rev Biophys* 39: 61–77.
- Woodson SA. 2011. RNA folding pathways and the self-assembly of ribosomes. *Acc Chem Res* 44: 1312–1319.
- Woolford JL, Baserga SJ. 2013. Ribosome biogenesis in the yeast *Saccharomyces cerevisiae*. *Genetics* 195: 643–681.
- Wu S, Kumcuoglu B, Yan K, Brown H, Zhang Y, Tan D, Gamalinda M, Yuan Y, Li Z, Jakovljevic J, Lei J, Dong M, Woolford JL, Gao N. 2016. Diverse roles of assembly factors revealed by structures of late nuclear pre-60S ribosomal particles. Submitted.
- Xie W, Qu L, Meng L, Liu C, Wu J, Shou C. 2013. PES1 regulates sensitivity of colorectal cancer cells to anticancer drugs. *Biochem Biophys Res Commun* 431: 460–465.
- Xue S, Barna M. 2012. Specialized ribosomes: a new frontier in gene regulation and organismal biology. *Nat Rev Mol Cell Biol* 13: 355–369.
- Yano R, Nomura M. 1991. Suppressor analysis of temperature-sensitive mutations of the largest subunit of RNA polymerase I in *Saccharomyces cerevisiae*: a suppressor gene encodes the second-largest subunit of RNA polymerase I. *Mol Cell Biol* 11: 754–764.

Yoshikatsu Y, Ishida Y-I, Sudo H, Yuasa K, Tsuji A, Nagahama M. 2015. NVL2, a nucleolar AAA-ATPase, is associated with the nuclear exosome and is involved in pre-rRNA processing. *Biochem Biophys Res Commun* 464: 780–786.

Zagulski M, Kressler D, B cam AM, Rytka J, Herbert CJ. 2003. Mak5p, which is required for the maintenance of the M1 dsRNA virus, is encoded by the yeast ORF YBR142w and is involved in the biogenesis of the 60S subunit of the ribosome. *Mol Genet Genomics* 270: 216–224.

Zanchin NI, Goldfarb DS. 1999. Nip7p interacts with Nop8p, an essential nucleolar protein required for 60S ribosome biogenesis, and the exosome subunit Rrp43p. *Mol Cell Biol* 19: 1518–1525.

Zhang J, Harnpicharnchai P, Jakovljevic J, Tang L, Guo Y, Oeffinger M, Rout MP, Hiley SL, Hughes T, Woolford JL. 2007. Assembly factors Rpf2 and Rrs1 recruit 5S rRNA and ribosomal proteins rpL5 and rpL11 into nascent ribosomes. *Genes Dev* 21: 2580–2592.